ISSN 1948-5204 (online)

World Journal of *Gastrointestinal Oncology*

World J Gastrointest Oncol 2022 July 15; 14(7): 1218-1374

Published by Baishideng Publishing Group Inc

World Journal of Gastrointestinal Oncology

Contents

Monthly Volume 14 Number 7 July 15, 2022

World Journal of Gastrointestinal Oncology

Monthly Volume 14 Number 7 July 15, 2022

Contents

NAME OF JOURNAL
World Journal of Gastrointestinal Oncology

ISSN
ISSN 1948-5204 (online)

LAUNCH DATE
February 15, 2009

FREQUENCY
Monthly

EDITORS-IN-CHIEF
Monjur Ahmed, Florin Burada

EDITORIAL BOARD MEMBERS
https://www.wjgnet.com/1948-5204/editorialboard.htm

PUBLICATION DATE
July 15, 2022

INSTRUCTIONS TO AUTHORS
https://www.wjgnet.com/bpg/gerinfo/204

GUIDELINES FOR ETHICS DOCUMENTS
https://www.wjgnet.com/bpg/GerInfo/287

GUIDELINES FOR NON-NATIVE SPEAKERS OF ENGLISH
https://www.wjgnet.com/bpg/gerinfo/240

PUBLICATION ETHICS
https://www.wjgnet.com/bpg/GerInfo/288

PUBLICATION MISCONDUCT
https://www.wjgnet.com/bpg/gerinfo/208

ARTICLE PROCESSING CHARGE
https://www.wjgnet.com/bpg/gerinfo/242

STEPS FOR SUBMITTING MANUSCRIPTS
https://www.wjgnet.com/bpg/GerInfo/239

ONLINE SUBMISSION
https://www.f6publishing.com

World Journal of Gastrointestinal Oncology

Submit a Manuscript: https://www.f6publishing.com

World J Gastrointest Oncol 2022 July 15; 14(7): 1218-1226

DOI: 10.4251/wjgo.v14.i7.1218

ISSN 1948-5204 (online)

FRONTIER

Gut microbiome and pancreatic cancer cachexia: An evolving relationship

Andrew Hendifar, Rasaq Akinsola, Hayato Muranaka, Arsen Osipov, Shant Thomassian, Natalie Moshayedi, Julianne Yang, Jonathan Jacobs, Suzanne Devkota, Neil Bhowmick, Jun Gong

Specialty type: Oncology

Provenance and peer review: Invited article; Externally peer reviewed.

Peer-review model: Single blind

Peer-review report's scientific quality classification

Grade A (Excellent): 0
Grade B (Very good): B, B
Grade C (Good): 0
Grade D (Fair): 0
Grade E (Poor): 0

P-Reviewer: Manojlovic N, Serbia; Yu L, Singapore

Received: March 3, 2022
Peer-review started: March 3, 2022
First decision: April 17, 2022
Revised: May 10, 2022
Accepted: June 20, 2022
Article in press: June 20, 2022
Published online: July 15, 2022

Andrew Hendifar, Rasaq Akinsola, Hayato Muranaka, Arsen Osipov, Shant Thomassian, Natalie Moshayedi, Neil Bhowmick, Jun Gong, Department of Medicine, Division of Hematology and Oncology, Cedars-Sinai Medical Center, Los Angeles, CA 90048, United States

Julianne Yang, The Vatche and Tamar Manoukian Division of Digestive Diseases, Department of Medicine, University of California, Los Angeles, CA 90095, United States

Jonathan Jacobs, Department of Medicine, David Geffen School of Medicine at UCLA, University of California, Los Angeles, Los Angeles, CA 90095, United States

Suzanne Devkota, Cedars-Sinai Medical Center, Department of Medicine, Inflammatory Bowel and Immunobiology Research Institute, University of California, Los Angeles, CA 90048, United States

Corresponding author: Jun Gong, MD, Assistant Professor, Department of Medicine, Division of Hematology and Oncology, Cedars-Sinai Medical Center, 8700 Beverly Blvd, AC 1042B, Los Angeles, CA 90048, United States. jun.gong@cshs.org

Abstract

Nearly 80% of patients with pancreatic ductal adenocarcinoma (PDAC) develop cachexia along their disease course. Cachexia is characterized by progressive weight loss, muscle wasting, and systemic inflammation and has been linked to poorer outcomes and impairments in quality of life. Management of PDAC cachexia has historically involved a multidisciplinary effort comprised of nutritional support, pancreatic enzyme replacement therapy, and/or pharmacologic interventions. Despite current interventions to mitigate PDAC cachexia, a significant proportion of patients continue to die from complications associated with cachexia underscoring the need for novel insights and treatments for this syndrome. We highlight the feasibility and effectiveness of a recent enteral feeding prospective trial at our institution to improve cachexia outcomes in patients with advanced PDAC. Additionally, we were among the first to characterize the stool microbiome composition in patients with advanced PDAC receiving enteral feeding for the treatment of cachexia. Novel insights into the relationship between enteral nutritional support, cachexia, and the gut microbiome are presented. These promising results are discussed in the context of a potential ability to modulate the stool microbiome as a new interventional strategy to mitigate PDAC cachexia.

Key Words: Gut microbiome; Pancreatic cancer; Stool; Cachexia; Inflammation; Weight

Core Tip: Cachexia is a hallmark of pancreatic cancer and is characterized by muscle wasting, weight loss, and systemic inflammation. Despite advancements in nutritional support, pancreatic enzyme replacement therapy, and pharmacologic interventions for treating pancreatic cancer cachexia, it continues to have a significant negative impact on patient outcomes. We detail the results of a recent prospective clinical trial wherein cachectic patients with advanced pancreatic cancer achieved weight stability with 12 wk of enteral feeding. Notably, gut microbiome changes and an increased abundance of a specific microbe associated with enteral feeding highlight a potentially novel approach to mitigate cachexia through microbial modulation.

Citation: Hendifar A, Akinsola R, Muranaka H, Osipov A, Thomassian S, Moshayedi N, Yang J, Jacobs J, Devkota S, Bhowmick N, Gong J. Gut microbiome and pancreatic cancer cachexia: An evolving relationship. *World J Gastrointest Oncol* 2022; 14(7): 1218-1226
URL: https://www.wjgnet.com/1948-5204/full/v14/i7/1218.htm
DOI: https://dx.doi.org/10.4251/wjgo.v14.i7.1218

INTRODUCTION

Pancreatic cancer is an aggressive malignancy characterized by progressive therapeutic resistance and a multifactorial syndrome of weight loss, muscle wasting, and systemic inflammation known as cachexia [1,2]. Cachexia is pervasive and an unfortunate hallmark of pancreatic cancer as nearly 85% of patients with pancreatic ductal adenocarcinoma (PDAC) will meet the definition of cancer cachexia along their disease course[3,4]. Cancer cachexia is generally defined as a multifactorial syndrome characterized by progressive loss of skeletal muscle mass (with or without loss of fat mass) that is not fully reversible through conventional means of nutritional support and leads to ongoing impairment in patient function [5]. Diagnostic criteria for cancer cachexia have been defined by international consensus guidelines as well (Table 1).

The management of PDAC cachexia is multidisciplinary and has historically been comprised of the following: Nutritional support with oral nutrition supplements and involvement of a registered dietitian, pancreatic enzyme replacement therapy, exercise, pharmacologic interventions, and in select cases, specialized nutrition support through the use of enteral or parenteral nutrition[4,6]. The importance of systemic therapy for the underlying PDAC cannot be underscored as well given that the negative impact of cancer cachexia on patient outcomes can be offset, to a degree, with systemic chemotherapy[7]. Despite the mechanisms of PDAC cachexia having been increasingly described, the cachexia syndrome in pancreatic cancer patients remains difficult to treat with a profoundly negative impact on outcomes including overall survival (OS), response to chemotherapy, and quality-of-life[6,7]. As such, novel interventions for PDAC cachexia are of high unmet need.

PANCAX-1

Our group has historically focused on the development of biomarkers and therapeutic strategies for PDAC cachexia across interventional and observational trials[1,8]. We conducted PANCAX-1 (NCT02400398), which was a single-institution, single-arm prospective clinical trial, to evaluate the feasibility and efficacy of enteral feeding on weight stability in cachectic patients with advanced pancreatic cancer[9,10]. Eligible patients included those aged > 18 years having been diagnosed with advanced or locally advanced pancreatic cancer and cachexia. Candidates were required to have a jejunal or gastrojejunal feeding tube placed prior to study intervention. Cachexia was defined using consensus criteria (Table 1). Anticancer therapy or previous surgical resection for pancreatic cancer was permitted. Patients were enrolled to receive the study intervention of a peptide-based formula (Peptamen 1.5) over three 4-week cycles (total of 12 wk) of enteral feeding as per protocol (Figure 1).

The primary endpoint was weight stability at 3 mo, defined as weight loss < 0.1 kg/baseline body mass index (BMI)-unit. Secondary endpoints included changes in body composition measurements, clinical metrics of function and activity, safety, and patient-reported outcomes (PROs).

Table 1 Consensus definitions of cancer cachexia[5]

Definition of cancer cachexia is met with one of the following
Weight loss > 5% over past 6 mo (in absence of simple starvation)
Body mass index < 20 and weight loss > 2%
Evidence of sarcopenia with weight loss > 2%[1]

[1]Generally accepted measures of sarcopenia include: mid upper-arm muscle area by anthropometry (men < 32 cm^2, women < 18 cm^2); appendicular skeletal muscle index determined by dual energy x-ray absorptiometry (men < 7.26 kg/m^2; women < 5.45 kg/m^2); lumbar skeletal muscle index determined by computed tomography imaging (men < 55 cm^2/m^2; women < 39 cm^2/m^2); whole body fat-free mass index without bone determined by bioelectrical impedance (men < 14.6 kg/m^2; women < 11.4 kg/m^2).

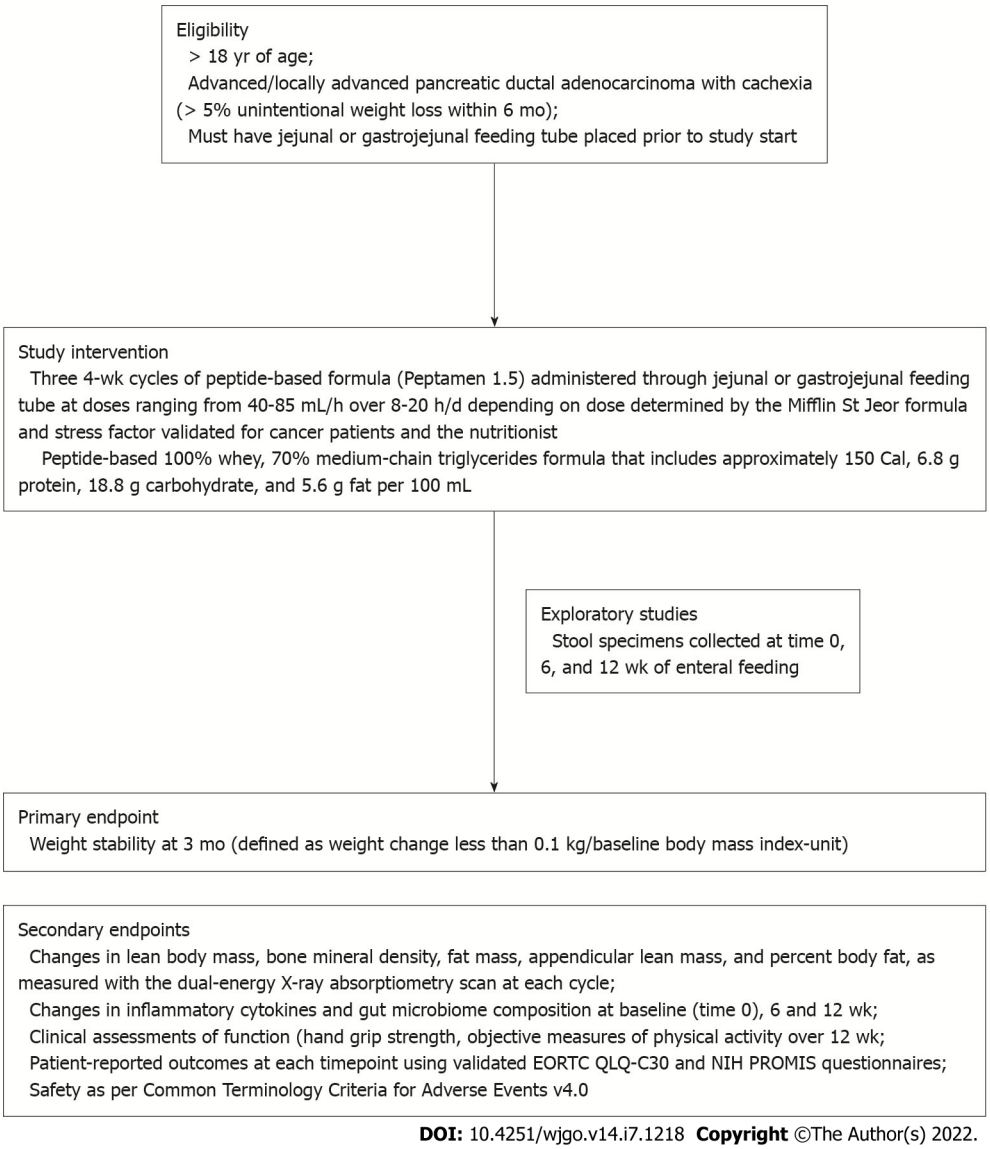

DOI: 10.4251/wjgo.v14.i7.1218

Figure 1 Study design of the single-institution, single-arm prospective PANCAX-1 trial evaluating the feasibility and efficacy of enteral feeding on weight stability in cachectic patients with advanced pancreatic cancer.

From April 2015-March 2019, a total of 31 patients were consented onto the study. From this, 16 patients were able to complete all 12 wk of enteral tube feeding and were deemed evaluable for the primary endpoint. The study achieved its primary endpoint whereby weight stability was achieved in 10/16 patients (62.5%). Additionally, enteral feeding was associated with improvement in key secondary outcomes including decreases in body fat mass and inflammatory markers (CRP) but increases in lean body mass (Table 2). Improvements were seen in PROs using both NIH PROMIS and EORTC QLQ-C30 scores from baseline to 12 wk of enteral feeding in this cohort[9].

Table 2 Key outcome measures in cachectic patients with advanced pancreatic cancer over 12 wk of enteral feeding

Outcome (*n* = 16)	Change (SD)
Average weight (kg)	+1.29 (5.8)
Body mass index (kg/m^2)	+0.6 (1.7)
% Body fat	-1.6 (5)
Bone mineral density (T-score)	-0.01 (0.02)
Body fat mass (g)	-602 (2794)
Lean body mass (g)	+1273.1 (4078)
Appendicular lean mass (kg/m^2)	+0.45 (0.62)
C-reactive protein (mg/mL)	-9.77 (SE 11.6)
Patient-reported outcomes	
NIH PROMIS (mean difference in score)	
Pain interference	-7.5 (P = 0.05)
Fatigue	-7.1 (P = 0.06)
Depression	-10.4 (P = 0.006)
EORTC QLQ-C30 (mean difference in score)	
Global health	+13.3 (P = 0.05)

THE GUT MICROBIOME AND CACHEXIA

The PANCAX-1 trial successfully demonstrated the feasibility and efficacy of enteral feeding alongside systemic chemotherapy for the treatment of cachexia in patients with advanced PDAC. Despite a drop in consented subjects who were unable to complete 12-wk of enteral feeding due to advanced disease, deteriorating performance status, and/or rapid changes in symptom burden as expected from a high-risk population, enteral feeding resulted in weight stability and improved PROs in cachectic patients with advanced pancreatic cancer. We next sought to identify predictive biomarkers associated with weight stability in this prospective cohort for insight into the possible mechanisms by which enteral feeding served an effective intervention for cachexia. In preplanned exploratory studies of the PANCAX-1 prospective cohort, blood and stool samples were collected longitudinally for profiling of inflammatory cytokines and the gut microbiome.

Our group characterized for the first time the gut microbiome composition in patients with advanced pancreatic cancer treated with enteral feeding for cachexia[11]. DNA extraction and sequencing of the 16S ribosomal RNA gene was performed on fecal samples, as previously described[12], with several unique findings (Table 3). Firstly, in stool samples collected over 12 wk of enteral feeding, differential abundance testing identified an increased relative abundance of the Gram-negative genus *Veillonella* (P = 0.0150) and the Gram-positive genus *Actinomyces* (P = 0.0390). As *Veillonella* represented a bacterial genus that increased in abundance over time with enteral feeding for PDAC cachexia, it was interesting to discover that a significantly increased abundance of *Veillonella* was also identified in baseline stool samples of cachectic patients who achieved weight stability with enteral feeding.

Veillonella are Gram-negative, anaerobic bacteria known for its lactate fermenting abilities and are nonpathogenic colonizers of the intestines and oral mucosa in humans whereby *Veillonella atypica* and its active metabolite propionate has been shown to enhance physical performance in mouse models[13]. Interestingly, in a separate cohort of cachectic patients comprised predominantly of subjects with pancreatic cancer, *Veillonella* was among the most abundant bacterial genera among cachectic cancer patients[14]. In a comparison of the oral microbiome collected from PDAC patients and healthy controls, *Veillonella* were among the genera in significantly greater abundance in salivary samples from healthy controls than those with PDAC[15]. Furthermore, when comparing subjects with resectable *vs* unresectable PDAC, *Veillonella* was found to be the most abundant bacterial genera in those with less advanced, resectable disease when compared to more advanced, unresectable disease. When compared to healthy controls, *Veillonella* had the lowest odds ratio (OR) for risk of PDAC development across all sampled oral bacteria (OR 0.187, 95% confidence interval 0.055-0.631, P = 0.007). The relative abundance of *Veillonella* in saliva samples was observed to show a gradual decline from healthy controls to those with resectable PDAC and unresectable PDAC. The lowest abundance of *Veillonella* was observed in saliva samples from subjects with unresectable PDAC, whereas the highest abundance of *Veillonella* was observed in the saliva from healthy subjects.

Table 3 Gut microbiome compositional changes in patients with advanced pancreatic cancer receiving 12 wk of enteral feeding for cachexia

Stool microbiome assessment[1]	Outcome
Relative abundance from baseline (time 0) to 12 wk (n = 6)	Increased abundance: *Veillonella* genera (P = 0.015); *Actinomyces* genera (P = 0.039). Decreased abundance: *Bacteroides* genera (P = 0.015); *Butyricicoccus* genera (P = 0.039)
Relative abundance in baseline stool samples from subjects achieving weight stability (n = 8)	Increased abundance: *Veillonella* genera (P = 0.0006). Decreased abundance: *Bifidobacterium* genera ($P = 2.35 \times 10^{-5}$)[2]
Diversity indices (n = 8)	Weight stability associated with reduced diversity by Chao1 index of richness (P = 0.0208) but not reduced species richness and evenness by Shannon index (P = 0.187)

[1]Performed through 16S ribosomal RNA gene sequencing.
[2]Taxa summary plot suggested that this finding was driven by a high percentage of this bacterium in one patient who had a much higher overall survival than the mean.

MICROBIAL INTERVENTIONS AS A POTENTIAL NEW THERAPEUTIC STRATEGY FOR CACHEXIA

The relationship between the gut microbiome and cachexia has long been implicated in earlier investigations wherein alterations in gut microbiome composition were associated with anorexia nervosa and low BMI states, body weight loss, low muscle mass, low appetite, and systemic inflammation[16]. However, the role that the gut microbiome plays in the cachexia process has been better established with studies on its impact with systemic inflammation and muscle wasting, which are hallmarks of cachexia[16-18].

Inflammation has classically served in host defense against pathogens but has increasingly been shown to be equally important in tissue repair, regeneration, and remodeling with programmed cell death including apoptosis, necroptosis, and pyroptosis representing means to clear dying cells and promote tissue homeostasis[19,20]. In this sense, localized transient inflammation is generally protective, helping the host to remove harmful stimuli including physical, chemical, carcinogenic, and infectious and facilitate degradation of dying cells as a nutritional source to facilitate tissue regeneration. However, the inflammatory response underlying cachexia often is characterized by impairment in the correct utilization of nutrients such that meeting energy and protein requirements in patients with cachexia without addressing inflammation can result in improper restoration of body composition as most proteins and energy are diverted to production of acute-phase proteins and adipose tissue, which in turn, can sustain and promote systemic inflammation[21]. In critically ill patients, for example, concepts of restrictive eating during acute phases of critical illness have been explored to potentially minimize the negative effects of overfeeding and systemic inflammation[22]. Evidence is emerging to suggest that specific bacteria within the gut microbiome may possess pro- and anti-inflammatory effects, providing another relationship between the microbiome and cachexia that could be exploited to counteract the systemic inflammation underlying cachexia[23].

Animal studies have illustrated several key findings of the gut microbiome-cachexia relationship: (1) Gut microbes can lead to muscle wasting through decreasing amino acid availability for the host or synthesis of noxious bacterial metabolites (*e.g.*, indoxyl sulfate and lipopolysaccharide or LPS) that activate PI3K/AKT, NF-κB, and MAPK (p38, JNK, ERK) signaling to upregulate Atrogin-1/MAFbx and MuRF1 genes encoding E3 ubiquitin ligases; (2) Pathogen-associated molecular patterns (PAMPs) from microbes (*e.g.*, circulating peptidoglycans, LPS, bacterial nucleic acids, short-chain fatty acids or SCFA, branched-chain amino acids or BCAAs, or flagellin) can induce muscle atrophy by stimulating the Toll-like receptor/NF-kB pathway; (3) Increased gut permeability in cachectic disorders and subsequent translocation of PAMPs from the gut lumen can stimulate pro-inflammatory cytokine cascades; and (4) Depletion of certain bacterial conditions can induce muscle wasting by activating the AMPK-FoxO3-Atrogin-1/MuRF1 cascade and BCAA catabolism, reducing expression of growth factors and muscle growth-related genes (IGF-1, myogenin, SIK1, and MyoD), increasing myostatin, and impairing neuromuscular junction function and mitochondrial function[16-18].

Based on this preclinical rationale, it is not surprising that early efforts for gut microbiota-targeted nutritional interventions of cachexia have already begun exploration. For example, administration of a mixture of *Lactobacillus reuteri* and *Lactobacillus gasseri* to cachectic mice with leukemia restored the levels of these bacteria in the gut while reducing inflammation and partially counteracting the induction of muscle atrophy markers[24]. Administration of bacterial metabolites have also shown applicability in the treatment of cachexia where pectic oligosaccharides given to leukemic mice with cachexia was able to delay the cachectic phenotype and spare fat mass while increasing abundance of *Bacteroides dorei*[25].

There is growing evidence to suggest that *Veillonella* represents a genus of gut bacteria that is protective against PDAC and performance enhancing in human subjects[13,15]. In our preplanned analyses of the gut microbiome in stool samples serially collected from a prospective cohort of enteral

fed patients with PDAC cachexia, we identified compositional changes in the gut microbiome and an increase in abundance of the bacterial genus *Veillonella* over time with enteral feeding associated with weight stability. We are therefore the first to posit another beneficial role of *Veillonella* as a microbe associated with weight stability in the treatment of cachexia. However, before positioning *Veillonella* as a potential future and novel intervention to mitigate cachexia, there are several lessons that can be learned from microbial manipulation strategies thus far.

FUTURE CONSIDERATIONS FOR CLINICAL TRANSLATION

Interventions to target the gut microbiome in cancer cachexia can largely be classified into: (1) Prebiotics, which are nondigestible substrates that can induce growth or activity of microorganisms in the host; (2) Probiotics that contain live microorganisms to be introduced to the host; and (3) Synbiotics, which are mixtures of live microorganisms and substrates utilized by the host (combination of prebiotics and probiotics)[17].

Recently, the double-blind, randomized phase II TRANSIT trial enrolled patients with unresectable or metastatic gastroesophageal junction adenocarcinoma who were planned to receive standard first-line chemotherapy and met criteria for cachexia to receive allogenic fecal microbiota transplantation (FMT) from obese donors or autologous FMT (control)[26]. Donor and recipients delivered fresh fecal samples within 6 h before use on day of fecal infusions wherein the feces were mixed until fully homogenized and the fecal solution filtered to remove food derived debris. The filtrate was then transferred to a 1000-mL sterile bottle and stored at room temperature. Enrolled subjects underwent bowel lavage with polyethylene glycol solution through a nasoduodenal tube to remove endogenous fecal contamination. This was followed by infusion of the gut microbiota solution over 30 minutes approximately. The primary outcome of this study was effect of allogenic FMT on satiety after 4 wk with secondary outcomes on cachexia domains including nutritional and appetite assessments and conventional cancer efficacy outcomes.

Between August 2016 to January 2019, 24 patients were randomized to receive allogenic FMT (n = 12) and autologous FMT (n = 12). Donors for allogenic FMT were all healthy overweight or obese subjects by BMI criteria. There was no significant difference in satiety levels, caloric intake, or change in any other measure related to cachexia between allogenic and autologous FMT groups. There was no difference in completion rates or adverse events associated with chemotherapy across groups either. However, those receiving allogenic FMT had higher disease-control rates at 12 wk, longer median OS (365 d *vs* 227 d), hazard ratio 0.38 (95% confidence interval: 0.14-1.05, P = 0.057) and longer progression-free survival (204 d *vs* 93 d) than those receiving autologous FMT. The microbiome composition from the allogenic recipients resembled the donor microbiome more closely after the FMT compared to baseline, suggestive of proper engraftment of donor microbiota.

The phase II TRANSIT trial, although negative, should be praised for testing the feasibility of such an approach in human subjects with cancer cachexia. There are multiple take-away points from this important study that need to be considered in future applications of microbial interventions in human subjects with cachexia. Firstly, although microbiome analyses revealed a significant shift in microbiome composition following allogenic FMT, a specific microbe or group of microbes mediating the beneficial oncological outcomes in the allogenic group were not identified. Is a healthy obese subject the ideal donor for FMT to treat cancer cachexia? An alternative mechanism could entail the administration of microbes isolated from stool of successfully treated patients for cachexia. This could arguably reflect the compositional changes in the gut microbiome indicative of a responding host to anti-cachexia therapy. The microbiome in an obese individual could also differ significantly from those of non-obese individuals and can induce weight gain or weight loss dependent on a variety of environmental and host biologic factors[26]. The uniqueness of the PANCAX-1 cohort lies in the fact that all subjects received enteral feeding as their primary source of nutrition thereby representing a homogeneous and internally controlled population for microbiome and metabolomics analyses. The finding that *Veillonella* was a microbe of interest with increased abundance over time with enteral feeding and was associated with weight stability in cachectic patients with advanced PDAC receiving enteral feeding provides an innovative opportunity to explore microbial interventional strategies for cachexia with this organism.

However, individual microbes may not be sufficient to elect pro- or anti-cachexia effects alone. Animal models have demonstrated that a series of functional and structural changes occur in the gut bacterial population during the development of cachexia[27]. Microbial dysbiosis has shown to play a role in shaping the gut microbiome and pancreatic tumorigenesis as well[28]. We showed that weight stabilizing, cachexia therapy through enteral feeding was associated with multiple taxonomic shifts including increased abundance of the *Veillonella* genus (P = 0.015) and *Actinomyces* genus (P = 0.039) and decreased abundance of the *Bacteroides* genus (P = 0.015) and *Butyricicoccus* genus (P = 0.039) (Table 3). In this sense, it would be prudent for future studies to evaluate the impact of microbial dysbiosis on cachexia, with emphasis on community microbes that altogether contribute to anti- or pro-cachexia effects in microbial interventional strategies for cachexia.

Lastly, it would be important to consider that microorganisms themselves may not be the key constituent for developing therapies against cachexia. Instead, the active metabolites of the gut microbiota may be just as (if not more) important in contributing to anti- or pro-cachexia effects. Here, studies have shown that branched-chain amino acids, LPS, polyamines, and metabolites of other biosynthetic pathways have correlated with altered microbial flora, tumorigenesis, and development of cachexia across animal models[28,29]. Therefore, the logical next step in addition to exploring the potential of *Veillonella* as a microbial intervention in the treatment of cachexia would be for metabolomics to profile the active metabolite(s) of this microorganism and microbial communities associated with weight stabilization on cachexia therapy. The impact of these metabolites as a mechanism to address the cachexia syndrome could then be formally evaluated in preclinical models [30].

CONCLUSION

Cachexia represents a multifactorial syndrome of weight loss, muscle wasting, and systemic inflammation that is pervasive across multiple advanced disease states. Using PDAC as a model, we identified a unique relationship between the gut microbiome and treatment of cachexia in a prospective cohort of advanced PDAC subjects treated with enteral feeding. Specifically, an increased abundance in the bacterial genus *Veillonella* was observed over time in stool samples of cachectic subjects effectively treated with weight-stabilizing intervention through 12 wk of enteral feeding. Our findings are hypothesis-generating and add to an exciting body of evidence suggesting a potential role for microbial-based interventions for cachexia. Future clinical translation of microbial modulation to mitigate cachexia will need to consider the role of microbial dysbiosis and microbial-derived metabolites in cachexia as well.

FOOTNOTES

Author contributions: Hendifar A and Gong J conceptualized the manuscript; Akinsola R, Muranaka H, Thomassian S, Moshayedi N, Yang J and Jacobs J analyzed the data; all authors have read and approve the final manuscript.

Supported by UCLA Clinical and Translational Science Institute UL1TR001881 Award.

Conflict-of-interest statement: All the authors report no relevant conflicts of interest for this article.

Country/Territory of origin: United States

ORCID number: Andrew Hendifar 0000-0002-2079-9177; Arsen Osipov 0000-0002-9000-7040; Jun Gong 0000-0001-8713-1406.

S-Editor: Gao CC
L-Editor: A
P-Editor: Gao CC

REFERENCES

1 **Gong J**, Guan M, Forsmark CE, Petzel MQ, Placencio-Hickok V, Hendifar A. Fecal elastase, an assay for exocrine pancreatic insufficiency, has clinical utility in patients with pancreatic ductal adenocarcinoma. *Therap Adv Gastroenterol* 2020; **13**: 1756284820964319 [PMID: 33354227 DOI: 10.1177/1756284820964319]

2 **Gong J**, Tuli R, Shinde A, Hendifar AE. Meta-analyses of treatment standards for pancreatic cancer. *Mol Clin Oncol* 2016; **4**: 315-325 [PMID: 26998283 DOI: 10.3892/mco.2015.716]

3 **Fearon KC**, Voss AC, Hustead DS; Cancer Cachexia Study Group. Definition of cancer cachexia: effect of weight loss, reduced food intake, and systemic inflammation on functional status and prognosis. *Am J Clin Nutr* 2006; **83**: 1345-1350 [PMID: 16762946 DOI: 10.1093/ajcn/83.6.1345]

4 **Hendifar AE**, Petzel MQB, Zimmers TA, Denlinger CS, Matrisian LM, Picozzi VJ, Rahib L; Precision Promise Consortium. Pancreas Cancer-Associated Weight Loss. *Oncologist* 2019; **24**: 691-701 [PMID: 30591550 DOI: 10.1634/theoncologist.2018-0266]

5 **Fearon K**, Strasser F, Anker SD, Bosaeus I, Bruera E, Fainsinger RL, Jatoi A, Loprinzi C, MacDonald N, Mantovani G, Davis M, Muscaritoli M, Ottery F, Radbruch L, Ravasco P, Walsh D, Wilcock A, Kaasa S, Baracos VE. Definition and classification of cancer cachexia: an international consensus. *Lancet Oncol* 2011; **12**: 489-495 [PMID: 21296615 DOI: 10.1016/S1470-2045(10)70218-7]

6 **Tan CR**, Yaffee PM, Jamil LH, Lo SK, Nissen N, Pandol SJ, Tuli R, Hendifar AE. Pancreatic cancer cachexia: a review of mechanisms and therapeutics. *Front Physiol* 2014; **5**: 88 [PMID: 24624094 DOI: 10.3389/fphys.2014.00088]

7 **Hendifar AE**, Chang JI, Huang BZ, Tuli R, Wu BU. Cachexia, and not obesity, prior to pancreatic cancer diagnosis worsens survival and is negated by chemotherapy. *J Gastrointest Oncol* 2018; **9**: 17-23 [PMID: 29564167 DOI: 10.21037/jgo.2017.11.10]

8 **Hendifar AE**, Kim S, Tighiouart M, Hautamaki E, Kim H, Ng C, Liu J-Y, Scher KS, Klempner SJ, Placencio-Hickok V, Gresham G, Gong J. A phase I study of nanoliposomal irinotecan and 5-fluorouracil/folinic acid in combination with interleukin-1-alpha antagonist for advanced pancreatic cancer patients with cachexia (OnFX). *J Clin Oncol* 2020; **38** 4634 PMID: Not applicable. [DOI: 10.1200/JCO.2020.38.15_suppl.4634]

9 **Gresham G**, Placencio-Hickok VR, Lauzon M, Nguyen T, Kim H, Mehta S, Paski S, Pandol SJ, Osipov A, Gong J, Jamil LH, Nissen N, Lo SK, Hendifar AE. Feasibility and efficacy of enteral tube feeding on weight stability, lean body mass, and patient-reported outcomes in pancreatic cancer cachexia. *J Cachexia Sarcopenia Muscle* 2021; **12**: 1959-1968 [PMID: 34609081 DOI: 10.1002/jcsm.12799]

10 **Hendifar AE**, Gresham G, Kim H, Guan M, Liu J-Y, Minton B, Bhuiyan D, Langeslay R, Rogatko A, Gong J, Placencio-Hickok V. A prospective trial of elemental enteral feeding in patients with pancreatic cancer cachexia (PANCAX-1). *J Clin Oncol* 2020; **38**: 726 [DOI: 10.1200/JCO.2020.38.4_suppl.726]

11 **Moshayedi N**, Yang J, Lagishetty V, Jacobs J, Placencio-Hickok V, Osipov A, Hendifar AE, Gong J. Fecal microbiome composition in pancreatic cancer cachexia and response to nutrition support. *J Clin Oncol* 2021; **39**: 4129 [DOI: 10.1200/JCO.2021.39.15_suppl.4129]

12 **Jacobs JP**, Lin L, Goudarzi M, Ruegger P, McGovern DP, Fornace AJ Jr, Borneman J, Xia L, Braun J. Microbial, metabolomic, and immunologic dynamics in a relapsing genetic mouse model of colitis induced by T-synthase deficiency. *Gut Microbes* 2017; **8**: 1-16 [PMID: 27874308 DOI: 10.1080/19490976.2016.1257469]

13 **Scheiman J**, Luber JM, Chavkin TA, MacDonald T, Tung A, Pham LD, Wibowo MC, Wurth RC, Punthambaker S, Tierney BT, Yang Z, Hattab MW, Avila-Pacheco J, Clish CB, Lessard S, Church GM, Kostic AD. Meta-omics analysis of elite athletes identifies a performance-enhancing microbe that functions *via* lactate metabolism. *Nat Med* 2019; **25**: 1104-1109 [PMID: 31235964 DOI: 10.1038/s41591-019-0485-4]

14 **Ubachs J**, Ziemons J, Soons Z, Aarnoutse R, van Dijk DPJ, Penders J, van Helvoort A, Smidt ML, Kruitwagen RFPM, Baade-Corpelijn L, Olde Damink SWM, Rensen SS. Gut microbiota and short-chain fatty acid alterations in cachectic cancer patients. *J Cachexia Sarcopenia Muscle* 2021; **12**: 2007-2021 [PMID: 34609073 DOI: 10.1002/jcsm.12804]

15 **Wei AL**, Li M, Li GQ, Wang X, Hu WM, Li ZL, Yuan J, Liu HY, Zhou LL, Li K, Li A, Fu MR. Oral microbiome and pancreatic cancer. *World J Gastroenterol* 2020; **26**: 7679-7692 [PMID: 33505144 DOI: 10.3748/wjg.v26.i48.7679]

16 **Genton L**, Mareschal J, Charretier Y, Lazarevic V, Bindels LB, Schrenzel J. Targeting the Gut Microbiota to Treat Cachexia. *Front Cell Infect Microbiol* 2019; **9**: 305 [PMID: 31572686 DOI: 10.3389/fcimb.2019.00305]

17 **Ziemons J**, Smidt ML, Damink SO, Rensen SS. Gut microbiota and metabolic aspects of cancer cachexia. *Best Pract Res Clin Endocrinol Metab* 2021; **35**: 101508 [PMID: 33648847 DOI: 10.1016/j.beem.2021.101508]

18 **Liu C**, Cheung WH, Li J, Chow SK, Yu J, Wong SH, Ip M, Sung JJY, Wong RMY. Understanding the gut microbiota and sarcopenia: a systematic review. *J Cachexia Sarcopenia Muscle* 2021; **12**: 1393-1407 [PMID: 34523250 DOI: 10.1002/jcsm.12784]

19 **Greten FR**, Grivennikov SI. Inflammation and Cancer: Triggers, Mechanisms, and Consequences. *Immunity* 2019; **51**: 27-41 [PMID: 31315034 DOI: 10.1016/j.immuni.2019.06.025]

20 **Yang Y**, Jiang G, Zhang P, Fan J. Programmed cell death and its role in inflammation. *Mil Med Res* 2015; **2**: 12 [PMID: 26045969 DOI: 10.1186/s40779-015-0039-0]

21 **Laviano A**, Koverech A, Mari A. Cachexia: clinical features when inflammation drives malnutrition. *Proc Nutr Soc* 2015; **74**: 348-354 [PMID: 25809872 DOI: 10.1017/S0029665115000117]

22 **Arabi YM**, Reintam Blaser A, Preiser JC. Less is more in nutrition: critically ill patients are starving but not hungry. *Intensive Care Med* 2019; **45**: 1629-1631 [PMID: 31531714 DOI: 10.1007/s00134-019-05765-0]

23 **Al Bander Z**, Nitert MD, Mousa A, Naderpoor N. The Gut Microbiota and Inflammation: An Overview. *Int J Environ Res Public Health* 2020; **17** [PMID: 33086688 DOI: 10.3390/ijerph17207618]

24 **Bindels LB**, Beck R, Schakman O, Martin JC, De Backer F, Sohet FM, Dewulf EM, Pachikian BD, Neyrinck AM, Thissen JP, Verrax J, Calderon PB, Pot B, Grangette C, Cani PD, Scott KP, Delzenne NM. Restoring specific lactobacilli levels decreases inflammation and muscle atrophy markers in an acute leukemia mouse model. *PLoS One* 2012; **7**: e37971 [PMID: 22761662 DOI: 10.1371/journal.pone.0037971]

25 **Bindels LB**, Neyrinck AM, Salazar N, Taminiau B, Druart C, Muccioli GG, François E, Blecker C, Richel A, Daube G, Mahillon J, de los Reyes-Gavilán CG, Cani PD, Delzenne NM. Non Digestible Oligosaccharides Modulate the Gut Microbiota to Control the Development of Leukemia and Associated Cachexia in Mice. *PLoS One* 2015; **10**: e0131009 [PMID: 26098097 DOI: 10.1371/journal.pone.0131009]

26 **de Clercq NC**, van den Ende T, Prodan A, Hemke R, Davids M, Pedersen HK, Nielsen HB, Groen AK, de Vos WM, van Laarhoven HWM, Nieuwdorp M. Fecal Microbiota Transplantation from Overweight or Obese Donors in Cachectic Patients with Advanced Gastroesophageal Cancer: A Randomized, Double-blind, Placebo-Controlled, Phase II Study. *Clin Cancer Res* 2021; **27**: 3784-3792 [PMID: 33883174 DOI: 10.1158/1078-0432.CCR-20-4918]

27 **de Maria YNLF**, Aciole Barbosa D, Menegidio FB, Santos KBNH, Humberto AC, Alencar VC, Silva JFS, Costa de Oliveira R, Batista ML Jr, Nunes LR, Jabes DL. Analysis of mouse faecal dysbiosis, during the development of cachexia, induced by transplantation with Lewis lung carcinoma cells. *Microbiology (Reading)* 2021; **167** [PMID: 34596506 DOI: 10.1099/mic.0.001088]

28 **Mendez R**, Kesh K, Arora N, Di Martino L, McAllister F, Merchant N, Banerjee S. Microbial dysbiosis and polyamine

metabolism as predictive markers for early detection of pancreatic cancer. *Carcinogenesis* 2020; **41**: 561-570 [PMID: 31369062 DOI: 10.1093/carcin/bgz116]

29 **Ni Y**, Lohinai Z, Heshiki Y, Dome B, Moldvay J, Dulka E, Galffy G, Berta J, Weiss GJ, Sommer MOA, Panagiotou G. Distinct composition and metabolic functions of human gut microbiota are associated with cachexia in lung cancer patients. *ISME J* 2021; **15**: 3207-3220 [PMID: 34002024 DOI: 10.1038/s41396-021-00998-8]

30 **Tsvetikova SA**, Koshel EI. Microbiota and cancer: host cellular mechanisms activated by gut microbial metabolites. *Int J Med Microbiol* 2020; **310**: 151425 [PMID: 32423739 DOI: 10.1016/j.ijmm.2020.151425]

World Journal of Gastrointestinal Oncology

Submit a Manuscript: https://www.f6publishing.com

World J Gastrointest Oncol 2022 July 15; 14(7): 1227-1238

DOI: 10.4251/wjgo.v14.i7.1227

ISSN 1948-5204 (online)

MINIREVIEWS

Prospects and applications of enucleation in solid pseudopapillary neoplasms of the pancreas

Rui Wang, Jing Li, Chun-Lu Tan, Xu-Bao Liu, Yong-Hua Chen

Specialty type: Gastroenterology and hepatology

Provenance and peer review: Invited article; Externally peer reviewed.

Peer-review model: Single blind

Peer-review report's scientific quality classification

Grade A (Excellent): 0
Grade B (Very good): B, B
Grade C (Good): C
Grade D (Fair): 0
Grade E (Poor): 0

P-Reviewer: Gaspar AF, Brazil; Sun LQ, China; Wang BG, United States

Received: March 13, 2022
Peer-review started: March 13, 2022
First decision: April 17, 2022
Revised: April 30, 2022
Accepted: June 21, 2022
Article in press: June 21, 2022
Published online: July 15, 2022

Rui Wang, Chun-Lu Tan, Xu-Bao Liu, Yong-Hua Chen, Department of Pancreatic Surgery, West China Hospital of Sichuan University, Chengdu 610037, Sichuan Province, China

Jing Li, Department of Operating Room, West China Hospital, Sichuan University/West China School of Nursing, Sichuan University, Chengdu 610037, Sichuan Province, China

Corresponding author: Yong-Hua Chen, MD, PhD, Adjunct Associate Professor, Department of Pancreatic Surgery, West China Hospital of Sichuan University, No. 37 Guoxue Alley, Wuhou District, Chengdu 610037, Sichuan Province, China. chenyonghua2007@163.com

Abstract

Solid pseudopapillary neoplasms (SPNs) of the pancreas are rare, low-grade, malignant neoplasms that are mostly seen in young women in the second and third decades of life and are quite uncommon in children. Standard resection for benign and borderline neoplasms of the pancreas is associated with a substantial risk of postoperative morbidity and long-term functional impairment, whereas enucleation leads to less morbidity and preserves healthy parenchyma as well as exocrine and endocrine function. Enucleation of SPNs has been increasingly reported to be feasible and safe for preserving the normal physiological function of the pancreas, especially in teenagers and children. This review summarizes findings published in recent years on the enucleation of SPNs as well as potential future developments and directions. Enucleation has undoubtedly come to stay as an alternative surgical procedure for SPNs. However, many questions remain unresolved, and future directions toward the best surgical indication, the prevention and intervention of complications, especially pancreatic fistula, intraoperative resection margin safety assessment, and long-term oncology prognosis remain to be evaluated and should be explored in future clinical trials.

Key Words: Solid pseudopapillary neoplasm; Enucleation; Pancreatic tumor; Distal pancreatectomy; Pancreaticoduodenectomy

Core Tip: Enucleation of solid pseudopapillary neoplasms (SPNs) has been increasingly reported to be feasible and safe for preserving pancreatic function, especially in teenagers and children. This review summarizes findings published in recent years on the enucleation of SPNs as well as potential future developments and directions. Enucleation has undoubtedly come to stay as an alternative surgical procedure for SPNs. However, many questions remain unresolved, and future directions toward the best surgical indication, the prevention and intervention of complications, especially pancreatic fistula, intraoperative resection margin safety assessment, and long-term oncology prognosis remain to be evaluated.

Citation: Wang R, Li J, Tan CL, Liu XB, Chen YH. Prospects and applications of enucleation in solid pseudopapillary neoplasms of the pancreas. *World J Gastrointest Oncol* 2022; 14(7): 1227-1238
URL: https://www.wjgnet.com/1948-5204/full/v14/i7/1227.htm
DOI: https://dx.doi.org/10.4251/wjgo.v14.i7.1227

INTRODUCTION

Solid pseudopapillary neoplasms (SPNs) of the pancreas account for approximately 1%-3% of all pancreatic neoplasms[1,2]. To date, surgery remains the only curative treatment for SPN patients[3-5]. Conventional pancreatectomy, such as pancreaticoduodenectomy and distal pancreatectomy, as the mainstream surgical options, has achieved good results and prognoses.

In recent years, enucleation, as an organ-sparing surgical method, has been increasingly widely used in the treatment of some benign and low-grade malignant tumors, including SPNs[1,4,6,7]. Compared to conventional pancreatectomy, enucleation can preserve the physiological function of the pancreas to the maximum extent while treating tumors, lengthen the life of patients, and improve their quality of life[1,7].

Enucleation has undoubtedly come to stay as an alternative surgical procedure for SPNs. However, to improve and widen the application of enucleation in SPNs, some problems must be solved in the future. This review article summarizes findings published in recent years on the enucleation of SPNs as well as potential future developments and directions.

FEASIBILITY AND ADVANTAGES OF ENUCLEATION APPLICATION IN SPNS

The low-grade malignancy of SPNs has been widely accepted, and reports of SPNs have become more extensive and in depth in recent years. To date, surgical treatment of SPNs, which has a 5-year survival rate of more than 95%, is still the only treatment that can achieve curative effects[2,3,8]. All patients who are eligible for surgical treatment should be encouraged to undergo relevant management, as surgery is indicated even if R1 resection is performed[8,9]. Surgery, if possible, is also a good option for patients with local progression and metastasis at the time of diagnosis, and distant metastasis is not an absolute contraindication to surgical treatment[3,9-12]. The specific surgical method is determined by the location, size, intraoperative pathology, and surrounding tissue invasion and distant metastasis of the tumor.

Clinical manifestations associated with SPNs are often nonspecific[5]. The most common symptom is abdominal pain[13]. For instance, patients with SPNs at the head of the pancreas do not experience obstructive jaundice and pancreatitis like those with other malignant pancreatic tumors[3]. In addition, some patients have no symptoms and are first discovered accidentally by epigastric imaging[4,10]. On the one hand, the awareness of the public about health management has gradually improved, and the state and individuals are paying increasing attention to timely physical examinations. On the other hand, with the expansion and improvement of imaging techniques worldwide, there has been an increase in the incidence of SPNs, and tumors are being increasingly detected at an early stage in asymptomatic patients. The earlier the tumor is detected, the smaller the tumor is likely to be, the more opportunities there are for surgical treatment, the more surgical options that are available, and the better the outcome.

In recent decades, the concepts of minimally invasive surgery and enhanced recovery after surgery have had a great influence on the surgical treatment of relevant diseases. In addition, technological innovation and research achievements provide support for and guarantee for the development of surgical strategies toward more minimally invasive and accurate directions. In the stage of rapid development of medicine, people pursue not only survival but also quality of life. For younger patients, especially pediatric patients, it is extremely critical to be able to treat the tumor and preserve normal function to the greatest extent to improve postoperative quality of life.

In fact, conventional pancreatectomy achieves the primary goal of negative margins while extensively removing the normal pancreatic parenchyma. Extensive excision of normal pancreatic tissue at the same time as tumor excision increases the risk of postoperative endocrine and exocrine pancreatic insufficiency[6]. Falconi *et al*[14] showed that the incidences of endocrine insufficiency in pancreatic parenchymal-preserving resection, distal pancreatectomy, and pancreaticoduodenectomy were 3%, 14%, and 18%, respectively. For wide surgical resection-induced pancreatic dysfunction, the lifetime psychological and physical effects of replacement therapy are enormous and unacceptable.

Compared with conventional surgical methods, enucleation removes the tumor while preserving as much of the normal pancreatic parenchyma as possible, which is closely related to the postoperative quality of life of patients, especially young patients. Importantly, according to recent studies[1,7,15], compared with conventional surgical methods, enucleation does not increase the risk of tumor recurrence or metastasis in SPN patients. Previous studies[1,2,7], including one of our studies, have reported the safety and efficacy of enucleation as an organ preservation method in the surgical management of SPNs, and it has some advantages over conventional pancreatectomy in some cases (Figure 1). Even if the tumor is located in the head of the pancreas, enucleation is safe and can ensure adequate margins[4,7,16]. Our previous study revealed that enucleation had a shorter duration of surgery, less blood loss, lower rate of exocrine insufficiency, and comparable morbidity compared with conventional pancreatectomy[7]. Compared with conventional pancreatectomy, enucleation does not require digestive tract reconstruction, reducing surgical complexity and the risk of associated postoperative complications.

In summary, enucleation, as a safe and effective surgical procedure, should be more widely used in appropriate patients. An increasing number of studies have reported that enucleation can be achieved successfully by laparotomy, laparoscopy, or even robotic techniques (Table 1).

PRECAUTIONS OF AND RELEVANT SUGGESTIONS FOR ENUCLEATION APPLICATION IN SPNS

For pediatric patients

There are differences in some clinical characteristics between children and adults, such as sex composition, mean diameter of the tumor, and common tumor sites[17]. Cho *et al*[1] showed that compared with conventional surgery in children, enucleation is safe and effective and reported some indications for enucleation. In that study, enucleation had a similar rate of morbidity and mortality as conventional pancreatectomy, prevented tumor recurrence, and reduced the incidence of postoperative pancreatic fistula. Even in pediatric patients who must undergo conventional pancreatectomy, the spleen should be preserved to prevent potentially dangerous infections associated with splenectomy. As a special population, the monitoring and management of pediatric patients should be strengthened to reduce other complications caused by prolonged hospitalization.

For pregnant patients

A diagnosis of SPN during pregnancy is rare and poses a threat to both the mother and the fetus. Sometimes, large cystic-solid masses of the pancreas found in pregnant women should be considered SPNs[18]. A 26-year-old woman who was diagnosed with SPN at 21 wk of gestation underwent tumor enucleation for SPN at 22 wk of gestation, and a healthy female infant was delivered vaginally at 39 wk and 5 d of gestation[10]. Similarly, another woman who was 26 years old underwent enucleation for SPN at 14 wk of gestation and gave birth to a mature female baby at 38 wk[18]. Surgery during pregnancy should be performed in cooperation with the surgeon and obstetrician to remove the tumor while ensuring the safety of the mother and fetus. Generally, the second trimester is the most favorable time window for surgical intervention for SPNs because fetal organogenesis is complete and the size of the fetus is adequate, which can reduce the influence of spontaneous abortion in early pregnancy and the influence of the large size of the fetus in late pregnancy on the difficulty of the operation[10].

Sex differences

Through observations and studies, there are certain differences between male and female patients that deserve attention. Approximately 90% of SPNs occur in adolescents and young adult women[19]. The male–female ratio is approximately 1:10, and SPNs are a common diagnosis in females under 40 years old undergoing pancreatectomy[2,3,16]. In our previous study, male patients, with an average age of 43.1 years, were older than female patients, and there were more asymptomatic male patients[20].

Overall, the tumors are significantly larger in females with SPNs than in males[21], but the tumors are more aggressive and develop at a later age in men[11]. In terms of composition, the mean solid component is significantly higher in male patients than in female patients[21]. For immunohistochemical staining, the expression of β-catenin is significantly decreased in male patients, but vimentin expression is significantly increased in male patients[21]. More research is expected to explain the underlying causes of these differences.

Table 1 Summary of selected patients with solid pseudopapillary neoplasms undergoing enucleation

Ref.	No.	Age	Sex	Tumor location	Tumor size (cm)	TM	PF (Grade)	DGE	NODM	Follow-up (mo)	PR/PM	Outcome	Type
Wang *et al*[7], 2018	31	11-49	27 F; 4 M	12 head; 9 neck; 9 body-tail; 1 multiple	2.0-14.5	NA	5 B; 1 C	No	NA	46.1 (mean)	No	Alive	30 EN; 1 LEN
Wang *et al*[12], 2018	15	NA	NA	NA	NA	NA	NA	NA	NA	NA	No	NA	EN
Cho *et al*[1], 2019	15	14.6 ± 10.7	14 F; 1 M	9 head; 6 body-tail	6.1 ± 2.9	NA	2 A; 8 B + C	NA	No	746.8-198.8	1 PR	NA	EN
Xu *et al*[24], 2021	14	NA	NA	NA	NA	NA	NA	NA	NA	NA	NA	NA	LEN
Wei *et al*[21], 2022	13	NA	8 F; 5 M	NA	NA	NA	NA	NA	NA	NA	2 PR	NA	EN
Li *et al*[31], 2011	9	NA	NA	NA	NA	NA	NA	NA	NA	NA	NA	NA	EN
Yalcin *et al*[17], 2019	9	10-16.5	8 F; 1 M	5 head; 2 head-neck; 1 neck; 1 body	2.0-10.0	NA	NA	NA	NA	17-136	NA	Alive	EN
Jin *et al*[28], 2020	8	NA	NA	Head	NA	NA	NA	NA	NA	NA	NA	NA	4 REN; 4 EN
Yu *et al*[32], 2015	5	NA	NA	NA	NA	NA	NA	NA	NA	NA	NA	NA	EN
Lu *et al*[25], 2017	5	NA	NA	NA	NA	NA	NA	NA	NA	NA	NA	NA	EN
Afridi *et al*[16], 2014	4	NA	NA	3 head	NA	NA	NA	NA	NA	NA	NA	NA	4 EN
Machado *et al*[11], 2008	3	NA	NA	NA	NA	NA	NA	NA	NA	NA	NA	NA	EN
Nakagohri *et al*[33], 2008	2	NA	NA	2 body-tail	NA	NA	NA	NA	NA	NA	NA	NA	EN
Butte *et al*[34], 2011	2	NA	NA	NA	NA	NA	NA	NA	NA	NA	NA	NA	EN
Sugito *et al*[35], 2012	2	11-15	2 F	1 head; 1 tail	NA	NA	No	No	No	36-144	NA	Alive	EN
Eric *et al*[2], 2021	1	32	F	Body-tail	2.0	NL	No	No	No	12	No	Alive	LEN
Salvia *et al*[36], 2007	1	NA	NA	Head	NA	NA	NA	NA	NA	NA	NA	NA	EN
Matos *et al*[37], 2009	1	16	NA	Body	2.5	NA	No	No	No	13	NA	Alive	LEN
Morikawa *et al*[38], 2013	1	NA	NA	NA	NA	NA	NA	NA	NA	NA	NA	NA	EN
Takamatsu *et al*[39], 2013	1	13	F	Tail	5.0	NA	1 A	NA	NA	24	No	Alive	LEN
Juric *et al*[40], 2014	1	16	F	1 head + 1 tail	Head 10.0; Tail 7.0	NL	No	No	No	24	No	Alive	EN
Karakas *et al*[41], 2015	1	18	F	Head	6.0	NL	No	No	No	3	No	Alive	EN
Namur *et al*[4], 2016	1	18	F	Head	4.5	NA	1 A	NA	NA	38	No	NA	EN

Stewart *et al*[42], 2016	1	NA	NA	NA	NA	NA	NA	NA	NA	NA	No	NA	EN
Esposito *et al*[43], 2017	1	5	M	Tail	NA	NA	No	No	No	NA	NA	NA	LEN
Tanaka *et al*[29], 2017	1	10	F	Head	3.0	NL	No	No	No	24	No	Alive	EN
Senthilnathan *et al*[27], 2017	1	NA	NA	Head	NA	NA	NA	NA	NA	NA	NA	NA	LEN
Scandavini *et al*[44], 2018	1	12	F	NA	NA	NA	No	No	No	159	NA	Alive	EN
Huang *et al*[10], 2018	1	26	F	Tail	13.0	NL	No	No	No	6	No	Alive	EN
Farhat *et al*[13], 2020	1	19	F	Tail	2.0	NA	Yes	No	No	209	No	Alive	EN
Feng *et al*[18], 2011	1	26	F	Head	9.5	NL	Yes	No	No	NA	NA	NA	EN

PF: Pancreatic fistula; DGE: Delayed gastric emptying; NODM: New-onset diabetes mellitus; PR: Postoperative recurrence; PM: Postoperative metastasis; F: Female; M: Male; NL: Normal level; EN: Enucleation; LEN: Laparoscopic enucleation; REN: Robotic enucleation; NA: Not available; Yes: Happened; No: No event.

Imaging examination is widely used in the diagnosis and differential diagnosis of various diseases. In a study of SPNs, the accuracies of imaging diagnoses for SPNs in male and female patients were 54.0% and 70.5%, respectively[21]. However, in imaging diagnoses, SPNs in male patients were more likely to be misdiagnosed as malignant tumors than those in female patients, with misdiagnosis rates of 37.7% and 10.7%, respectively[21]. These results suggest that when imaging alone is insufficient to determine a diagnosis or differential diagnosis, other examinations, such as preoperative pathological examination, may be necessary to supplement the deficiency in imaging and improve the overall diagnostic accuracy for SPNs.

Furthermore, older age is an independent risk factor for recurrence[21] and is significantly associated with tumor recurrence[22]. In addition, as there are no significant differences in margin status, peripheral tissue invasion, postoperative complications, disease-free survival, or overall survival between male and female patients, the prognosis of SPNs has been reported to be similar between male and female patients[21]. Therefore, for elderly male and female patients with SPNs, surgery should be more radical, and postoperative follow-up should be more frequent[11].

Histopathological features

A definite pathological diagnosis can guarantee the application of enucleation in SPN. Endoscopic ultrasound-guided fine-needle aspiration (EUS-FNA) can achieve pathological tissue acquisition, and SPNs can be diagnosed preoperatively and differentiated from other diseases. Lubezky *et al*[3] reported that the sensitivity and specificity of EUS-FNA were 90.9% and 100%, respectively. In addition, intraoperative frozen sections are important for determining the presence of an involved margin. If intraoperative frozen sectioning reveals invasive features (such as adenocarcinoma or carcinoma), conventional surgery should be performed[7].

In fact, there is still no consensus on the malignant characteristics of SPNs[1,8]. In 2010, the World Health Organization (WHO) classified SPNs as a low-grade malignant neoplasm. Prior to this, the

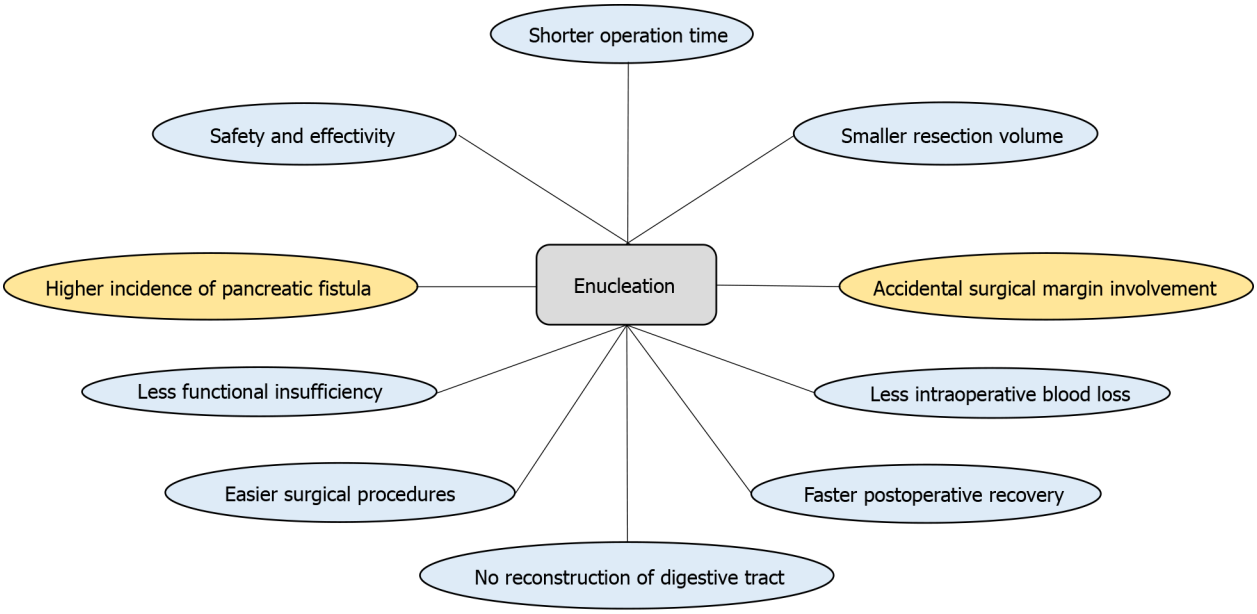

DOI: 10.4251/wjgo.v14.i7.1227

Figure 1 Advantages (blue) and disadvantages (yellow) of enucleation compared with conventional pancreatectomy in solid pseudopapillary neoplasms.

malignant components of solid pseudopapillary carcinoma (SPC) of the pancreas were defined by the WHO as vascular invasion, perineural invasion, or deep invasion into the surrounding pancreatic parenchyma. Importantly, recurrence and metastasis of SPNs may occur even in the absence of microscopic features similar to SPC of the pancreas, and these features may not cause malignant behavior[1,8]. For example, in a study, 98 of 351 patients with SPNs presented with malignant features, but recurrence occurred in 9 of the 317 patients who underwent surgery for SPNs and had a follow-up of more than 6 mo[8]. Among these nine patients who relapsed after surgery, eight had R0 resection and six did not meet the WHO definition of SPC[8].

In summary, there is no consensus on the malignant characteristics of SPNs of the pancreas, and the malignant components of SPC of the pancreas may not be absolute contraindications for enucleation with negative surgical margin. However, it should be noted that during enucleation of SPNs with peripheral tissue invasion, more peritumor pancreatic tissue should be resected than that resected during enucleation of SPNs without peripheral tissue invasion.

Relationship between the tumor and surrounding tissue

SPNs can occur anywhere in the pancreas[2], even outside the pancreas[23], and they can be solid, solid-cystic, or cystic in composition. For enucleation, it is important to carefully evaluate the tumor size, location, depth of implantation into the pancreas, and distance between the pancreatic duct and tumor margin because it may be difficult to distinguish between the tumor and normal tissue and the relationship between the surrounding organs during surgery. While laparoscopic resection of tumors deeply embedded in the pancreas is technically feasible and safe compared to that of superficial tumors, it is more challenging[24]. Accidental damage to important surrounding structures may result in serious complications. If the main pancreatic duct (MPD) is damaged during enucleation, there is an increased risk of forced conversion of enucleation to conventional pancreatectomy, postoperative pancreatic leakage, and iatrogenic pancreatic duct stenosis.

Postoperative pancreatic fistula

Enucleation has been reported to be associated with a higher risk of postoperative pancreatic leakage, and pancreatic leakage is more serious than conventional pancreatectomy, especially in patients with tumors larger than 3 cm and tumors close to the MPD[1,7,14,25]. Cho *et al*[1] reported that the most common postoperative complication in pediatric patients was postoperative pancreatic fistula (POPF). Although the overall incidence of pancreatic leakage was similar in the enucleation and conventional pancreatectomy groups, mild grade A symptoms mainly occurred in the conventional pancreatectomy group, and the incidence of grades B and C symptoms was more common in the enucleation group, which consequently prolonged the duration of maintaining drainage with POPF in the enucleation group[1]. Patients with tumors at the head and neck of the pancreas had a higher incidence of complications than those with tumors at other sites after enucleation for pancreatic benign tumors[6]. However, it should be noted that postoperative pancreatic fistula was not associated with further progression to

pancreatic insufficiency after pancreatectomy[14]. Because of the higher incidence of pancreatic fistula as a short-term complication after enucleation, it is not advised to choose a conventional surgical approach imprudently that will increase the risk of postoperative pancreatic dysfunction.

Although the results of current conservative treatments for pancreatic leakage are good, more methods for reducing postoperative pancreatic leakage are expected.

Pancreatic excision and onset of diabetes mellitus

Kwon *et al*[26] found that the pancreatic resection volume (in milliliters) and resected volume ratio (in percentage) were associated with the onset of diabetes mellitus after distal pancreatectomy, especially in patients with a high pancreatic resected volume ratio (> 35.6%) in distal pancreatectomy. It is suggested to preserve as much normal pancreatic tissue as possible under the condition of ensuring a positive margin to reduce the risk of postoperative dysfunction. For patients diagnosed with severe impairment of pancreatic function before surgery, conventional pancreatectomy, which enables negative margins to be achieved more easily, should be considered.

Different types of enucleation

Enucleation has been gradually completed *via* laparotomy, laparoscopy, and robotic approaches, each of which has certain characteristics. For example, open enucleation is more suitable for tumors that are deep or posterior lesions and located to the right of the superior mesenteric vein[6]. Laparoscopic tumor enucleation is also feasible for the treatment of some SPN patients and has certain advantages[2,27]. Laparoscopic enucleation has a clear and magnifying optical field, which can make the resection more detailed and may be beneficial to the protection of the MPD[24]. Compared with open surgery, the robotic approach provides an alternative for SPNs in the head of the pancreas without increasing the incidence of clinically relevant pancreatic fistula or other major complications, and patients can obtain a favorable prognosis[28]. There are few reports on surgical procedures for enucleation in patients with SPNs, and some surgical details can be seen in these articles[6,24,28,29], including our previous one[7].

Surgical key points of enucleation

The main procedures for enucleation are summarized in Figure 2, and some keys to enucleation are described below. Some preoperative and intraoperative auxiliary examinations are closely related to the correct diagnosis and evaluation of the relationship between the tumor and the surrounding tissues, such as the MPD, common bile duct (CBD), and mesenteric vessels. Although the measurement is less precise, in patients with postoperative complications, computed tomography can be used to detect tumors close to the MPD, and a distance between the tumor and the MPD of less than 2-3 mm is a risk factor for postoperative pancreatic leakage[15]. Intraoperative ultrasound can be further used to evaluate the tumor and provide guidance for surgical resection. Importantly, multiple lesions may occur in patients with SPNs[7].

Correctly exposing the location of the tumor is critical for surgery because it can appear anywhere in the pancreas. In the process of enucleation, the tumor can be taped to expose the boundary between the tumor and normal tissue more clearly, which is conducive to the complete enucleation of the tumor and the preservation of normal pancreatic parenchyma[7]. Similarly, traction sutures are beneficial for enucleation of solid pancreatic tumors[6]. In the dissection of tumors from the surrounding normal pancreatic parenchyma, the use of monopolar cautery is more efficient than the use of an ultrasonic scalpel for fine dissection[6]. Parenchymal sutures and a tissue sealant can be used in patients whose hemostasis and pancreatostasis cannot be satisfactorily managed with bipolar cautery and ultrasound scalpel[7].

Pancreatic duct stents can be used in patients with a small distance between the tumor and the pancreatic duct to facilitate intraoperative identification of the location of the pancreatic duct and reduce the risk of accidental intraoperative injury to the pancreatic duct. If the mass is near the confluence region, a Foley catheter can be inserted into the CBD to avoid accidental injury during surgery[25]. The possibility of damaging the MPD can be reduced by preoperative endoscopic implantation of pancreatic duct stents as intraoperative guidance[6].

The integrity of the MPD and CBD can be confirmed by intraoperative cholangiopancreatography with methylene blue[25]. For patients with proven MPD or CBD damage, polyprolene sutures can be used to repair or rebuild the tube[25]. The Roux-Y loop can be used to treat patients with suspected MPD injury or a wide wounded area (diameter > 3 cm) of the pancreatic parenchyma[7]. For patients with severe MPD damage, a fine silicon tube can be inserted into the MPD as a stent, and the other side of the silicon tube can be inserted through the papilla into the duodenal cavity, which is fixed with soluble sutures[23].

Drainage tubes and some measures to the enucleated sites are applied to reduce postoperative complications, unnecessary invasive procedures, and even reoperation. Some surgeons who apply fibrin glue and absorbable fibrin sealant patches to the enucleated sites in most patients[6]. In a case report of SPN, a drainage stent was placed in the MPD of the patient before surgery, and the surgeon used only interrupted sutures to close the pancreatic parenchymal defect after enucleation[29]. Even without the use of drainage tubes, the patient was discharged 2 wk after surgery without postoperative complic-

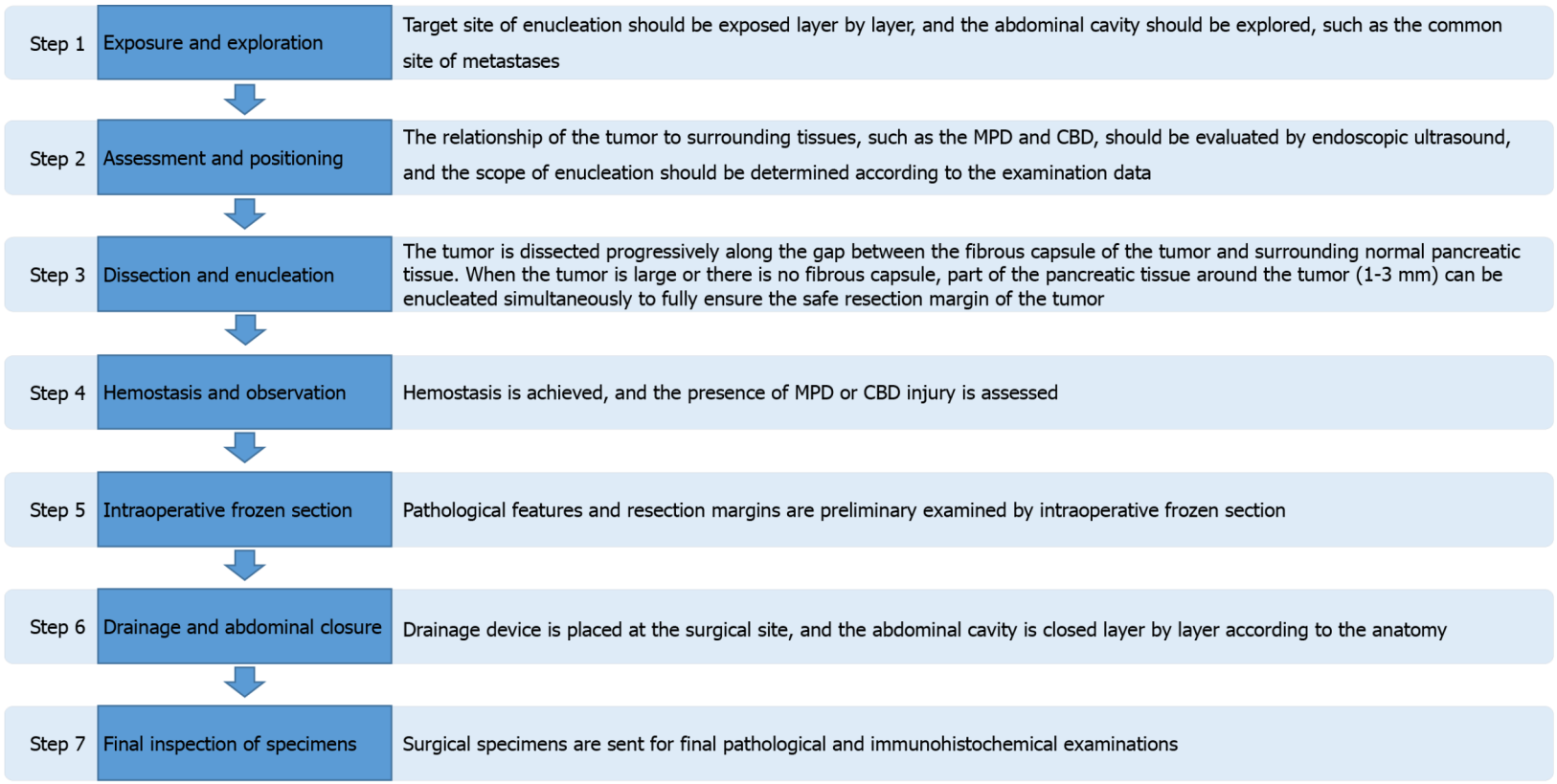

DOI: 10.4251/wjgo.v14.i7.1227

Figure 2 Main procedures of pancreatic enucleation. MPD: Main pancreatic duct; CBD: Common bile duct.

ations[29]. In the future, more research findings and inventions are expected to reduce the incidence of pancreatic leakage after enucleation.

For benign pancreatic tumors

For benign pancreatic tumors, Falconi *et al*[14] revealed that atypical resection has an acceptable risk of postoperative complications and significantly reduces the risk of long-term complications. Lu *et al*[25] reported that enucleation is recommended for benign or low-grade tumors of the proximal pancreas, and large tumors and proximity to the MPD are not absolute contraindications, although the postoperative fistula rate would be high. Laparoscopic enucleation is safe and effective for benign and low-grade malignancies and is associated with favorable perioperative outcomes[6]. Although these findings relate to benign or low-grade pancreatic tumors, they may also apply to SPNs, which are a

member of the group.

UNANSWERED QUESTIONS REGARDING ENUCLEATION IN SPNS AND FUTURE PROSPECTS

What are the best surgical indications?

According to the above findings, it can be concluded that the lower the degree of malignancy of the tumor, the farther the distance from the MPD to the tumor margin, and the smaller the volume of the removed pancreatic tissue, the more suitable enucleation is. However, the specific critical value still lacks relevant data, so there is no unified view. Higher-level evidence is needed to further explore the following questions: How do the location and size of the tumor affect the indications for enucleation due to anatomic factors? What is the effect of tumor components on indications, and are solid or cystic component tumors more suitable for enucleation? Can surgical indications for enucleation be relaxed for people seeking a higher quality of life, and what are the indications for this group?

How can complications, especially pancreatic fistula, be prevented and intervened?

Common postoperative complications, such as pancreatic leakage and emerging diabetes, are related to the exocrine and endocrine functions of the pancreas. The problems related to pancreatic leakage have been presented in the section about postoperative pancreatic fistula and surgical procedures of enucleation mentioned in this paper. New-onset diabetes mellitus (NODM) should be monitored for a long time to prevent multisystem harm caused by the loss of glucose homeostasis. Due to the uneven distribution of islets in the pancreas, the resection volume of patients with NODM caused by resection at different sites needs to be further studied to guide the control and prediction of postoperative NODM.

How can the surgical margin be guaranteed?

Enucleation is expected to preserve normal pancreatic function and improve postoperative quality of life by preserving normal pancreatic tissue to a large extent. However, several cases of positive surgical margins in SPN patients undergoing enucleation have been reported[1,17]. To treat tumors while preserving organ function, we need to pay attention to the following points: First, further research and investigation are needed to determine the appropriate distance from the tumor to the surgical margin. Second, tumor characteristics, such as the composition, size, and shape of the tumor as well as its relationship with surrounding blood vessels, should be carefully evaluated by intraoperative ultrasound and other equipment, and then the resection scope can be determined. Finally, the determination of negative margins by intraoperative frozen section is of great significance to the prognosis of patients. We recommend multipoint biopsies on the tissue margins of the three-dimensional structure of the tumor to confirm the status of the margins, especially the dorsal side of the tumor in the visual blind area during surgery.

What is the prognosis of long-term oncology?

Although the majority of patients have a good prognosis, approximately 15% of patients present with malignant signs of peripheral organ invasion and metastatic disease[14]. The absence of malignant histological appearance cannot completely exclude the risk of postoperative metastasis and recurrence, so regular oncological follow-up and long-term surveillance are important for the early detection and further treatment of metastasis and recurrence.

In a small number of patients, distant metastasis can occur in the peritoneum, perirenal lymph nodes, colon, small intestine, and other sites[30]. Usually, the most common site of postoperative metastasis is the liver[2]. When a suspicious liver mass is detected during postoperative follow-up, it should be differentiated from primary hepatocellular carcinoma and nonpancreatic metastatic tumors. Percutaneous liver biopsy with immunohistochemistry can be used to confirm the diagnosis. Even if liver metastases occur, patients with SPNs can achieve long-term survival with timely surgical treatment.

To date, there are still no good tumor markers of suggesting the occurrence, development, recurrence, and metastasis of SPNs. Laboratory tests, including tumor markers, are nonspecific[3,4]. With regard to current imaging techniques and the development of tumor markers associated with SPNs, imaging is of higher value during follow-up. It is expected that more studies will be conducted to find relevant markers that can detect abnormalities early and provide help for the early diagnosis and treatment of this tumor. In addition, surgery-related complications, such as pancreatectomy-related diabetes mellitus, need to be monitored because most patients have no obvious symptoms early on.

CONCLUSION

Enucleation has undoubtedly come to stay as an alternative surgical procedure for SPNs. However, many questions remain unresolved, and future directions toward the best surgical indication, the prevention and intervention of complications, especially pancreatic fistula, intraoperative resection margin safety assessment, and long-term oncology prognosis remain to be evaluated and should be explored in future clinical trials.

FOOTNOTES

Author contributions: Wang R and Li J contributed equally to this work; Chen YH and Liu XB conceptualized and designed the manuscript; Wang R, Li J, and Tan CL drafted the manuscript; all authors revised the manuscript for important intellectual content; Liu XB and Chen YH supervised the work of the manuscript; Liu XB obtained research funding; all authors have read and approved the final manuscript.

Supported by the Key Research and Development Projects in Sichuan Province, No. 2019YFS0043; and the 1·3·5 Project for Disciplines of Excellence, West China Hospital, Sichuan University, No. ZY2017302-1.3.5.

Conflict-of-interest statement: The authors have no conflicts of interest to declare. No benefits in any form were received or will be received from a commercial party related directly or indirectly to the subject of this article.

Country/Territory of origin: China

ORCID number: Rui Wang 0000-0003-0829-152X; Yong-Hua Chen 0000-0001-8485-0755.

S-Editor: Yan JP
L-Editor: Wang TQ
P-Editor: Yan JP

REFERENCES

1 **Cho YJ**, Namgoong JM, Kim DY, Kim SC, Kwon HH. Suggested Indications for Enucleation of Solid Pseudopapillary Neoplasms in Pediatric Patients. *Front Pediatr* 2019; **7**: 125 [PMID: 31001506 DOI: 10.3389/fped.2019.00125]
2 **Eric D**, Milosavljevic V, Gonzalez-Urquijo M, Tadic B, Veselinovic M, Grubor N, Jelic D, Bjelovic M. Laparoscopic enucleation of Frantz's tumor of the pancreas: Case report and literature review. *Ann Med Surg (Lond)* 2021; **64**: 102221 [PMID: 33796288 DOI: 10.1016/j.amsu.2021.102221]
3 **Lubezky N**, Papoulas M, Lessing Y, Gitstein G, Brazowski E, Nachmany I, Lahat G, Goykhman Y, Ben-Yehuda A, Nakache R, Klausner JM. Solid pseudopapillary neoplasm of the pancreas: Management and long-term outcome. *Eur J Surg Oncol* 2017; **43**: 1056-1060 [PMID: 28238521 DOI: 10.1016/j.ejso.2017.02.001]
4 **Namur GN**, Ribeiro TC, Souto MM, Figueira ER, Bacchella T, Jureidini R. MINIMALLY INVASIVE SURGERY FOR PSEUDOPAPILLARY NEOPLASM OF THE PANCREAS. *Arq Bras Cir Dig* 2016; **29**: 97-101 [PMID: 27438035 DOI: 10.1590/0102-6720201600020008]
5 **Silano F**, de Melo Amaral RB, Santana RC, Neves VC, Ardengh JC, do Amaral PCG. Yield of surgery in solid pseudopapillary neoplasms of the pancreas: A case series and literature review. *World J Gastrointest Oncol* 2021; **13**: 589-599 [PMID: 34163575 DOI: 10.4251/wjgo.v13.i6.589]
6 **Song KB**, Kim SC, Hwang DW, Lee JH, Lee DJ, Lee JW, Jun ES, Sin SH, Kim HE, Park KM, Lee YJ. Enucleation for benign or low-grade malignant lesions of the pancreas: Single-center experience with 65 consecutive patients. *Surgery* 2015; **158**: 1203-1210 [PMID: 25633730 DOI: 10.1016/j.surg.2014.10.008]
7 **Wang X**, Chen YH, Tan CL, Zhang H, Xiong JJ, Chen HY, Ke NW, Liu XB. Enucleation of pancreatic solid pseudopapillary neoplasm: Short-term and long-term outcomes from a 7-year large single-center experience. *Eur J Surg Oncol* 2018; **44**: 644-650 [PMID: 29525465 DOI: 10.1016/j.ejso.2018.01.085]
8 **Kang CM**, Choi SH, Kim SC, Lee WJ, Choi DW, Kim SW; Korean Pancreatic Surgery Club. Predicting recurrence of pancreatic solid pseudopapillary tumors after surgical resection: a multicenter analysis in Korea. *Ann Surg* 2014; **260**: 348-355 [PMID: 24743622 DOI: 10.1097/SLA.0000000000000583]
9 **Hosokawa I**, Shimizu H, Ohtsuka M, Kato A, Yoshitomi H, Furukawa K, Takayashiki T, Ishihara T, Yokosuka O, Miyazaki M. Preoperative diagnosis and surgical management for solid pseudopapillary neoplasm of the pancreas. *J Hepatobiliary Pancreat Sci* 2014; **21**: 573-578 [PMID: 24535774 DOI: 10.1002/jhbp.96]
10 **Huang TT**, Zhu J, Zhou H, Zhao AM. Solid pseudopapillary neoplasm of pancreas in pregnancy treated with tumor

enucleation: Case report and review of the literature. *Niger J Clin Pract* 2018; **21**: 1234-1237 [PMID: 30156213 DOI: 10.4103/njcp.njcp_39_18]

11 **Machado MC**, Machado MA, Bacchella T, Jukemura J, Almeida JL, Cunha JE. Solid pseudopapillary neoplasm of the pancreas: distinct patterns of onset, diagnosis, and prognosis for male versus female patients. *Surgery* 2008; **143**: 29-34 [PMID: 18154930 DOI: 10.1016/j.surg.2007.07.030]

12 **Wang P**, Wei J, Wu J, Xu W, Chen Q, Gao W, Jiang K, Miao Y. Diagnosis and treatment of solid-pseudopapillary tumors of the pancreas: A single institution experience with 97 cases. *Pancreatology* 2018; **18**: 415-419 [PMID: 29548800 DOI: 10.1016/j.pan.2017.12.012]

13 **Farhat W**, Ammar H, Amine Said M, Mizouni A, Bouazzi A, Abdessaied N, Ben Mabrouk M, Ben Ali A. Solid pseudopapillary neoplasm of the pancreas: a report of 10 cases and literature review. *ANZ J Surg* 2020; **90**: 1683-1688 [PMID: 31989788 DOI: 10.1111/ans.15701]

14 **Falconi M**, Mantovani W, Crippa S, Mascetta G, Salvia R, Pederzoli P. Pancreatic insufficiency after different resections for benign tumours. *Br J Surg* 2008; **95**: 85-91 [PMID: 18041022 DOI: 10.1002/bjs.5652]

15 **Brient C**, Regenet N, Sulpice L, Brunaud L, Mucci-Hennekine S, Carrère N, Milin J, Ayav A, Pradere B, Hamy A, Bresler L, Meunier B, Mirallié E. Risk factors for postoperative pancreatic fistulization subsequent to enucleation. *J Gastrointest Surg* 2012; **16**: 1883-1887 [PMID: 22872510 DOI: 10.1007/s11605-012-1971-x]

16 **Afridi SA**, Kazaryan AM, Marangos IP, Røsok BI, Fretland ÅA, Yaqub S, Edwin B. Laparoscopic surgery for solid pseudopapillary tumor of the pancreas. *JSLS* 2014; **18**: 236-242 [PMID: 24960486 DOI: 10.4293/108680813X13753907291837]

17 **Yalçın B**, Yağcı-Küpeli B, Ekinci S, Orhan D, Oğuz B, Varan A, Kutluk T, Akyüz C. Solid pseudopapillary neoplasm of the pancreas in children: Hacettepe experience. *ANZ J Surg* 2019; **89**: E236-E240 [PMID: 31033126 DOI: 10.1111/ans.15111]

18 **Feng JF**, Chen W, Guo Y, Liu J. Solid pseudopapillary tumor of the pancreas in a pregnant woman. *Acta Gastroenterol Belg* 2011; **74**: 560-563 [PMID: 22319967]

19 **Maffuz A**, Bustamante Fde T, Silva JA, Torres-Vargas S. Preoperative gemcitabine for unresectable, solid pseudopapillary tumour of the pancreas. *Lancet Oncol* 2005; **6**: 185-186 [PMID: 15737835 DOI: 10.1016/S1470-2045(05)01770-5]

20 **Cai YQ**, Xie SM, Ran X, Wang X, Mai G, Liu XB. Solid pseudopapillary tumor of the pancreas in male patients: report of 16 cases. *World J Gastroenterol* 2014; **20**: 6939-6945 [PMID: 24944486 DOI: 10.3748/wjg.v20.i22.6939]

21 **Wei G**, Luo Q, Fang J, Li X, Shi Y, Li Y, Sun L. The Sex Features of Patients With Solid Pseudopapillary Neoplasms of the Pancreas: A Retrospective Study. *Front Oncol* 2022; **12**: 844182 [PMID: 35252013 DOI: 10.3389/fonc.2022.844182]

22 **Karsenti D**, Caillol F, Chaput U, Perrot B, Koch S, Vuitton L, Jacques J, Valats JC, Poincloux L, Subtil C, Chabrun E, Williet N, Vanbiervliet G, Belkhodja H, Charachon A, Wangermez M, Coron E, Cholet F, Privat J, Le Baleur Y, Bichard P, Ah Soune P, Lecleire S, Palazzo M; from the GRAPHE. Safety of Endoscopic Ultrasound-Guided Fine-Needle Aspiration for Pancreatic Solid Pseudopapillary Neoplasm Before Surgical Resection: A European Multicenter Registry-Based Study on 149 Patients. *Pancreas* 2020; **49**: 34-38 [PMID: 31856077 DOI: 10.1097/MPA.0000000000001460]

23 **Wu H**, Huang YF, Liu XH, Xu MH. Extrapancreatic solid pseudopapillary neoplasm followed by multiple metastases: Case report. *World J Gastrointest Oncol* 2017; **9**: 497-501 [PMID: 29290920 DOI: 10.4251/wjgo.v9.i12.497]

24 **Xu J**, Li F, Zhan H, Liu H, Wu D, Hu S, Wang L. Laparoscopic enucleation of pancreatic tumours: a single-institution experience of 66 cases. *ANZ J Surg* 2021; **91**: 106-110 [PMID: 33205607 DOI: 10.1111/ans.16450]

25 **Lu WJ**, Cai HL, Ye MD, Wu YL, Xu B. Enucleation of non-invasive tumors in the proximal pancreas: indications and outcomes compared with standard resections. *J Zhejiang Univ Sci B* 2017; **18**: 906-916 [PMID: 28990381 DOI: 10.1631/jzus.B1600597]

26 **Kwon JH**, Kim SC, Shim IK, Song KB, Lee JH, Hwang DW, Park KM, Lee YJ. Factors Affecting the Development of Diabetes Mellitus After Pancreatic Resection. *Pancreas* 2015; **44**: 1296-1303 [PMID: 26390413 DOI: 10.1097/MPA.0000000000000404]

27 **Senthilnathan P**, Dhaker KC, Kaje V, Naidu SB, Sarvani M, Sabnis SC, Srivatsan Gurumurthy S, Nalakilli VP, Anand Vijay N, Rajapandian S, Praveen Raj P, Parthasarathi R, Palanivelu C. Laparoscopic management of solid pseudo papillary neoplasm of pancreas in tertiary care center from south India. *Pancreatology* 2017; **17**: 927-930 [PMID: 29054814 DOI: 10.1016/j.pan.2017.09.003]

28 **Jin JB**, Qin K, Yang Y, Shi YS, Wu ZC, Deng XX, Chen H, Cheng DF, Shen BY, Peng CH. Robotic pancreatectomy for solid pseudopapillary tumors in the pancreatic head: A propensity score-matched comparison and analysis from a single center. *Asian J Surg* 2020; **43**: 354-361 [PMID: 31327550 DOI: 10.1016/j.asjsur.2019.05.016]

29 **Tanaka K**, Misawa T, Haruki K, Saito R, Gocho T, Akiba T. Enucleation of solid pseudopapillary tumor with a preoperative nasopancreatic drainage stent in a child. *Asian J Endosc Surg* 2017; **10**: 438-441 [PMID: 28635016 DOI: 10.1111/ases.12397]

30 **Agaimy A**, Haller F. CTNNB1 (β-Catenin)-altered Neoplasia: A Review Focusing on Soft Tissue Neoplasms and Parenchymal Lesions of Uncertain Histogenesis. *Adv Anat Pathol* 2016; **23**: 1-12 [PMID: 26645457 DOI: 10.1097/PAP.0000000000000104]

31 **Li Z**, Zhang Z, Liu X, Hu W, Mai G, Zhang Y, Lu H, Zeng Y, Tian B. Solid pseudopapillary tumor of the pancreas: the surgical procedures. *Surg Today* 2011; **41**: 91-96 [PMID: 21191697 DOI: 10.1007/s00595-009-4225-0]

32 **Yu P**, Cheng X, Du Y, Yang L, Xu Z, Yin W, Zhong Z, Wang X, Xu H, Hu C. Solid Pseudopapillary Neoplasms of the Pancreas: a 19-Year Multicenter Experience in China. *J Gastrointest Surg* 2015; **19**: 1433-1440 [PMID: 26001371 DOI: 10.1007/s11605-015-2862-8]

33 **Nakagohri T**, Kinoshita T, Konishi M, Takahashi S, Gotohda N. Surgical outcome of solid pseudopapillary tumor of the pancreas. *J Hepatobiliary Pancreat Surg* 2008; **15**: 318-321 [PMID: 18535771 DOI: 10.1007/s00534-007-1264-z]

34 **Butte JM**, Brennan MF, Gönen M, Tang LH, D'Angelica MI, Fong Y, Dematteo RP, Jarnagin WR, Allen PJ. Solid pseudopapillary tumors of the pancreas. Clinical features, surgical outcomes, and long-term survival in 45 consecutive patients from a single center. *J Gastrointest Surg* 2011; **15**: 350-357 [PMID: 20824369 DOI: 10.1007/s11605-010-1337-1]

35 **Sugito K**, Furuya T, Kaneda H, Masuko T, Ohashi K, Inoue M, Ikeda T, Koshinaga T, Tomita R, Maebayashi T. Long-

term follow-up of nutritional status, pancreatic function, and morphological changes of the pancreatic remnant after pancreatic tumor resection in children. *Pancreas* 2012; **41**: 554-559 [PMID: 22158069 DOI: 10.1097/MPA.0b013e318232a6e2]

36 **Salvia R**, Bassi C, Festa L, Falconi M, Crippa S, Butturini G, Brighenti A, Capelli P, Pederzoli P. Clinical and biological behavior of pancreatic solid pseudopapillary tumors: report on 31 consecutive patients. *J Surg Oncol* 2007; **95**: 304-310 [PMID: 17326131 DOI: 10.1002/jso.20685]

37 **Matos JM**, Grützmann R, Agaram NP, Saeger HD, Kumar HR, Lillemoe KD, Schmidt CM. Solid pseudopapillary neoplasms of the pancreas: a multi-institutional study of 21 patients. *J Surg Res* 2009; **157**: e137-e142 [PMID: 19818965 DOI: 10.1016/j.jss.2009.03.091]

38 **Morikawa T**, Onogawa T, Maeda S, Takadate T, Shirasaki K, Yoshida H, Ishida K, Motoi F, Naitoh T, Rikiyama T, Katayose Y, Egawa S, Unno M. Solid pseudopapillary neoplasms of the pancreas: an 18-year experience at a single Japanese Institution. *Surg Today* 2013; **43**: 26-32 [PMID: 23114787 DOI: 10.1007/s00595-012-0345-z]

39 **Takamatsu S**, Nagano H, Ohtsukasa S, Kawachi Y, Maruyama H. A case of spontaneous ruptured solid pseudopapillary tumor of pancreas resected by laparoscopic surgery. *Case Rep Med* 2013; **2013**: 953240 [PMID: 23737801 DOI: 10.1155/2013/953240]

40 **Jurić I**, Pogorelić Z, Stepan JG, Kuzmić IP. Extremely rare presentation of Frantz's tumour: synchronous localisation in the pancreatic head and tail. *Scott Med J* 2014; **59**: e8-e12 [PMID: 25035290 DOI: 10.1177/0036933014543222]

41 **Karakas S**, Dirican A, Soyer V, Koç S, Ersan V, Ates M. A pancreatic pseudopapillary tumor enucleated curatively. *Int J Surg Case Rep* 2015; **10**: 118-120 [PMID: 25828476 DOI: 10.1016/j.ijscr.2015.03.040]

42 **Stewart CL**, Meguid C, Chapman B, Schulick R, Edil BH. Evolving Trends Towards Minimally Invasive Surgery for Solid-Pseudopapillary Neoplasms. *Ann Surg Oncol* 2016; **23**: 4165-4168 [PMID: 27510845 DOI: 10.1245/s10434-016-5491-x]

43 **Esposito C**, De Lagausie P, Escolino M, Saxena A, Holcomb GW 3rd, Settimi A, Becmeur F, van der Zee D. Laparoscopic Resection of Pancreatic Tumors in Children: Results of a Multicentric Survey. *J Laparoendosc Adv Surg Tech A* 2017; **27**: 533-538 [PMID: 28225638 DOI: 10.1089/lap.2016.0630]

44 **Scandavini C**, Valente R, Rangelova E, Segersvärd R, Arnelo U, Permert J, Svensson PJ, Stenman J, Del Chiaro M. Pancreatectomies for pancreatic neoplasms in pediatric and adolescent age: A single institution experience. *Pancreatology* 2018; **18**: 204-207 [PMID: 29277262 DOI: 10.1016/j.pan.2017.12.009]

World Journal of Gastrointestinal Oncology

Submit a Manuscript: https://www.f6publishing.com

World J Gastrointest Oncol 2022 July 15; 14(7): 1239-1251

DOI: 10.4251/wjgo.v14.i7.1239

ISSN 1948-5204 (online)

ORIGINAL ARTICLE

Basic Study

KIFC3 promotes proliferation, migration and invasion of esophageal squamous cell carcinoma cells by activating EMT and β-catenin signaling

Wei-Wei Hao, Feng Xu

Specialty type: Oncology

Provenance and peer review: Unsolicited article; Externally peer reviewed.

Peer-review model: Single blind

Peer-review report's scientific quality classification

Grade A (Excellent): 0
Grade B (Very good): B, B
Grade C (Good): 0
Grade D (Fair): 0
Grade E (Poor): 0

P-Reviewer: Exbrayat JM, France; Oguma J, Japan

Received: November 18, 2021
Peer-review started: November 18, 2021
First decision: January 12, 2022
Revised: January 26, 2022
Accepted: March 26, 2022
Article in press: March 26, 2022
Published online: July 15, 2022

Wei-Wei Hao, Feng Xu, Department of Gastroenterology, The First Affiliated Hospital of Zhengzhou University, Zhengzhou 450052, Henan Province, China

Corresponding author: Feng Xu, MD, Chief Doctor, Professor, Department of Gastroenterology, The First Affiliated Hospital of Zhengzhou University, No. 1 Jianshe East Road, Zhengzhou 450052, Henan Province, China. xufengmd@sina.com

Abstract

BACKGROUND

Esophageal squamous cell carcinoma (ESCC) is one of the most common malignancies. A total of 45 kinesin superfamily proteins (KIFs) have been identified in humans, among which several family members have demonstrated varied functions in tumor pathobiology *via* different mechanisms, including regulation of cell cycle progression and metastasis. KIFC3 has microtubule motor activity and is involved in cancer cell invasion and migration, as well as survival. However, the role of KIFC3 in ESCC is still unknown.

AIM

To evaluate the role of KIFC3 in ESCC and the underlying mechanisms.

METHODS

Expression of KIFC3 was evaluated in ESCC tissues and adjacent normal esophageal tissues. The prognostic value of KIFC3 was analyzed using Kaplan–Meier Plotter. Colony formation, EdU assays, cell cycle analysis, Transwell assay, immunofluorescence, and western blotting were performed in ESCC cell lines after transfection with pLVX-Puro-KIFC3-shRNA- and pLVX-Puro-KIFC3-expressing lentiviruses. A xenograft tumor model in nude mice was used to evaluate the role of KIFC3 in tumorigenesis. Inhibitor of β-catenin, XAV-939, was used to clarify the mechanism of KIFC3 in ESCC. To analyze the differences between groups, *t* test and nonparametric tests were used. $P < 0.05$ was considered statistically significant.

RESULTS

Immunohistochemical staining indicated that KIFC3 was upregulated in ESCC tissues compared with adjacent normal tissues. Kaplan–Meier Plotter revealed that overexpressed KIFC3 was associated with poor prognosis in ESCC patients.

Colony formation and EdU assay showed that KIFC3 overexpression promoted cell proliferation, while KIFC3 knockdown inhibited cell proliferation in ESCC cell lines. In addition, cell cycle analysis showed that KIFC3 overexpression promoted cell cycle progression. KIFC3 knockdown suppressed ESCC tumorigenesis *in vivo*. Transwell assay and western blotting revealed that KIFC3 overexpression promoted cell migration and invasion, as well as epithelial–mesenchymal transition (EMT), while KIFC3 knockdown showed the opposite results. Mechanistically, KIFC3 overexpression promoted β-catenin signaling in KYSE450 cells; however, the role of KIFC3 was abolished by XAV-939, the inhibitor of β-catenin signaling.

CONCLUSION

KIFC3 was overexpressed in ESCC and was associated with poor prognosis. Furthermore, KIFC3 promoted proliferation, migration and invasion of ESCC *via* β-catenin signaling and EMT.

Key Words: Esophageal squamous cell carcinoma; KIFC3; β-catenin; Cell proliferation; Cell migration; Cell invasion

Core tip: Esophageal squamous cell carcinoma (ESCC) is one of the most dangerous malignancies affecting human health. However, the mechanism of ESCC is still unclear. We revealed that KIFC3 was upregulated in ESCC. In addition, overexpressed KIFC3 was associated with poor prognosis in ESCC patients. *In vitro* and *in vivo* experiments revealed that KIFC3 promoted the proliferation, migration and invasion of ESCC cells by activating epithelial–mesenchymal transition and β-catenin signaling. Our study strongly suggests that KIFC3 may be a potential new therapeutic target for ESCC.

Citation: Hao WW, Xu F. KIFC3 promotes proliferation, migration and invasion of esophageal squamous cell carcinoma cells by activating EMT and β-catenin signaling. *World J Gastrointest Oncol* 2022; 14(7): 1239-1251
URL: https://www.wjgnet.com/1948-5204/full/v14/i7/1239.htm
DOI: https://dx.doi.org/10.4251/wjgo.v14.i7.1239

INTRODUCTION

Esophageal cancer is one of the most dangerous tumors affecting humans, ranking seventh in incidence and sixth in mortality worldwide[1]. The main histological type of esophageal cancer in western countries is adenocarcinoma, while that in Asian countries is squamous cell carcinoma, where it has high incidence and mortality[2-4]. Although clinicians and researchers have made great efforts to unravel the pathophysiology of esophageal cancer, the mechanism of esophageal squamous cell carcinoma (ESCC) is still unknown[5-7]. Recent research has shown that dysregulation of *TP53* and cell cycle regulators are prominent characteristics of ESCC, which may also be detected in precursor lesions, but the molecular progression from dysplasia to invasive ESCC remains unclear[3,8]. Further studies are urgently needed to reveal the underlying molecular mechanisms and discover effective treatment targets to improve ESCC survival.

The kinesin superfamily proteins (KIFs) are a group of proteins that function as microtubule-based motors for transporting cellular cargo and playing crucial roles in chromosomal and spindle movements during mitosis and meiosis[9]. There are 45 KIFs identified in humans; among which, several have demonstrated varied functions in tumor pathobiology *via* different mechanisms, including regulation of cell cycle progression and metastasis[10-12]. Among these members, KIFC3 has negative end-directed microtubule motor activity and plays roles in Golgi positioning and integration, as well as in apical transport, in epithelial cells[13,14]. Studies of null mice have revealed that KIFC3 is dispensable for normal development and reproduction[15]. Overexpression of KIFC3 may mediate docetaxel resistance in breast cancer cells[16]. KIFC3 expression was positively associated with cell invasion and migration, and overexpressed KIFC3 was associated with shorter overall survival in hepatocellular carcinoma[17]. However, the role of KIFC3 in ESCC has not yet been reported. In view of the importance of cell cycle regulators in the development of ESCC and the involvement of KIFC3 in mitosis, we speculated that this protein might be involved in the occurrence and development of ESCC.

In this study, we aimed to examine KIFC3 expression in ESCC and further explore its role and the relevant mechanisms in ESCC tumor progression, in an attempt to provide promising insights into the mechanism of this disease and possible therapeutic targets.

MATERIALS AND METHODS

Human tissue specimens

Primary ESCC tumor tissues and corresponding nontumor tissue specimens were collected from the First Affiliated Hospital of Zhengzhou University. All experiments were carried out in accordance with the Declaration of Helsinki (amended in 2013). All procedures were supervised and approved by the Ethics Committee of the First Affiliated Hospital of Zhengzhou University (No. 2021-KY-0446-001).

Cell lines and cultures

The human ESCC cell lines KYSE30, KYSE150, KYSE450, KYSE510 and Eca109 and human normal esophageal epithelial cell line Het-1A were obtained from the Type Culture Collection of the Chinese Academy of Sciences and cultured in RPMI-1640 medium supplemented with fetal bovine serum (FBS) (10%) at 37°C in 5% CO_2.

Western blotting

Total proteins were extracted using RIPA buffer supplemented with 1% phenylmethylsulfonyl fluoride and 1% Protease Inhibitor Cocktail. Protein concentration was measured using the BCA kit (Beyotime, China). Proteins were separated using SDS-PAGE and transferred onto a polyvinylidene difluoride membrane. After blocking with 5% fresh milk for 1 h, the membranes were incubated with a specific primary antibody overnight at 4°C, followed by incubation with the corresponding secondary antibody for 1 h. Finally, the bands on the membranes were detected using the ECL detection system (Thermo) and quantified using Quantity One Software version 4.3. Primary antibodies for KIFC3, E-cadherin, N-cadherin, vimentin, proliferating cell nuclear antigen (PCNA), cyclin D1, β-actin, and secondary antibodies were purchased from Proteintech (China), matrix metalloproteinase (MMP)7 and c-Myc were purchased from Abcam (Cambridge, MA, USA), and β-catenin was purchased from Cell Signaling Technology (Danvers, MA, USA).

Transfection

pLVX-Puro-KIFC3-shRNA- and pLVX-Puro-KIFC3-expressing lentiviruses were designed and provided by Genechem (China). KYSE150 cells were transfected with pLVX-Puro-KIFC3-shRNA- expressing lentiviruses and KYSE450 cells with pLVX-Puro-KIFC3-expressing lentiviruses, while control cells were transfected with empty vectors. After transfection with lentiviruses, 2 μg/mL puromycin dihydrochloride (Beyotime) was added for 6–8 d to establish stable cell lines. Knockdown and overexpression efficiency were validated using western blotting, and the validated cell lines were recorded as KYSE150shNC, KYSE150shKIFC3, KYSE450oeNC and KYSE450oeKIFC3.

Colony formation assay

The cancer cells were seeded in a six-well plate at 1000 cells/well and cultured for 14 d. The colonies were washed once with phosphate-buffered saline (PBS), fixed with 1 mL 4% paraformaldehyde for 15 min, and stained with 1 mL 0.5% crystal violet for 30 min. After washing with deionized distilled water, the images were captured using a digital camera. The number of colonies was then counted.

Cell cycle analysis

The cancer cells were seeded in a six-well plate at 2.5 × 10^5 cells per well. When the cell density was 60%, cells were collected, washed with cold PBS twice, and then fixed in 70% ethanol at 4°C overnight. The cells were washed with cold PBS twice, and then incubated with RNaseA (0.1 mg/mL) and propidium iodide (0.02 mg/mL) at 37°C for 30 min in the dark. The cell cycle was detected using flow cytometry.

Transwell assay

A Transwell assay was used to detect cell migration and invasion. For the invasion assay, 100 μL Matrigel (serum-free medium diluted 1:8) was added to the upper chamber of the Transwell chamber (Corning, USA). After shaking well, the gel was incubated at 37°C and solidified for 2–4 h. Cells were seeded at 10^4 per well in the upper chamber with 100 μL serum-free medium. For the lower chamber, 500 μL medium (20% FBS) was added. After 24 h, the cells that passed through the filter were fixed with 4% paraformaldehyde for 30 min, stained with 0.5% crystal violet for 30 min, and washed with PBS. Finally, the cells were examined under a fluorescence microscope (BX51; Olympus, Japan). The migration assay was similar to the invasion assay, with the difference that no Matrigel was added to the upper chamber.

Immunofluorescence

KYSE150 and KYSE450 cells were seeded onto glass coverslips in 24-well plates overnight. The cells were then washed with PBS and fixed with 4% paraformaldehyde for 15 min at 25°C. Next, the cells were permeabilized for 15 min with 0.3% Triton X-100 in PBS. The cells were then blocked with 5% BSA in PBS for 1 h at 25°C and then incubated overnight at 4°C with the primary antibody against β-catenin

(1:100 dilution) overnight; normal goat serum was used as a negative control. The treated cells were incubated with an FITC-labeled or Cy3-labeled goat anti-rabbit IgG (H+L) highly cross-adsorbed secondary antibody (Beyotime) in the dark for 1 h. The nuclei were visualized after staining with 2 μg/mL DAPI (Biosharp, China) for 10 min at 25°C. The glass coverslips were sealed with antifade reagent (Biosharp) and examined under a fluorescence microscope (BX51; Olympus).

Xenograft tumor experiment using nude mice

All animal research procedures were approved by the Ethics Committee of the First Affiliated Hospital of Zhengzhou University (No. 2021-KY-0446-001). All animal experiments were carried out in accordance with the National Institutes of Health Guide for the Care and Use of Laboratory Animals (NIH Publications No. 8023, revised 1978). Male BALB/c nude mice (age 4 wk) were purchased from Beijing Life River Experimental Animal Technology Co. Ltd. and kept in a temperature-controlled specific pathogen free environment with a regular light/dark cycle and provided with adequate rodent diet and water. Ten mice were randomly divided into KYSE150shNC and KYSE150shKIFC3 groups. There were five mice in each group. KYSE150shNC cells (10^6) and KYSE150shKIFC3 cells (10^6) were collected, washed with PBS, suspended in 200 μL PBS, and subcutaneously implanted into the right flank of the dorsal region of nude mice. A Vernier caliper was used to measure tumor sizes every 3 d, and the tumor volume (TV) was calculated using the following formula: TV (mm^3) = $0.5 \times d^2 \times D$, where d is the shortest diameter and D is the longest diameter. After nine measurements, the longest diameter of tumor reached 15 mm. All mice were killed and the tumor specimens were collected and weighed.

Immunohistochemistry

Immunohistochemical staining was performed using an UltraSensitive TM SP kit and DAB kit (Maixin, China). Tumor tissues were embedded in paraffin and cut into 4-μm sections. The deparaffinized sections were incubated with a primary antibody against KIFC3 (1: 200 dilution, Abcam, #ab154419) or Ki-67 (1:100 dilution, Abcam, #ab16667) overnight at 4°C, and normal goat serum was used as a negative control. After washing, the tissue sections were then incubated with a biotinylated anti-rabbit secondary antibody (1:200 dilution, Aspen, #AS-1107) for 1 h at 25°C. The sections were subsequently incubated with horseradish-peroxidase-conjugated streptavidin (Beyotime, #A0303) and developed using 3, 3-diaminobenzidine. An optical microscope (BX51; Olympus) was used to observe the specimens. Two observers, who were blinded to the data of the samples, evaluated, counted and analyzed the positive cells. The proportion of positive tumor cells was scored as follows: 1 (< 10% positive tumor cells), 2 (10%–50% positive tumor cells), 3 (50%–75% positive tumor cells), and 4 (> 75% positive tumor cells). The intensity of staining was graded according to the following criteria: 0 (no staining), 1 (weak staining = light yellow), 2 (moderate staining = yellow brown), and 3 (strong staining = brown). The staining index was calculated as the product of the proportion of positive cells times the staining intensity score (range: 0–12). The median of staining index was used as the cut-off value; the staining index higher than the cut-off value was identified as high expression, while that less than the cut-off value was identified as low expression.

Statistical analysis

Graphpad Prism 7 was used for all analyses. Data are expressed as the mean ± SD. To analyze the differences between groups, *t* test and nonparametric tests were used. $P < 0.05$ was considered statistically significant.

RESULTS

KIFC3 expression is upregulated in ESCC and is associated with poor prognosis

To investigate KIFC3 expression, ESCC tissues and adjacent nontumor tissues were collected from 34 patients (26 male and 8 female, aged 47–72 years) with ESCC. Immunohistochemical assays showed that KIFC3 expression was lower in ESCC tissues than in adjacent nontumor tissues (Figure 1A). Moreover, data from Kaplan–Meier Plotter (https://kmplot.com/analysis) revealed that lower expression of KIFC3 was associated with better overall survival in patients with ESCC (Figure 1B). These results indicate that KIFC3 plays an important role in ESCC development. To explore the role of KIFC3 in ESCC cells, its expression level was evaluated in ESCC cell lines Eca109, KYSE30, KYSE150, KYSE450 and KYSE510, as well as normal esophageal epithelial cell line Het-1A. KYSE450 and KYSE150 cells displayed the lowest and highest expression levels of KIFC3, respectively (Figure 1C). Therefore, KYSE450 cells were used for subsequent overexpression assays, while KYSE150 cells were used for knockdown assays. Western blotting verified that the corresponding cell lines were successfully constructed (Figure 1D).

KIFC3 promotes cell proliferation in ESCC cells

To investigate the effect of KIFC3 in ESCC, colony-formation and EdU assays were performed to

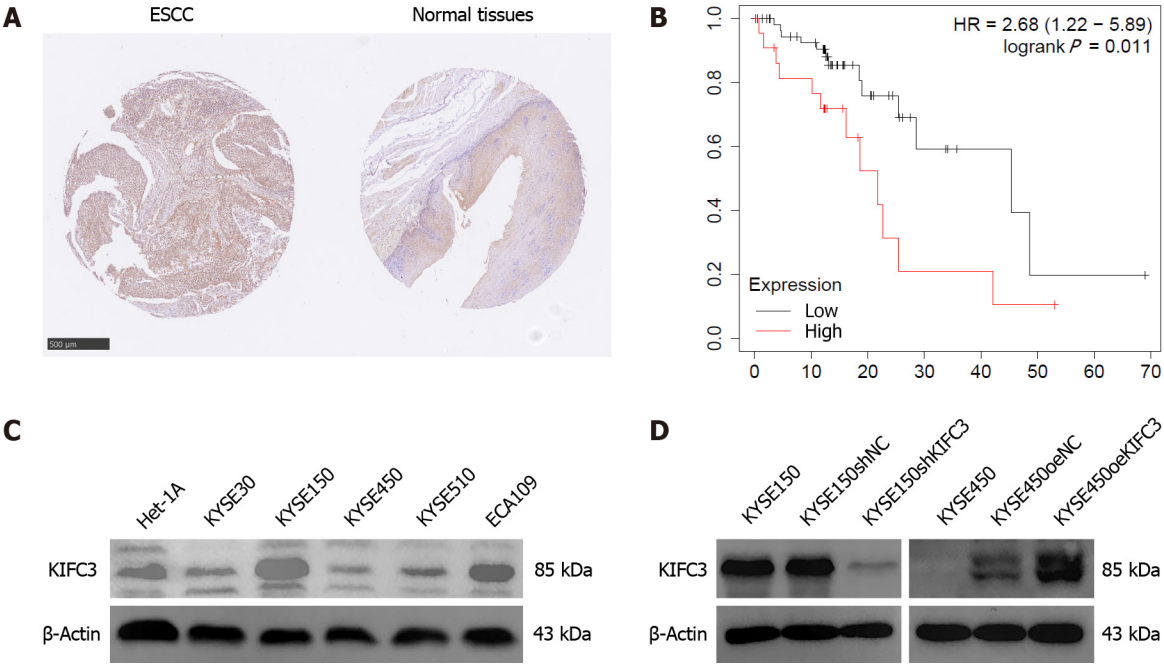

Figure 1 KIFC3 is overexpressed in ESCC tissues and is associated with poor prognosis. A: Immunohistochemistry shows that KIFC3 is overexpressed in ESCC tissues compared with adjacent normal tissues, scale bar: 500 μm; B: Kaplan–Meier Plotter shows that high levels of KIFC3 are associated with poor prognosis in ESCC patients; C: Western blotting shows expression of KIFC3 in ESCC cell lines and normal esophageal epithelial cell line Het-1A; D: Western blotting shows that KIFC3-knockdown and KIFC3-overexpressed cell lines are constructed successfully. ESCC: Esophageal squamous cell carcinoma; KIFC3: Kinesin family member C3.

observe the proliferation of KYSE150 and KYSE450 cells. The results showed that the colony-formation capacity was decreased after knockdown of KIFC3 in KYSE150 cells, while KIFC3 overexpression promoted colony-formation capacity in KYSE450 cells (Figure 2A and 2B). EdU assay showed that KIFC3 knockdown inhibited the proliferation of KYSE150 cells, while its overexpression promoted proliferation of KYSE450 cells (Figure 2C and 2D). In addition, KIFC3 knockdown inhibited the expression of PCNA, while its overexpression promoted PCNA expression (Figure 2E), which indicated that KIFC3 promoted proliferation in ESCC cells at the molecular level.

KIFC3 promotes cell cycle progression in ESCC cells

To further investigate the role of KIFC3 in cell cycle progression, cell cycle analysis was conducted. The percentage of G0/1 phase in KYSE150shKIFC3 group was significantly higher, and percentage of S and G2/M phase was lower than that in KYSE150shNC group (Figure 3A), while the percentage of G0/1 phase in KYSE450oeKIFC3 group was significantly lower, and percentage of S and G2/M phase was higher than that in KYSE450oeNC group (Figure 3B). At the molecular level, KIFC3 knockdown caused a decrease while KIFC3 overexpression promoted the expression of cyclin D1, which plays an important role in the transition from G1 to S phase (Figure 3C and 3D). These results indicate that KIFC3 positively regulates cell cycle in ESCC cells.

KIFC3 promotes tumor growth in vivo

Based on the *in vitro* data above, we further investigated the role of KIFC3 using xenograft tumors *in vivo*. All animals were in a fit state during the experiment and all *in vivo* data were included in the analysis. The transplanted tumors grew rapidly in the KYSE150shNC group but were suppressed in the KYSE150shKIFC3 group (Figure 4A and 4B), and the weight of tumors in the KYSE150shKIFC3 group was significantly lower (Figure 4C). Immunohistochemistry of tumors showed that the expression of Ki-67 was decreased significantly in the KYSE150shKIFC3 group (Figure 4D), proving that KIFC3 knockdown inhibited the proliferation of ESCC *in vivo* at the molecular level. Taken together, KIFC3 promotes ESCC proliferation *in vivo*.

KIFC3 promotes migration and invasion via epithelial–mesenchymal transition in ESCC cells

To detect whether KIFC3 exerts effects on the migration and invasion of ESCC cells, Transwell migration and invasion assays were used. Accelerated cell migration was observed in the KYSE450oeKIFC3 group compared with the KYSE450oeNC group, while it was less active in the KYSE150shKIFC3 group than in the KYSE150shNC group (Figure 5A and 5C). Transwell invasion showed similar results (Figure 5B and 5D). To further explore the molecular mechanism of KIFC3-promoted migration and invasion, we detected the expression of E-cadherin, N-cadherin and vimentin,

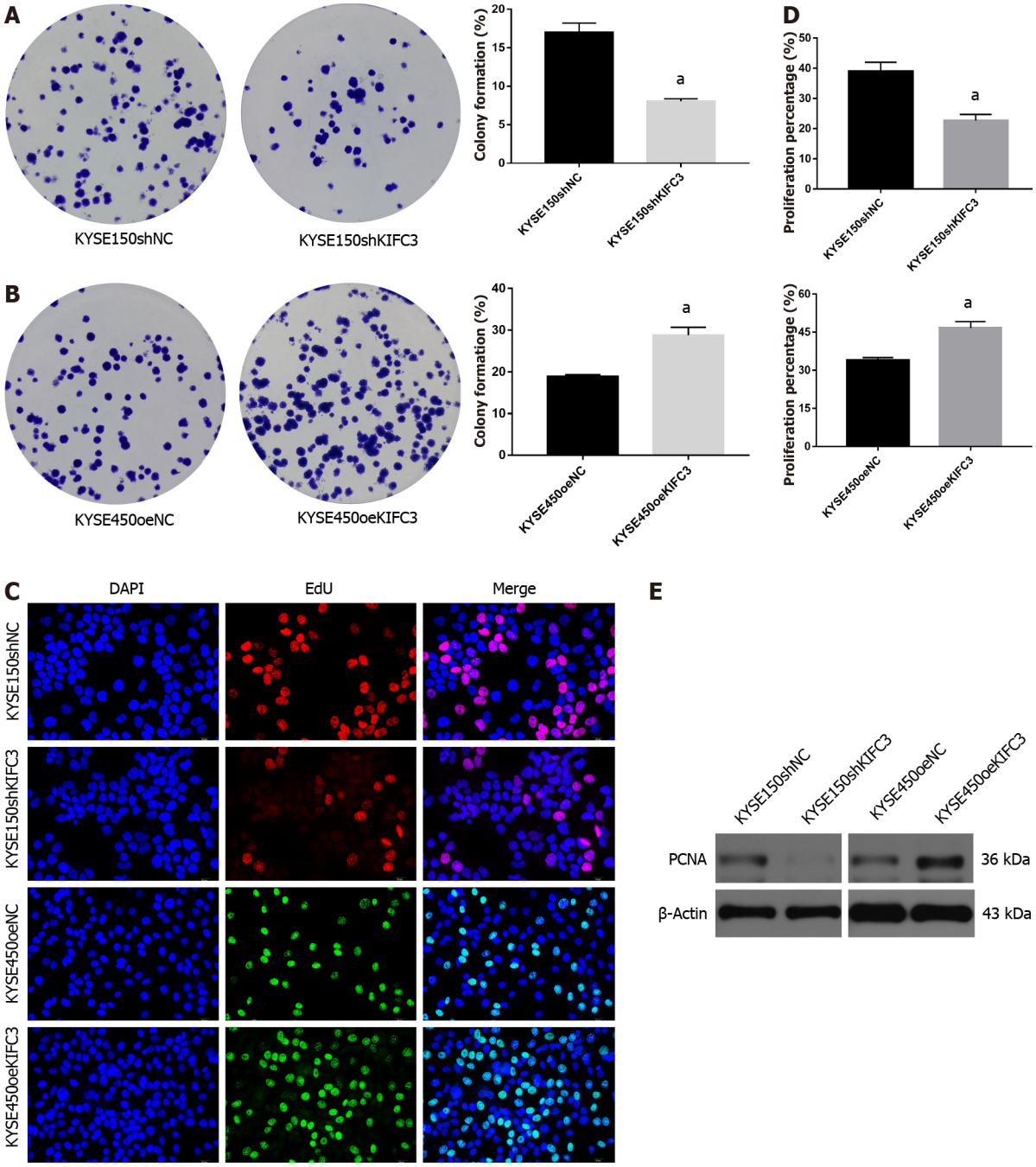

Figure 2 KIFC3 promotes proliferation in human ESCC cells. A: Colony-formation assay shows that KIFC3 knockdown inhibits colony formation in KYSE150 cells; B: Colony-formation assay shows that KIFC3 overexpression promotes colony formation in KYSE450 cells; C: EdU proliferation assay shows that KIFC3 knockdown inhibits proliferation in KYSE150 cells, while its overexpression promotes proliferation in KYSE450 cells, scale bar: 20 μm; D: Statistical analysis of the data shown in C; E: Western blotting shows that KIFC3 promotes the expression of proliferating cell nuclear antigen in ESCC cells. $^{a}P < 0.05$ *versus* the control group. ESCC: Esophageal squamous cell carcinoma; KIFC3: Kinesin family member C3.

which are key molecules of epithelial–mesenchymal transition (EMT). The results indicated that N-cadherin and vimentin, which are associated with the mesenchyme phenotype and indicate a higher possibility of tumor migration and invasion, were decreased, while E-cadherin, which is associated with the epithelial phenotype, increased after KIFC3 knockdown. In KIFC3-overexpressing cells, the expression of N-cadherin, vimentin and E-cadherin showed the opposite results (Figure 5E and 5F). These results indicate that KIFC3 promotes migration and invasion through EMT in ESCC cells.

KIFC3 promotes expression of β-catenin in ESCC cells

Previous studies have demonstrated that β-catenin plays an essential role in the proliferation, migration, and invasion of ESCC cells. In our study, western blotting showed that β-catenin protein expression in KYSE150shKIFC3 group was decreased significantly compared with that in the KYSE150shNC group (Figure 6A and 6B), while expression of β-catenin was increased significantly in the KYSE450oeKIFC3

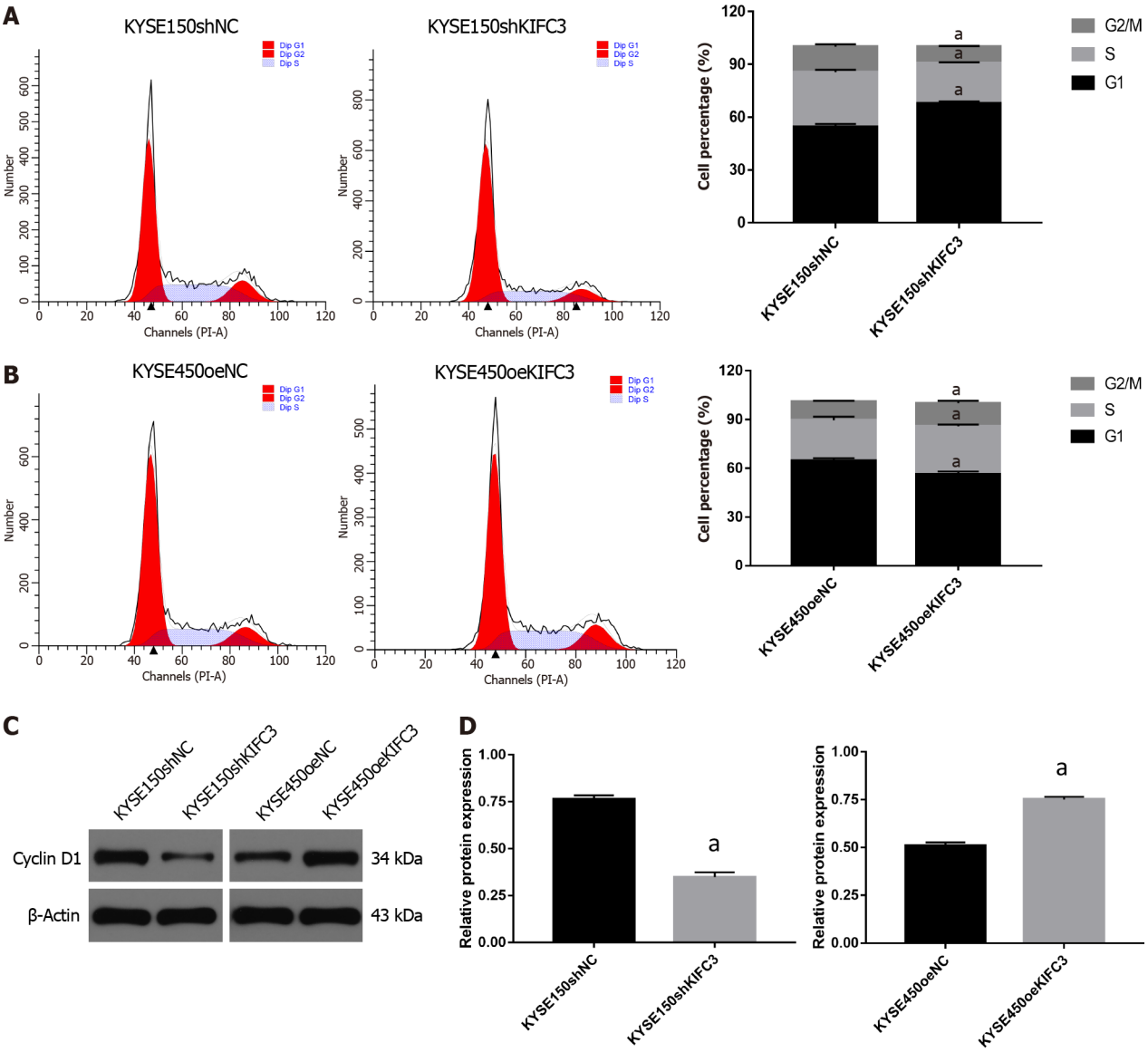

Figure 3 KIFC3 promotes the progression of cell cycle in ESCC cells. A: Cell cycle analysis showing that KIFC3 knockdown induces cell cycle arrest in KYSE150 cells; B: Cell cycle analysis showing that KIFC3 overexpression promotes the progression of cell cycle in KYSE450 cells; C: Western blotting showing that KIFC3 knockdown decreases the expression of cyclin D1 in KYSE150 cells, while KIFC3 overexpression increased the expression of cyclin D1 in KYSE450 cells; D: Statistical analysis of the data presented in C. $^{a}P < 0.05$ *versus* the control group. ESCC: Esophageal squamous cell carcinoma; KIFC3: Kinesin family member C3.

group compared to that in the KYSE450oeNC group (Figure 6A and 6B). Immunofluorescence showed the same results; β-catenin expression was decreased after KIFC3 knockdown and increased after KIFC3 overexpression (Figure 6C). These results suggest that KIFC3 promotes β-catenin expression in ESCC cells.

KIFC3 promotes the progression of ESCC via β-catenin signaling

To explore the role of β-catenin signaling in KIFC3-promoted proliferation, migration and invasion, we used XAV-939, an inhibitor of β-catenin. KYSE450oeNC and KYSE450oeKIFC3 cells were treated with XAV-939, and the expression of proteins downstream of β-catenin, which play an important role in proliferation, migration, and invasion was evaluated. Although the expression of c-myc, cyclin D1 and MMP7 was increased after KIFC3 overexpression ($P < 0.05$), when β-catenin was inhibited by XAV-939, the levels of c-myc, cyclin D1 and MMP7 were decreased even when KIFC3 was overexpressed ($P < 0.05$) (Figure 6D and 6E). These results suggest that KIFC3 promotes the progression of ESCC *via* β-catenin signaling.

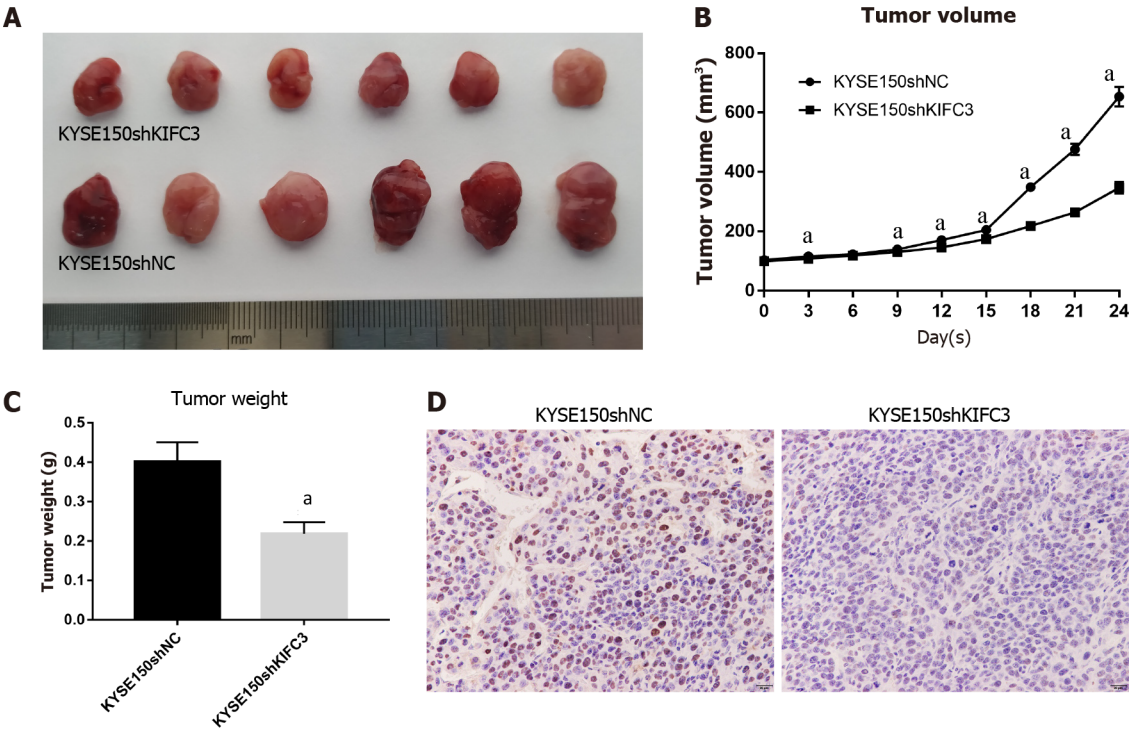

Figure 4 KIFC3 knockdown inhibits the growth of ESCC cells *in vivo*. A: Images of tumors formed in nude mice; B: Volume curves of xenograft tumors; C: Weight of xenograft tumors; D: Immunohistochemistry showing that KIFC3 knockdown inhibits the expression of Ki-67, scale bar: 20 μm. $^{a}P < 0.05$ *versus* the control group. ESCC: Esophageal squamous cell carcinoma; KIFC3: Kinesin family member C3.

DISCUSSION

ESCC is one of the most malignant tumors that impose a significant medical burden on the health system. Although several gene mutations that could increase the susceptibility to ESCC have been identified[8], the exact mechanism that induces tumor progression is still unclear. KIFC3 has been reported to be overexpressed in a number of cancers and may be involved in cell cycle and cell proliferation, which suggests that KIFC3 is an oncogene, thus arousing our interest in its possible role in ESCC progression.

In the present study, we found that KIFC3 was upregulated in ESCC tissues compared to adjacent nontumor tissues. Data from the Kaplan–Meier Plotter website indicated that high levels of KIFC3 expression were correlated with poor ESCC prognosis. These findings indicate that KIFC3 may be involved in the development of ESCC, and that high expression of KIFC3 may be a prognostic factor in ESCC. Functional assays showed that knockdown of KIFC3 suppressed proliferation in KYSE150 cells, and the cell cycle was arrested compared with that in KYSE150shNC cells. Migration and invasion were inhibited in KYSE150shKIFC3 cells. Compared with KYSE450oeNC cells, cell proliferation, migration, and invasion were activated in KYSE450oeKIFC3 cells, further demonstrating that KIFC3 promoted the progression of ESCC cells. Furthermore, KIFC3 knockdown inhibited ESCC proliferation *in vivo*. Given the above results, we may consider KIFC3 as a tumor marker associated with the progression and prognosis of ESCC.

EMT plays a potential role in the promotion of tumor invasiveness, metastasis and resistance to apoptotic stimuli, and it is marked by downregulation of epithelial biomarkers, such as E-cadherin, and the upregulation of mesenchymal biomarkers, such as N-cadherin and vimentin. Cells undergoing EMT can acquire greater mobility and become prometastatic[18-20]. EMT is known to play an important role in the metastasis of ESCC[21-23]. In addition, members of the KIF family are involved in the regulation of EMT and thus affect the migration and invasion of tumors[24-26]. In our study, KIFC3 knockdown suppressed the migration and invasion of KYSE150 cells, accompanied by the upregulation of E-cadherin and downregulation of N-cadherin and vimentin, while KIFC3 overexpression showed the opposite results in KYSE450 cells. These results indicate that KIFC3 promotes the migration and invasion of ESCC cells by inhibiting EMT.

β-Catenin signaling has been shown to be associated with the regulation of processes such as proliferation and invasion, which are involved in the occurrence and progression of cancers[27,28]. Moreover, the deactivation of β-catenin has been a potential treatment target in ESCC[29-31]. Thus, regulation of β-catenin may play an important role in the development of ESCC. It has been reported that in HEK293 cells depleted of centrosomes, normal accumulation of β-catenin in response to Wnt signaling is attenuated[32]. KIFC3 regulates centrosome cohesion in a microtubule-dependent manner[14].

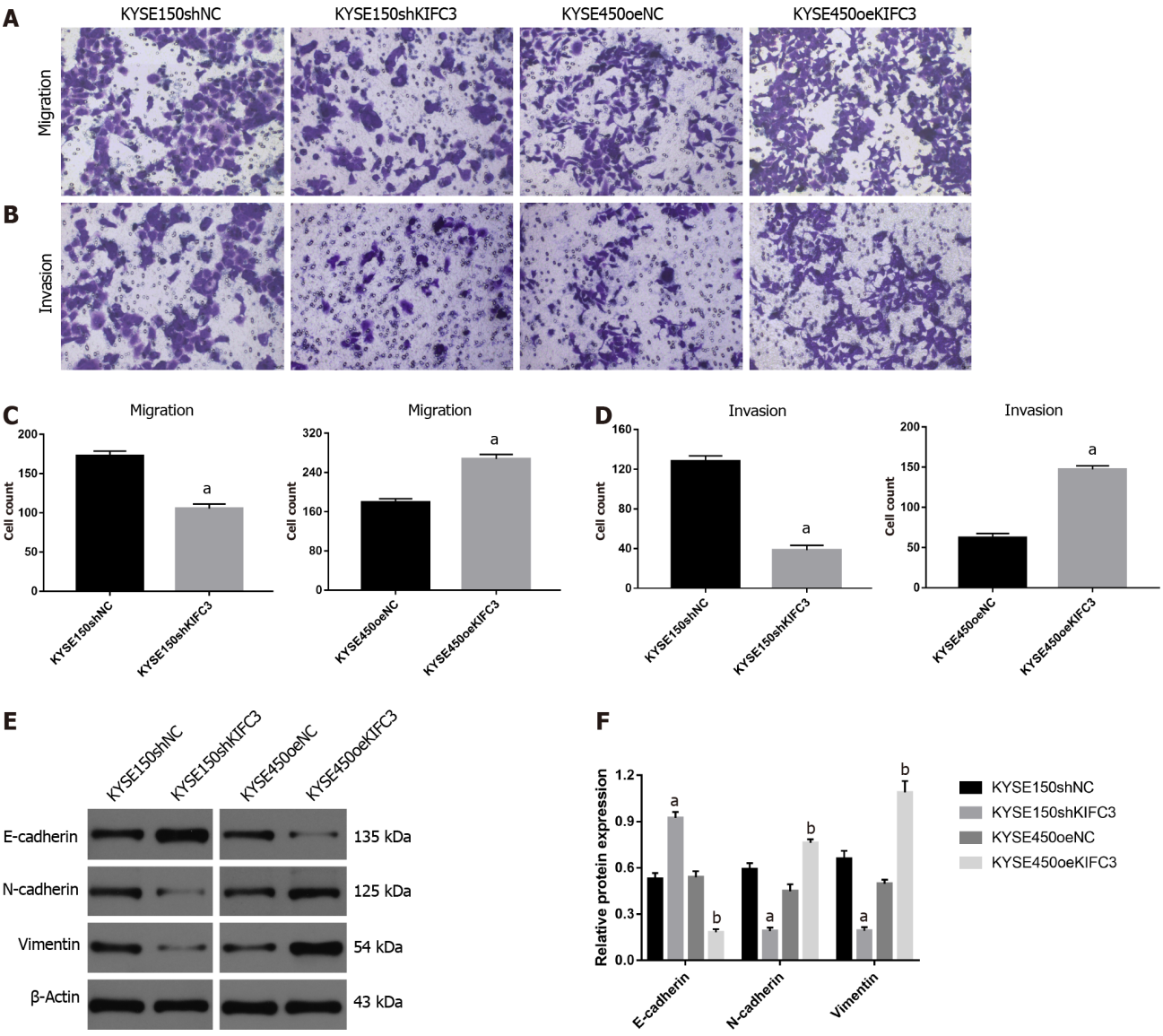

Figure 5 KIFC3 promotes migration, invasion, and EMT in human ESCC cells. A: Transwell migration assay showing that KIFC3 knockdown inhibits migration in KYSE150 cells, while its overexpression promotes migration in KYSE450 cells, scale bar: 20 μm; B: Transwell invasion assay showing that KIFC3 knockdown inhibits invasion in KYSE150 cells, while its overexpression promotes invasion in KYSE450 cells, scale bar: 20 μm; C: Statistical analysis of cell migration; D: Statistical analysis of cell invasion; E: Western blotting showing that KIFC3 knockdown inhibits epithelial-mesenchymal transition (EMT), while KIFC3 overexpression promotes EMT in ESCC cells; F: Statistical analysis of E. $^{a}P < 0.05$ *vs* the KYSE150shNC group, $^{b}P < 0.05$ *vs* the KYSE450oeNC group. ESCC: Esophageal squamous cell carcinoma; EMT: Epithelial–mesenchymal transition; KIFC3: Kinesin family member C3.

Collectively, the relationship between KIFC3 and β-catenin is worth exploring. In the present study, KIFC3 overexpression promoted the expression of β-catenin and downstream molecules of β-catenin signaling, such as cyclin D1, c-myc and MMP7. However, after treatment with XAV-939, an inhibitor of β-catenin, KIFC3-induced upregulation of cyclin D1, c-Myc, and MMP7 was blocked, which means that β-catenin plays a vital role in KIFC3-induced tumor progression. Although further investigation is required to clarify the exact mechanism underlying the effect of KIFC3 on β-catenin, our research demonstrated that KIFC3 promotes tumor progression *via* β-catenin signaling in ESCC.

CONCLUSION

KIFC3 is upregulated in ESCC, and KIFC3 overexpression is associated with poor prognosis in ESCC patients. KIFC3 promotes the proliferation, migration, and invasion of ESCC cells by activating EMT and β-catenin signaling. Overall, our study provides a comprehensive understanding of KIFC3 in ESCC and its underlying mechanisms, which strongly suggests that KIFC3 may be a potential new therapeutic target for ESCC treatment.

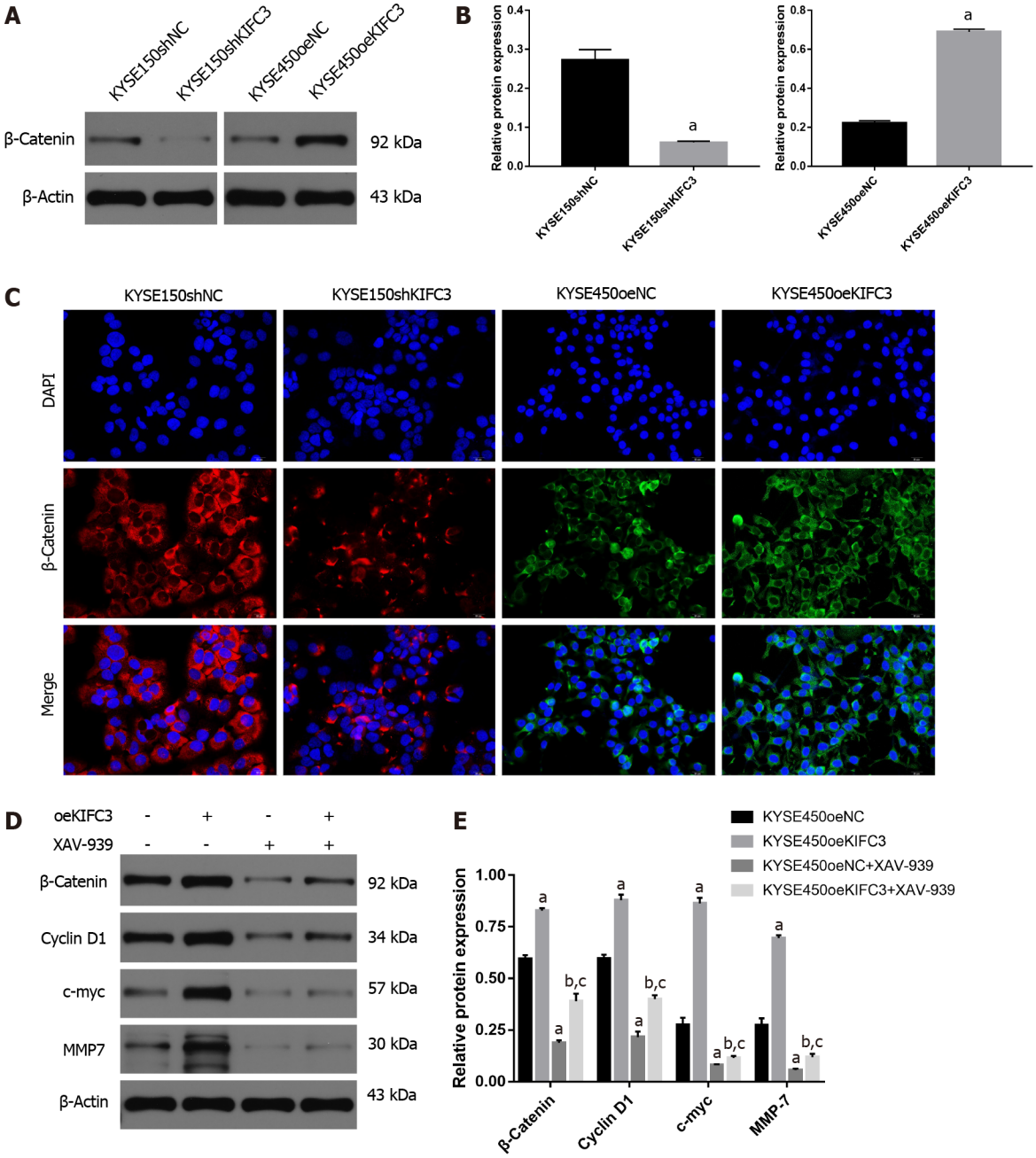

Figure 6 KIFC3 promotes the progression of ESCC *via* β-catenin signaling. A: Western blotting showing that KIFC3 knockdown inhibits, while its overexpresssion promotes the expression of β-catenin in ESCC cells; B: Statistical analysis of the data presented in A; C: Immunofluorescence showing that KIFC3 knockdown inhibits, while its overexpression promotes the expression of β-catenin, scale bar: 20 μm; D: Inhibitor of β-catenin, XAV-939 is used to treat KYSE450oeNC and KYSE450oeKIFC3 cells, then western blotting is used to detect downstream molecules of β-catenin signaling; E: Statistical analysis of the data presented in D. $^{a}P < 0.05$ *vs* the KYSE450oeNC group, $^{b}P < 0.05$ *versus* the KYSE450oeNC+ XAV-939 group, $^{c}P < 0.05$ *vs* the KYSE450oeKIFC3 group. ESCC: Esophageal squamous cell carcinoma; KIFC3: Kinesin family member C3.

ARTICLE HIGHLIGHTS

Research background

Esophageal squamous cell carcinoma (ESCC) is one of the most common malignancies. The mechanism of ESCC is still unclear.

Research motivation

Kinesin family member (KIF)C3 has microtubule motor activity and may be involved in mitotic progression. KIFC3 was also shown to be involved in cell invasion and migration, as well as in survival, in hepatocellular carcinoma.

Research objectives
To elucidate the role of KIFC3 in ESCC and the underlying mechanisms.

Research methods
The expression of KIFC3 was evaluated in ESCC tissues and normal tissues. In addition, KIFC3 knockdown and KIFC3-overexpressing cell lines were constructed and then colony formation, EdU assays, cell cycle analysis, Transwell assays, and western blotting were performed to explore the underlying mechanisms of action. A xenograft tumor model in nude mice was used to verify the role of KIFC3 in tumorigenesis.

Research results
We showed that KIFC3 was upregulated in ESCC tissues and was associated with poor prognosis. KIFC3 promoted cell proliferation, mitosis progression, migration and invasion. In addition, KIFC3 knockdown suppressed ESCC tumorigenesis in an *in vivo* model. Mechanistically, we validated the involvement of KIFC3 β-catenin signaling and epithelial–mesenchymal transition (EMT) in ESCC progression.

Research conclusions
We found that KIFC3 was overexpressed in ESCC, and the expression of this protein was associated with prognosis in ESCC patients. Furthermore, KIFC3 promoted proliferation, migration, and invasion of ESCC *via* β-catenin signaling and EMT.

Research perspectives
Although the detailed mechanism underlying the effect of KIFC3 in promoting ESCC progression should be studied more carefully in our next research, we believe our research strongly suggests that KIFC3 may be a potential new therapeutic target for ESCC treatment.

FOOTNOTES

Author contributions: Hao WW designed and performed experiments, analyzed data, and wrote the article; Xu F conceived the study, analyzed the data, and revised the article; all authors have read and approved the final manuscript.

Institutional review board statement: The study was reviewed and approved by the Institutional Review Board at the First Hospital of Zhengzhou University (No. 2021-KY-0446-001).

Institutional animal care and use committee statement: All animal research procedures were approved by the Ethics Committee of the First Affiliated Hospital of Zhengzhou University (No. 2021-KY-0446-001). All animal experiments were carried out in accordance with the National Institutes of Health Guide for the Care and Use of Laboratory Animals (NIH Publications No. 8023, revised 1978).

Conflict-of-interest statement: The authors declare no conflicts of interest.

Data sharing statement: No additional data are available.

ARRIVE guidelines statement: The authors have read the ARRIVE guidelines, and the manuscript was prepared and revised according to the ARRIVE guidelines.

Country/Territory of origin: China

ORCID number: Weiwei Hao 0000-0002-5156-6878; Feng Xu 0000-0002-5205-781X.

S-Editor: Wu YXJ
L-Editor: Kerr C
P-Editor: Yuan YY

REFERENCES

1 **Siegel RL**, Miller KD, Fuchs HE, Jemal A. Cancer Statistics, 2021. *CA Cancer J Clin* 2021; **71**: 7-33 [PMID: 33433946 DOI: 10.3322/caac.21654]
2 **Fan J**, Liu Z, Mao X, Tong X, Zhang T, Suo C, Chen X. Global trends in the incidence and mortality of esophageal cancer from 1990 to 2017. *Cancer Med* 2020; **9**: 6875-6887 [PMID: 32750217 DOI: 10.1002/cam4.3338]
3 **Smyth EC**, Lagergren J, Fitzgerald RC, Lordick F, Shah MA, Lagergren P, Cunningham D. Oesophageal cancer. *Nat Rev Dis Primers* 2017; **3**: 17048 [PMID: 28748917 DOI: 10.1038/nrdp.2017.48]
4 **Thrumurthy SG**, Chaudry MA, Thrumurthy SSD, Mughal M. Oesophageal cancer: risks, prevention, and diagnosis. *BMJ* 2019; **366**: l4373 [PMID: 31289038 DOI: 10.1136/bmj.l4373]
5 **Cao W**, Lee H, Wu W, Zaman A, McCorkle S, Yan M, Chen J, Xing Q, Sinnott-Armstrong N, Xu H, Sailani MR, Tang W, Cui Y, Liu J, Guan H, Lv P, Sun X, Sun L, Han P, Lou Y, Chang J, Wang J, Gao Y, Guo J, Schenk G, Shain AH, Biddle FG, Collisson E, Snyder M, Bivona TG. Multi-faceted epigenetic dysregulation of gene expression promotes esophageal squamous cell carcinoma. *Nat Commun* 2020; **11**: 3675 [PMID: 32699215 DOI: 10.1038/s41467-020-17227-z]
6 **Triantafyllou T**, Wijnhoven BPL. Current status of esophageal cancer treatment. *Chin J Cancer Res* 2020; **32**: 271-286 [PMID: 32694894 DOI: 10.21147/j.issn.1000-9604.2020.03.01]
7 **Yang YM**, Hong P, Xu WW, He QY, Li B. Advances in targeted therapy for esophageal cancer. *Signal Transduct Target Ther* 2020; **5**: 229 [PMID: 33028804 DOI: 10.1038/s41392-020-00323-3]
8 **Liu X**, Zhang M, Ying S, Zhang C, Lin R, Zheng J, Zhang G, Tian D, Guo Y, Du C, Chen Y, Chen S, Su X, Ji J, Deng W, Li X, Qiu S, Yan R, Xu Z, Wang Y, Cui J, Zhuang S, Yu H, Zheng Q, Marom M, Sheng S, Hu S, Li R, Su M. Genetic Alterations in Esophageal Tissues From Squamous Dysplasia to Carcinoma. *Gastroenterology* 2017; **153**: 166-177 [PMID: 28365443 DOI: 10.1053/j.gastro.2017.03.033]
9 **Hirokawa N**, Noda Y, Okada Y. Kinesin and dynein superfamily proteins in organelle transport and cell division. *Curr Opin Cell Biol* 1998; **10**: 60-73 [PMID: 9484596 DOI: 10.1016/s0955-0674(98)80087-2]
10 **Qureshi Z**, Ahmad M, Yang WX, Tan FQ. Kinesin 12 (KIF15) contributes to the development and tumorigenicity of prostate cancer. *Biochem Biophys Res Commun* 2021; **576**: 7-14 [PMID: 34474246 DOI: 10.1016/j.bbrc.2021.08.072]
11 **Wu YP**, Ke ZB, Zheng WC, Chen YH, Zhu JM, Lin F, Li XD, Chen SH, Cai H, Zheng QS, Wei Y, Xue XY, Xu N. Kinesin family member 18B regulates the proliferation and invasion of human prostate cancer cells. *Cell Death Dis* 2021; **12**: 302 [PMID: 33753726 DOI: 10.1038/s41419-021-03582-2]
12 **Zou JX**, Duan Z, Wang J, Sokolov A, Xu J, Chen CZ, Li JJ, Chen HW. Kinesin family deregulation coordinated by bromodomain protein ANCCA and histone methyltransferase MLL for breast cancer cell growth, survival, and tamoxifen resistance. *Mol Cancer Res* 2014; **12**: 539-549 [PMID: 24391143 DOI: 10.1158/1541-7786.MCR-13-0459]
13 **Xu Y**, Takeda S, Nakata T, Noda Y, Tanaka Y, Hirokawa N. Role of KIFC3 motor protein in Golgi positioning and integration. *J Cell Biol* 2002; **158**: 293-303 [PMID: 12135985 DOI: 10.1083/jcb.200202058]
14 **Hata S**, Pastor Peidro A, Panic M, Liu P, Atorino E, Funaya C, Jäkle U, Pereira G, Schiebel E. The balance between KIFC3 and EG5 tetrameric kinesins controls the onset of mitotic spindle assembly. *Nat Cell Biol* 2019; **21**: 1138-1151 [PMID: 31481795 DOI: 10.1038/s41556-019-0382-6]
15 **Yang Z**, Xia Ch, Roberts EA, Bush K, Nigam SK, Goldstein LS. Molecular cloning and functional analysis of mouse C-terminal kinesin motor KifC3. *Mol Cell Biol* 2001; **21**: 765-770 [PMID: 11154264 DOI: 10.1128/MCB.21.3.765-770.2001]
16 **De S**, Cipriano R, Jackson MW, Stark GR. Overexpression of kinesins mediates docetaxel resistance in breast cancer cells. *Cancer Res* 2009; **69**: 8035-8042 [PMID: 19789344 DOI: 10.1158/0008-5472.CAN-09-1224]
17 **Chen J**, Li S, Zhou S, Cao S, Lou Y, Shen H, Yin J, Li G. Kinesin superfamily protein expression and its association with progression and prognosis in hepatocellular carcinoma. *J Cancer Res Ther* 2017; **13**: 651-659 [PMID: 28901309 DOI: 10.4103/jcrt.JCRT_491_17]
18 **Lamouille S**, Xu J, Derynck R. Molecular mechanisms of epithelial-mesenchymal transition. *Nat Rev Mol Cell Biol* 2014; **15**: 178-196 [PMID: 24556840 DOI: 10.1038/nrm3758]
19 **Mittal V**. Epithelial Mesenchymal Transition in Tumor Metastasis. *Annu Rev Pathol* 2018; **13**: 395-412 [PMID: 29414248 DOI: 10.1146/annurev-pathol-020117-043854]
20 **Navas T**, Kinders RJ, Lawrence SM, Ferry-Galow KV, Borgel S, Hollingshead MG, Srivastava AK, Alcoser SY, Makhlouf HR, Chuaqui R, Wilsker DF, Konaté MM, Miller SB, Voth AR, Chen L, Vilimas T, Subramanian J, Rubinstein L, Kummar S, Chen AP, Bottaro DP, Doroshow JH, Parchment RE. Clinical Evolution of Epithelial-Mesenchymal Transition in Human Carcinomas. *Cancer Res* 2020; **80**: 304-318 [PMID: 31732654 DOI: 10.1158/0008-5472.CAN-18-3539]
21 **Cai R**, Wang P, Zhao X, Lu X, Deng R, Wang X, Su Z, Hong C, Lin J. LTBP1 promotes esophageal squamous cell carcinoma progression through epithelial-mesenchymal transition and cancer-associated fibroblasts transformation. *J Transl Med* 2020; **18**: 139 [PMID: 32216815 DOI: 10.1186/s12967-020-02310-2]
22 **Tang Q**, Lento A, Suzuki K, Efe G, Karakasheva T, Long A, Giroux V, Islam M, Wileyto EP, Klein-Szanto AJ, Nakagawa H, Bass A, Rustgi AK. Rab11-FIP1 mediates epithelial-mesenchymal transition and invasion in esophageal cancer. *EMBO Rep* 2021; **22**: e48351 [PMID: 33403789 DOI: 10.15252/embr.201948351]
23 **Zhang J**, Luo A, Huang F, Gong T, Liu Z. SERPINE2 promotes esophageal squamous cell carcinoma metastasis by activating BMP4. *Cancer Lett* 2020; **469**: 390-398 [PMID: 31730904 DOI: 10.1016/j.canlet.2019.11.011]
24 **Gao Y**, Zheng H, Li L, Zhou C, Chen X, Zhou X, Cao Y. KIF3C Promotes Proliferation, Migration, and Invasion of Glioma Cells by Activating the PI3K/AKT Pathway and Inducing EMT. *Biomed Res Int* 2020; **2020**: 6349312 [PMID: 33150178 DOI: 10.1155/2020/6349312]
25 **Han J**, Wang F, Lan Y, Wang J, Nie C, Liang Y, Song R, Zheng T, Pan S, Pei T, Xie C, Yang G, Liu X, Zhu M, Wang Y, Liu Y, Meng F, Cui Y, Zhang B, Meng X, Zhang J, Liu L. KIFC1 regulated by miR-532-3p promotes epithelial-to-mesenchymal transition and metastasis of hepatocellular carcinoma *via* gankyrin/AKT signaling. *Oncogene* 2019; **38**: 406-420 [PMID: 30115976 DOI: 10.1038/s41388-018-0440-8]
26 **Li J**, Diao H, Guan X, Tian X. Kinesin Family Member C1 (KIFC1) Regulated by Centrosome Protein E (CENPE)

Promotes Proliferation, Migration, and Epithelial-Mesenchymal Transition of Ovarian Cancer. *Med Sci Monit* 2020; **26**: e927869 [PMID: 33361741 DOI: 10.12659/MSM.927869]

27 **Liu C**, Wang L, Liu X, Tan Y, Tao L, Xiao Y, Deng P, Wang H, Deng Q, Lin Y, Jie H, Zhang H, Zhang J, Peng Y, Zhou Z, Sun Q, Cen X, Zhao Y. Cytoplasmic SHMT2 drives the progression and metastasis of colorectal cancer by inhibiting β-catenin degradation. *Theranostics* 2021; **11**: 2966-2986 [PMID: 33456583 DOI: 10.7150/thno.48699]

28 **Zhang Y**, Wang X. Targeting the Wnt/β-catenin signaling pathway in cancer. *J Hematol Oncol* 2020; **13**: 165 [PMID: 33276800 DOI: 10.1186/s13045-020-00990-3]

29 **Wang T**, Wang J, Ren W, Liu ZL, Cheng YF, Zhang XM. Combination treatment with artemisinin and oxaliplatin inhibits tumorigenesis in esophageal cancer EC109 cell through Wnt/β-catenin signaling pathway. *Thorac Cancer* 2020; **11**: 2316-2324 [PMID: 32657048 DOI: 10.1111/1759-7714.13570]

30 **Wei B**, Wang Y, Wang J, Cai X, Xu L, Wu J, Liu W, Gu Y, Guo W, Xu Q. Apatinib suppresses tumor progression and enhances cisplatin sensitivity in esophageal cancer *via* the Akt/β-catenin pathway. *Cancer Cell Int* 2020; **20**: 198 [PMID: 32514243 DOI: 10.1186/s12935-020-01290-z]

31 **Zhang L**, Zhou S, Guo E, Chen X, Yang J, Li X. DCLK1 inhibition attenuates tumorigenesis and improves chemosensitivity in esophageal squamous cell carcinoma by inhibiting β-catenin/c-Myc signaling. *Pflugers Arch* 2020; **472**: 1041-1049 [PMID: 32533239 DOI: 10.1007/s00424-020-02415-z]

32 **Vora SM**, Fassler JS, Phillips BT. Centrosomes are required for proper β-catenin processing and Wnt response. *Mol Biol Cell* 2020; **31**: 1951-1961 [PMID: 32583737 DOI: 10.1091/mbc.E20-02-0139]

World Journal of Gastrointestinal Oncology

Submit a Manuscript: https://www.f6publishing.com

World J Gastrointest Oncol 2022 July 15; 14(7): 1252-1264

DOI: 10.4251/wjgo.v14.i7.1252

ISSN 1948-5204 (online)

ORIGINAL ARTICLE

Basic Study

Claudin 18.2 is a potential therapeutic target for zolbetuximab in pancreatic ductal adenocarcinoma

Xi Wang, Cheng-Sheng Zhang, Xu-Yuan Dong, Yuan Hu, Bao-Jun Duan, Jun Bai, Yin-Ying Wu, Lin Fan, Xin-Hua Liao, Ye Kang, Peng Zhang, Meng-Yang Li, Jiao Xu, Zhi-Jun Mao, Hui-Tong Liu, Xiao-Long Zhang, Li-Fei Tian, En-Xiao Li

Specialty type: Pathology

Provenance and peer review: Unsolicited article; Externally peer reviewed.

Peer-review model: Single blind

Peer-review report's scientific quality classification

Grade A (Excellent): 0
Grade B (Very good): 0
Grade C (Good): C, C
Grade D (Fair): 0
Grade E (Poor): 0

P-Reviewer: Plougmann JI, Denmark; Sato H, Japan
A-Editor: Nakaji K, Japan

Received: December 31, 2021
Peer-review started: December 31, 2021
First decision: March 10, 2022
Revised: March 22, 2022
Accepted: May 28, 2022
Article in press: May 28, 2022
Published online: July 15, 2022

Xi Wang, Xu-Yuan Dong, Yuan Hu, Yin-Ying Wu, En-Xiao Li, Department of Medical Oncology, The First Affiliated Hospital of Xi'an Jiaotong University, Xi'an 710061, Shaanxi Province, China

Xi Wang, Bao-Jun Duan, Jun Bai, Department of Medical Oncology, Shaanxi Provincial People's Hospital, Xi'an 710068, Shaanxi Province, China

Cheng-Sheng Zhang, Ye Kang, Meng-Yang Li, Jiao Xu, Department of Cancer Precision Medicine, Med-X Institute, The First Affiliated Hospital of Xi'an Jiaotong University, Xi'an 710061, Shaanxi Province, China

Cheng-Sheng Zhang, Peng Zhang, Cancer Center, The First Affiliated Hospital of Xi'an Jiaotong University, Xi'an 710061, Shaanxi Province, China

Lin Fan, Xin-Hua Liao, Department of General Surgery, The First Affiliated Hospital of Xi'an Jiaotong University, Xi'an 710061, Shaanxi Province, China

Zhi-Jun Mao, Xiao-Long Zhang, Li-Fei Tian, Department of General Surgery, Shaanxi Provincial People's Hospital, Xi'an 710068, Shaanxi Province, China

Hui-Tong Liu, Department of Orthopedics, Shaanxi Provincial People's Hospital, Xi'an 710068, Shaanxi Province, China

Corresponding author: En-Xiao Li, PhD, Professor, Department of Medical Oncology, The First Affiliated Hospital of Xi'an Jiaotong University, No. 277 West Yanta Road, Xi'an 710061, Shaanxi Province, China. doclienxiao@sina.com

Abstract

BACKGROUND

Pancreatic ductal adenocarcinoma (PDAC) is frequently diagnosed and treated in advanced tumor stages with poor prognosis. More effective screening programs and novel therapeutic means are urgently needed. Recent studies have regarded tight junction protein claudin 18.2 (CLDN18.2) as a candidate target for cancer treatment, and zolbetuximab (formerly known as IMAB362) has been developed against CLDN18.2. However, there are few data reported thus far related to the clinicopathological characteristics of CLDN18.2 expression for PDAC.

AIM
To investigate the expression of CLDN18.2 in PDAC patients and subsequently propose a new target for the treatment of PDAC.

METHODS
The Cancer Genome Atlas, Genotype-Tissue Expression, Gene Expression Omnibus, and European Genome-phenome Archive databases were first employed to analyze the *CLDN18* gene expression in normal pancreatic tissue compared to that in pancreatic cancer tissue. Second, we analyzed the expression of CLDN18.2 in 93 primary PDACs, 86 para-cancer tissues, and 13 normal pancreatic tissues by immunohistochemistry. Immunostained tissues were assessed applying the histoscore. subsequently, they fell into two groups according to the expression state of CLDN18.2. Furthermore, the correlations between CLDN18.2 expression and diverse clinicopathological characteristics, including survival, were investigated.

RESULTS
The gene expression of *CLDN18* was statistically higher ($P < 0.01$) in pancreatic tumors than in normal tissues. However, there was no significant correlation between *CLDN18* expression and survival in pancreatic cancer patients. CLDN18.2 was expressed in 88 (94.6%) of the reported PDACs. Among these tumors, 50 (56.8%) cases showed strong immunostaining. The para-cancer tissues were positive in 81 (94.2%) cases, among which 32 (39.5%) of cases were characterized for strong staining intensities. Normal pancreatic tissue was identified solely *via* weak immunostaining. Finally, CLDN18.2 expression significantly correlated with lymph node metastasis, distant metastasis, nerve invasion, stage, and survival of PDAC patients, while there was no correlation between CLDN18.2 expression and localization, tumor size, patient age and sex, nor any other clinicopathological characteristic.

CONCLUSION
CLDN18.2 expression is frequently increased in PDAC patients. Thus, it may act as a potential therapeutic target for zolbetuximab in PDAC.

Key Words: Pancreatic ductal adenocarcinoma; Claudin 18.2, Immunohistochemistry; Therapeutic target; Diagnosis; Prognosis

Core Tip: Claudin 18.2 (CLDN18.2) shows a high rate of expression in pancreatic ductal adenocarcinoma (PDAC) but displays little expression in normal pancreatic tissue. CLDN18.2 expression significantly correlates with lymph node metastasis, distant metastasis, nerve invasion, stage, and survival of PDAC patients. Thus, CLDN18.2 may act as an ideal therapeutic target, and a considerable number of PDAC patients may be in eligible for a CLDN18.2-targeted therapeutic approach.

Citation: Wang X, Zhang CS, Dong XY, Hu Y, Duan BJ, Bai J, Wu YY, Fan L, Liao XH, Kang Y, Zhang P, Li MY, Xu J, Mao ZJ, Liu HT, Zhang XL, Tian LF, Li EX. Claudin 18.2 is a potential therapeutic target for zolbetuximab in pancreatic ductal adenocarcinoma. *World J Gastrointest Oncol* 2022; 14(7): 1252-1264
URL: https://www.wjgnet.com/1948-5204/full/v14/i7/1252.htm
DOI: https://dx.doi.org/10.4251/wjgo.v14.i7.1252

INTRODUCTION

Pancreatic cancer is the eleventh most frequently diagnosed cancer and the sixth most common cause of cancer-related deaths in China, being only slightly lower than the rates reported from the United States and United Kingdom[1]. However, the overall incidence and mortality rates of pancreatic cancer are expected to increase further[2]. Pancreatic ductal adenocarcinoma (PDAC) accounts for more than 90% of all pancreatic neoplasms. Yet, there is no effective screening tool for early detection of PDAC, and patients lack specific clinical symptoms at early stages. Thus, most patients are usually diagnosed at the advanced stage with distant metastases and are not suitable for curable surgery, aggravating its poor prognosis[3]. It is therefore urgent to develop nonsurgical therapeutic approaches for effective treatment of PDAC.

For systemic palliative treatment of unresectable PDAC patients, chemotherapy is the first-line approach. The majority of patients are treated with FOLFIRINOX (5-fluorouracil/irinotecan/oxaliplatin)[4] and gemcitabine-based chemotherapy, including combinations of gemcitabine and nanoparticle albumin-bound paclitaxel (nab-paclitaxel)[5], gemcitabine, and erlotinib[6]. These combination therapies exhibit an improvement in median and 1-year survival rates as compared with gemcitabine alone. However, the chemosensitivity of PDAC is moderate, and as the benefits of adding erlotinib are marginal but the toxicity of the combination is higher, erlotinib has not been widely adopted[6].

Immunotherapy has great success in treating many types of cancers, whereas it has not been very successful against PDAC. Most clinical outcomes of immunotherapy with immune checkpoint inhibitors, chimeric antigen receptor T cells, immunomodulators, and vaccines were not satisfactory[7]. Therefore, immunotherapy is not recommended as a conventional treatment by the guidelines for PDAC. However, we cannot totally deny the immunotherapeutic potential. With a deeper level understanding of the PDAC immunology and mechanisms of immunotherapeutic resistance, immunotherapy may achieve great success in treating PDAC. A clinical trial showed that BL-8040, a CXCR4 antagonist, in combination with pembrolizumab and chemotherapy for pancreatic cancer enhanced the objective response rate, disease control rate, and median duration in PDAC[8]. Another study revealed that combination treatment of a vaccine p53MVA and pembrolizumab (an immune checkpoint inhibitor of programmed death protein 1) had higher cure rate or longer survival time than the control group, but there were still many patients who suffered grade 1-2 adverse events, despite the small sample size[9]. Therefore, combination immunotherapy with or without chemoradiotherapy may be one of the future directions of immunotherapy application for treating PDAC. Novel treatments and early detection tools are still urgently needed for this highly aggressive and lethal disease.

Claudin 18 (CLDN18) is a highly specific tight junction protein, encoded by the *CLDN18* gene, regulating paracellular barrier functions. Its two isoforms are known as isoform 1 (CLDN18.1) and isoform 2 (CLDN18.2). Expression of CLDN18.2 has been revealed to be confined to short lived differentiated gastric epithelial cells of the primary gastric carcinoma and normal gastric mucosa, which suggesting its potential as a candidate therapeutic target in cancer treatment[10,11]. CLDN18.2 expression has also been reported in PDAC[12,13].

Zolbetuximab is a highly potent and tumor cell-selective therapeutic antibody that directly targets the tight junction molecule CLDN18.2, a proliferation-promoting transmembrane protein[14]. Zolbetuximab is currently in clinical testing. The phase II clinical trial (FAST: NCT01630083) revealed that zolbetuximab combined with first-line chemotherapy significantly improved the overall survival, progression-free survival and the objective response rate with acceptable safety and tolerability in patients with CLDN18.2-positive advanced/recurrent gastric cancers and gastroesophageal junction cancers[15]. Furthermore, health-related quality of life was sustained for a longer duration in patients who received zolbetuximab plus chemotherapy compared with those who received chemotherapy alone [16]. This prompted us to consider clinical testing of zolbetuximab in PDAC. Since few data are available regarding the clinicopathological characteristics of CLDN18.2 expression for PDAC, this study was designed and carried out as a part of the prefeasibility program for such clinical trials.

MATERIALS AND METHODS

Data extraction from multiple databases

Expression of the *CLDN18* gene in normal pancreatic tissue and pancreaticcancer was analyzed using TNMplot.com (https://tnmplot.com/analysis/)[17] and Xena (http://xena.ucsc.edu/compare-tissue/)[18], which allow for online analysis of The Cancer Genome Atlas (TCGA), Genotype-Tissue Expression, and Gene Expression Omnibus (GEO) data. In this study, TCGA and GEO offered the pancreatic tumor samples and solid tissue normal samples from individuals with cancer, while the Genotype-Tissue Expression offered normal tissue from individuals who did not have cancer. In addition, we used KM plotter to assess the effect of CLDN18 on survival in pancreatic cancer (https://kmplot.com/analysis/), which is based on the databases of TCGA, GEO, and European Genome-phenome Archive.

Sample collection

The primary tumor samples and para-cancer tissues as well as normal pancreatic tissues were collected between 2018 and 2020 at the Institute of Pathology of the First Affiliated Hospital of Xi'an Jiaotong University (Xi'an, Shaanxi Province, China). We included patients with pathologically confirmed PDAC. Patients with a tumor type different from PDAC were excluded. Each tissue had gone through gross sectioning and histological detection by qualified pathologists. The date of patients' deaths was collected from the hospital records. Follow-up data of the patients who were still alive were obtained from the telephone follow-up and hospital records. The histopathological diagnosis and grading followed the recommendations of the World Health Organization, and the tumor stage was confirmed in accordance with the 8th edition of American Joint Committee on Cancer staging system. Sampling of tissues and clinical data for scientific purposes was approved by the ethics committee of The First

Affiliated Hospital of Xi'an Jiaotong University. Additionally, tissue microarrays spotted with samples of primary PDAC and para-cancer tissues were bought from Shanghai Zhuo hao Pharmaceutical Technology Co., LTD (Shanghai, China) (Cat. No. PAC1602).

Immunohistochemistry

Immunohistochemistry (IHC) was performed on slides of 4% buffered formalin-fixed paraffin-embedded samples. Deparaffinized tissue slice were stained with hematoxylin and eosin. Immunohistochemical CLDN18.2 staining used the anti-CLDN18.2 antibody (Rabbit monoclonal EPR19202, Cat No. ab222512; Abcam, Cambridge, United Kingdom) in 1:500 dilution on a BOND-MAX automated staining system with Leica Bond Polymer Refine Detection Kit (Leica Biosystems, Wetzlar, Germany).

Scoring of CLDN18.2 staining

Scoring of 93 primary PDACs, 86 para-cancer tissues, and 13 normal pancreatic tissues was assessed by using a semi-quantitative pathology histoscore (H-score), defined as a method combined both percentages of positive-expression cells in the tissue slice and immunostaining intensities (hereinafter referred to as IHC-score). The IHC-score was on account of the membranous staining intensity level of CLDN18.2 from 0 to 1+ (weak), 2+ (intermediate), or 3+ (strong). Only membranous staining was retained for scoring. Nuclear and/or cytoplasmic CLDN18.2 expression was just noted but not scored. Tissue was assessed as IHC-score 0 (no staining was detectable), 1+ (faint membranous staining was partially showed), 2+ (moderate membranous staining was observed), or 3+ (strong membranous staining was present in the tissue section). In brief, the H-score was calculated according to the formula: (0 × percentage of immunonegative cells) + (1 × percentage of weakly stained cells) + (2 × percentage of intermediately stained cells) + (3 × percentage of strongly stained cells). Thus, the H-scoring ranged from 0 (a tissue sample that is completely negative) to a maximum of 300 (a tissue sample in which all the cells show a 3+ staining), which can separate samples with a predominantly high staining intensity from samples with a predominantly low staining intensity more distinctively. All samples of this study were assessed by two pathologists working independently. In case of discrepancies in the assessments, the sections were discussed to reach a final agreement.

For the purpose of finding correlations between CLDN18.2 expression and clinicopathological characteristics of PDAC patients, the tissues were divided into two groups according to the median H-score: negative/low (≤ median) and positive/high (> median).

Assessment of heterogeneous expression

During the process of reviewing both IHC-score and H-score, we found the obvious intratumoral heterogeneity in PDAC. Due to lack of accredited guideline to evaluate the heterogeneity between PDAC patients, some literature materials were referenced and we classified the heterogeneity according to the IHC-score, if 3+ and 0 were present meanwhile in one tumor tissue and accounted for more than 50% combined, we thought the strong heterogeneous expression was showed[14]. Additionally, we assessed the immunostaining patterns of these heterogeneous tumors. Some tumor cells of PDAC showed diffusely distribution with low or no IHC staining, which we referred to as "scattered". Another heterogeneity pattern of tumors with a "downward gradient" pattern displayed an obvious decline in intensity of the immunostaining towards the deep of the tissue.

Statistical analysis

SPSS version 24.0 (IBM Corp., Armonk, NY, United States) was used for statistical analyses. For assessing the correlation between non-ordinal variables, we applied the χ^2 test and Fisher's exact test. To make up for the false discovery rate in the correlations, we used the Simes' procedure, also known as Benjamini-Hochberg procedure. Multivariate analysis was performed to evaluate if a significant factor correlated to CLDN18.2 expression was an independent factor. The Kaplan-Meier method was used to determine median survival with 95%CIs and Log-rank test was applied to assess the differences between median survivals. Furthermore, Cox's regression model was performed for the Multivariate survival analysis. $P < 0.05$ was accepted as demonstration of significant differences.

RESULTS

Identification of gene expression data of CLDN18 in pancreatic cancer from databases

The TNMplot.comanalysis involved 108 normal tissues and 248 pancreatic tumors. We found that the gene expression of *CLDN18* in pancreatic tumors was much higher than that in normal tissues, and the difference was statistically significant ($P < 0.01$) (Figure 1A). Xena analysis of the gene expression of *CLDN18* in 167 normal tissues and 183 pancreatic tumors yielded results that were consistent with those from TNMplot.com (Figure 1B). KM plotter assessment of the effect of *CLDN18* expression on survival in 177 pancreatic cancer patients revealed no significant correlation between *CLDN18* expression and survival (Figure 1C).

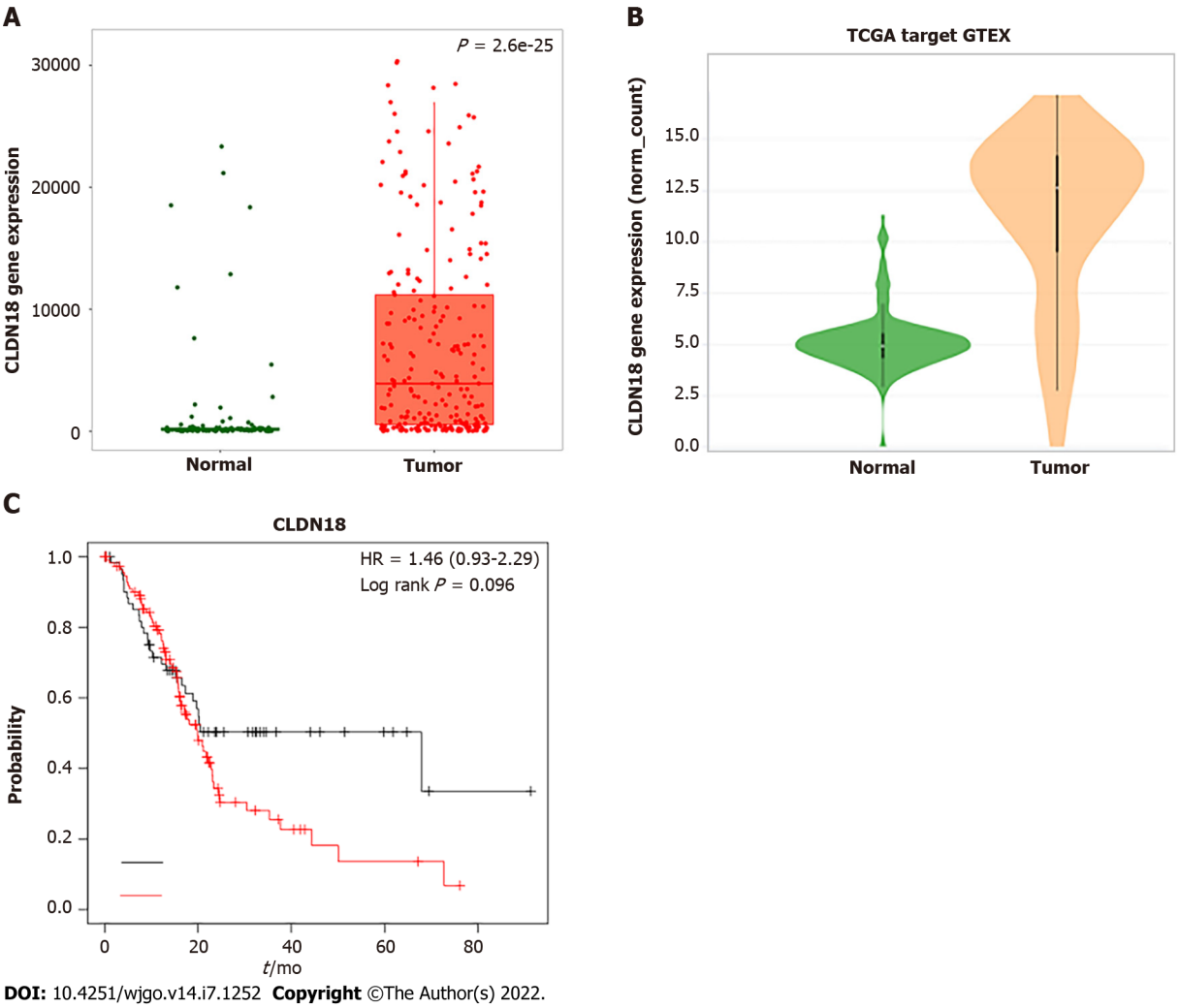

DOI: 10.4251/wjgo.v14.i7.1252

Figure 1 Online analysis of gene expression of claudin 18 and its effected survival in pancreatic cancer using the database. A: Analysis of claudin18 expression in normal pancreatic tissue and pancreatic cancer using the TNMplot.com (https://tnmplot.com/analysis/) based on The Cancer Genome Atlas (TCGA), Genotype-Tissue Expression (GTEX), and Gene Expression Omnibus (GEO) databases; B: Analysis of claudin18 expression in normal pancreatic tissue and pancreatic cancer using Xena (http://xena.ucsc.edu/compare-tissue/) based on TCGA and GTEX databases; C: Assessment of the claudin18 effect on survival in pancreatic cancer using KM plotter (https://kmplot.com/analysis/) based on GEO, European Genome-phenome Archive, and TCGA databases. HR: Hazard ratio.

CLDN18.2 expression in non-neoplastic pancreatic tissue

We observed a set of non-neoplastic pancreatic tissue samples (n = 13) for CLDN18.2 expression. All histological cell types and distinct structures of normal pancreatic tissue, such as duct cells, acinar cells, and endocrine cells, were observed. CLDN18.2-specific staining was not detectable in any of the normal pancreatic tissue cells. Representative images are displayed in Supplementary Figure 1.

CLDN18.2 expression in para-cancer tissue

Eighty-six para-cancer tissues of PDAC were analyzed for CLDN18.2 expression. We found that 81 (94.2%) cases showed the positive fraction ≥ 1%, in which 32 (39.5%) cases were characterized as strong staining intensities (Table 1).

CLDN18.2 expression in primary PDAC

In total, 93 cases of primary PDAC were analyzed for CLDN18.2 expression. The average age was 63.48 (51.6%). PDAC samples were poorly differentiated (*i.e.* grade 3). Twenty-seven (29.0%) cases were classified as pT3/4. Thirty-six (38.7%) cases had already-confirmed lymph node invasion (pN1/2), twenty-three (24.7%) cases were confirmed as nerve invasion, and fourteen (15.1%) cases presented distant metastasis at the time of first diagnosis (Table 2).

CLDN18.2 presented quite high expression rate in PDAC patients, with 88 (94.6%) PDACs showed positive expression (Table 1), in which most patients showed compositive IHC-intensity. Fifty (56.8%) cases were scored up to IHC 3+, eighty-six (97.7%) cases were scored equivalent to but no more than IHC 2+, seventy-seven (87.5%) cases were no higher than IHC 1+ (representative images are displayed in Figure 2A). The supreme expression of CLDN18.2 IHC 3+ was discovered with 94.0% of tumor cells,

Table 1 Classification of sample types investigated by claudin 18.2 staining

Sample type	Samples, *n*	CLDN18.2 expression	
		Positive fraction ≥ 1%, *n* (%)	Staining intensity = 3+, *n* (%)
PDAC	93	88 (94.6)	50 (56.8)
Para-cancerous	86	81 (94.2)	32 (39.5)
Normal	13	0 (0.0)	0 (0.0)

CLDN18.2: Claudin 18.2; PDAC: Pancreatic ductal adenocarcinoma.

observable in 1 case. The IHC-score distribution of CLDN18.2 in this study is exhibited in Figure 2B. Figure 2C summed up the distribution and frequency of the H-scores.

CLDN18.2 correlates with lymph node metastasis, distant metastasis, nerve invasion, and stage

Group comparison analysis revealed that CLDN18.2 correlated with lymph node metastasis, distant metastasis, nerve invasion, and stage (Table 2). In our study, the N category was assessed in 93 cases, including N0 (n = 57), N1 (n = 27), and N2 (n= 9). CLDN18.2 positivity showed the following distribution of N categories: N0 in 23 (40.4%) cases; N1 in 15 (55.6%) cases; and N2 in 8 (88.9%) cases. There was a statistically significant difference between them (P = 0.019). When we stratified the lymph node metastasis, we found the difference also existed (P = 0.034). CLDN18.2 expression was predominantly increased in the cases of lymph node invasion (pN1/2). A similar observation was also made for distant metastasis. Compared to patients with M0, the expression of CLDN18.2 significantly increased in PDAC patients with distant metastases (78.6% *vs* 44.3%, P = 0.022). Moreover, we found that 17 cases with nerve invasion showed positive CLDN18.2 expression, while the patients without nerve invasion showed much lower expression (73.9% *vs* 38.5%, P = 0.006), the difference between two group was statistically significant.

Furthermore, it is interesting to note that the relative proportion of positive CLDN18.2 expression was not different between the four stage groups (I, II, III and IV). But when we stratified it, the correlation was observed. CLDN18.2 expression was significantly increased in III + IV stages than that in I + II stages (70.4% *vs* 40.9%, P = 0.012). The cases with stage IV showed significantly higher CLDN18.2 expression than I + II + III stages (78.6% *vs* 44.3%, P = 0.022).

To evaluate if any of the significant factors correlated to CLDN18.2 expression was an independent factor, we performed multivariate analysis. We found that the significant factors of stage, lymph node metastasis, distant metastasis, and nerve invasion related to the expression of CLDN18.2 as independent factors. Corresponding P values were all less than 0.05.

We demonstrated that the expression of CLDN18.2 had no relevance with T category and grading (Table 2). No other clinicopathological characteristic of PDAC patient, for example, age, sex, tumor site, CA199, local infiltration, vascular invasion, or vessel carcinoma embolus, correlated with CLDN18.2 expression.

CLDN18.2 is frequently heterogeneously expressed in PDAC

In our study, almost all tumors showed compositive IHC-intensity with IHC 3+ and IHC 0 were present meanwhile in one tumor tissue, revealing the expression of CLDN18.2 had a high tendency to heterogeneous expression. In order to elaborate the degree of tumor heterogeneity, it was considered that if both strong and negative expressions were existed simultaneously and accounted for more than 50% combined, the tumor showed strong heterogeneity. Nine (9.7%) tumors met these criteria. We assessed the different immunostaining distribution patterns of these heterogeneous tumors. Six (66.7%) PDACs showed a "scattered" pattern, which had diffusely distribution with low or no IHC staining in tumor cells. Three (33.3%) PDACs displayed a "downward gradient", with weaker staining intensity towards the depth of the tumor. Representative images are displayed in Supplementary Figure 2.

CLDN18.2 and survival

Tumor-specific survival data were available in 80 cases and no correlation was discovered between the cancer specific survival and expression of CLDN18.2 (Figure 3A). Nevertheless, when stratified analysis was applied to verify the influence of diverse CLDN18.2 expression on various tumor stages (American Joint Committee on Cancer) and different N category and M category, the correlation was discovered. The study revealed that the expression of CLDN18.2 correlated with cancer survival of PDAC patients with stage III, stage IV, and distant metastasis meaningfully (Figure 3B-I). This suggests the CLDN18.2-positive patients with late stage and distant metastasis may have a poorer prognosis.

Table 2 Claudin 18.2 expression and correlation with clinicopathological characteristics of pancreatic ductal adenocarcinoma

Clinicopathological parameter	Variable	Total valid, *n* (%)	CLDN18.2 expression		*P* value
			Positive, *n* (%)	Negative, *n* (%)	
Age	< 63	49 (52.7)	23 (46.9)	26 (53.1)	0.680
	≥ 63	44 (47.3)	23 (52.3)	21 (47.7)	
Sex	Female	44 (47.3)	24 (54.5)	20 (45.5)	0.409
	Male	49 (52.7)	22 (44.9)	27 (55.1)	
Localization	Head and neck	52 (65.0)	23 (44.2)	29 (55.8)	0.350
	Body and tail	28 (35.0)	16 (57.1)	12 (42.9)	
CA199	High[1]	65 (81.3)	33 (50.8)	32 (49.2)	0.570
	Normal[2]	15 (18.7)	6 (40.0)	9 (60.0)	
T category	T1	14 (15.1)	6 (42.9)	8 (57.1)	0.773
	T2	47 (50.5)	24 (51.1)	23 (48.9)	
	T3	26 (28.0)	14 (53.8)	12 (46.2)	
	T4	6 (6.4)	2 (33.3)	4 (66.7)	
	T1 + T2	61 (65.6)	30 (49.2)	31 (50.8)	1.000
	T3 + T4	32 (34.4)	16 (50.0)	16 (50.0)	
	T1	14 (15.1)	6 (42.9)	8 (57.2)	0.773
	T2 + T3 + T4	79 (84.9)	40 (50.6)	39 (49.4)	
N category	N0	57 (61.3)	23 (40.4)	34 (59.6)	0.019[a]
	N1	27 (29.0)	15 (55.6)	12 (44.4)	
	N2	9 (9.7)	8 (88.9)	1 (11.1)	
	N0	57 (61.3)	23 (40.4)	34 (59.6)	0.034[a]
	N1 + N2	36 (38.7)	23 (63.9)	13 (36.1)	
M category	M0	79 (84.9)	35 (44.3)	44 (55.7)	0.022[a]
	M1	14 (15.1)	11 (78.6)	3 (21.4)	
AJCC stage	I	38 (40.9)	16 (42.1)	22 (57.9)	0.058
	II	28 (30.1)	11 (39.3)	17 (60.7)	
	III	13 (14.0)	8 (61.5)	5 (38.5)	
	IV	14 (15.0)	11 (78.6)	3 (21.4)	
	I	38 (40.9)	16 (42.1)	22 (57.9)	0.293
	II + III + IV	55 (59.1)	30 (54.5)	25 (45.5)	
	I + II	66 (71)	27 (40.9)	39 (59.1)	0.012[a]
	III + IV	27 (29)	19 (70.4)	8 (29.6)	
	I + II + III	79 (84.9)	35 (44.3)	44 (55.7)	0.022[a]
	IV	14 (15.1)	11 (78.6)	3 (21.4)	
Local infiltration	Yes	57 (71.3)	29 (50.9)	28 (49.1)	0.625
	No	23 (28.7)	10 (43.5)	13 (56.5)	
Vascular invasion	Yes	12 (15.0)	7 (58.3)	5 (41.7)	0.542
	No	68 (85.0)	32 (47.1)	36 (52.9)	
Nerve invasion	Yes	23 (28.7)	17 (73.9)	6 (26.1)	0.006[b]
	No	57 (71.3)	22 (38.6)	35 (61.4)	
Vessel carcinoma embolus	Yes	27 (33.8)	13 (48.1)	14 (51.9)	1.000

	No	53 (66.2)	26 (49.1)	27 (50.9)	
Grading	G1/G2	45 (48.4)	20 (44.4)	25 (55.6)	0.409
	G3	48 (51.6)	26 (54.2)	22 (45.8)	

[a]$P < 0.05$.
[b]$P < 0.01$.
[1]High indicates CA199 > 39 U/mL.
[2]Normal indicates CA199 ≤ 39 U/mL.
AJCC: American Joint Committee on Cancer; CLDN18.2: Claudin 18.2.

DISCUSSION

PDAC is still difficult to diagnose and has a poor prognosis. The main aim of this study was to investigate CLDN18.2 expression in a large PDAC patient population using IHC and then find its correlation with diverse clinicopathological characteristics, including survival in order to detect possible distinctive features of CLDN18-positive PDACs and assess whether it is a suitable indication for clinical development of zolbetuximab, the therapeutic antibody directed against CLDN18.2.

Previous studies reported CLDN18 expression in 50%-90% of pancreatic cancer[12,13,19]. These studies involved patients with different cancer types and different stages, and they used different grade staining protocols and various anti-CLDN18 antibodies or sera, which is a drawback because of cross-reactivity to CLDN18.1. Furthermore, different approaches to analyze and score CLDN18 positivity status were implemented. Therefore, it was not suitable to completely rely on these data for a clinical development program. To further add to the validity and reliability of the obtained data, we used H-score to assess the CLDN18.2 expression, which combined both the fraction of stained tumor cells and intensity of cell surface staining. It can separate the sample's staining intensity more distinctively. Based on this, our study has the following major key findings, which are novel and support indications for clinical testing of zolbetuximab in PDAC patients.

The ideal therapeutic target should show high and specific expression in the tumor and show a very low or no expression in normal tissues. The majority of PDACs in our study showed a high rate of CLDN18.2 positivity, but all normal pancreatic tissue showed CLDN18.2 negativity. Thus, CLDN18.2 may act as an ideal therapeutic target, and a considerable number of PDAC patients would be eligible for a CLDN18.2-targeting therapeutic approach. However, we need to realize that the expression of a target does not necessarily mean that a patient will definitely benefit from the respective targeting drug. The clinical curative effect may depend on the intensity of expression[20], the fraction of positive tumor cells, or may not be associated at all to the target expression state[21]. Well-controlled clinical trials should be designed to investigate the therapeutic agent of our CLDN18.2-targeting approach. It is noteworthy that almost 86 (92.5%) tumors assessed in this study presented at least 2+ cell surface expression of CLDN18.2, and the majority of tumor tissue displayed a relatively high fraction of positive cells (median was 50%). This indicates that even if the clinical benefit requires high expression of CLDN18.2, a considerable number of PDAC patients will still be eligible.

In addition, the correlation analysis revealed that the fractions of positive cells and the intensities of membrane staining of CLDN18.2 were significantly higher in lymph node-positive tumors, distant metastatic tumors, nerve invasion tumors, and stage III/IV PDAC patients. Lymph node positivity and distant metastasis were independent factors for poor prognosis in PDAC[22]. Moreover, CLDN18.2 expression correlated to cancer survival of PDAC patients with stage III, stage IV, and distant metastasis meaningfully, which was not in accordance with the result from the database (Figure 1C and Figure 3). The reason for this inconsistency may be that the database analyzed the relevance between gene expression and cancer survival, whereas our research explored the relationship between protein expression and cancer survival. The survival data from the database was analyzed but not stratified. This result also needs to be verified in more substantial pancreatic cancer patients. Besides, CLDN18.2 expression was not associated with tumor size, differentiation, localization, CA199, local infiltration, vascular invasion, nor vessel carcinoma embolus. These data revealed that CLDN18.2 might play a role as an oncogene in the development and progression of pancreatic cancer, and the expression of this gene could promote the aggressiveness of tumor cells. Therefore, CLDN18.2 has the potential to act as a risk assessment and as a prognostic indicator for PDAC.

While some researchers have reported weak expression of CLDN18 in normal pancreatic tissue[19], others have denied it. Our study confirmed that CLDN18.2 was not expressed in normal pancreatic tissue including all different cell types prevalent in the pancreas. More interestingly, we found that CLDN18.2 expression was increased in para-cancer tissues and higher in PDAC tissues. This gradual upward trend of CLDN18.2 expression has not been reported before, which suggests that CLDN18.2 is silenced in normal pancreatic tissue but strongly activated during the course of malignant occurrence and development. However, there is little research reporting the molecular mechanism of CLDN18.2. Combined with the previous correlation analysis results, we thus hypothesize that CLDN18.2 may be

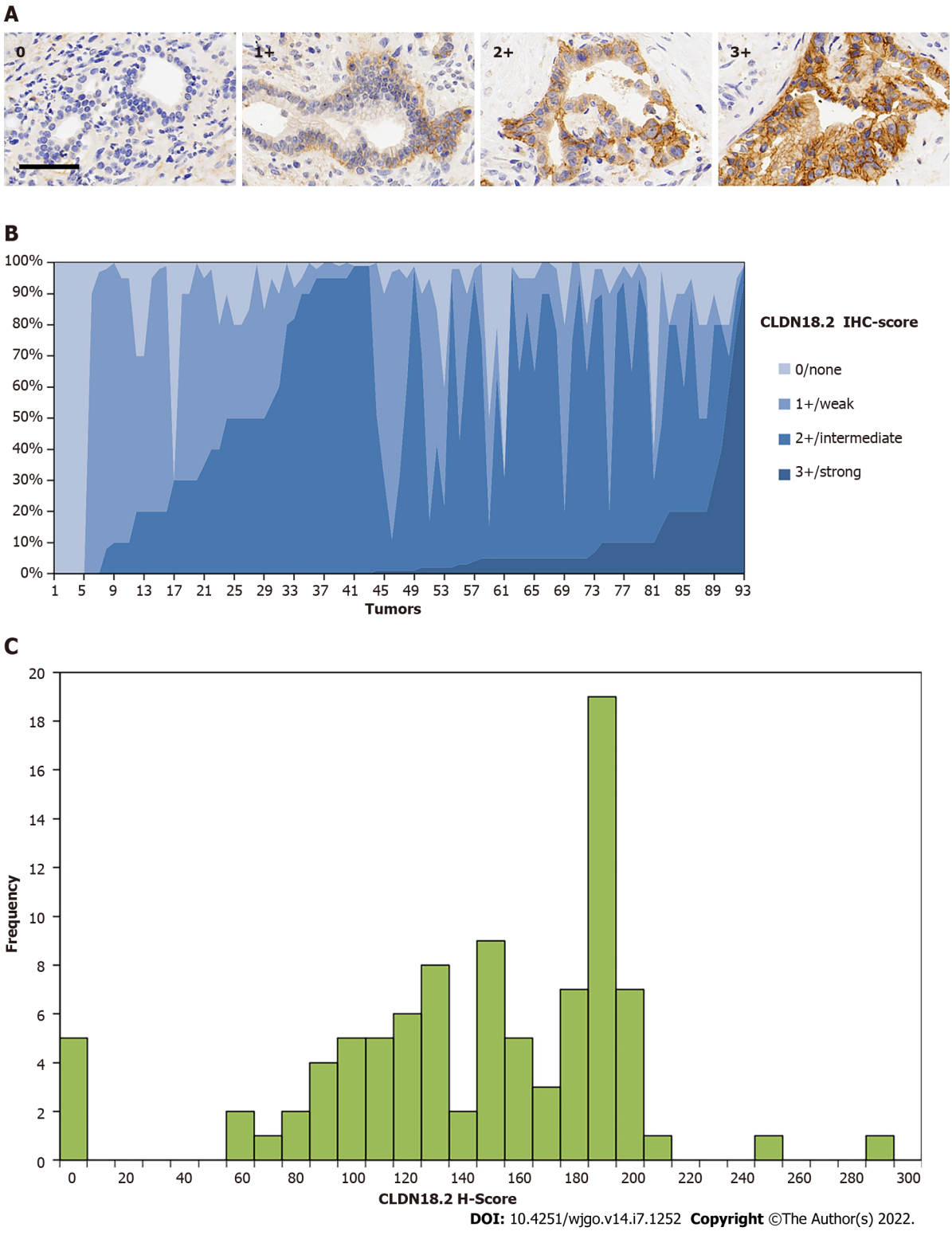

DOI: 10.4251/wjgo.v14.i7.1252

Figure 2 Expression of claudin 18.2 in primary pancreatic ductal adenocarcinoma. A: Examples of claudin 18.2 (CLDN18.2)-positive pancreatic ductal adenocarcinoma tissues with 0/none, 1+/weak, 2+/intermediate, and 3+/ strong staining intensity. Scale bar 100 μm; B: Overall expression intensity of claudin 18.2. Eighty-eight (94.6%) primary pancreatic ductal adenocarcinoma tissues showed positivity for CLDN18.2 expression. In the positive cases, most showed compositive immunohistochemistry (IHC)-intensity. Fifty (56.8%) cases were scored up to IHC 3+, 86 (97.7%) cases were scored up to but no higher than IHC 2+, and 77 (87.5%) cases were no higher than IHC 1+; C: Histoscore (H-Score) distribution in the study. Minimum H-Score was 0; Maximum H-score was 292. Median H-score of positive tumors was 150.

involved in the tumor migration process, but further experiments are needed to test this hypothesis and explore the exact molecular mechanism of CLDN18.2.

Moreover, the differential expression of CLDN18.2 in normal pancreatic tissue and pancreatic neoplasm suggests that CLDN18.2 can be used as a diagnostic marker for PDAC. This has been reported in other studies. Li *et al*[23] reported the sensitivity of CLDN18 for identifying the gastric and pancreato-

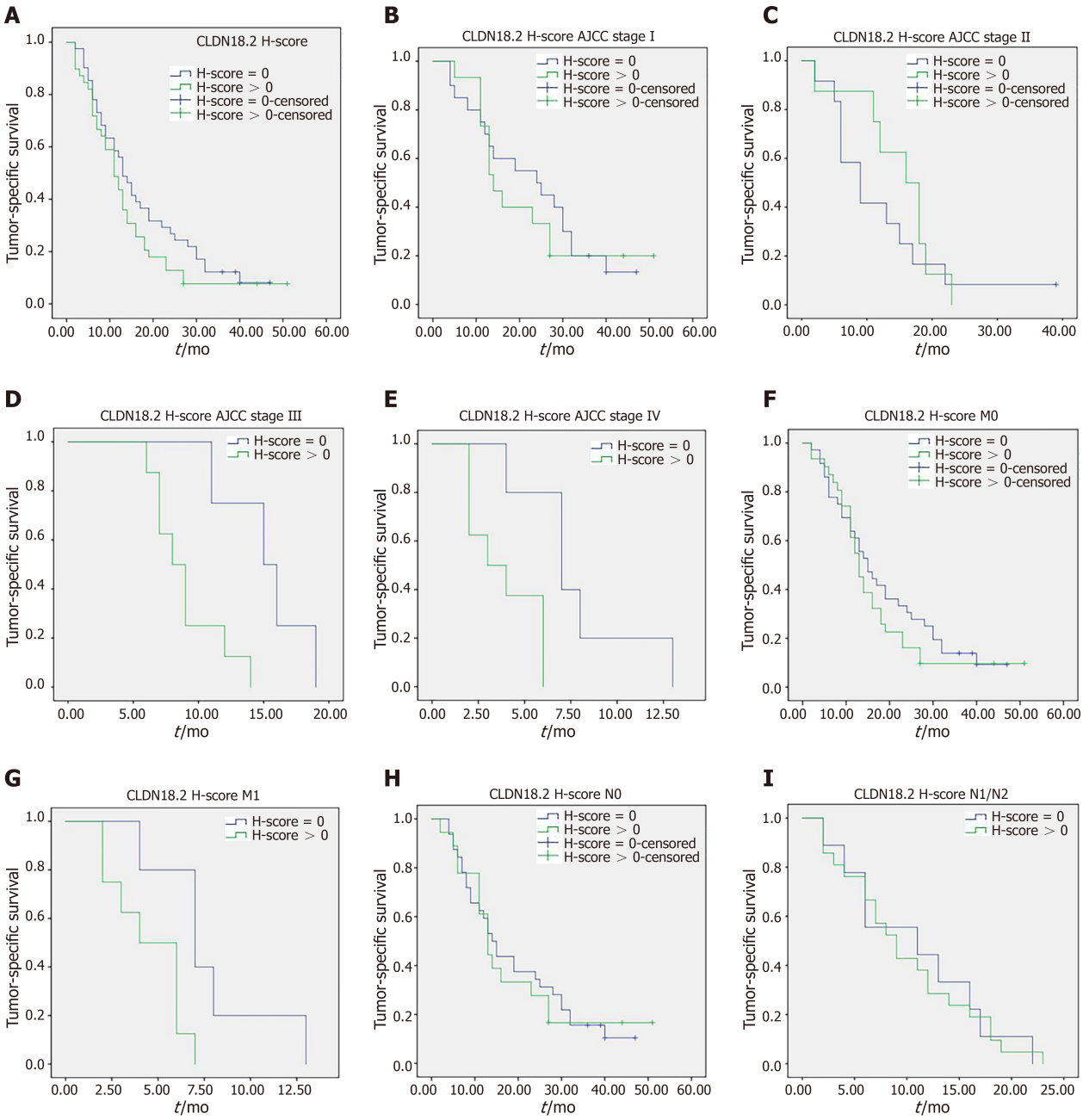

DOI: 10.4251/wjgo.v14.i7.1252

Figure 3 Claudin 18.2 and survival. A: There was no significant correlation between tumor-specific survival and claudin 18.2 expression in tumor cells (41 *vs* 39 patients; median survival 13 mo *vs* 11 mo; $P = 0.176$); B: 20 *vs* 15 patients in stage I disease with median survival 24 mo *vs* 14 mo ($P = 0.666$); C: 12 *vs* 8 patients in stage II disease with median survival 9 mo *vs* 16 mo ($P = 0.480$); D: 4 *vs* 8 patients in stage III disease with median survival 15 mo *vs* 8 mo ($P = 0.012$); E: 5 *vs* 8 patients in stage IV disease with median survival 7 mo *vs* 3 mo ($P = 0.009$); F: 36 *vs* 31 patients in M0 disease with median survival 15 mo *vs* 13 mo ($P = 0.351$); G: 5 *vs* 8 patients in M1 disease with median survival 7 mo *vs* 4 mo ($P = 0.024$); H: 32 *vs* 18 patients in N0 disease with median survival 14 mo *vs* 13 mo ($P = 0.825$); I: 9 *vs* 21 patients in N1/N2 disease with median survival 11 mo *vs* 9 mo ($P = 0.920$). *P* values were obtained *via* log-rank-test. AJCC: American Joint Committee on Cancer; H-score: Histoscore.

biliary tract as primary tumor sites was 79% and the specificity was 93%. The positive and negative predictive values were 76% and 94%, respectively, which indicated that CLDN18 represented a sensitive and specific marker for stomach and pancreatobiliary adenocarcinoma that might be a useful diagnostic tool in routine surgical pathology. However, CLDN18.2 heterogeneity poses a challenge to diagnostic evaluations. In the light of distributions of IHC-score and H-score, this research demonstrated a universal phenomenon of CLDN18.2 expression heterogeneity in PDAC (Supplementary Figure 2), and then we describe heterogeneity types, which likely bring huge challenges to scientific explore and clinical practice. For example, one small tumor specimen with a scattered pattern may lead a serious misjudgment of total expression rate. In addition, the occurrence of the "downward gradient" staining pattern that shows obvious decline in intensity of the immunostaining towards the depth of the tissue may have some impact on biopsy within the deep of PDAC tissue specimen, which mainly allow

evaluation of the superficial malignant tumor tissues. Therefore, we should obtain as much tissue as possible when taking a biopsy so that the accuracy of diagnosis can be further improved.

This study suffered from a few limitations that deserve to be underlined. First, our study was limited by the types of samples. We described and illustrated CLDN18.2 expression in PDAC but not in other types of pancreatic tumors, such as adenosquamous carcinoma and pancreatic endocrine neoplasms. Second, we were limited by the numbers of samples. More large-scale studies need to be conducted to further analyze CLDN18.2 expression in PDAC in the future.

CONCLUSION

In general, this research describes a specified illustration for the expression of CLDN18.2 and its relationship with different clinicopathological elements in PDAC. We conclude CLDN18.2 is a potential therapeutic target for the treatment of PDAC.

ARTICLE HIGHLIGHTS

Research background

Pancreatic ductal adenocarcinoma (PDAC) is frequently diagnosed and treated in advanced tumor stages with a poor prognosis. More effective screening programs and novel therapeutic means are urgently needed. The tight junction protein claudin 18.2 (CLDN18.2) has been proved as a novel candidate drug target for cancer treatment, and zolbetuximab (formerly known as IMAB362) has been developed against CLDN18.2. Due to the few data available for clinicopathological characteristics of CLDN18.2 expression in PDAC, this study was performed to evaluate CLDN18.2 expression and to determine whether it can act as a potential therapeutic target for PDAC patients.

Research motivation

Zolbetuximab is a highly potent and tumor cell-selective therapeutic antibody that directly targets the tight junction molecule CLDN18.2. Zolbetuximab is currently in clinical testing and has shown good therapeutic effect. This prompted us to consider clinical testing of zolbetuximab in PDAC. Since few data are available for clinicopathological characteristics of the expression of CLDN18.2 in PDAC, this study is part of the prefeasibility program for such clinical trials.

Research objectives

The present study designed to investigate the CLDN18.2 expression in PDAC patients, and subsequently analyze its relevance with diverse clinicopathological characteristics of PDAC, and then propose a novel target for the cancer treatment of PDAC.

Research methods

The databases, including The Cancer Genome Atlas, Genotype-Tissue Expression, Gene Expression Omnibus, and European Genome-phenome Archive, were used to analyze the expression of the *CLDN18* gene in normal pancreatic tissue and pancreatic cancer. Immunohistochemistry was used to analyze the expression of CLDN18.2 in 93 primary PDACs, 86 para-cancer tissues, and 13 normal pancreatic tissues. Immunostained tissues were assessed applying the histoscore and subsequently fell into two groups according to detection of any or no CLDN18.2 expression. Furthermore, the correlations between CLDN18.2 expression and diverse clinicopathological characteristics, including survival, were investigated.

Research results

Reports found in the searched databases showed that the gene expression of *CLDN18* in pancreatic tumors was much higher than that in normal tissues. Moreover, the difference was statistically significant ($P < 0.01$), and there was no significant correlation between CLDN18 expression and survival in pancreatic cancer patients. CLDN18.2 was expressed in 88 (94.6%) PDACs. Of these tumors, 50 (56.8%) cases showed strong immunostaining. The para-cancer tissues were positive in 81 (94.2%) cases, in which 32 (39.5%) cases were characterized as having strong staining intensities. Normal pancreatic tissue showed only weak immunostaining. CLDN18.2 expression significantly correlated with lymph node metastasis, distant metastasis, nerve invasion, stage, and survival of PDAC patients, while there was no correlation between CLDN18.2 expression and localization, tumor size, patient age and sex, nor any other clinicopathological characteristic.

Research conclusions

CLDN18.2 expression is frequently increased in PDAC patients. Thus, it may act as a potential

therapeutic target for zolbetuximab in pancreatic ductal adenocarcinoma.

Research perspectives

This study is part of the prefeasibility program for some clinical trials that applied zolbetuximab in PDAC patients.

ACKNOWLEDGEMENTS

The authors would like to acknowledge all staff members of the department of Cancer Precision Medicine, Med-X Institute for skillful technical assistance.

FOOTNOTES

Author contributions: Wang X, Zhang CS, Dong XY, Duan BJ, Bai J, Wu YY and Li EX designed and coordinated the study; Wang X, Hu Y, Kang Y, Li MY, Xu J and Zhang P performed the experiments and acquired and analyzed the data; Fan L and Liao XH supervised the study design and collected the clinical sample; Wang X and Zhang CS interpreted the data and wrote the manuscript; All authors contributed to the critical revisionfor important intellectual content and provided final approval of the manuscript.

Supported by the Basic Research Project of Natural Science of Shaanxi Province, No.2020JQ-943, 2021JQ-916 and 2021JQ-914; Research Project of Chinese Society of Clinical Oncology-Sai Sheng Fund, No. Y-2020Sciclone/qn-0181; Science and Technology Support Program of Shaanxi Provincial People's Hospital, No. 2021JY-26, 2021JY-38, 2021JY-50 and 2021BJ-13; Research Fund Project of Shaanxi Provincial People's Hospital, No. 2021YJY-18; and China Postdoctoral Science Foundation, No. 2021M702607.

Institutional review board statement: The study was reviewed and approved by the First Affiliated Hospital of Xi'an Jiaotong University Institutional Review Board (No. XJTU1AF2019LSL-C001).

Conflict-of-interest statement: The authors declare that the research was conducted in the absence of any commercial or financial relationships that could be construed as a potential conflict of interest.

Data sharing statement: No additional data are available.

Country/Territory of origin: China

ORCID number: Xi Wang 0000-0001-9516-0397; Cheng-Sheng Zhang 0000-0003-4792-7009; Xu-Yuan Dong 0000-0003-2037-7852; Yuan Hu 0000-0003-3267-1565; Bao-Jun Duan 0000-0002-8375-7951; Jun Bai 0000-0002-9063-3631; Yin-Ying Wu 0000-0002-4132-2714; Lin Fan 0000-0001-8260-1886; Xin-Hua Liao 0000-0003-2171-9287; Ye Kang 0000-0002-5735-8295; Peng Zhang 0000-0002-5673-4404; Meng-Yang Li 0000-0001-8270-2994; Jiao Xu 0000-0002-6702-8855; Zhi-Jun Mao 0000-0001-5689-5307; Hui-Tong Liu 0000-0003-4585-7932; Xiao-Long Zhang 0000-0003-3107-7046; Li-Fei Tian 0000-0001-8374-3683; En-Xiao Li 0000-0001-5225-0173.

S-Editor: Zhang H
L-Editor: A
P-Editor: Yu HG

REFERENCES

1 **Qiu H**, Cao S, Xu R. Cancer incidence, mortality, and burden in China: a time-trend analysis and comparison with the United States and United Kingdom based on the global epidemiological data released in 2020. *Cancer Commun (Lond)* 2021; **41**: 1037-1048 [PMID: 34288593 DOI: 10.1002/cac2.12197]
2 **Ilic M**, Ilic I. Epidemiology of pancreatic cancer. *World J Gastroenterol* 2016; **22**: 9694-9705 [PMID: 27956793 DOI: 10.3748/wjg.v22.i44.9694]
3 **Yu S**, Zhang C, Xie KP. Therapeutic resistance of pancreatic cancer: Roadmap to its reversal. *Biochim Biophys Acta Rev Cancer* 2021; **1875**: 188461 [PMID: 33157162 DOI: 10.1016/j.bbcan.2020.188461]
4 **Conroy T**, Desseigne F, Ychou M, Bouché O, Guimbaud R, Bécouarn Y, Adenis A, Raoul JL, Gourgou-Bourgade S, de la

Fouchardière C, Bennouna J, Bachet JB, Khemissa-Akouz F, Péré-Vergé D, Delbaldo C, Assenat E, Chauffert B, Michel P, Montoto-Grillot C, Ducreux M; Groupe Tumeurs Digestives of Unicancer; PRODIGE Intergroup. FOLFIRINOX versus gemcitabine for metastatic pancreatic cancer. *N Engl J Med* 2011; **364**: 1817-1825 [PMID: 21561347 DOI: 10.1056/NEJMoa1011923]

5 **Von Hoff DD**, Ervin T, Arena FP, Chiorean EG, Infante J, Moore M, Seay T, Tjulandin SA, Ma WW, Saleh MN, Harris M, Reni M, Dowden S, Laheru D, Bahary N, Ramanathan RK, Tabernero J, Hidalgo M, Goldstein D, Van Cutsem E, Wei X, Iglesias J, Renschler MF. Increased survival in pancreatic cancer with nab-paclitaxel plus gemcitabine. *N Engl J Med* 2013; **369**: 1691-1703 [PMID: 24131140 DOI: 10.1056/NEJMoa1304369]

6 **Moore MJ**, Goldstein D, Hamm J, Figer A, Hecht JR, Gallinger S, Au HJ, Murawa P, Walde D, Wolff RA, Campos D, Lim R, Ding K, Clark G, Voskoglou-Nomikos T, Ptasynski M, Parulekar W; National Cancer Institute of Canada Clinical Trials Group. Erlotinib plus gemcitabine compared with gemcitabine alone in patients with advanced pancreatic cancer: a phase III trial of the National Cancer Institute of Canada Clinical Trials Group. *J Clin Oncol* 2007; **25**: 1960-1966 [PMID: 17452677 DOI: 10.1200/JCO.2006.07.9525]

7 **Wu J**, Cai J. Dilemma and Challenge of Immunotherapy for Pancreatic Cancer. *Dig Dis Sci* 2021; **66**: 359-368 [PMID: 32140943 DOI: 10.1007/s10620-020-06183-9]

8 **Bockorny B**, Semenisty V, Macarulla T, Borazanci E, Wolpin BM, Stemmer SM, Golan T, Geva R, Borad MJ, Pedersen KS, Park JO, Ramirez RA, Abad DG, Feliu J, Muñoz A, Ponz-Sarvise M, Peled A, Lustig TM, Bohana-Kashtan O, Shaw SM, Sorani E, Chaney M, Kadosh S, Vainstein Haras A, Von Hoff DD, Hidalgo M. BL-8040, a CXCR4 antagonist, in combination with pembrolizumab and chemotherapy for pancreatic cancer: the COMBAT trial. *Nat Med* 2020; **26**: 878-885 [PMID: 32451495 DOI: 10.1038/s41591-020-0880-x]

9 **Chung V**, Kos FJ, Hardwick N, Yuan Y, Chao J, Li D, Waisman J, Li M, Zurcher K, Frankel P, Diamond DJ. Evaluation of safety and efficacy of p53MVA vaccine combined with pembrolizumab in patients with advanced solid cancers. *Clin Transl Oncol* 2019; **21**: 363-372 [PMID: 30094792 DOI: 10.1007/s12094-018-1932-2]

10 **Sahin U**, Koslowski M, Dhaene K, Usener D, Brandenburg G, Seitz G, Huber C, Türeci O. Claudin-18 splice variant 2 is a pan-cancer target suitable for therapeutic antibody development. *Clin Cancer Res* 2008; **14**: 7624-7634 [PMID: 19047087 DOI: 10.1158/1078-0432.CCR-08-1547]

11 **Türeci O**, Koslowski M, Helftenbein G, Castle J, Rohde C, Dhaene K, Seitz G, Sahin U. Claudin-18 gene structure, regulation, and expression is evolutionary conserved in mammals. *Gene* 2011; **481**: 83-92 [PMID: 21571049 DOI: 10.1016/j.gene.2011.04.007]

12 **Wöll S**, Schlitter AM, Dhaene K, Roller M, Esposito I, Sahin U, Türeci Ö. Claudin 18.2 is a target for IMAB362 antibody in pancreatic neoplasms. *Int J Cancer* 2014; **134**: 731-739 [PMID: 23900716 DOI: 10.1002/ijc.28400]

13 **Türeci Ö**, Mitnacht-Kraus R, Wöll S, Yamada T, Sahin U. Characterization of zolbetuximab in pancreatic cancer models. *Oncoimmunology* 2019; **8**: e1523096 [PMID: 30546962 DOI: 10.1080/2162402X.2018.1523096]

14 **Dottermusch M**, Krüger S, Behrens HM, Halske C, Röcken C. Expression of the potential therapeutic target claudin-18.2 is frequently decreased in gastric cancer: results from a large Caucasian cohort study. *Virchows Arch* 2019; **475**: 563-571 [PMID: 31332522 DOI: 10.1007/s00428-019-02624-7]

15 **Sahin U**, Türeci Ö, Manikhas G, Lordick F, Rusyn A, Vynnychenko I, Dudov A, Bazin I, Bondarenko I, Melichar B, Dhaene K, Wiechen K, Huber C, Maurus D, Arozullah A, Park JW, Schuler M, Al-Batran SE. FAST: a randomised phase II study of zolbetuximab (IMAB362) plus EOX versus EOX alone for first-line treatment of advanced CLDN18.2-positive gastric and gastro-oesophageal adenocarcinoma. *Ann Oncol* 2021; **32**: 609-619 [PMID: 33610734 DOI: 10.1016/j.annonc.2021.02.005]

16 **Lordick F**, Al-Batran SE, Ganguli A, Morlock R, Sahin U, Türeci Ö. Patient-reported outcomes from the phase II FAST trial of zolbetuximab plus EOX compared to EOX alone as first-line treatment of patients with metastatic CLDN18.2+ gastroesophageal adenocarcinoma. *Gastric Cancer* 2021; **24**: 721-730 [PMID: 33755863 DOI: 10.1007/s10120-020-01153-6]

17 **Bartha Á**, Győrffy B. TNMplot.com: A Web Tool for the Comparison of Gene Expression in Normal, Tumor and Metastatic Tissues. *Int J Mol Sci* 2021; **22** [PMID: 33807717 DOI: 10.3390/ijms22052622]

18 **Goldman MJ**, Craft B, Hastie M, Repečka K, McDade F, Kamath A, Banerjee A, Luo Y, Rogers D, Brooks AN, Zhu J, Haussler D. Visualizing and interpreting cancer genomics data *via* the Xena platform. *Nat Biotechnol* 2020; **38**: 675-678 [PMID: 32444850 DOI: 10.1038/s41587-020-0546-8]

19 **Tanaka M**, Shibahara J, Fukushima N, Shinozaki A, Umeda M, Ishikawa S, Kokudo N, Fukayama M. Claudin-18 is an early-stage marker of pancreatic carcinogenesis. *J Histochem Cytochem* 2011; **59**: 942-952 [PMID: 21832145 DOI: 10.1369/0022155411420569]

20 **Van Cutsem E**, Bang YJ, Feng-Yi F, Xu JM, Lee KW, Jiao SC, Chong JL, López-Sanchez RI, Price T, Gladkov O, Stoss O, Hill J, Ng V, Lehle M, Thomas M, Kiermaier A, Rüschoff J. HER2 screening data from ToGA: targeting HER2 in gastric and gastroesophageal junction cancer. *Gastric Cancer* 2015; **18**: 476-484 [PMID: 25038874 DOI: 10.1007/s10120-014-0402-y]

21 **Eich ML**, Athar M, Ferguson JE 3rd, Varambally S. EZH2-Targeted Therapies in Cancer: Hype or a Reality. *Cancer Res* 2020; **80**: 5449-5458 [PMID: 32978169 DOI: 10.1158/0008-5472.CAN-20-2147]

22 **Silvestris N**, Brunetti O, Bittoni A, Cataldo I, Corsi D, Crippa S, D'Onofrio M, Fiore M, Giommoni E, Milella M, Pezzilli R, Vasile E, Reni M. Clinical Practice Guidelines for Diagnosis, Treatment and Follow-Up of Exocrine Pancreatic Ductal Adenocarcinoma: Evidence Evaluation and Recommendations by the Italian Association of Medical Oncology (AIOM). *Cancers (Basel)* 2020; **12** [PMID: 32599886 DOI: 10.3390/cancers12061681]

23 **Li WT**, Jeng YM, Yang CY. Claudin-18 as a Marker for Identifying the Stomach and Pancreatobiliary Tract as the Primary Sites of Metastatic Adenocarcinoma. *Am J Surg Pathol* 2020; **44**: 1643-1648 [PMID: 32925194 DOI: 10.1097/PAS.0000000000001583]

World Journal of Gastrointestinal Oncology

Submit a Manuscript: https://www.f6publishing.com

World J Gastrointest Oncol 2022 July 15; 14(7): 1265-1280

DOI: 10.4251/wjgo.v14.i7.1265

ISSN 1948-5204 (online)

ORIGINAL ARTICLE

Clinical and Translational Research

Differences of core genes in liver fibrosis and hepatocellular carcinoma: Evidence from integrated bioinformatics and immunohistochemical analysis

Yue Li, Shou-Li Yuan, Jing-Ya Yin, Kun Yang, Xin-Gang Zhou, Wen Xie, Qi Wang

Specialty type: Gastroenterology and hepatology

Provenance and peer review: Unsolicited article; Externally peer reviewed.

Peer-review model: Single blind

Peer-review report's scientific quality classification

Grade A (Excellent): A
Grade B (Very good): B, B
Grade C (Good): 0
Grade D (Fair): 0
Grade E (Poor): 0

P-Reviewer: Mukthinuthalapati VVPK, United States; Papadopoulos VP, Greece; Silva LD, Brazil

Received: January 25, 2022
Peer-review started: January 25, 2022
First decision: May 9, 2022
Revised: May 18, 2022
Accepted: June 26, 2022
Article in press: June 26, 2022
Published online: July 15, 2022

Yue Li, Kun Yang, Xin-Gang Zhou, Department of Pathology, Beijing Ditan Hospital, Capital Medical University, Beijing 100015, China

Yue Li, Beijing Key Laboratory of Emerging Infectious Diseases, Beijing 100015, China

Shou-Li Yuan, Key Laboratory of Animal Ecology and Conservation Biology, Institute of Zoology, Beijing 100101, China

Jing-Ya Yin, Wen Xie, Qi Wang, Center of Liver Diseases, Beijing Ditan Hospital, Capital Medical University, Beijing 100015, China

Corresponding author: Qi Wang, MD, PhD, Reader (Associate Professor), Center of Liver Diseases, Beijing Ditan Hospital, Capital Medical University, No. 8 East Jingshun Street, Chaoyang District, Beijing 100015, China. wangqidl04@ccmu.edu.cn

Abstract

BACKGROUND

Liver fibrosis and hepatocellular carcinoma (HCC) are common adverse consequences of chronic liver injury. The interaction of various risk factors may cause them to happen. Identification of specific biomarkers is of great significance for understanding the occurrence, development mechanisms, and determining the novel tools for diagnosis and treatment of both liver fibrosis and HCC.

AIM

To identify liver fibrosis-related core genes, we analyzed the differential expression pattern of core genes in liver fibrosis and HCC.

METHODS

Gene expression profiles of three datasets, GSE14323, GSE36411, and GSE89377, obtained from the Gene Expression Omnibus (GEO) database, were analyzed, and differentially expressed genes (DEGs) between patients with liver cirrhosis and healthy controls were identified by screening *via* R software packages and online tool for Venn diagrams. The WebGestalt online tool was used to identify DEGs enriched in biological processes, molecular functions, cellular components, and Kyoto Encyclopedia of Genes and Genomes pathways. The protein–protein interactions of DEGs were visualized using Cytoscape with STRING. Next, the

expression pattern of core genes was analyzed using Western blot and immunohistochemistry in a carbon tetrachloride (CCl_4)-induced liver cirrhosis mouse model and in patient liver samples. Finally, Kaplan-Meier curves were constructed using the Kaplan-Meier plotter online server.

RESULTS

Forty-five DEGs (43 upregulated and 2 downregulated genes) associated with liver cirrhosis were identified from three GEO datasets. Ten hub genes were identified, which were upregulated in liver cirrhosis. Western blot and immunohistochemical analyses of the three core genes, decorin (*DCN*), dermatopontin (*DPT*), and SRY-box transcription factor 9 (*SOX9*), revealed that they were highly expressed in the CCl_4-induced liver cirrhosis mouse model. The expression levels of DCN and SOX 9 were positively correlated with the degree of fibrosis, and SOX 9 level in HCC patients was significantly higher than that in fibrosis patients. However, high expression of DPT was observed only in patients with liver fibrosis, and its expression in HCC was low. The gene expression profiling interactive analysis server (GEPIA) showed that SOX9 was significantly upregulated whereas DCN and DPT were significantly downregulated in patients with HCC. In addition, the Kaplan-Meier curves showed that HCC patients with higher SOX9 expression had significantly lower 5-year survival rate, while patients with higher expression of DCN or DPT had significantly higher 5-year survival rates.

CONCLUSION

The expression levels of *DCN*, *DPT*, and *SOX9* were positively correlated with the degree of liver fibrosis but showed different correlations with the 5-year survival rates of HCC patients.

Key Words: Liver cirrhosis; Hepatocellular carcinoma; Bioinformatical analysis; Decorin; Dermatopontin; SRY-box transcription factor 9

Core Tip: GSE14323, GSE36411, and GSE89377 are available from the Gene Expression Omnibus database. Forty-five differentially expressed genes and 10 hub genes were identified between cirrhotic and healthy livers. quantitative polymerase chain reaction, Western blot, and immunohistochemical analyses showed that decorin (DCN), dermatopontin (DPT), and SRY-box transcription factor 9 (SOX9) were highly expressed in the CCl_4-induced cirrhotic mouse model. The expression level of SOX9 was also significantly increased in HCC patients,and was associated with the fibrosis stage.. However, overexpression of DPT was only observed in patients with liver fibrosis. The Kaplan-Meier curves showed that HCC patients with higher SOX9 expression had significantly lower 5-year survival rate, while patients with higher expression of DCN or DPT had higher 5-year survival rates.

Citation: Li Y, Yuan SL, Yin JY, Yang K, Zhou XG, Xie W, Wang Q. Differences of core genes in liver fibrosis and hepatocellular carcinoma: Evidence from integrated bioinformatics and immunohistochemical analysis. *World J Gastrointest Oncol* 2022; 14(7): 1265-1280

URL: https://www.wjgnet.com/1948-5204/full/v14/i7/1265.htm

DOI: https://dx.doi.org/10.4251/wjgo.v14.i7.1265

INTRODUCTION

Chronic liver infection, including chronic hepatitis B (CHB), chronic hepatitis C, alcoholic liver disease, and non-alcoholic fatty liver disease can all result in liver fibrosis. Primary liver cancer is the seventh most common cancer worldwide[1]. Hepatocellular carcinoma (HCC), which is the dominant type of liver cancer, accounts for approximately 75% of all liver cancers worldwide[2] and is the second most fatal disease in China[3]. Liver cirrhosis is an advanced stage of liver fibrosis and is characterized by limited regeneration capacity and serious complications[4]. Most HCCs develop in the background of chronic liver injury, hepatic inflammation, and liver fibrosis. Unfortunately, to date, there are still no effective treatment strategies for liver cirrhosis, and the limited number of specific biomarkers for HCC related to fibrosis further compounds the problem of its diagnosis and treatment[5,6].

The pathogenesis of liver fibrosis and HCC is complex as the interaction of many factors may lead to their occurrence. In recent years, with the optimization of gene sequencing platforms, several differentially expressed genes (DEGs) have been identified using bioinformatics analysis[7,8]. To date, there is a huge collection of data stored in the Gene Expression Omnibus (GEO) database of gene expression that

can be explored to find the relevant DEGs for a diseased condition. Chan *et al*[9] identified DEGs between cirrhotic and non-cirrhotic livers using microarray gene analysis. Many human genes may show differential expression patterns and functions with the onset of fibrosis and/or HCC. However, the study by Chan *et al*[9] was limited by the small sample size, which only included 24 patients with cirrhosis and 16 patients without cirrhosis. The results obtained solely from either bioinformatics or experimental approach may not elucidate relevant DEGs. Hence, integrating bioinformatics methods with experimental techniques may help us to better understand the underlying mechanisms behind fibrosis/HCC pathogenesis.

In this study, we analyzed three databases from GEO, R software packages and online tools to identify DEGs, including upregulated and downregulated genes between liver fibrosis and HCC. The molecular function, cellular component, biological process, and Kyoto Encyclopedia of Genes and Genomes (KEGG) pathways of DEGs were then assessed. We also constructed a protein-protein interaction (PPI) network using Cytoscape for further analysis. Using these methods, hub genes were identified and subjected to KEGG pathway enrichment analysis. Finally, real-time quantitative polymerase chain reaction (qPCR), Western blotting, and immunohistochemistry of the liver tissue samples from mouse model and patients were carried out to identify novel biomarkers of liver fibrosis. Our study identified fibrosis-related core genes and compared their phenotypic differences between liver fibrosis and HCC.

MATERIALS AND METHODS

Patient liver samples collection

Liver tissue samples were collected from 5 healthy controls, 40 patients with CHB (n = 28) and CHB-associated HCC (n = 12) at the Beijing Ditan Hospital, Capital Medical University, Beijing, China. The diagnosis of CHB was based on the "Guidelines on prevention and treatment of chronic hepatitis B in China"[10]. Chronic HBV infection is defined as the persistence of HBsAg in blood serum for at least 6 mo. Patients who were diagnosed for Hepatitis C viral infection, drug-induced liver disease, non-alcoholic liver disease, alcoholic liver disease, autoimmune liver disease, cholestatic liver disease, or hereditary metabolic liver disease were excluded. All samples were analyzed by a clinician and two independent pathologists with no prior knowledge of demographic and clinical data. The degree of liver inflammation and fibrosis were scored according to the METAVIR system[11], and liver samples were divided into five groups: normal control, fibrosis grade 0 (S0), fibrosis grade 1-2 (S1-2), fibrosis grade 3-4 (S3-4), and HCC group. Meanwhile, we collected the clinical data, including sex, age, HBeAg, HBV DNA, alanine transaminase, aspartate transaminase, total bilirubin, albumin, cholinesterase and alpha-fetoprotein. The study protocol conformed to the ethical guidelines of the 1975 Declaration of Helsinki, as approved by the Ethics Committee of Beijing Ditan Hospital.

Animals

Six-week-old male C57BL/6 mice were purchased from Vital River Laboratory Animal Technology Co., Ltd, Beijing, China. All mice were housed in a specific pathogen free laboratory animal house (Institute of Zoology of Beijing, Chinese Academy of Sciences, China) at 24 ℃ with a 12 h light/dark cycle. All animal studies were approved by the Institutional Animal Care and Use Committee of the Institute of Zoology, Chinese Academy of Sciences.

Twelve male C57BL/6 mice were randomly divided into two groups: control group and carbon tetrachloride (CCl_4)-treated group. To induce liver cirrhosis, CCl_4 (0.5 μL/g) mixed with corn oil was intraperitoneally injected into the mice three times per week for 12 wk. The control group was injected with an equal volume of corn oil. CCl_4 was purchased from Sigma-Aldrich (St. Louis, MO, United States).

Histological and immunohistochemical analysis

For hematoxylin and eosin (HE) staining, Masson's trichrome staining, and immunohistochemical analysis, liver tissues collected from mouse model or patients were fixed with 4% paraformaldehyde solution and embedded in paraffin. For histological analysis, 5 μm thick sections were stained and observed under 10 × or 20 × objective lens. Masson's trichrome kit (G1281, Solarbio, Beijing, China) was used according to the manufacturer's instructions.

For immunohistochemical staining, 5% bovine serum albumin in 0.1% TritonX-100 tris-buffered saline was used as the blocking solution. The samples were incubated overnight at 4 ℃ with anti-decorin (DCN) (ab277636, Abcam), anti-dermatopontin (DPT) (10537-1-AP, Proteintech), and anti-SRY-box transcription factor 9 (SOX9) (ab185966; Abcam) antibodies. After incubation with a peroxidase-conjugated secondary antibody, the signal was visualized using a diaminobenzidine peroxidase substrate kit. The collagen area or positive area of immunohistochemical staining was quantified using ImageJ 1.52a software.

Real-time qPCR

Total RNA from liver tissues was isolated using TRIzolTM reagent (Thermo Fisher Scientific, MA, United States). Isolated RNA was reverse-transcribed into complementary DNA (cDNA) using a high-capacity cDNA reverse transcription kit (Promega, WI, United States). The relative expression of genes was detected by real-time fluorescence qPCR system (Light Cycler 480, Roche, Sweden) with SYBR green master mix (Promega, WI, United States). The primer sequences used in this study were listed in Supplementary Table 1. Statistical significance between the control and CCl_4-treated groups was defined at $P < 0.05$.

Western blotting

Total protein from liver tissues was extracted using radioimmunoprecipitation assay buffer. The protein concentration of the samples was measured by bicinchoninic acid assay. The same concentration of protein was loaded to 10% sodium dodecyl sulfate polyacrylamide gel and then transferred to a polyvinylidene fluoride membrane. The membranes were incubated overnight at 4°C in anti-α-SMA (ab5694, Abcam), anti-DCN (ab277636, Abcam), anti-DPT (10537-1-AP, Proteintech), and anti-SOX9 (ab185966, Abcam) antibodies. All signals were visualized by density scanning (Image Quant TL7.0; GE Healthcare Biosciences, Uppsala, Sweden). The intensity of the bands was analyzed using ImageJ 1.52a software.

Microarray and gene expression analysis

The RNA expression data of human cirrhotic and healthy livers were collected from the GEO database (http://www.ncbi.nlm.nih.gov/geo). The GSE14323, GSE36411, and GSE89377 datasets contained gene expression data collected from 41, 21, and 12 cirrhotic and 19, 21, and 13 healthy liver tissues, respectively. The GEOquery R software package was used to download the GEO data and platform information. Then, the gene ID conversion was performed, and the maximum value of genes with the same name was selected. Ggplot2 package was used to plot the boxplot and density of the expression levels for each sample. Ggfortify package was used to perform the principal component analysis (PCA). DEGs between the cirrhosis and healthy liver tissue groups were identified using limma package by limiting the value of adjustment: *P*-value (adjust. $P < 0.05$) and the absolute value of logFC ($|\log FC| > 1.2$ or 0.6). A volcano map was generated using the ggplot2 package, and Venn diagram online tool (http://bioinformatics.psb.ugent.be/webtools/Venn/) was used to draw a Venn map. The DEGs were verified using the ONCOMINE server (https://www.Oncomine.org/resource/), which is an online available microarray database[12].

Gene ontology and pathway enrichment analysis

WebGestalt online tool (http://www.webgestalt.org) was used to identify DEGs enriched in biological processes, molecular functions, cellular component-related pathways, and KEGG pathways. The *P*-value of less than 0.05 was considered statistically significant.

PPI network construction and identification of hub genes

STRING online database (https://string-db.org/; version 11.5) was used to build the PPI network[13]. The DEGs were submitted to the STRING database to construct the PPI network. Cytoscape (version 3.7.2) was used to draw the PPI network of DEGs, and the cytoHubba plugin was used to identify hub genes[14].

Gene expression level in HCC and survival analysis

Gene expression profiling interactive analysis (GEPIA) online server (http://gepia.cancer-pku.cn/) was used to analyze the RNA sequencing expression data of tumors and healthy samples from the cancer genome atlas and genotype tissue expression projects[15]. We used this server to check whether the identified hub genes were differentially expressed in HCC tissues. Overall 5-year survival rates according to gene expression were obtained using the Kaplan-Meier Plotter (http://kmplot.com/analysis/index.php?p=service&cancer=liver_rnaseq)[16].

Statistical analyses

GraphPad Prism 6.0 (GraphPad Software Inc. La Jolla, CA, United States) was used for statistical analysis. Data were presented as mean ± SE or SD (for normally distributed data) or median with interquartile range (for non-normally distributed data). Statistically significant differences were determined using a two-tailed Student's *t*-test or analysis of variance (ANOVA). Statistical significance was set and marked as $^{a}P < 0.05$, $^{b}P < 0.01$, $^{c}P < 0.001$, and $^{d}P < 0.0001$. Replicates are indicated in the figure legends, and (n) represents the number of experimental replicates.

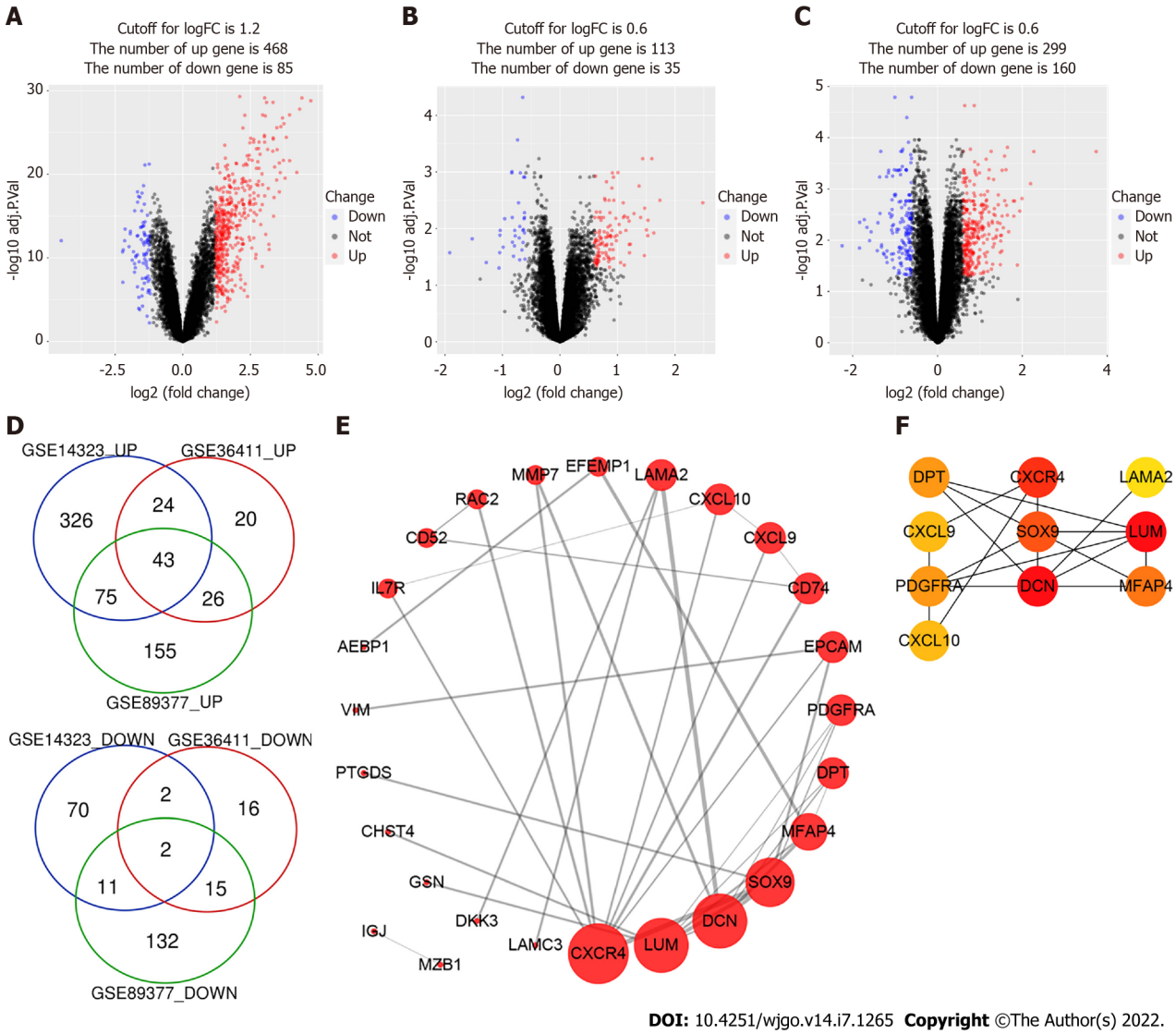

DOI: 10.4251/wjgo.v14.i7.1265

Figure 1 Identification of differentially expressed genes. A-C: The volcano plots of GSE14323, GSE36411 and GSE89377. The red dots and blue dots represent up-regulated and downregulated genes, respectively; D: The Venn diagram software identified 45 common differentially expressed genes (DEGs) in three datasets (GSE14323, GSE36411 and GSE89377), including 43 upregulated genes and 2 downregulated genes; E: protein-protein interaction network of DEGs was constructed by STRING online database and drew by Cytoscape software; F: Top 10 hub genes of DEGs were identified by cytoHubba plug-in of Cytoscape and their importance were represented by their color's shade.

RESULTS

Identification of DEGs

We analyzed three gene expression datasets, GSE14323, GSE36411, and GSE89377, which included data from 74 cirrhotic and 53 healthy liver tissue samples in total. The analysis of processed sample data showed that the gene expression levels in different samples were primarily the same (Supplementary Figure 1). PCA showed that cirrhotic and healthy groups constituted individual clusters (Supplementary Figure 2). Using limma package, we extracted 553, 148, and 459 DEGs from GSE14323, GSE36411, and GSE89377 datasets, respectively (Figure 1A-C). Using Venn diagram online tool, we identified 45 DEGs (43 upregulated genes and 2 downregulated genes) associated with cirrhosis from the three datasets (Figure 1D, Table 1).

Gene Ontology and KEGG pathway analysis of DEGs

To understand the function of identified DEGs, we carried out Gene Ontology (GO) and KEGG pathways analyses using Webgestalt online server. The GO analysis results were listed according to *P*-values (Table 2), which showed that DEGs were significantly enriched in extracellular matrix organization (GO: 0030198), extracellular matrix structural constituent (GO: 0005201), collagen-containing extracellular matrix (GO: 0062023), extracellular matrix (GO: 0031012), cell adhesion (GO: 0007155), biological adhesion (GO: 0022610), and taxis (GO: 0042330). KEGG pathway analysis showed

Table 1 Gene expression profiles of GSE14323, GSE36411 and GSE89377 have 45 differentially expressed genes, including 2 downregulated genes and 43 upregulated genes in the fibrotic liver compared to normal liver

DEGs	Genes		
Upregulated	C-X-C chemokine receptor type 4 (*CXCR4*)	SH3 domain-containing YSC84-like protein 1 (*SH3YL1*)	Laminins containing the α2 (*LAMA2*)
	Lumican (*LUM*)	DNA-binding protein inhibitor ID-3 (*ID3*)	Microfibril-associated glycoprotein 4 (*MFAP4*)
	Prostaglandin-H2 D-isomerase (*PTGDS*)	Aldo-keto reductase family 1 member B10 (*AKR1B10*)	Marginal zone B- and B1-Cell-specific protein (*MZB1*)
	Dickkopf-related protein 3 (*DKK3*)	Ras-related protein Rac2 (*RAC2*)	Suppressor of lin-12-like protein 3 (*SEL1L3*)
	Dermatopontin (*DPT*)	Annexin A13 (*ANXA13*)	Defensin Beta 1 (*DEFB1*)
	H-2 class II histocompatibility antigen gamma chain (*CD74*)	CAMPATH-1 antigen (*CD52*)	Protein unc-93 homolog A (*UNC93A*)
	FXYD domain-containing ion transport regulator 2 (*FXYD2*)	Adipocyte enhancer-binding protein 1 (*AEBP1*)	Interleukin-7 receptor subunit alpha (*IL7R*)
	C-X-C motif chemokine 9 (*CXCL9*)	C-X-C motif chemokine 10 (*CXCL10*)	Ribonuclease pancreatic (*RNASE1*)
	SRY-Box transcription factor 9 (*SOX9*)	Gelsolin (*GSN*)	Carbohydrate sulfotransferase 4 (*CHST4*)
	Vimentin (*VIM*)	Galectin-3-binding protein (*LGALS3BP*)	Platelet-derived growth factor receptor alpha (*PDGFRA*)
	Lectin, galactoside-binding soluble 4 (*LGALS4*)	Laminin subunit gamma-3 (*LAMC3*)	Claudin-10 (*CLDN10*)
	Joining chain of multimeric IgA and IgM (*JCHAIN*)	Ectonucleotide pyrophosphatase/phosphodiesterase family member 2 (*ENPP2*)	Cholesterol 25-hydroxylase (*CH25H*)
	Apolipoprotein L3 (*APOL3*)	Decorin (*DCN*)	Complement component C7 (*C7*)
	Epithelial cell adhesion molecule (*EPCAM*)	Keratin type I cytoskeletal 23 (*KRT23*)	EGF-containing fibulin-like extracellular matrix protein 1 (*EFEMP1*)
	Matrix metallopeptidase 7 (*MMP7*)		
Downregulated	Small conductance calcium-activated potassium channel protein 2 (*KCNN2*)	Cytochrome P450 2C19 (*CYP2C19*)	

DEGs: Differentially expressed genes.

that the DEGs involved in the chemokine signaling pathway, focal adhesion, regulation of actin cytoskeleton, leukocyte transendothelial migration, pathways in cancer, and cytokine–cytokine receptor interaction, and arachidonic acid metabolism were highly enriched in patients with liver cirrhosis (Table 3).

PPI network construction and identification of hub genes

PPI network analysis aids in studying the molecular mechanisms of the disease pathogenesis. Using String v11 and Cytoscape software, we constructed a PPI network with 26 nodes and 36 edges (Figure 1E). These genes were upregulated in liver cirrhosis. The top 10 hub genes were identified using the CytoHubba plugin of Cytoscape, which included C-X-C motif chemokine ligand 9 (*CXCL9*), *CXCL10,* C-X-C motif chemokine receptor 4 (*CXCR4*), *DCN*, *DPT,* laminin subunit alpha 2 (*LAMA2*), lumican (*LUM*), microfibril associated protein 4 (*MFAP4*), platelet-derived growth factor receptor alpha (*PDGFRA*), and *SOX9* (Figure 1F).

Expression of hub genes in the liver tissue of CCl_4-induced cirrhosis mice

To study the role of the 10 hub genes in liver cirrhosis, we generated a CCl_4-induced liver cirrhosis mouse model (Figure 2A–B). The relative mRNA levels of these genes were shown in Figure 2C. Compared to those in the control group, seven genes (*CXCR4, DCN, DPT, LAMA2, LUM, MFAP4,* and *SOX9*) were significantly upregulated in the liver cirrhosis mice, while the expression levels of *PDGFRA, CXCL9*, and *CXCL10* were not significantly different between the two groups. For further validation, we performed Western blotting and immunohistochemical analysis (Figure 2D, Figure 3). These results confirmed that the protein levels of DCN, DPT, and SOX9 were significantly upregulated in the liver tissue of cirrhotic mice.

Table 2 Gene Ontology analysis of differentially expressed genes (top 10 according to *P*-value)

Gene set	Description	Count	*P* value
GO: 0030198	Extracellular matrix organization	11	3.38E-10
GO: 0043062	Extracellular structure organization	11	1.56E-9
GO: 0005201	Extracellular matrix structural constituent	7	7.48E-8
GO: 0062023	Collagen-containing extracellular matrix	9	1.53E-7
GO: 0031012	Extracellular matrix	10	1.78E-7
GO: 0007155	Cell adhesion	15	2.78E-7
GO: 0022610	Biological adhesion	15	3.00E-7
GO: 0006935	Chemotaxis	10	0.000001284
GO: 0042330	Taxis	10	0.000001323
GO: 0005198	Structural molecule activity	11	0.000001624

Table 3 Kyoto Encyclopedia of Genes and Genomes pathway analysis of differentially expressed genes in fibrotic liver

Gene set	Description	*P* value	Genes
hsa04062	Chemokine signaling pathway	0.00	*CXCR4, CXCL9, CXCL10, RAC2*
hsa04510	Focal adhesion	0.01	*LAMA2, LAMC3, PDGFRA, RAC2*
hsa04810	Regulation of actin cytoskeleton	0.01	*CXCR4, GSN, PDGFRA, RAC2*
hsa04670	Leukocyte transendothelial migration	0.01	*CLDN10, CXCR4, RAC2*
hsa05200	Pathways in cancer	0.01	*CXCR4, IL7R, LAMA2, LAMC3, PDGFRA, RAC2*
hsa05416	Viral myocarditis	0.02	*LAMA2*
hsa04060	Cytokine-cytokine receptor interaction	0.02	*CXCL9, CXCL10, CXCR4, IL7R*
hsa00590	Arachidonic acid metabolism	0.02	*CYP2C19, PTGDS*
hsa04976	Bile secretion	0.03	*FXYD2, KCNN2*
hsa04024	cAMP signaling pathway	0.02	*FXYD2, RAC2, SOX9*

DCN, DPT and SOX9 expression and liver fibrosis progression in patients

To further explore the relationship between DCN, DPT, and SOX9 protein expression and progression of liver cirrhosis, we collected liver biopsy tissue samples from 5 healthy controls, 28 patients with CHB, and 12 patients with CHB-associated HCC. All liver tissues were divided into 5 groups (normal, S0, S1-2, S3-4, and HCC) according to METAVIR system. The clinical profile of the patients enrolled in the study is summarized in Table 4. The results showed that males were the majority in S3-4 and HCC groups. The age, TBil, ALB, and CHE values in all groups and the AFP value in non-HCC group were in normal distribution, and the median AFP value in the HCC group was higher than the upper limit of normal value. In patients with CHB, HBV DNA was detected as positive, and most ALT and AST levels were elevated, which was consistent with the inflammatory activity of the liver. Most patients with HCC were detected negative for HBV DNA, which is related to antiviral treatment. Liver samples from patients with fibrosis showed increased collagen deposition, inflammatory cell infiltration, or atypical cells viewed with HE and Masson's trichrome staining (Figure 4).

Immunohistochemical results showed that the expression levels of DCN and SOX9 increased with the aggravation of liver fibrosis (Figure 4, Figure 5A, Figure 5C) and were significantly higher in the HCC group than those in healthy controls and fibrotic groups (Figure 4, Figure 5D, and Figure 5F). Further, compared with healthy controls, DPT expression was significantly increased in patients with liver fibrosis, particularly in the S3-S4 group but extremely reduced in patients with HCC (Figure 5B, Figure 5E). In addition, we found that DCN was mostly expressed in the portal vein region, which was highly consistent with the distribution of collagen fibers, while SOX9 and DPT were mostly expressed in hepatocytes and several other types of cells (Figure 4).

DCN, DPT, and SOX9 expression and survival rate of patients with HCC

Due to the differential expression pattern and distribution, we decided to analyze the correlation between DCN, DPT, and SOX9 expression levels and the survival rate of patients with HCC. The GEPIA

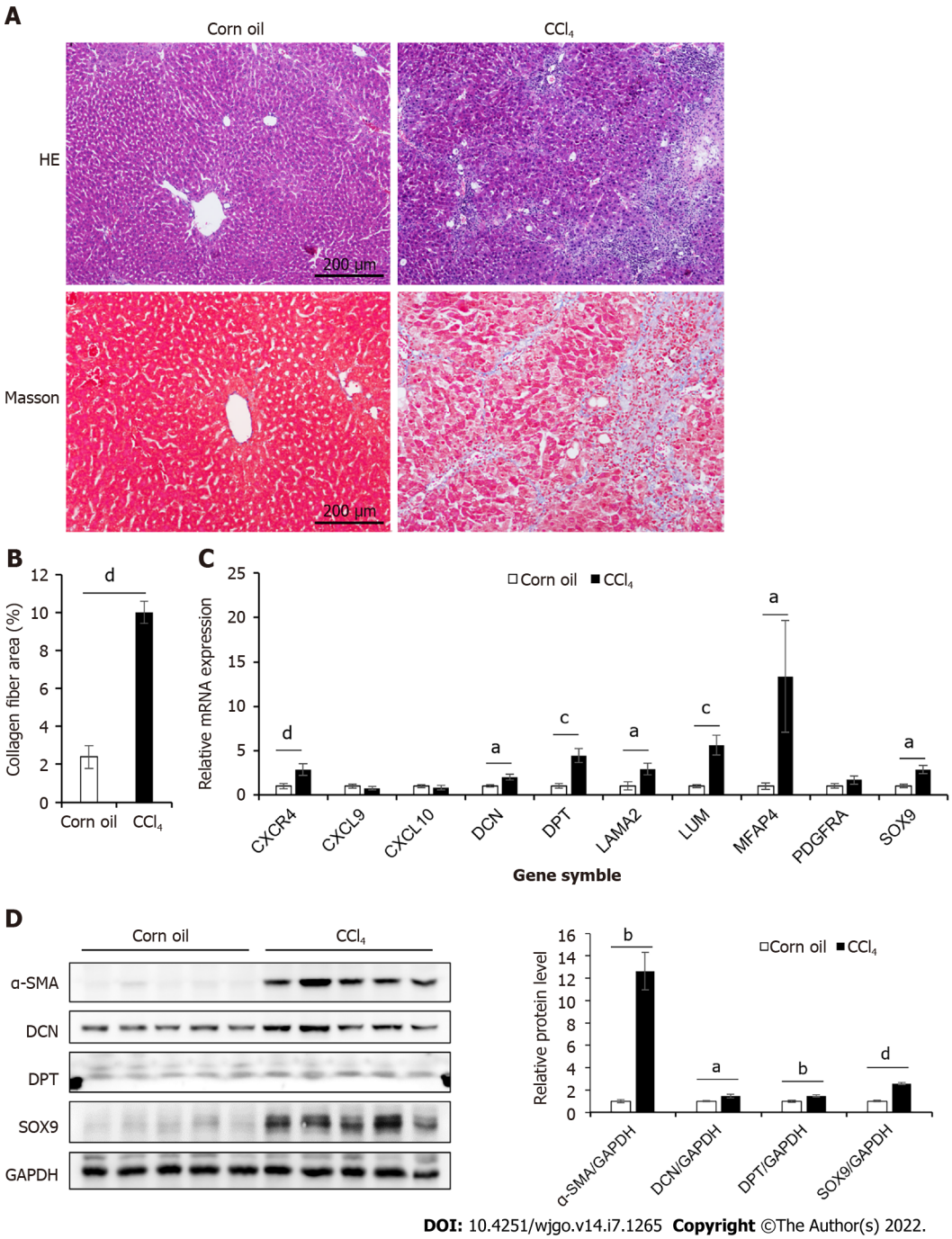

DOI: 10.4251/wjgo.v14.i7.1265

Figure 2 Expression of hub genes in the liver tissue of CCl_4-induced mouse mice. A: Masson's trichrome and HE staining of control and CCl_4-induced liver cirrhosis mouse liver tissues; B: Collagen area in Masson's trichrome staining (n = 7 or 8); C: The mRNA expression levels of 10 hub genes of control and CCl_4-induced cirrhosis mouse liver tissues (n = 6); D: The protein expression levels of α-SMA, Decorin (DCN), Dermatopontin (DPT), and SRY-box transcription factor 9 (SOX9) in liver tissues of mice in two groups. The right panel showed the result of quantitative analysis (n = 4). All data were presented as mean ± SE. Two-tailed Student's t test were performed. $^aP < 0.05$, $^bP < 0.01$, $^cP < 0.001$, $^dP < 0.0001$.

server was used to detect the mRNA expression levels in tissues of patients 369 liver hepatocellular carcinoma (LIHC) and 160 normal tissues (Figure 6A-C). The results showed that SOX9 was significantly upregulated whereas DCN and DPT were significantly downregulated in patients with LIHC.

Kaplan-Meier curves, depicting samples from these 369 patients with HCC, showed that the 5-year survival rate of patients with high expression of SOX 9 was significantly reduced, while that of patients with high expression of DCN or DPT was increased (Figure 6D-F).

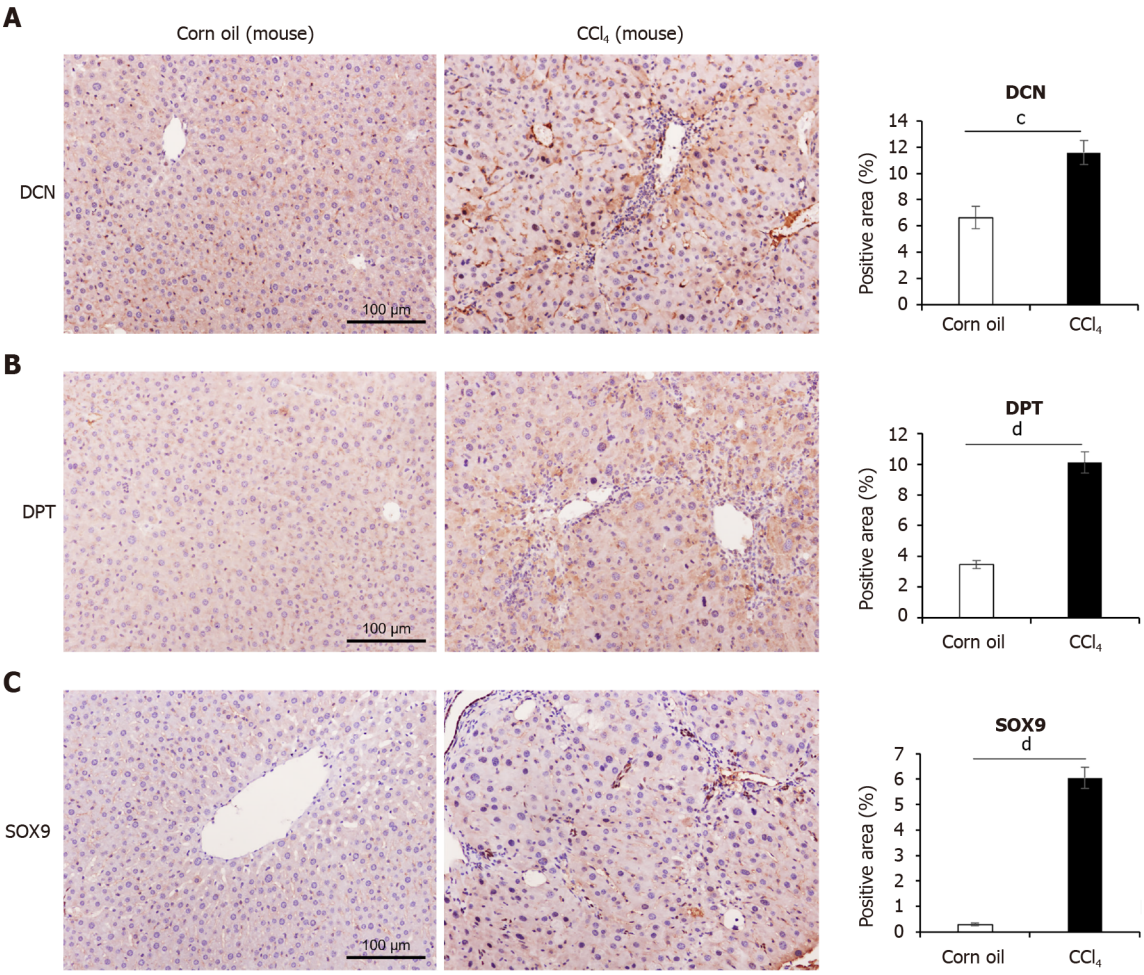

DOI: 10.4251/wjgo.v14.i7.1265

Figure 3 Comparison of decorin, dermatopontin, and SRY-box transcription factor 9 expression in CCl_4-induced mouse model. A: Immunohistochemical (IHC) analyses of the expression of Decorin (DCN) and the percentage of positive area were shown, n = 9 or 11; B: IHC analyses of the expression of Dermatopontin (DPT) and the percentage of positive area were shown (n = 9 or 10); C: IHC analyses of the expression of SRY-box transcription factor 9 (SOX9) and the percentage of positive area were shown (n = 9 or 10). All data were presented as mean ± SE. Two-tailed Student's t test were performed. ^cP < 0.001, ^dP < 0.0001.

DISCUSSION

Fibrosis is a common pathological symptom of severe liver damage caused by various chronic liver diseases. The most common primary liver cancer, HCC, occurs most often in people inflicted with chronic liver diseases[17]. Understanding the molecular mechanisms underlying cirrhosis can help in the development of effective treatments. Although bioinformatics tools can be used to study the relationship between gene function, liver fibrosis, and HCC, it is necessary to comprehensively analyze gene expression levels and distribution in the context of disease pathology *via in vivo* experiments.

GEO is an international public resource bank for high-throughput microarray and next-generation sequencing of functional genome datasets submitted by research groups. In this study, we identified 45 DEGs from GSE14323, GSE36411, and GSE89377 datasets in the GEO database for an in-depth analysis of their biological function. Most of these DEGs have been associated with liver diseases. *CXCL9, ENPP2, CH25H, KRT23, IL7R, APOL3,* and *GSN* are involved in HCV or HBV infection[18-23]. *AEBP1, C7,* and *LUM* are overexpressed in non-alcoholic steatohepatitis (NASH)[24-26]. *CHST4, DEFB1, EFEMP1, MMP7,* and *SOX9* are associated with cholestasis[27-31]. *AKR1B10, CLDN10, DKK3, EPCAM, LGALS4,* and *ITM2A* are upregulated in patients with HCC[32-38]. The combined data-mining of three datasets from different sources yielded 45 DEGs, further indicating that the GEO database is indeed a useful resource for understanding the mechanism of liver diseases and using the GEO database can increase the efficiency of published resources.

Next, for detailed characterization of hub gene functions, we selected three representative genes (*DCN, DPT,* and *SOX9*), since their expression was consistently found to be associated with liver cirrhosis. We established a CCl_4-induced mice model and verified their mRNA and protein levels using qPCR, Western blotting, and immunohistochemistry to confirm the expression and main pathophysiological functions. The results confirmed that DCN, DPT, and SOX9 were significantly overex-

Table 4 Clinical and histologic data for healthy controls, chronic hepatitis B and hepatocellular carcinoma patients

	Control (*n* = 5)	CHB-S0 (*n* = 4)	CHB-S1-2 (*n* = 13)	CHB-S3-4 (*n* = 11)	HCC (*n* = 12)
Sex (M/F), *n*	3/2	2/2	6/7	8/3	11/1
Age, yr, mean ± SD	41.8 ± 9.5	33.0 ± 10.3	38.2 ± 8.1	40.3 ± 6.1	52.8 ± 10.5
HBeAg(+), *n*	0	2	9	7	3
HBV DNA, logIU/mL, median with IQR	-	5.5 (2.4, 8.5)	5.0 (2.5, 7.0)	4.7 (2.0, 6.6)	0 (0, 3.0)
ALT, U/L, median with IQR	19.2 (16.8, 28.7)	56.6 (45.0, 75.8)	39.3 (17.9, 66.3)	51.3 (29.6, 70.0)	54.7 (24.1, 105.8)
AST, U/L, median with IQR	20.7 (19.4, 22.5)	36.3 (27.2, 44.6)	27.3 (20.9, 39.9)	31.8 (23.8, 49.7)	54.8 (27.9, 111.6)
TBil, μmol/L, mean ± SD	18.9 ± 14.1	14.0 ± 4.3	12.8 ± 4.9	12.9 ± 4.8	16.8 ± 14.6
ALB, g/L, mean ± SD	45.9 ± 4.8	47.8 ± 4.3	46.5 ± 3.9	44.4 ± 5.0	41.3 ± 5.3
CHE, IU/L, mean ± SD	6191.3 ± 1908.0	11514.5 ± 3416.1	8887.5 ± 1964.8	7708.5 ± 2064.4	6538.7 ± 7065.7
AFP, ng/ml, mean ± SD or median with IQR	2.5 ± 1.4	2.0 ± 0.8	4.7 ± 6.1	11.3 ± 22.1	37.9 (9.3, 388.9)

F: Female; M: Male; ALT: Alanine transaminase; AST: Aspartate transaminase; TBil: Total bilirubin; ALB: Albumin; CHE: Cholinesterase; AFP: Alpha-fetoprotein; IQR: Interquartile range; HCC: Hepatocellular carcinoma; CHB: Chronic hepatitis B.

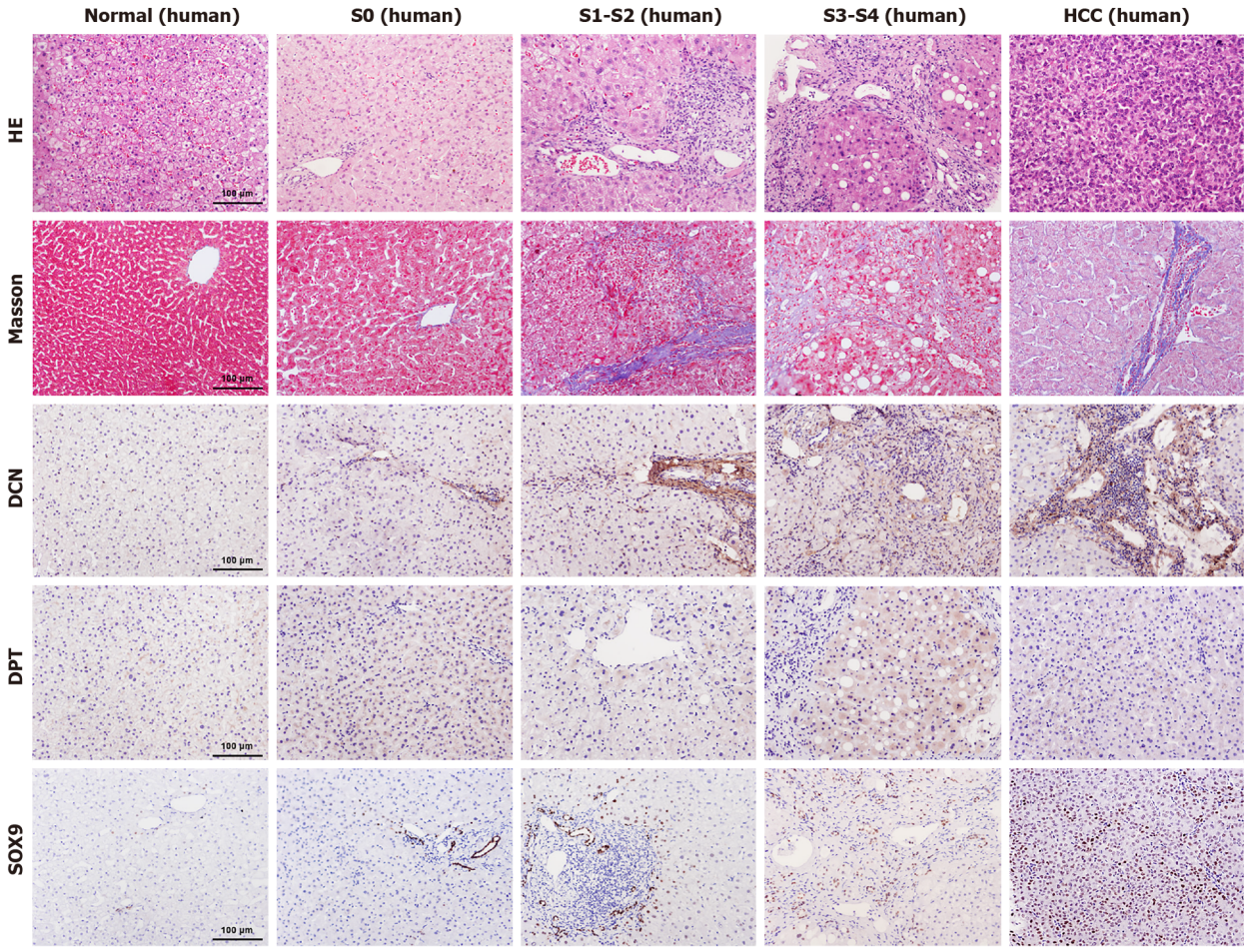

DOI: 10.4251/wjgo.v14.i7.1265

Figure 4 Comparison of decorin, dermatopontin, and SRY-box transcription factor 9 expression in human liver tissues. The expression levels of Decorin (DCN), Dermatopontin (DPT) and SRY-box transcription factor 9 (SOX9) in normal, S0, S1-S2, S3-S4, Hepatocellular carcinoma (HCC) groups were analyzed by immunohistochemistry. The H&E staining and Masson's trichrome staining were shown also.

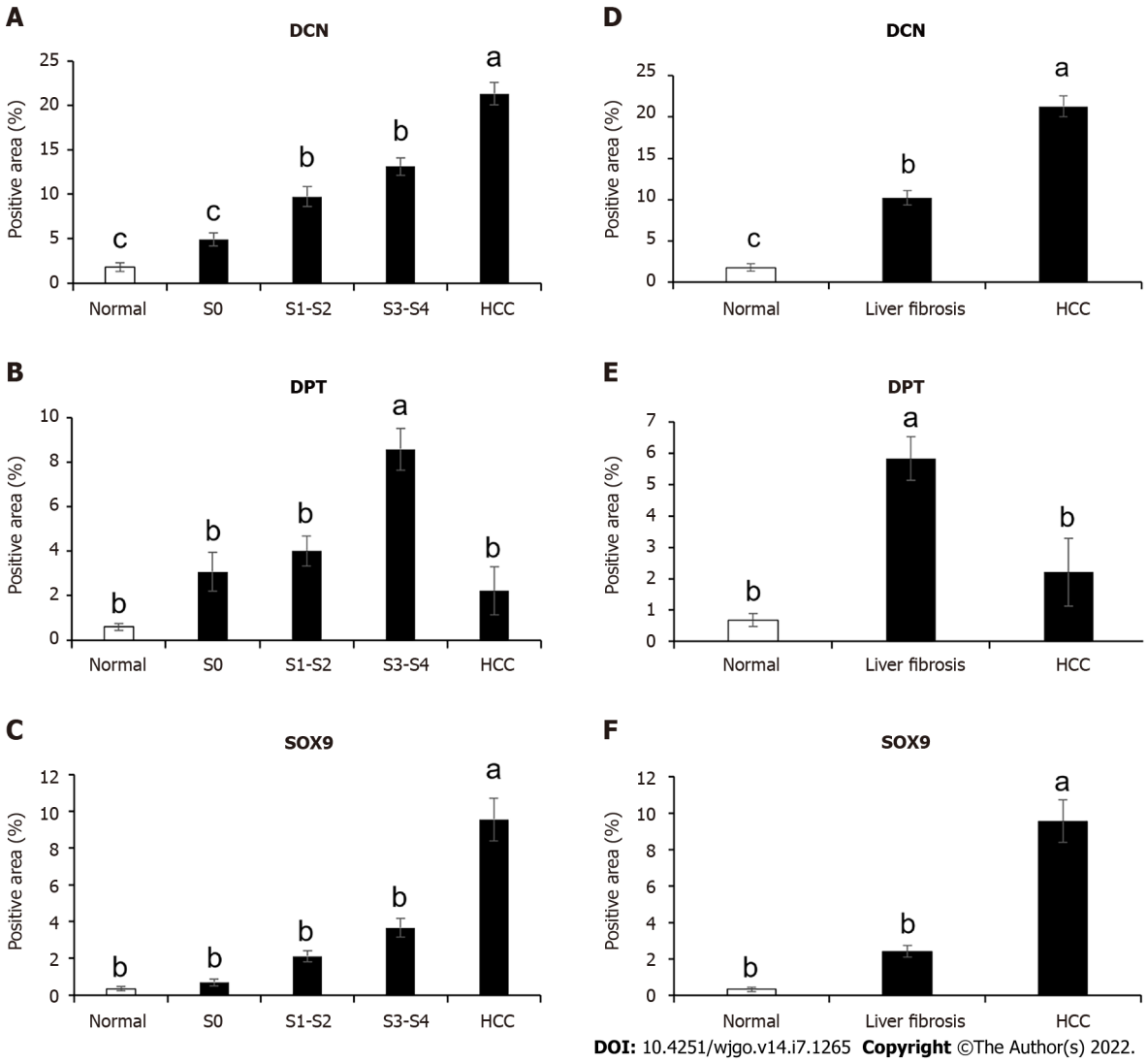

DOI: 10.4251/wjgo.v14.i7.1265

Figure 5 Expression levels analysis of decorin, dermatopontin, and SRY-box transcription factor 9 in human liver tissues. A-C: The percentage of positive area of decorin (DCN) , dermatopontin (DPT) and SRY-box transcription factor 9 (SOX9) among normal (n = 5 or 7), S0 (n = 3 or 4), S1-S2 (n = 10 or 12), S3-S4 (n = 8, 9 or 11) and hepatocellular carcinoma (HCC) (n = 11, 12 or 14) groups were counted; D-F: The percentage of positive area of DCN , DPT and SOX9 in normal (n = 5 or 7), liver fibrosis (n = 22, 23 or 26) and HCC (n = 11, 12 or 14) groups were counted. All data were presented as mean ± SE.One-way ANOVA with multiple comparisons and Tukey's post-test were performed, $^{a}P < 0.05$, $^{b}P < 0.01$, $^{c}P < 0.001$.

pressed in human and mouse fibrotic liver; however, there were differences in the relationship between their expression levels and the survival rate of patients with HCC.

The *DCN* gene encodes a member of the small leucine-rich proteoglycan family of proteins, which can act as a tumor repressor in a variety of cancers[39]. DCN is a regulator of matrix assembly and not only targets transforming growth factor-beta 1 (TGF-β1) but is also involved in the maturation of collagen fibrils[40,41]. The enhanced deposition of DCN reflects the stimulatory effect of overproduction of TGF-β1[41]. Dudás *et al*[42] indicated that high amounts of TGF-β1 colocalize with DCN within the fibrotic areas of the liver using a cohort of liver pathologies, including chronic hepatitis, fibrosis, and cirrhosis, which is consistent with our results. However, contrary to our results, Shang *et al*[43] found DCN mRNA expression to be downregulated and not upregulated in patients with HCC *via* gene expression profile analyses. Although GEPIA analysis showed that the mRNA expression level of DCN in ILHC was lower than that normal tissues, the heterogeneity within each group, especially the ILHC group, was very different. In addition, our results were based on immunohistochemical analysis, different from the expression profile of the whole liver tissue used by Shang *et al*[43]. From the distribution of immunohistochemical sections, we concluded that almost all the increase in DCN expression was localized in the collagen-intensive area of the portal region and not in the hepatic lobule, which indicates that the upregulated DCN significantly represents an increase in matrix assembly. These may partly explain why the increased DCN is not associated with the lower 5-year survival rate of HCC patients, and why the expression pattern of DCN expression analyzed by GEPIA server was different from our study. Considering these inconsistent results, the expression, location and function of DCN deserves further study.

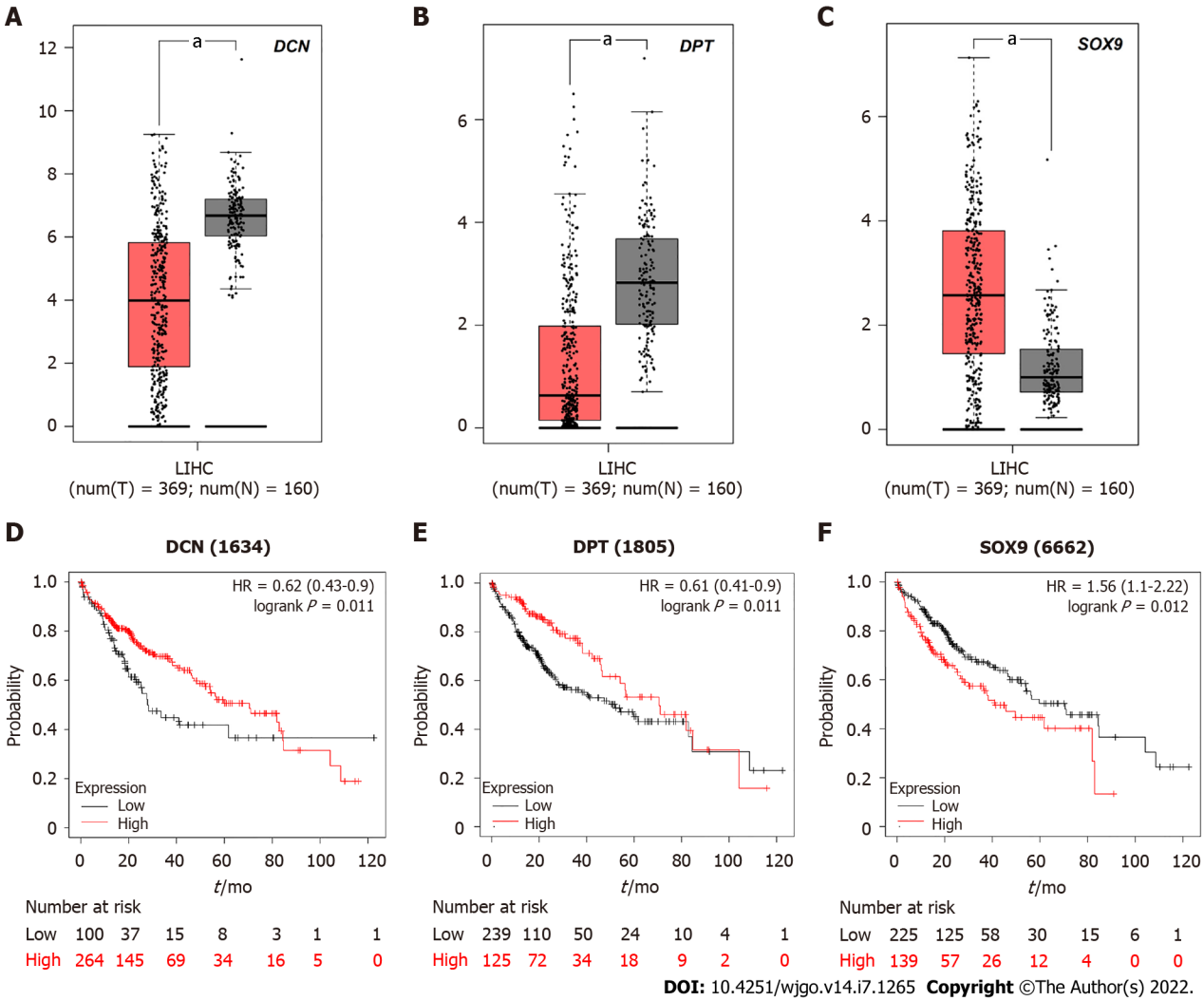

DOI: 10.4251/wjgo.v14.i7.1265

Figure 6 The relationship between decorin, dermatopontin, SRY-box transcription factor 9 expression and survival rate of hepatocellular carcinoma patients. A-C: Decorin (DCN), dermatopontin (DPT), and SRY-box transcription factor 9 (SOX9) were analyzed by gene expression profiling interactive analysis server (GEPIA) to determine their expression level differences between hepatocellular carcinoma (HCC) and normal liver tissues. Red box represents tumor tissue and gray box represents normal tissue; D-F: Prognostic information of hub genes. Kaplan-Meier plotter online tool was used to identify the prognostic information of DCN, DPT and SOX9, which associated with the survival rate of HCC patients ($^aP < 0.05$).

DPT is a downstream target of the vitamin D receptor. Fu *et al*[44] reported that mRNA expression of DPT was significantly downregulated in HCC, while its protein was weakly expressed in tumorous tissues compared to that in non-tumorous tissues. However, Lefebvre *et al*[45] suggested that DPT is upregulated in active NASH and fibrosis, and it is necessary for collagen deposition in profibrotic conditions. Our results also confirmed that the expression of DPT increased with the aggravation of liver fibrosis. Interestingly, a previous study showed that DPT interacts with DCN, which influences collagen fibrillogenesis and increases TGF-β1 signaling[46]. Our study identified these two molecules in a combined screening, suggesting that both DPT and DCN play an important role in the occurrence and development of liver fibrosis and HCC. However, the interactions between them needs to be further studied.

During tumorigenesis, SOX9 is upregulated in various tumors and plays an essential role in tumor progression as an oncogene[29], which regulates cellular proliferation, senescence, and self-renewal and is highly expressed in liver cancer stem cells[47]. In addition, SOX9 was the earliest marker expressed by biliary precursors[48]. It has been confirmed as a transcription factor that regulates bile duct development and contributes to liver regeneration and fibrosis[47]. In this study, we confirmed that SOX9 was positively correlated with the degree of fibrosis, and the high expression of SOX9 indicated a decline in the 5-year survival rate of patients with HCC, which is consistent with the results of other studies. In addition, our results showed that SOX9 was enriched and expressed in bile duct cells in mouse and human fibrotic livers, and the expression levels of SOX9 in hepatocytes were also increased significantly in patients with HCC. This observation can be explained by the fact that SOX9 mediates the transdifferentiation of hepatocytes into bile duct epithelial cells[47]. However, the detailed molecular mechanism of SOX9 overexpression in hepatocytes requires further elucidation.

Our current study has some limitations. First, we only analyzed the transcriptome, and many studies have shown that epigenetic modifications and non-coding RNAs also play an important role in the progression of liver diseases[33,49]. Secondly, the sample size in terms of number of patients was small, and immunohistochemistry was a semi-quantitative method. In addition, although our study had identified the signal transduction pathway involved in liver cirrhosis and HCC, it lacked in-depth analysis on the mechanism of action of these molecules, which needed to be further studied using *in vivo* studies or knock-out mice.

CONCLUSION

We screened GEO databases and obtained 45 DEGs and 10 hub genes (particularly *DCN, DPT,* and *SOX9*) in cirrhotic liver tissues. Upregulated expression of DCN, DPT, and SOX9 was all positively correlated with the degree of fibrosis, but there may be differences between their correlation with the 5-year survival rate of HCC patients.

ARTICLE HIGHLIGHTS

Research background

Liver fibrosis and hepatocellular carcinoma (HCC) are common adverse consequences of chronic liver injury. Establishing more effective biomarkers is important for understanding the pathogenesis, occurrence, development mechanisms of liver fibrosis and HCC, as well as to identify new diagnostic and therapeutic tools.

Research motivation

Bioinformatics has screened out many differentially expressed genes related to liver fibrosis; however, it is unknown whether these genes are different in animal and human liver fibrosis tissues, especially among the different fibrotic degrees. Therefore, we should carefully analyze the research results of bioinformatics.

Research objectives

To identify liver fibrosis-related core genes, we observed and compared the differential expression pattern of core genes in patients with liver fibrosis and HCC.

Research methods

In this study, we analyzed the expression pattern of hub genes of fibrosis and HCC. Bioinformatics analyses, quantitative polymerase chain reaction, Western blot, and immunohistochemistry of liver tissues from mouse model and patients were performed to identify novel biomarkers of liver fibrosis and HCC.

Research results

Ten hub genes (*CXCL9, CXCL10, CXCR4, DCN, DPT, LAMA2, LUM, MFAP4, PDGFRA,* and *SOX9*) associated with cirrhosis were screened from GSE14323, GSE36411, and GSE89377 datasets. DCN, DPT, and SOX9 were highly expressed in the CCl_4-induced mouse model of liver cirrhosis and fibrotic patient liver samples, and their expression levels were associated with the degree of fibrosis. In patients with HCC, SOX9 was upregulated, while DCN and DPT were downregulated. However, the 5-year survival rate of HCC patients with high SOX 9 expression was significantly reduced, which is different from DPT or DCN.

Research conclusions

We screened and identified 10 hub genes related to fibrosis. The expression levels of DCN, DPT, and SOX were positively correlated with the degree of liver fibrosis but showed different correlations with the survival rate of patients with HCC.

Research perspectives

The integrated approach of bioinformatics and molecular biology is more efficient to research multi-factorial diseases, such as liver fibrosis and liver cancer. Future studies on the differences on DCN, DPT, and SOX9 expression may help in the better understanding of the mechanisms involved in the development of liver fibrosis and HCC.

FOOTNOTES

Author contributions: Li Y and Yuan SL contributed equally to this work; Wang Q and Xie W designed the research and were co-corresponding authors; Yuan SL, Li Y, Yin JY, Yang K and Zhou XG performed the experiments; Yuan SL and Li Y analyzed the data; Yuan SL, Li Y and Wang Q wrote the manuscript; Yuan SL provided vital reagents and analytical tools; all authors read and approved the final manuscript.

Supported by the Beijing Natural Science Foundation, No. 7222097; Beijing Hospitals Authority the Digestive Medical Coordinated Development Center, No. XXZ0401; National Natural Science Foundation of China, No. 82000555 and No. 81900547; and Beijing Municipal Science and Technology Commission, No. D171100003117005.

Institutional review board statement: The study protocol conforms to the ethical guidelines of the 1975 Declaration of Helsinki as reflected in a priori approval by the Ethics Committee of Beijing Ditan Hospital No. 2021-034-01.

Informed consent statement: Patients were not required to give informed consent to the study because the analysis used anonymous clinical data and liver tissue samples.

Conflict-of-interest statement: All the authors report no relevant conflicts of interest for this article.

Data sharing statement: Publicly available datasets were analyzed in this study, which can be found here: GSE14323, GSE36411 and GSE89377. Technical appendix, statistical code, and data set available from the corresponding author at wangqidl04@ccmu.edu.cn. No additional data are available.

Country/Territory of origin: China

ORCID number: Yue Li 0000-0002-7412-7632; Shou-Li Yuan 0000-0002-4733-9891; Jing-Ya Yin 0000-0002-9707-2363; Kun Yang 0000-0003-0688-4962; Xin-Gang Zhou 0000-0002-4211-3017; Wen Xie 0000-0002-7314-8175; Qi Wang 0000-0002-0269-1568.

Corresponding Author's Membership in Professional Societies: Beijing Medical Association Hepatology Branch.

S-Editor: Gong ZM
L-Editor: A
P-Editor: Li X

REFERENCES

1 **Bosetti C**, Turati F, La Vecchia C. Hepatocellular carcinoma epidemiology. *Best Pract Res Clin Gastroenterol* 2014; **28**: 753-770 [PMID: 25260306 DOI: 10.1016/j.bpg.2014.08.007]
2 **Harris PS**, Hansen RM, Gray ME, Massoud OI, McGuire BM, Shoreibah MG. Hepatocellular carcinoma surveillance: An evidence-based approach. *World J Gastroenterol* 2019; **25**: 1550-1559 [PMID: 30983815 DOI: 10.3748/wjg.v25.i13.1550]
3 **Chen Z**, Xie H, Hu M, Huang T, Hu Y, Sang N, Zhao Y. Recent progress in treatment of hepatocellular carcinoma. *Am J Cancer Res* 2020; **10**: 2993-3036 [PMID: 33042631]
4 **Chen W**, Zheng R, Baade PD, Zhang S, Zeng H, Bray F, Jemal A, Yu XQ, He J. Cancer statistics in China, 2015. *CA Cancer J Clin* 2016; **66**: 115-132 [PMID: 26808342 DOI: 10.3322/caac.21338]
5 **Zhou WC**, Zhang QB, Qiao L. Pathogenesis of liver cirrhosis. *World J Gastroenterol* 2014; **20**: 7312-7324 [PMID: 24966602 DOI: 10.3748/wjg.v20.i23.7312]
6 **Thomson MJ**, Lok AS, Tapper EB. Optimizing medication management for patients with cirrhosis: Evidence-based strategies and their outcomes. *Liver Int* 2018; **38**: 1882-1890 [PMID: 29845749 DOI: 10.1111/liv.13892]
7 **Huang X**, Li Y, Guo X, Zhu Z, Kong X, Yu F, Wang Q. Identification of differentially expressed genes and signaling pathways in chronic obstructive pulmonary disease *via* bioinformatic analysis. *FEBS Open Bio* 2019; **9**: 1880-1899 [PMID: 31419078 DOI: 10.1002/2211-5463.12719]
8 **Jiang CH**, Yuan X, Li JF, Xie YF, Zhang AZ, Wang XL, Yang L, Liu CX, Liang WH, Pang LJ, Zou H, Cui XB, Shen XH, Qi Y, Jiang JF, Gu WY, Li F, Hu JM. Bioinformatics-based screening of key genes for transformation of liver cirrhosis to hepatocellular carcinoma. *J Transl Med* 2020; **18**: 40 [PMID: 32000807 DOI: 10.1186/s12967-020-02229-8]
9 **Chan KM**, Wu TH, Wu TJ, Chou HS, Yu MC, Lee WC. Bioinformatics microarray analysis and identification of gene expression profiles associated with cirrhotic liver. *Kaohsiung J Med Sci* 2016; **32**: 165-176 [PMID: 27185598 DOI: 10.1016/j.kjms.2016.03.008]
10 **Chinese Society of Infectious Diseases**; Chinese Medical Association; Chinese Society of Hepatology, Chinese Medical Association. [The guidelines of prevention and treatment for chronic hepatitis B (2019 version)]. *Zhonghua Gan Zang Bing*

Za Zhi 2019; **27**: 938-961 [PMID: 31941257 DOI: 10.3760/cma.j.issn.1007-3418.2019.12.007]
11 **Bedossa P**, Poynard T. An algorithm for the grading of activity in chronic hepatitis C. The METAVIR Cooperative Study Group. *Hepatology* 1996; **24**: 289-293 [PMID: 8690394 DOI: 10.1002/hep.510240201]
12 **Rhodes DR**, Kalyana-Sundaram S, Mahavisno V, Varambally R, Yu J, Briggs BB, Barrette TR, Anstet MJ, Kincead-Beal C, Kulkarni P, Varambally S, Ghosh D, Chinnaiyan AM. Oncomine 3.0: genes, pathways, and networks in a collection of 18,000 cancer gene expression profiles. *Neoplasia* 2007; **9**: 166-180 [PMID: 17356713 DOI: 10.1593/neo.07112]
13 **Szklarczyk D**, Gable AL, Lyon D, Junge A, Wyder S, Huerta-Cepas J, Simonovic M, Doncheva NT, Morris JH, Bork P, Jensen LJ, Mering CV. STRING v11: protein-protein association networks with increased coverage, supporting functional discovery in genome-wide experimental datasets. *Nucleic Acids Res* 2019; **47**: D607-D613 [PMID: 30476243 DOI: 10.1093/nar/gky1131]
14 **Shannon P**, Markiel A, Ozier O, Baliga NS, Wang JT, Ramage D, Amin N, Schwikowski B, Ideker T. Cytoscape: a software environment for integrated models of biomolecular interaction networks. *Genome Res* 2003; **13**: 2498-2504 [PMID: 14597658 DOI: 10.1101/gr.1239303]
15 **Tang Z**, Li C, Kang B, Gao G, Zhang Z. GEPIA: a web server for cancer and normal gene expression profiling and interactive analyses. *Nucleic Acids Res* 2017; **45**: W98-W102 [PMID: 28407145 DOI: 10.1093/nar/gkx247]
16 **Menyhárt O**, Nagy Á, Győrffy B. Determining consistent prognostic biomarkers of overall survival and vascular invasion in hepatocellular carcinoma. *R Soc Open Sci* 2018; **5**: 181006 [PMID: 30662724 DOI: 10.1098/rsos.181006]
17 **Müller M**, Bird TG, Nault JC. The landscape of gene mutations in cirrhosis and hepatocellular carcinoma. *J Hepatol* 2020; **72**: 990-1002 [PMID: 32044402 DOI: 10.1016/j.jhep.2020.01.019]
18 **Marrocco C**, Rinalducci S, Mohamadkhani A, D'Amici GM, Zolla L. Plasma gelsolin protein: a candidate biomarker for hepatitis B-associated liver cirrhosis identified by proteomic approach. *Blood Transfus* 2010; **8** Suppl 3: s105-s112 [PMID: 20606740 DOI: 10.2450/2010.017S]
19 **Guzmán-Fulgencio M**, Berenguer J, Jiménez-Sousa MA, Pineda-Tenor D, Aldámiz-Echevarria T, García-Broncano P, Carrero A, García-Álvarez M, Tejerina F, Diez C, Vazquez-Morón S, Resino S. Association between IL7R polymorphisms and severe liver disease in HIV/HCV coinfected patients: a cross-sectional study. *J Transl Med* 2015; **13**: 206 [PMID: 26123260 DOI: 10.1186/s12967-015-0577-y]
20 **Xiang Y**, Tang JJ, Tao W, Cao X, Song BL, Zhong J. Identification of Cholesterol 25-Hydroxylase as a Novel Host Restriction Factor and a Part of the Primary Innate Immune Responses against Hepatitis C Virus Infection. *J Virol* 2015; **89**: 6805-6816 [PMID: 25903345 DOI: 10.1128/JVI.00587-15]
21 **Shrivastava S**, Meissner EG, Funk E, Poonia S, Shokeen V, Thakur A, Poonia B, Sarin SK, Trehanpati N, Kottilil S. Elevated hepatic lipid and interferon stimulated gene expression in HCV GT3 patients relative to non-alcoholic steatohepatitis. *Hepatol Int* 2016; **10**: 937-946 [PMID: 27193023 DOI: 10.1007/s12072-016-9733-6]
22 **Farquhar MJ**, Humphreys IS, Rudge SA, Wilson GK, Bhattacharya B, Ciaccia M, Hu K, Zhang Q, Mailly L, Reynolds GM, Ashcroft M, Balfe P, Baumert TF, Roessler S, Wakelam MJO, McKeating JA. Autotaxin-lysophosphatidic acid receptor signalling regulates hepatitis C virus replication. *J Hepatol* 2017; **66**: 919-929 [PMID: 28126468 DOI: 10.1016/j.jhep.2017.01.009]
23 **Kinast V**, Leber SL, Brown RJP, Vieyres G, Behrendt P, Eßbach C, Strnad P, Vondran FWR, Cornberg M, Wex C, Pietschmann T, Haybaeck J, Todt D, Steinmann E. Identification of Keratin 23 as a Hepatitis C Virus-Induced Host Factor in the Human Liver. *Cells* 2019; **8** [PMID: 31216713 DOI: 10.3390/cells8060610]
24 **Gerhard GS**, Hanson A, Wilhelmsen D, Piras IS, Still CD, Chu X, Petrick AT, DiStefano JK. AEBP1 expression increases with severity of fibrosis in NASH and is regulated by glucose, palmitate, and miR-372-3p. *PLoS One* 2019; **14**: e0219764 [PMID: 31299062 DOI: 10.1371/journal.pone.0219764]
25 **Wolff G**, Taranko AE, Meln I, Weinmann J, Sijmonsma T, Lerch S, Heide D, Billeter AT, Tews D, Krunic D, Fischer-Posovszky P, Müller-Stich BP, Herzig S, Grimm D, Heikenwälder M, Kao WW, Vegiopoulos A. Diet-dependent function of the extracellular matrix proteoglycan Lumican in obesity and glucose homeostasis. *Mol Metab* 2019; **19**: 97-106 [PMID: 30409703 DOI: 10.1016/j.molmet.2018.10.007]
26 **Hou W**, Janech MG, Sobolesky PM, Bland AM, Samsuddin S, Alazawi W, Syn WK. Proteomic screening of plasma identifies potential noninvasive biomarkers associated with significant/advanced fibrosis in patients with nonalcoholic fatty liver disease. *Biosci Rep* 2020; **40** [PMID: 31860081 DOI: 10.1042/BSR20190395]
27 **Huang CC**, Chuang JH, Chou MH, Wu CL, Chen CM, Wang CC, Chen YS, Chen CL, Tai MH. Matrilysin (MMP-7) is a major matrix metalloproteinase upregulated in biliary atresia-associated liver fibrosis. *Mod Pathol* 2005; **18**: 941-950 [PMID: 15696117 DOI: 10.1038/modpathol.3800374]
28 **Jinawath N**, Chamgramol Y, Furukawa Y, Obama K, Tsunoda T, Sripa B, Pairojkul C, Nakamura Y. Comparison of gene expression profiles between Opisthorchis viverrini and non-Opisthorchis viverrini associated human intrahepatic cholangiocarcinoma. *Hepatology* 2006; **44**: 1025-1038 [PMID: 17006947 DOI: 10.1002/hep.21330]
29 **Yovchev MI**, Xue Y, Shafritz DA, Locker J, Oertel M. Repopulation of the fibrotic/cirrhotic rat liver by transplanted hepatic stem/progenitor cells and mature hepatocytes. *Hepatology* 2014; **59**: 284-295 [PMID: 23840008 DOI: 10.1002/hep.26615]
30 **Lou Y**, Tian GY, Song Y, Liu YL, Chen YD, Shi JP, Yang J. Characterization of transcriptional modules related to fibrosing-NAFLD progression. *Sci Rep* 2017; **7**: 4748 [PMID: 28684781 DOI: 10.1038/s41598-017-05044-2]
31 **Klag T**, Thomas M, Ehmann D, Courth L, Mailänder-Sanchez D, Weiss TS, Dayoub R, Abshagen K, Vollmar B, Thasler WE, Stange EF, Berg CP, Malek NP, Zanger UM, Wehkamp J. β-Defensin 1 Is Prominent in the Liver and Induced During Cholestasis by Bilirubin and Bile Acids *via* Farnesoid X Receptor and Constitutive Androstane Receptor. *Front Immunol* 2018; **9**: 1735 [PMID: 30100908 DOI: 10.3389/fimmu.2018.01735]
32 **Cheung ST**, Leung KL, Ip YC, Chen X, Fong DY, Ng IO, Fan ST, So S. Claudin-10 expression level is associated with recurrence of primary hepatocellular carcinoma. *Clin Cancer Res* 2005; **11**: 551-556 [PMID: 15701840]
33 **Ding Z**, Qian YB, Zhu LX, Xiong QR. Promoter methylation and mRNA expression of DKK-3 and WIF-1 in hepatocellular carcinoma. *World J Gastroenterol* 2009; **15**: 2595-2601 [PMID: 19496188 DOI: 10.3748/wjg.15.2595]
34 **Huang GW**, Ding X, Chen SL, Zeng L. Expression of claudin 10 protein in hepatocellular carcinoma: impact on survival. *J*

Cancer Res Clin Oncol 2011; **137**: 1213-1218 [PMID: 21647678 DOI: 10.1007/s00432-011-0987-z]

35 **Bacigalupo ML**, Manzi M, Rabinovich GA, Troncoso MF. Hierarchical and selective roles of galectins in hepatocarcinogenesis, liver fibrosis and inflammation of hepatocellular carcinoma. *World J Gastroenterol* 2013; **19**: 8831-8849 [PMID: 24379606 DOI: 10.3748/wjg.v19.i47.8831]

36 **Ye X**, Li C, Zu X, Lin M, Liu Q, Liu J, Xu G, Chen Z, Xu Y, Liu L, Luo D, Cao Z, Shi G, Feng Z, Deng H, Liao Q, Cai C, Liao DF, Wang J, Jin J, Cao D. A Large-Scale Multicenter Study Validates Aldo-Keto Reductase Family 1 Member B10 as a Prevalent Serum Marker for Detection of Hepatocellular Carcinoma. *Hepatology* 2019; **69**: 2489-2501 [PMID: 30672601 DOI: 10.1002/hep.30519]

37 **Zhang Z**, Li J, He T, Ouyang Y, Huang Y, Liu Q, Wang P, Ding J. The competitive endogenous RNA regulatory network reveals potential prognostic biomarkers for overall survival in hepatocellular carcinoma. *Cancer Sci* 2019; **110**: 2905-2923 [PMID: 31335995 DOI: 10.1111/cas.14138]

38 **Zhang Z**, Wen H, Weng J, Feng L, Liu H, Hu X, Zeng F. Silencing of EPCAM suppresses hepatic fibrosis and hepatic stellate cell proliferation in mice with alcoholic hepatitis *via* the PI3K/Akt/mTOR signaling pathway. *Cell Cycle* 2019; **18**: 2239-2254 [PMID: 31378124 DOI: 10.1080/15384101.2019.1642067]

39 **Zhang W**, Ge Y, Cheng Q, Zhang Q, Fang L, Zheng J. Decorin is a pivotal effector in the extracellular matrix and tumour microenvironment. *Oncotarget* 2018; **9**: 5480-5491 [PMID: 29435195 DOI: 10.18632/oncotarget.23869]

40 **Zhang G**, Ezura Y, Chervoneva I, Robinson PS, Beason DP, Carine ET, Soslowsky LJ, Iozzo RV, Birk DE. Decorin regulates assembly of collagen fibrils and acquisition of biomechanical properties during tendon development. *J Cell Biochem* 2006; **98**: 1436-1449 [PMID: 16518859 DOI: 10.1002/jcb.20776]

41 **Baghy K**, Iozzo RV, Kovalszky I. Decorin-TGFβ axis in hepatic fibrosis and cirrhosis. *J Histochem Cytochem* 2012; **60**: 262-268 [PMID: 22260996 DOI: 10.1369/0022155412438104]

42 **Dudás J**, Kovalszky I, Gallai M, Nagy JO, Schaff Z, Knittel T, Mehde M, Neubauer K, Szalay F, Ramadori G. Expression of decorin, transforming growth factor-beta 1, tissue inhibitor metalloproteinase 1 and 2, and type IV collagenases in chronic hepatitis. *Am J Clin Pathol* 2001; **115**: 725-735 [PMID: 11345837 DOI: 10.1309/J8CD-E9C8-X4NG-GTVG]

43 **Shang YK**, Li F, Zhang Y, Liu ZK, Wang ZL, Bian H, Chen ZN. Systems analysis of key genes and pathways in the progression of hepatocellular carcinoma. *Medicine (Baltimore)* 2018; **97**: e10892 [PMID: 29879025 DOI: 10.1097/MD.0000000000010892]

44 **Fu Y**, Feng MX, Yu J, Ma MZ, Liu XJ, Li J, Yang XM, Wang YH, Zhang YL, Ao JP, Xue F, Qin W, Gu J, Xia Q, Zhang ZG. DNA methylation-mediated silencing of matricellular protein dermatopontin promotes hepatocellular carcinoma metastasis by α3β1 integrin-Rho GTPase signaling. *Oncotarget* 2014; **5**: 6701-6715 [PMID: 25149533 DOI: 10.18632/oncotarget.2239]

45 **Lefebvre P**, Lalloyer F, Baugé E, Pawlak M, Gheeraert C, Dehondt H, Vanhoutte J, Woitrain E, Hennuyer N, Mazuy C, Bobowski-Gérard M, Zummo FP, Derudas B, Driessen A, Hubens G, Vonghia L, Kwanten WJ, Michielsen P, Vanwolleghem T, Eeckhoute J, Verrijken A, Van Gaal L, Francque S, Staels B. Interspecies NASH disease activity whole-genome profiling identifies a fibrogenic role of PPARα-regulated dermatopontin. *JCI Insight* 2017; **2** [PMID: 28679947 DOI: 10.1172/jci.insight.92264]

46 **Okamoto O**, Fujiwara S, Abe M, Sato Y. Dermatopontin interacts with transforming growth factor beta and enhances its biological activity. *Biochem J* 1999; **337** (Pt 3): 537-541 [PMID: 9895299]

47 **Suda H**, Yoshii D, Yamamura K, Yokouchi Y, Inomata Y. New insight into reactive ductular cells of biliary atresia provided by pathological assessment of SOX9. *Pediatr Surg Int* 2014; **30**: 481-492 [PMID: 24658905 DOI: 10.1007/s00383-014-3497-7]

48 **Furuyama K**, Kawaguchi Y, Akiyama H, Horiguchi M, Kodama S, Kuhara T, Hosokawa S, Elbahrawy A, Soeda T, Koizumi M, Masui T, Kawaguchi M, Takaori K, Doi R, Nishi E, Kakinoki R, Deng JM, Behringer RR, Nakamura T, Uemoto S. Continuous cell supply from a Sox9-expressing progenitor zone in adult liver, exocrine pancreas and intestine. *Nat Genet* 2011; **43**: 34-41 [PMID: 21113154 DOI: 10.1038/ng.722]

49 **Yang JJ**, Tao H, Deng ZY, Lu C, Li J. Non-coding RNA-mediated epigenetic regulation of liver fibrosis. *Metabolism* 2015; **64**: 1386-1394 [PMID: 26362725 DOI: 10.1016/j.metabol.2015.08.004]

World Journal of Gastrointestinal Oncology

Submit a Manuscript: https://www.f6publishing.com

World J Gastrointest Oncol 2022 July 15; 14(7): 1281-1294

DOI: 10.4251/wjgo.v14.i7.1281

ISSN 1948-5204 (online)

ORIGINAL ARTICLE

Case Control Study

Efficacy of neoadjuvant chemotherapy for initially resectable colorectal liver metastases: A retrospective cohort study

Kazuhisa Takeda, Yu Sawada, Yasuhiro Yabushita, Yuki Honma, Takafumi Kumamoto, Jun Watanabe, Ryusei Matsuyama, Chikara Kunisaki, Toshihiro Misumi, Itaru Endo

Specialty type: Oncology

Provenance and peer review: Unsolicited article; Externally peer reviewed.

Peer-review model: Single blind

Peer-review report's scientific quality classification

Grade A (Excellent): A, A
Grade B (Very good): B
Grade C (Good): C
Grade D (Fair): 0
Grade E (Poor): 0

P-Reviewer: Barisani D, Italy; de Melo FF, Brazil; Habashy HO, Egypt; Planellas P, Spain
A-Editor: Zhou S, United States

Received: February 1, 2022
Peer-review started: February 1, 2022
First decision: April 17, 2022
Revised: April 29, 2022
Accepted: June 4, 2022
Article in press: June 4, 2022
Published online: July 15, 2022

Kazuhisa Takeda, Yu Sawada, Jun Watanabe, Chikara Kunisaki, Gastroenterological Center, Yokohama City University Medical Center, Yokohama 232-0024, Japan

Yasuhiro Yabushita, Yuki Honma, Takafumi Kumamoto, Ryusei Matsuyama, Itaru Endo, Department of Gastroenterological Surgery, Yokohama City University Graduate School of Medicine, Yokohama 236-0004, Jordan

Toshihiro Misumi, Department of Biostatistics, Yokohama City University Graduate School of Medicine, Yokohama 236-0004, Japan

Corresponding author: Kazuhisa Takeda, PhD, Assistant Professor, Gastroenterological Center, Yokohama City University Medical Center, 4-57 Urafune-cho, Minami-ku, Yokohama 232-0024, Japan. kazu1968@yokohama-cu.ac.jp

Abstract

BACKGROUND

The liver is the most common metastatic site of colorectal cancer. Hepatectomy is the mainstay of treatment for patients with colorectal liver metastases (CRLMs). However, there are cases of early recurrence after upfront hepatectomy alone. In selected high-risk patients, neoadjuvant chemotherapy (NAC) may improve long-term survival.

AIM

To determine the efficacy of NAC for initially resectable CRLMs.

METHODS

Among 644 patients who underwent their first hepatectomy for CRLMs at our institution, 297 resectable cases were stratified into an upfront hepatectomy group (238 patients) and a NAC group (59 patients). Poor prognostic factors for upfront hepatectomy were identified using multivariate logistic regression analysis. Propensity score matching was used to compare clinical outcomes between the upfront hepatectomy and NAC groups, according to the number of poor prognostic factors. Survival curves were estimated using the Kaplan–Meier method and compared using the log-rank test.

RESULTS

Preoperative carcinoembryonic antigen levels (≥ 10 ng/mL) (P = 0.003), primary

histological type (other than well/moderately differentiated) (P = 0.04), and primary lymph node metastases (≥ 1) (P = 0.04) were identified as independent poor prognostic factors for overall survival (OS) in the upfront hepatectomy group. High-risk status was defined as the presence of two or more risk factors. After propensity score matching, 50 patients were matched in each group. Among high-risk patients, the 5-year OS rate was significantly higher in the NAC group (13 patients) than in the upfront hepatectomy group (18 patients) (100% *vs* 34%; P = 0.02).

CONCLUSION

NAC may improve the prognosis of high-risk patients with resectable CRLMs who have two or more risk factors.

Key Words: Colorectal neoplasms; Neoadjuvant therapy; Neoplasm metastasis; Prognosis; Risk factors; Survival

Core Tip: Hepatectomy is the mainstay of treatment for patients with colorectal liver metastases (CRLMs). However, there are cases of early recurrence after upfront hepatectomy alone. In selected high-risk patients, neoadjuvant chemotherapy (NAC) may improve long-term survival. Although several studies have identified risk factors for recurrence and prognosis after hepatectomy for CRLMs, they could not show a benefit of NAC for resectable CRLMs. This article demonstrated the effectiveness of NAC for initially resectable CRLMs, based on risk stratification according to prognostic factors.

Citation: Takeda K, Sawada Y, Yabushita Y, Honma Y, Kumamoto T, Watanabe J, Matsuyama R, Kunisaki C, Misumi T, Endo I. Efficacy of neoadjuvant chemotherapy for initially resectable colorectal liver metastases: A retrospective cohort study. *World J Gastrointest Oncol* 2022; 14(7): 1281-1294
URL: https://www.wjgnet.com/1948-5204/full/v14/i7/1281.htm
DOI: https://dx.doi.org/10.4251/wjgo.v14.i7.1281

INTRODUCTION

Colorectal cancer (CRC) is a leading cause of cancer-related deaths worldwide. Approximately 20% of patients with CRC present with synchronous distant metastases, and another 20% develop metachronous metastases[1].

The liver is the most common metastatic site of CRC[2]. Hepatectomy is the mainstay of treatment for patients with colorectal liver metastases (CRLMs). The 5-year overall survival (OS) rate after curative hepatectomy has been reported to range from 45 to 61%. However, the postoperative recurrence rate is high (approximately 75%), especially in the remnant liver[3]. To improve surgical outcomes, neoadjuvant chemotherapy (NAC) has been used to treat initially resectable CRLMs. In the EORTC 40983 trial[4], 364 patients with resectable CRLMs were randomly assigned to a perioperative 5-fluorouracil/folinic acid/oxaliplatin (FOLFOX4) group and a surgery alone group. Better recurrence-free survival, but no OS benefit, was observed in patients in the chemotherapy group. Therefore, upfront hepatectomy is recommended for patients with resectable CRLMs[3,5].

Several studies[6-9] have identified risk factors for recurrence and prognosis after hepatectomy for CRLMs, including positive lymph node status of the primary colorectal lesion, appearance time, largest tumor diameter, number and distribution of CRLMs, and preoperative carcinoembryonic antigen (CEA)/carbohydrate antigen 19-9 Levels. A greater number of risk factors were associated with early recurrence or poor prognosis. Hence, there are cases of early recurrence after upfront hepatectomy alone in the resectable CRLMs, and in selected high-risk patients, NAC may improve long-term survival. We investigated the effectiveness of NAC for initially resectable CRLMs, based on risk stratification according to prognostic factors.

MATERIALS AND METHODS

Study design

A total of 644 patients underwent their first hepatectomy for CRLMs at our institution between January 1992 and December 2019. Among them, 297 resectable cases were included in this study. Among these cases, patients with synchronous liver metastases who received liver-first surgery or simultaneous

resection of CRLM and the primary lesion were excluded. Patients were stratified into an upfront hepatectomy group (238 patients) and a NAC group (59 patients) (Figure 1). No patient received preoperative chemotherapy before resection of the primary lesion. Poor prognostic factors for upfront hepatectomy were identified using multivariate logistic regression analysis. Propensity score matching was performed using baseline characteristics, and clinical outcomes were compared between the groups, according to the number of poor prognostic factors.

Clinicopathological characteristics

The following clinicopathological variables were analyzed: Patient-related: Age (< 60 *vs* ≥ 60 years), sex (male *vs* female), and initial CEA level (< 10 *vs* ≥ 10 ng/mL); primary tumor-related: Site of the primary lesion (right *vs* left), primary histological type (well/moderately differentiated *vs* others), lymph node metastases (0 *vs* ≥ 1), depth of tumor invasion [adjacent organ invasion (T4b) *vs* others], lymphatic invasion (0 *vs* ≥ 1), and venous invasion (0 *vs* ≥ 1); liver metastasis-related: Number (1–3 *vs* ≥ 4), maximum diameter (< 40 *vs* ≥ 40 mm), appearance time (synchronous *vs* metachronous), and tumor distribution (unilobar *vs* bilobar); and treatment-related: Staged hepatectomy (performed *vs* not performed), surgical margins (exposed *vs* not exposed), and adjuvant chemotherapy after primary resection and after hepatectomy (administered *vs* not administered). In addition, left-sided tumors included carcinomas in the descending colon, sigmoid colon, and rectum; and right-sided tumors included carcinomas in the cecum, ascending colon, and transverse colon.

Propensity score matching was performed to minimize the differences in baseline characteristics between the upfront hepatectomy and NAC groups. The propensity score for each patient was estimated by logistic regression analysis using the primary tumor- and liver metastasis-related variables.

Indications for NAC

The criteria for resectable CRLMs were: (1) No extrahepatic metastases; (2) Liver tumor in one lobe only, or no more than three tumors in both lobes; (3) Favorable tumor location, without invasion of major vascular structures; (4) Maximum tumor diameter ≤ 80 mm; and (5) Sufficient planned residual liver volume[10]. The criteria for unresectable CRLMs were uncontrollable extrahepatic metastases and insufficient residual liver capacity. Originally, NAC was administered to those with marginally resectable CRLMs who did not satisfy either of these criteria[10]. However, there were patients who underwent upfront hepatectomy (at their own request) although they met the criteria for NAC initially. Conversely, there were patients who received NAC although they met the criteria for resectable CRLM initially. Therefore, patients who met the criteria for resectable CRLM included those who underwent upfront hepatectomy or received NAC.

NAC

Patients received NAC according to the abovementioned criteria. Some patients in the NAC group were treated with chemotherapy by another physician, who considered the CRLMs to be unresectable. However, when the patients were referred to our hospital, the CRLMs were judged to have met the criteria for resection prior to the start of chemotherapy. Regarding NAC regimens, fluoracyl and folinic acid had been used. After oxaliplatin- and irinotecan-based regimens became available, these were widely used as NAC. The combined use of molecularly-targeted agents was also considered, based on *RAS* status. Hepatic arterial infusion was considered for elderly patients, or those who could not continue systemic chemotherapy due to side effects. The response to NAC was evaluated by contrast-enhanced computed tomography (CT)/magnetic resonance imaging, according to the Response Evaluation Criteria in Solid Tumors (version 1.1)[11]. The number of treatment cycles varied because of the retrospective nature of the study. Hepatectomy was performed ≥ 4 wk after the last administration of chemotherapy. When bevacizumab was used, an interval of ≥ 6 wk was maintained.

Adjuvant chemotherapy after hepatectomy

Adjuvant chemotherapy (hepatic arterial or intravenous infusion or systemic or oral administration of fluoracyl and folinic acid, oxaliplatin, or irinotecan) was considered for all patients who underwent hepatectomy[10]. However, it has not been administered actively since 2019, as few studies have shown a survival benefit[12,13].

Hepatectomy

Hepatectomy with negative surgical margins was performed in principle with non-anatomical procedures. Anatomical hepatectomy was performed, if it was advantageous, in terms of complete resection (R0), operative time, blood loss, or invasiveness. Portal vein embolization or two-stage hepatectomy was planned when the remnant prognostic score was low, based on volumetry, the indocyanine green retention rate, and patients' age[14]. Intraoperative ultrasonography was performed in all cases to detect occult tumors undetected by preoperative imaging, and to confirm the anatomical relationships between tumors and vasculobiliary structures, and the absence of residual tumors in the remnant liver. Parenchymal dissection was performed mainly using ultrasonic dissectors[14]. R0

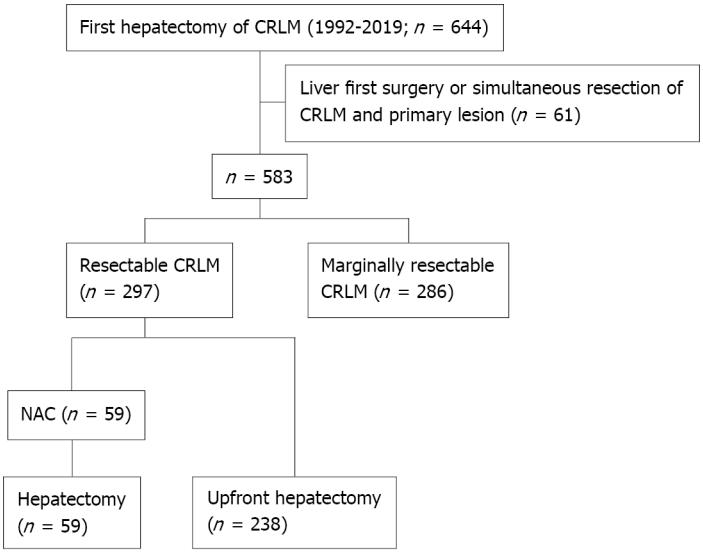

DOI: 10.4251/wjgo.v14.i7.1281

Figure 1 Study flow diagram. NAC: Neoadjuvant chemotherapy; CRLM: Colorectal liver metastases.

resection was considered complete when the pathologist assessed free resection margins.

Outcomes

OS was defined as the time from hepatectomy until death from any cause. Disease-free survival (DFS) was defined as the time from hepatectomy until the first recurrence. Tumor response was evaluated according to the Response Evaluation Criteria in Solid Tumors (version 1.1)[11]. Synchronous CRLMs were defined as metastases to the liver at the time of resection of the primary CRC.

Follow-up

Patients were examined for recurrence after hepatectomy using contrast-enhanced CT (every 4–6 mo), blood tests, and tumor markers (every 2–3 mo). When recurrence in the remnant liver was suspected, magnetic resonance imaging was performed, and the appearance of new lesions was investigated. Extrahepatic recurrence in the chest and pelvis was detected on CT. Fluorodeoxyglucose positron emission tomography was sometimes performed to detect other distant metastases. Recurrence was diagnosed when imaging studies confirmed new lesions showing typical features of CRC/CRLMs, compared with previous images. Recurrent CRLMs were treated with repeat resection, if applicable. When there was no indication for resection, chemotherapy, radiotherapy, or palliative care was chosen.

Statistical analyses

Quantitative variables were expressed as medians (interquartile ranges), and categorical variables as numbers and percentages. Continuous data were compared using the Mann–Whitney *U* test, and categorical data using the chi-square test. Survival curves were estimated using the Kaplan–Meier method and compared using the log-rank test. Multivariate analysis was performed using stepwise logistic regression. Statistically significant variables in the univariate analysis were included in the multivariate analysis. All statistical analyses were conducted using SPSS Base 11.0 J (Chicago, IL, United States). A P value < 0.05 was considered statistically significant.

RESULTS

Baseline characteristics before propensity score matching

Before propensity score matching, there were 238 patients in the upfront hepatectomy group and 59 patients in the NAC group (Table 1). Variables that were significantly different between the upfront hepatectomy and NAC groups included age (≥ 60 years) (P < 0.001), primary tumor location (right) (P = 0.03), lymph node metastases (≥ 1) (P < 0.001), depth of tumor invasion [adjacent organ invasion (T4b)] (P = 0.01), number of liver metastases (≥ 4) (P < 0.001), appearance time (synchronous) (P < 0.001), tumor distribution (bilobar) (P < 0.001), and staged hepatectomy (performed) (P = 0.04). The NAC regimens were as follows: Oxaliplatin-based chemotherapy (35 patients), with molecularly-targeted agents [bevacizumab (14 patients), cetuximab (three patients), and panitumumab (seven patients)]; irinotecan-based chemotherapy (four patients), with molecularly-targeted agents [bevacizumab (two patients) and panitumumab (two patients)]; oxaliplatin- and irinotecan-based chemotherapy (nine patients), with

Table 1 Patient characteristics before propensity score matching

Variables		Upfront hepatectomy (*n* = 238)	NAC (*n* = 59)	*P* value
Patient-related				
Age	< 60	123	14	< 0.001
	≥ 60	115	45	
Gender	Male	184	39	0.07
	Female	54	20	
CEA level (ng/mL)	< 10	73	19	0.82
	≥ 10	165	40	
Primary tumor-related				
Site	Right	34	15	0.03
	Left	204	44	
Histology	Well/moderately differentiated	236	57	0.128
	Others	2	2	
Lymph node metastases	0	144	17	< 0.001
	≥ 1	94	42	
Depth of invasion	Adjacent organ invasion (T4b)	14	9	0.01
	Others	224	50	
Lymphatic invasion	0	146	29	0.08
	≥ 1	92	30	
Venous invasion	0	91	18	0.27
	≥ 1	147	41	
Liver metastasis-related				
Number	1–3	233	48	< 0.001
	≥ 4	5	11	
Size (max)	< 40	180	18	0.06
	≥ 40	58	41	
Timing of the appearance	Synchronous	40	37	< 0.001
	Metachronous	198	22	
Distribution	Unilobar	211	38	< 0.001
	Bilobar	27	21	
Treatment-related				
Staged hepatectomy	Performed	0	1	0.04
	Not performed	238	58	
Surgical margin	Exposed	13	6	0.186
	Not exposed	225	53	
Adjuvant chemotherapy after primary resection	Administered	69	32	< 0.001
	Not administered	169	27	
Adjuvant chemotherapy after hepatectomy	Administered	86	23	0.684
	Not administered	152	36	

CEA: Carcinoembryonic antigen; NAC: Neoadjuvant chemotherapy.

molecularly-targeted agents [bevacizumab (six patients) and cetuximab (one patient)]; fluorouracil and folinic acid (nine patients), with cisplatin (seven patients); and chemotherapy, including hepatic arterial infusion (two patients). Responses to NAC were defined as follows: Complete response (no patient), partial response (34 patients), stable disease (22 patients), or progressive disease (three patients). The median number of treatment cycles was 6 (range from 2 to 25).

Prognostic factors for upfront hepatectomy

In univariate analysis, preoperative CEA levels (≥ 10 ng/mL) (P = 0.01), primary histological type (other than well/moderately differentiated) (P = 0.01), primary lymph node metastases (≥ 1) (P = 0.001), lymphatic invasion (≥ 1) (P = 0.02), and adjuvant chemotherapy (performed) (P = 0.02) were associated with poor OS in the upfront hepatectomy group (238 patients). Preoperative CEA levels [hazard ratio (HR), 1.948; 95% confidence interval (CI): 1.252–3.031; P = 0.003], primary histological type (HR, 2.971; 95%CI: 1.038–8.503; P = 0.04), and primary lymph node metastases (HR, 1.623; 95%CI: 1.020–2.583; P = 0.04) were independent prognostic factors in multivariate analysis (Table 2).

The 5-year OS rates of patients with zero (59 patients), one (108 patients), and two (71 patients) risk factors were 83%, 73%, and 46%, respectively. No patient had three risk factors. High-risk patients were defined as those with two or more risk factors, while low-risk patients were defined as those with zero or one risk factor. The 5-year OS rate of high-risk patients (71 patients) was significantly worse than that of low-risk patients (167 patients) (46.4% *vs* 76.4%; P < 0.001) (Figure 2).

Baseline characteristics after propensity score matching

Fifty patients in the upfront hepatectomy group were matched with 50 patients in the NAC group. Patients with insufficient preoperative data or without a suitable match were excluded. After matching preoperative baseline characteristics, treatment-related factors (staged hepatectomy, surgical margins, and adjuvant chemotherapy) were comparable between the two groups (Table 3). The NAC regimens after propensity score matching were as follows: Oxaliplatin-based chemotherapy (30 patients), with molecularly-targeted agents [bevacizumab (11 patients), cetuximab (three patients), and panitumumab (seven patients)]; irinotecan-based chemotherapy (four patients), with molecularly-targeted agents [bevacizumab (two patients) and panitumumab (two patients)]; oxaliplatin- and irinotecan-based chemotherapy (eight patients), with molecularly-targeted agents [bevacizumab (five patients) and cetuximab (one patient)]; fluorouracil and folinic acid (six patients), with cisplatin (four patients); and chemotherapy, including hepatic arterial infusion (two patients). Responses to NAC were defined as follows: Partial response (30 patients), stable disease (17 patients), or progressive disease (three patients). In total, there were 30 responders and 20 non-responders. The median number of treatment cycles was 6 (range from 2 to 25). The upfront hepatectomy group comprised 18 high-risk patients and 32 low-risk patients. The NAC group comprised 13 high-risk patients and 37 low-risk patients (Table 3). The background characteristics were comparable when stratified by high- and low-risk, respectively.

Clinical outcomes after propensity score matching

Short-term outcomes, including the amount of intraoperative bleeding, frequency of red blood cell transfusions, postoperative complications, and length of postoperative hospital stay, were not significantly different between the two groups. In the NAC group, there was one complication of Clavien–Dindo grade IV. In this patient, five cycles of irinotecan-based chemotherapy were administered as NAC. Partial resection of segments 7 and 8, with right hepatic vein reconstruction, was performed 4 wk after the last cycle of NAC. Laparotomy hemostasis was performed on postoperative day 5, due to bleeding from the surface of the hepatic dissection.

Regarding long-term outcomes, there was no significant difference in the 5-year OS rate between the upfront hepatectomy and NAC groups (63% *vs* 83%; P = 0.13) after propensity score matching. Among low-risk patients, there was also no significant difference in the 5-year OS rate (84.1% *vs* 81.0%; P = 0.79) (Figure 3A) or 5-year DFS rate (47.3% *vs* 46.3%; P = 0.71) (Figure 3B) between the two groups. Conversely, among high-risk patients, the 5-year OS rate was significantly higher in the NAC group than in the upfront hepatectomy group (100% *vs* 34.4%; P = 0.02) (Figure 3C). However, there was no significant difference in the 5-year DFS rate between the two groups (P = 0.37) (Figure 3D).

Recurrence after hepatectomy was observed in 30 (60%) patients in the upfront hepatectomy group and 24 (48%) patients in the NAC group. The difference between them was not statistically significant. The lung and remnant liver were the most frequent sites of recurrence in the upfront hepatectomy and NAC groups, respectively, and there was no significant difference in the distribution of initial recurrence sites. Regarding the initial treatment strategy for recurrence, resection and chemotherapy were adopted in 26.7% and 57.7% of patients in the upfront hepatectomy group and 25.0% and 66.7% of patients in the NAC group, respectively. The differences between them were not statistically significant (Table 4). Especially among high-risk patients, recurrence was observed in 15 (83%) of the 18 patients in the upfront hepatectomy group. Resection was adopted as the initial treatment strategy for recurrence in four patients, chemotherapy in six patients, and other therapies in five patients. None of the patients who received chemotherapy were converted to resection, and resection could only be performed in 27% of patients with recurrence. Conversely, recurrence was observed in nine (69%) of the 13 high-risk

Table 2 Prognostic factors for upfront hepatectomy

Variables		*n*	5-yr OS rate (%)	*P* value	Hazard ratio (95%CI)	*P* value
Patient-related						
Age (yr)	< 60	60	65.7	0.24		
	≥ 60	178	66.7			
Sex	Male	167	66.5	0.28		
	Female	71	65.8			
CEA level (ng/mL)	< 10	122	75	0.01	1.948 (1.252–3.031)	0.003
	≥ 10	116	58.4			
Primary tumor-related						
Site	Left	190	56.2	0.14		
	Right	48	68.5			
Histology	Well/moderately differentiated	234	67.1	0.01	2.971 (1.038–8.503)	0.04
	Others	4	25			
Lymph node metastases	0	108	79	0.001	1.623 (1.020–2.583)	0.04
	≥ 1	130	56.6			
Depth of invasion	Adjacent organ invasion (T4b)	19	64.8	0.64		
	Others	219	66.4			
Lymphatic invasion	0	116	73.1	0.02	1.418 (0.897–2.242)	0.135
	≥ 1	122	60.8			
Venous invasion	0	81	69.7	0.73		
	≥ 1	157	63.9			
Number	1–3	228	67.5	0.07		
	≥ 4	10	38.1			
Maximum diameter (mm)	< 40	180	70.9	0.05		
	≥ 40	58	52.9			
Timing of the appearance	Synchronous	54	61.2	0.94		
	Metachronous	184	67.8			
Distribution	Unilobar	198	67.1	0.12		
	Bilobar	40	63			
Treatment-related						
Staged hepatectomy	Performed	0	–	–		
	Not performed	238	66.3			
Surgical margins	Exposed	19	40.1	0.09		
	Not exposed	219	69			
Adjuvant chemotherapy after primary resection	Administered	69	64.9	0.16		
	Not administered	169	66.7			
Adjuvant chemotherapy after hepatectomy	Administered	126	56.2	0.02	0.646 (0.414–1.009)	0.05
	Not administered	112	71.7			

CEA: Carcinoembryonic antigen; CI: Confidence interval; OS: Overall survival.

patients in the NAC group. Resection was adopted as the initial treatment strategy for recurrence in two patients. Chemotherapy was adopted as the initial treatment strategy for recurrence in seven patients (the same regimen was used in all responders; a different regimen was used in non-responders), three of

Table 3 Patient characteristics after propensity score matching

Variables		Upfront hepatectomy group (*n* = 50)	NAC group (*n* = 50)	*P* value
Patient-related				
Age (yr)	< 60	14	10	0.349
	≥ 60	36	40	
Sex	Male	33	34	0.832
	Female	17	16	
CEA level (ng/mL)	< 10	28	34	0.216
	≥ 10	22	16	
Primary tumor-related				
Site	Right	10	14	0.349
	Left	40	36	
Histology	Well/moderately differentiated	49	50	0.315
	Others	1	0	
Lymph node metastases	0	15	15	1.0
	≥ 1	35	35	
Depth of invasion	Adjacent organ invasion (T4b)	5	3	0.461
	Others	45	47	
Lymphatic invasion	0	19	23	0.418
	≥ 1	31	27	
Venous invasion	0	16	15	0.829
	≥ 1	34	35	
Liver metastasis-related				
Number	1–3	44	42	0.564
	≥ 4	6	8	
Maximum diameter (mm)	< 40	15	15	1.0
	≥ 40	35	35	
Timing of the appearance	Synchronous	28	28	1.0
	Metachronous	22	22	
Distribution	Unilobar	33	33	1.0
	Bilobar	17	17	
Treatment-related				
Staged hepatectomy	Performed	0	1	0.315
	Not performed	50	49	
Surgical margins	Exposed	4	4	1.0
	Not exposed	46	46	
Adjuvant chemotherapy after primary resection	Administered	17	29	0.144
	Not administered	23	21	
Adjuvant chemotherapy after hepatectomy	Administered	23	17	0.221
	Not administered	27	33	
Risk stratification	High-risk	18	13	0.515

	Low-risk	32	37

CEA: Carcinoembryonic antigen; NAC: Neoadjuvant chemotherapy.

Table 4 Recurrence patterns/treatment after propensity score matching

	Upfront hepatectomy group (*n* = 50)	NAC group (*n* = 50)	*P* value
Recurrence	30	24	0.229
Recurrence site[1]			
Liver	12	11	0.106
Lung	17	9	
Peritoneum	0	4	
Other	4	3	
Initial treatment for recurrence[2]			
Resection	8 (26.7)	6 (25.0)	0.623
Chemotherapy	17 (56.7)	16 (66.7)	
Other	5 (16.6)	2 (8.3)	

[1]Duplication (+).
[2]Number (%) of patients with recurrence.
NAC: Neoadjuvant chemotherapy.

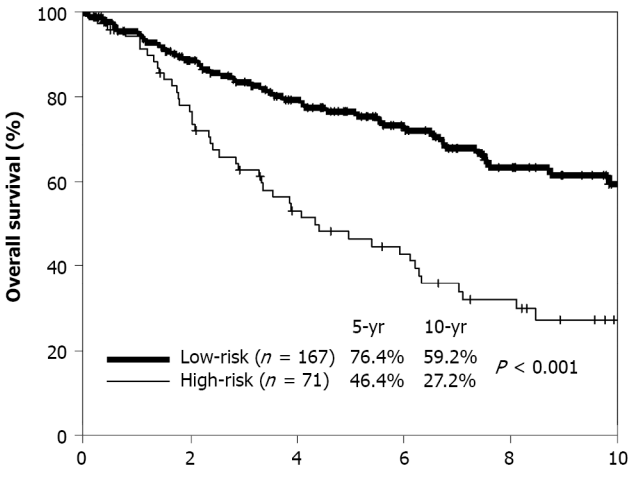

DOI: 10.4251/wjgo.v14.i7.1281

Figure 2 Kaplan–Meier curves of 5-yr overall survival stratified by risk. Patients in the high-(71 patients) and low-(167 patients) risk groups are represented by the thin and thick lines, respectively.

whom were converted to resection (Table 5). Consequently, resection was performed in 56% of patients with recurrence in the NAC group, which was higher than the proportion of high-risk patients in the upfront hepatectomy group (27%). The 5-year OS rate after the first recurrence in the NAC group was significantly higher than that in the upfront hepatectomy group (66.7% *vs* 17.9%; $P = 0.04$).

DISCUSSION

This study revealed a significantly worse OS rate of patients in resectable CRLMs with two or more risk factors [primary histological type (other than well/moderately differentiated), lymph node metastases (≥ 1), and preoperative CEA levels (≥ 10 g/mL)] who met the high-risk criteria compared to those who met the low-risk criteria. Among high-risk patients, the OS rate of those who received NAC was

Table 5 Initial treatment strategy for recurrence in high-risk patients

Case	NAC regimen	Course	Efficacy	First recurrence site	Initial treatment for recurrence	Conversion Therapy
1	FU, FOL + CDDP	2	SD	Peritoneum	LV/5-FU + CPT-11 (IFL)	Resection
2	FU, FOL + CDDP	2	SD	Liver	LV/5-FU + CPT-11 (IFL)	Resection
3	FU, FOL	2	PD	Other	FOLFOX + Bmab	
4	FU, FOL + CDDP	4	SD	Lung	Resection	
5	FOLFOX + Bmab	8	PD	Liver	FOLFIRI + Bmab	Resection
6	XELOX + Bmab	14	SD	Lung	IRIS + Bmab	
7	FOLFOX + Cmab	6	PR	Liver	Resection	
8	IRI + Pmab	6	PR	Peritoneum	IRI + Pmab	
9	FOLFIRI + Bmab	6	PR	Liver	FOLFIRI + Bmab	

Bmab: Bevacizumab; CDDP: Cisplatin; Cmab: Cetuximab; FOL: Folinic acid; FOLFIRI: Fluorouracil + leucovorin + irinotecan; FOLFOXR: Folinic acid + fluorouracil + oxaliplatin; FU: Fluorouracil; IFL: I-leucovorin + fluorouracil + irinotecan; IRI: Irinotecan; IRIS: Irinotecan + s-1; Pmab: Panitumumab; XELOX: Capecitabine + oxaliplatin; NAC: Neoadjuvant chemotherapy.

significantly higher than that of those who underwent upfront hepatectomy after propensity score matching. It is a novel finding that the efficacy of NAC for resectable CRLMs was demonstrated after risk stratification and propensity score matching.

The definition of resectable CRLM varies in the literature[3,4,6,15]. In studies that examined the effectiveness of NAC for resectable CRLMs, resectable CRLM was defined as a maximum of four tumors [4]; four or fewer tumors with a maximum diameter of < 5 cm[3]; or (1) A ≥ 30% residual liver volume (regardless of tumor number and size); (2) Resectable or already resected primary tumor; and (3) No unresectable extrahepatic metastases[16]. Some studies did not show a benefit of NAC for resectable CRLMs[3,4]. This may be because the criteria for resectable CRLMs were not specific enough to restrict the patient group to those for whom NAC is truly effective. Even when NAC was shown to be effective, it was considered without propensity score matching[16]. The definition of resectable CRLM in our database is more detailed and the efficacy of NAC was assessed by risk stratification.

We demonstrated that the OS rate, but not the DFS rate, of high-risk patients was significantly higher in the NAC group than in the upfront hepatectomy group. The post-recurrence clinical course after the first hepatectomy differed between the two groups. The treatment strategy for recurrence showed that chemotherapy was initially selected most frequently in both the upfront hepatectomy and NAC groups, although resection of not only the intrahepatic, but also the extrahepatic, recurrence site is crucial for prolonging the survival of patients with CRLMs[17]. However, in the NAC group, there were conversion cases from chemotherapy to resection, and consequently, there were more resection cases in the NAC group than in the upfront hepatectomy group (56% *vs* 27%), although this was not significant. Based on these results, the reason for a better OS rate among high-risk patients in the NAC group may be that the most effective and tolerable chemotherapy regimen has already been established in patients receiving NAC before their first hepatectomy, and appropriate regimens may be available from the start of treatment for recurrence. In fact, the OS rate of the NAC group after recurrence was significantly higher than that of the upfront hepatectomy group ($P = 0.04$).

Conversely, disadvantages of NAC include the risk that hepatectomy may not be performed in patients who do not respond to NAC. We showed that the effect of chemotherapy was progressive in 6% of NAC cases. To avoid missing the timing of hepatectomy, it is important to evaluate the efficacy of chemotherapy every 2–3 cycles. Other disadvantages of NAC include liver damage and perioperative complications induced by the NAC drugs. Sinusoidal dilation caused by oxaliplatin and steatohepatitis caused by irinotecan have been reported[18]. Furthermore, prolonged systemic NAC alters the liver parenchyma and increases morbidity after major resection[19]. Although many centers specializing in hepatobiliary procedures have reported mortality rates of < 5% after major liver surgery, the morbidity of hepatectomy may have increased with the advent of NAC, due to the hepatic parenchymal damage caused by chemotherapy[5]. The short-term outcomes of the NAC group in this study were comparable to those of a previous study[5]. However, one case of postoperative bleeding was observed after irinotecan-based chemotherapy. As hepatectomy was performed after a sufficient drug interval, no sinusoidal dilation or steatohepatitis was observed in the resected specimen. Postoperative bleeding in this case may have resulted from a complicated hepatic dissection surface. Therefore, careful surgical procedures are required, even after a sufficient drug interval.

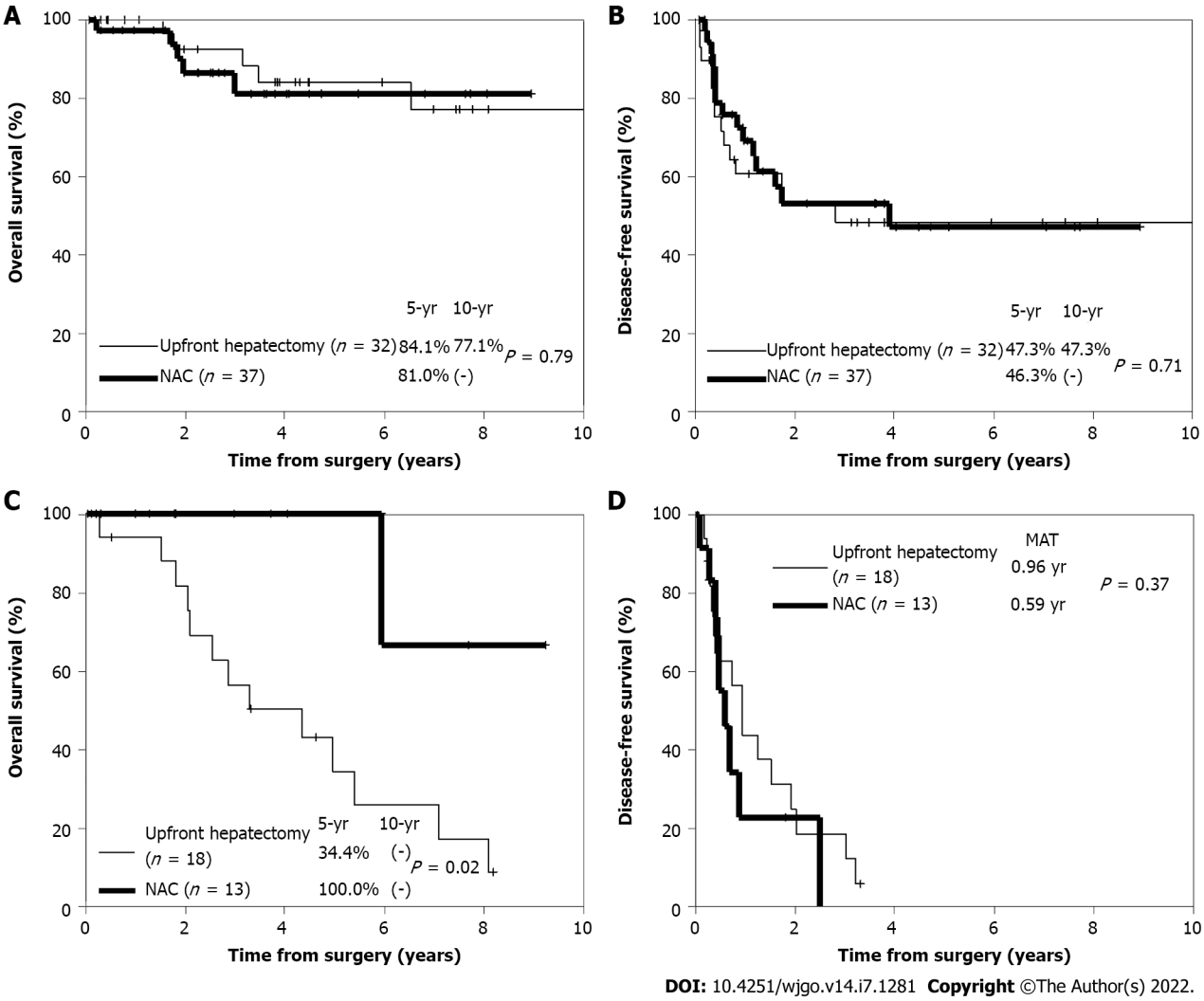

DOI: 10.4251/wjgo.v14.i7.1281

Figure 3 Kaplan–Meier curves. A and C: 5-yr overall survival; B: 5-yr disease-free survival (DFS) in low-risk patients in the upfront hepatectomy (thin line) (32 patients) and neoadjuvant chemotherapy (NAC) (thick line) (37 patients) groups after propensity score matching; D: 5-yr DFS in high-risk patients in the upfront hepatectomy (thin line) (18 patients) and NAC (thick line) (13 patients) groups after propensity score matching. NAC: Neoadjuvant chemotherapy.

Limits of the study

This study has several limitations. The first is its single-center design with limited sample size. Second, its retrospective nature introduces the inevitable risk of selection bias, which could not be completely eradicated, despite using propensity score matching to reduce confounding by indication. Lastly, it has been reported that molecular biological factors, such as *RAS* status and microsatellite instability, are prognostic[20,21]. However, this information was unavailable in the present study.

CONCLUSION

Our findings suggest that NAC may improve the prognosis of patients with resectable CRLMs who have at least two of the following risk factors: Preoperative CEA levels (≥ 10 ng/mL), primary histological type (other than well/moderately differentiated), and lymph node metastases (≥ 1). Future prospective, multicenter studies with larger sample sizes are needed to validate these findings

ARTICLE HIGHLIGHTS

Research background

Colorectal cancer (CRC) is a leading cause of cancer-related deaths worldwide. The liver is the most common metastatic site of CRC, and hepatectomy is the mainstay of treatment for patients with colorectal liver metastases (CRLMs). Upfront hepatectomy is recommended for patients with resectable

CRLMs. However, there are cases of early recurrence after upfront hepatectomy alone in the resectable CRLMs. In selected patients, neoadjuvant chemotherapy (NAC) may improve long-term survival.

Research motivation

Identifying the poor prognostic factors for upfront hepatectomy in resectable CRLMs and investigating the effectiveness of NAC are urgently needed to improve long-term survival of patients with resectable CRLMs.

Research objectives

To determine the efficacy of NAC for initially resectable CRLMs.

Research methods

Among 644 patients who underwent their first hepatectomy for CRLMs at our institution, 297 resectable cases were stratified into an upfront hepatectomy group (238 patients) and NAC group (59 patients). Poor prognostic factors for upfront hepatectomy were identified using multivariate logistic regression analysis. Propensity score matching was used, and clinical outcomes between the upfront hepatectomy and NAC groups were compared according to the number of poor prognostic factors. Survival curves were estimated using the Kaplan–Meier method and compared using the log-rank test.

Research results

As independent poor prognostic factors for overall survival (OS) in the upfront hepatectomy group, preoperative carcinoembryonic antigen (CEA) levels (≥ 10 ng/mL) (P = 0.003), primary histological type (other than well/moderately differentiated) (P = 0.04), and primary lymph node metastases (≥ 1) (P = 0.04) were identified. High-risk status was defined as the presence of two or more risk factors. Fifty patients were matched in upfront hepatectomy and NAC groups respectively, after propensity score matching. Among high-risk patients, the 5-year OS rate was significantly higher in the NAC group (13 patients) than in the upfront hepatectomy group (18 patients) (100% *vs* 34%; P = 0.02).

Research conclusions

NAC was effective in patients with resectable CRLMs who had at least two of the following risk factors: Preoperative CEA levels (≥ 10 ng/mL), primary histological type (other than well/moderately differentiated), and lymph node metastases (≥ 1).

Research perspectives

NAC therapy may improve the prognosis of high-risk patients with resectable CRLMs.

FOOTNOTES

Author contributions: Takeda K, Sawada Y, Yabushita Y, Honma Y, Kumamoto T and Watanabe J performed the research; Takeda K drafted the manuscript; Kunisaki C, Misumi T and Endo I revised the manuscript critically; all authors read and approved the final manuscript.

Institutional review board statement: The study was reviewed and approved for publication by our Institutional Reviewer.

Informed consent statement: The requirement for written informed consent was waived owing to the retrospective nature of the study.

Conflict-of-interest statement: All the authors report no relevant conflicts of interest for this article.

Data sharing statement: The original anonymous dataset is available on request from the corresponding author at kazu1968@yokohama-cu.ac.jp.

STROBE statement: The authors have read the STROBE Statement—checklist of items, and the manuscript was prepared and revised according to the STROBE Statement—checklist of items.

Country/Territory of origin: Japan

ORCID number: Kazuhisa Takeda 0000-0001-8092-6206; Yu Sawada 0000-0002-5641-1103; Yasuhiro Yabushita 0000-0003-1090-1614; Yuki Honma 0000-0001-6560-2895; Takafumi Kumamoto 0000-0002-9928-4386; Jun Watanabe 0000-0002-7187-3664; Ryusei Matsuyama 0000-0001-5131-0023; Chikara Kunisaki 0000-0002-0843-8766; Toshihiro Misumi 0000-0001-8339-2895; Itaru Endo 0000-0001-5520-8114.

S-Editor: Fan JR
L-Editor: A
P-Editor: Fan JR

REFERENCES

1 **de Ridder JAM**, van der Stok EP, Mekenkamp LJ, Wiering B, Koopman M, Punt CJA, Verhoef C, de Wilt JH. Management of liver metastases in colorectal cancer patients: A retrospective case-control study of systemic therapy *vs* liver resection. *Eur J Cancer* 2016; **59**: 13-21 [PMID: 26994469 DOI: 10.1016/j.ejca.2016.02.003]
2 **Ishida K**, Uesugi N, Hasegawa Y, Sugimoto R, Takahara T, Otsuka K, Nitta H, Kawasaki T, Wakabayashi G, Sugai T. Proposal for novel histological findings of colorectal liver metastases with preoperative chemotherapy. *Pathol Int* 2015; **65**: 367-373 [PMID: 25940915 DOI: 10.1111/pin.12300]
3 **Hirokawa F**, Asakuma M, Komeda K, Shimizu T, Inoue Y, Kagota S, Tomioka A, Uchiyama K. Is neoadjuvant chemotherapy appropriate for patients with resectable liver metastases from colorectal cancer? *Surg Today* 2019; **49**: 82-89 [PMID: 30255329 DOI: 10.1007/s00595-018-1716-x]
4 **Nordlinger B**, Sorbye H, Glimelius B, Poston GJ, Schlag PM, Rougier P, Bechstein WO, Primrose JN, Walpole ET, Finch-Jones M, Jaeck D, Mirza D, Parks RW, Mauer M, Tanis E, Van Cutsem E, Scheithauer W, Gruenberger T; EORTC Gastro-Intestinal Tract Cancer Group; Cancer Research UK; Arbeitsgruppe Lebermetastasen und–tumoren in der Chirurgischen Arbeitsgemeinschaft Onkologie (ALM-CAO); Australasian Gastro-Intestinal Trials Group (AGITG); Fédération Francophone de Cancérologie Digestive (FFCD). Perioperative FOLFOX4 chemotherapy and surgery *vs* surgery alone for resectable liver metastases from colorectal cancer (EORTC 40983): long-term results of a randomised, controlled, phase 3 trial. *Lancet Oncol* 2013; **14**: 1208-1215 [PMID: 24120480 DOI: 10.1016/S1470-2045(13)70447-9]
5 **Boostrom SY**, Nagorney DM, Donohue JH, Harmsen S, Thomsen K, Que F, Kendrick M, Reid-Lombardo KM. Impact of neoadjuvant chemotherapy with FOLFOX/FOLFIRI on disease-free and overall survival of patients with colorectal metastases. *J Gastrointest Surg* 2009; **13**: 2003-9; discussion 2009 [PMID: 19760306 DOI: 10.1007/s11605-009-1007-3]
6 **Fong Y**, Fortner J, Sun RL, Brennan MF, Blumgart LH. Clinical score for predicting recurrence after hepatic resection for metastatic colorectal cancer: analysis of 1001 consecutive cases. *Ann Surg* 1999; **230**: 309-18; discussion 318 [PMID: 10493478 DOI: 10.1097/00000658-199909000-00004]
7 **Kanemitsu Y**, Kato T. Prognostic models for predicting death after hepatectomy in individuals with hepatic metastases from colorectal cancer. *World J Surg* 2008; **32**: 1097-1107 [PMID: 18200429 DOI: 10.1007/s00268-007-9348-0]
8 **Iwatsuki S**, Dvorchik I, Madariaga JR, Marsh JW, Dodson F, Bonham AC, Geller DA, Gayowski TJ, Fung JJ, Starzl TE. Hepatic resection for metastatic colorectal adenocarcinoma: a proposal of a prognostic scoring system. *J Am Coll Surg* 1999; **189**: 291-299 [PMID: 10472930 DOI: 10.1016/s1072-7515(99)00089-7]
9 **Mann CD**, Metcalfe MS, Leopardi LN, Maddern GJ. The clinical risk score: emerging as a reliable preoperative prognostic index in hepatectomy for colorectal metastases. *Arch Surg* 2004; **139**: 1168-1172 [PMID: 15545561 DOI: 10.1001/archsurg.139.11.1168]
10 **Tanaka K**, Nojiri K, Kumamoto T, Takeda K, Endo I. R1 resection for aggressive or advanced colorectal liver metastases is justified in combination with effective prehepatectomy chemotherapy. *Eur J Surg Oncol* 2011; **37**: 336-343 [PMID: 21277151 DOI: 10.1016/j.ejso.2011.01.007]
11 **Eisenhauer EA**, Therasse P, Bogaerts J, Schwartz LH, Sargent D, Ford R, Dancey J, Arbuck S, Gwyther S, Mooney M, Rubinstein L, Shankar L, Dodd L, Kaplan R, Lacombe D, Verweij J. New response evaluation criteria in solid tumours: revised RECIST guideline (version 1.1). *Eur J Cancer* 2009; **45**: 228-247 [PMID: 19097774 DOI: 10.1016/j.ejca.2008.10.026]
12 **Portier G**, Elias D, Bouche O, Rougier P, Bosset JF, Saric J, Belghiti J, Piedbois P, Guimbaud R, Nordlinger B, Bugat R. Multicenter randomized trial of adjuvant fluorouracil and folinic acid compared with surgery alone after resection of colorectal liver metastases: FFCD ACHBTH AURC 9002 trial. *J Clin Oncol* 2006; **24**: 4976-4982 [DOI: 10.1200/jco.2006.06.8353]
13 **Hasegawa K**, Saiura A, Takayama T, Miyagawa S, Yamamoto J, Ijichi M, Teruya M, Yoshimi F, Kawasaki S, Koyama H, Oba M, Takahashi M, Mizunuma N, Matsuyama Y, Watanabe T, Makuuchi M, Kokudo N. Adjuvant Oral Uracil-Tegafur with Leucovorin for Colorectal Cancer Liver Metastases: A Randomized Controlled Trial. *PLoS One* 2016; **11**: e0162400 [PMID: 27588959 DOI: 10.1371/journal.pone.0162400]
14 **Tanaka K**, Shimada H, Kubota K, Ueda M, Endo I, Sekido H, Togo S. Effectiveness of prehepatectomy intra-arterial chemotherapy for multiple bilobar colorectal cancer metastases to the liver: a clinicopathologic study of peritumoral vasculobiliary invasion. *Surgery* 2005; **137**: 156-164 [PMID: 15674195 DOI: 10.1016/j.surg.2004.07.007]
15 **Gayowski TJ**, Iwatsuki S, Madariaga JR, Selby R, Todo S, Irish W, Starzl TE. Experience in hepatic resection for metastatic colorectal cancer: analysis of clinical and pathologic risk factors. *Surgery* 1994; **116**: 703-10; discussion 710 [PMID: 7940169]
16 **Ninomiya M**, Emi Y, Motomura T, Tomino T, Iguchi T, Kayashima H, Harada N, Uchiyama H, Nishizaki T, Higashi H, Kuwano H. Efficacy of neoadjuvant chemotherapy in patients with high-risk resectable colorectal liver metastases. *Int J Clin Oncol* 2021; **26**: 2255-2264 [PMID: 34519930 DOI: 10.1007/s10147-021-02024-5]
17 **Imai K**, Yamashita YI, Miyamoto Y, Nakagawa S, Okabe H, Hashimoto D, Chikamoto A, Baba H. The predictors and

oncological outcomes of repeat surgery for recurrence after hepatectomy for colorectal liver metastases. *Int J Clin Oncol* 2018; **23**: 908-916 [PMID: 29619592 DOI: 10.1007/s10147-018-1273-8]

18 **Vauthey JN**, Pawlik TM, Ribero D, Wu TT, Zorzi D, Hoff PM, Xiong HQ, Eng C, Lauwers GY, Mino-Kenudson M, Risio M, Muratore A, Capussotti L, Curley SA, Abdalla EK. Chemotherapy regimen predicts steatohepatitis and an increase in 90-day mortality after surgery for hepatic colorectal metastases. *J Clin Oncol* 2006; **24**: 2065-2072 [PMID: 16648507 DOI: 10.1200/JCO.2005.05.3074]

19 **Karoui M**, Penna C, Amin-Hashem M, Mitry E, Benoist S, Franc B, Rougier P, Nordlinger B. Influence of preoperative chemotherapy on the risk of major hepatectomy for colorectal liver metastases. *Ann Surg* 2006; **243**: 1-7 [PMID: 16371728 DOI: 10.1097/01.sla.0000193603.26265.c3]

20 **Jácome AA**, Vreeland TJ, Johnson B, Kawaguchi Y, Wei SH, Nancy You Y, Vilar E, Vauthey JN, Eng C. The prognostic impact of RAS on overall survival following liver resection in early *vs* late-onset colorectal cancer patients. *Br J Cancer* 2021; **124**: 797-804 [PMID: 33208919 DOI: 10.1038/s41416-020-01169-w]

21 **Fujiyoshi K**, Yamamoto G, Takahashi A, Arai Y, Yamada M, Kakuta M, Yamaguchi K, Akagi Y, Nishimura Y, Sakamoto H, Akagi K. High concordance rate of KRAS/BRAF mutations and MSI-H between primary colorectal cancer and corresponding metastases. *Oncol Rep* 2017; **37**: 785-792 [PMID: 28000889 DOI: 10.3892/or.2016.5323]

World Journal of Gastrointestinal Oncology

Submit a Manuscript: https://www.f6publishing.com

World J Gastrointest Oncol 2022 July 15; 14(7): 1295-1306

DOI: 10.4251/wjgo.v14.i7.1295

ISSN 1948-5204 (online)

ORIGINAL ARTICLE

Retrospective Cohort Study

Increased 5-hydroxymethylcytosine is a favorable prognostic factor of *Helicobacter pylori*-negative gastric cancer patients

Ying-Li Fu, Yan-Hua Wu, Dong-Hui Cao, Zhi-Fang Jia, Ao Shen, Jing Jiang, Xue-Yuan Cao

Specialty type: Gastroenterology and hepatology

Provenance and peer review: Unsolicited article; Externally peer reviewed.

Peer-review model: Single blind

Peer-review report's scientific quality classification

Grade A (Excellent): A
Grade B (Very good): B
Grade C (Good): 0
Grade D (Fair): 0
Grade E (Poor): 0

P-Reviewer: Jeong SH, South Korea; Kirkik D, Turkey
A-Editor: Zhu JQ, China

Received: January 11, 2022
Peer-review started: January 11, 2022
First decision: March 13, 2022
Revised: March 18, 2022
Accepted: May 28, 2022
Article in press: May 28, 2022
Published online: July 15, 2022

Ying-Li Fu, Yan-Hua Wu, Dong-Hui Cao, Zhi-Fang Jia, Jing Jiang, Division of Clinical Research, The First Hospital of Jilin University, Changchun 130000, Jilin Province, China

Ao Shen, Xue-Yuan Cao, Department of Gastric and Colorectal Surgery, The First Hospital of Jilin University, Changchun 130000, Jilin Province, China

Corresponding author: Xue-Yuan Cao, PhD, Professor, Research Scientist, Department of Gastric and Colorectal Surgery, The First Hospital of Jilin University, Xinmin Street, Changchun 130000, Jilin Province, China. jd3d2ub@jlu.edu.cn

Abstract

BACKGROUND

Most gastric cancer (GC) patients are diagnosed at middle or late stage because the symptoms in early stage are obscure, which causes higher mortality rates of GC. *Helicobacter pylori* (*H. pylori*) was identified as a class I carcinogen and leads to aberrant DNA methylation/hydroxymethylation. 5-hydroxymethylcytosine (5-hmC) plays complex roles in gene regulation of tumorigenesis and can be considered as an activating epigenetic mark of hydroxymethylation.

AIM

To explore the association between 5-hmC levels and the progression and prognosis of GC patients with or without *H. pylori* infection.

METHODS

A retrospective cohort study was conducted to estimate the predicted value of 5-hmC level in the progression and prognosis of GC patients with different *H. pylori* infection status. A total of 144 GC patients were recruited.

RESULTS

The levels of 5-hmC were significantly decreased in tumor tissues (0.076 ± 0.048) compared with the matched control tissues (0.110 ± 0.057, $P = 0.001$). A high level of 5-hmC was an independent significant favorable predictor of overall survival in GC patients (hazard ratio = 0.61, 95% confidence interval: 0.38-0.98, $P = 0.040$), the *H. pylori*-negative GC subgroup (hazard ratio = 0.30, 95% confidence interval: 0.13-0.68, $P = 0.004$) and the GC patients with TNM stage I or II (hazard ratio = 0.32, 95% confidence interval: 0.13-0.77, $P = 0.011$).

CONCLUSION

Increased 5-hmC is a favorable prognostic factor in GC, especially for *H. pylori*-negative subgroups.

Key Words: 5-hydroxymethylation; 5-hydroxymethylcytosine; *Helicobacter pylori*; Gastric cancer; Prognosis

Core Tip: *Helicobacter pylori* (*H. pylori*) was identified as a class I carcinogen and leads to aberrant DNA methylation/hydroxymethylation. 5-hydroxymethylcytosine plays complex roles in the gene regulation of tumorigenesis and is considered an activating epigenetic mark of hydroxymethylation. We conducted a retrospective cohort study to estimate the predictive value of 5-hydroxymethylcytosine levels in the progression and prognosis of gastric cancer patients with different *H. pylori* infection statuses. The results indicated that increasing 5-hydroxymethylcytosine is a favorable prognostic factor in gastric cancer patients who were not infected with *H. pylori*, but no associations were observed in *H. pylori*-positive gastric cancer patients.

Citation: Fu YL, Wu YH, Cao DH, Jia ZF, Shen A, Jiang J, Cao XY. Increased 5-hydroxymethylcytosine is a favorable prognostic factor of *Helicobacter pylori*-negative gastric cancer patients. *World J Gastrointest Oncol* 2022; 14(7): 1295-1306
URL: https://www.wjgnet.com/1948-5204/full/v14/i7/1295.htm
DOI: https://dx.doi.org/10.4251/wjgo.v14.i7.1295

INTRODUCTION

Gastric cancer (GC) is a serious disease with over 1 million estimated new cases annually around the world, and it is the fifth most diagnosed malignancy worldwide[1]. Due to the symptoms in early stage being obscure, most GC patients are diagnosed at middle or late stage, which causes higher mortality rates, and accounted for 769000 deaths globally in 2020[1].

Recent comprehensive analyses showed that many GC-related pathways are more frequently altered by aberrant DNA methylation than by mutations[2], and the degree of accumulation of aberrant DNA methylation is highly correlated with GC risk[3,4].

Helicobacter pylori (*H. pylori*) was identified as a class I carcinogen leading to gastric adenocarcinoma by the World Health Organization[5]. *H. pylori*-induced chronic inflammation plays a direct role in the induction of aberrant DNA methylation. The methylation level in an *H. pylori*-positive group was 2.5-34.1 times higher than a negative group. *H. pylori* eradication leads to a decrease in DNA methylation levels[6,7].

A promising method to reverse the progression of GC is effective demethylation treatment. The passive demethylation agents (5-azacytidine/decitabine), which relies on DNA methyltransferase, are not effective in the treatment of solid tumors and have serious side effects. A newly proposed classical active demethylation process involves oxidizing 5-methylcytosine to 5-hydroxymethylcytosine (5-hmC) and further downstream products by the ten-eleven translocation (TET) family. The median product, 5-hmC, is considered an activating epigenetic marker, and it plays complex roles in gene regulation of tumorigenesis[8-10]. Significant reductions in 5-hmC levels have been found in hematological malignancies, such as breast cancer, colon cancer, prostate cancer and melanoma. A few small size studies analyzed the association between 5-hmC levels and GC, but the evidence is still lacking[11,12], especially for the *H. pylori*-induced GC.

In the current study, we explored the level of 5-hmC and *H. pylori* infection in a relatively large scale GC patient cohort to assess the association between 5-hmC level and the malignant progression of the tumor and the overall survival of GC patients with different *H. pylori* infection status.

MATERIALS AND METHODS

Ethics statement

This study was approved by the Institutional Review Board of the First Hospital of Jilin University. All participants provided written informed consent prior to joining the study.

Study population

A total of 158 patients with histologically diagnosed GC who underwent radical gastrectomy at the Department of Gastric and Colorectal Surgery in the First Hospital of Jilin University (Changchun, China) during 2007 to 2017 were recruited in this cohort study. For each patient, 5 mL of peripheral blood before surgery and 0.5 cm^3 of tumor tissue were collected. Among the patients, 38 specimens of 0.5 cm^3 adjacent tissue were collected during the operation. All patients did not undergo chemotherapy or radiotherapy before surgery. Demographic information (sex, age) and principal clinical pathological information (histological grade, TNM stage, tumor size, neural invasion, vascular invasion, *etc*.) were collected. The tumor histological grade was evaluated by the World Health Organization criteria. TNM stages were classified according to the 8th edition of the TNM staging system of the Union for International Cancer Control/American Joint Committee on Cancer (2017). Patients with the following conditions were excluded from this study: (1) Patients with distant metastasis or a positive surgical margin; (2) Patients who died due to complications of the surgical procedure during the perioperative period; and (3) Patients who were lost at the first time of interview.

Follow-up

Follow-up for all patients was implemented at 3 mo, 6 mo, 12 mo and annually afterwards until death or the end of the follow-up. Information on general status and postoperative chemotherapy were collected during each follow-up. If the patients had died, the date of death and potential cause were recorded. The duration from the date of surgery to the date of death or the last successful interview date was defined as the survival time. If the patient was lost to follow-up, survival time was defined as the duration from the date of surgery to the date of the last successful interview.

5-hmC quantification and test for H. pylori infection

The genomic DNA from primary tumors and paired noncancerous mucosa tissues were extracted using a QIAamp DNA Mini Kit (Qiagen, Hilden, Germany) according to the manufacturer's instructions. The 5-hmC content of genomic DNA was determined with a Quest 5-hmC DNA enzyme-linked immunosorbent assay (ELISA) Kit (Zymo Research, Irvine, CA, United States) according to the manufacturer's instructions. Assays were performed using 4 μg/mL anti-5-hmC polyclonal antibodies, loading 200 ng of DNA per well. Absorbance at 405 nm was evaluated using a SynergyH1 microplate reader and Gen5 software (BioTek, Winooski, VT, United States). The amount of 5-hmC was calculated as a percentage based on a standard curve generated using kit controls and the median value was used as the cutoff of 5-hmC level category. Values above the median value were considered to be the 5-hmC high group (≥ 0.106%), and those below the median value were considered the 5-hmC low group (< 0.106%).

A commercial ELISA kit for *H. pylori* immunoglobulin G (Biohit, Helsinki, Finland) was used to detect the serum *H. pylori* immunoglobulin G antibodies. The antibody titers were quantified by optical density readings according to the manufacturer's protocol, and titers higher than the threshold value of 30 EIU were considered as positive for *H. pylori* infection.

Statistical analysis

Continuous variables that followed a normal distribution were shown as the mean ± standard deviation. Independent samples were compared by two-sample *t*-test, and matched-paired samples were compared by paired *t*-test. Categorical variables were presented as frequencies with percentages and were compared with the χ^2 test or Fisher's exact test when appropriate.

Survival curves within each stratification of variables were plotted by the Kaplan-Meier method and compared by log-rank test. The forward stepwise multivariate Cox proportional hazard model was used to evaluate the prognostic role of clinical characteristics and 5-hmC level. Hazard ratios (HRs) with their 95% confidence intervals (Cis) were calculated. All analyses were conducted with the SPSS program (version 21.0; IBM Corp., Armonk, NY, United States) or GraphPad Prism 5.0 (La Jolla, CA, United States). A two-tailed P value < 0.05 indicated statistical significance.

RESULTS

In the present study, 144 GC patients were involved for the final prognostic analysis and were followed up until August 2021. The median survival time was 73.59 mo. During the follow-up period, 75 (52.1%) patients died, 68 (47.2%) patients remained alive, and 1 (0.7%) patient was lost to follow-up (Figure 1).

Among the 38 paired tissues, the 5-hmC levels were significantly reduced in tumor tissues (0.076 ± 0.048) compared with the matched control tissues (0.110 ± 0.057, P = 0.001) (Figure 2A).

Among the 144 subjects, there were 99 (68.7%) males, and the median age was 62.82 (range 39–90) years old. The mean 5-hmC level of the 144 GC patients was 0.104 ± 0.062. We investigated possible correlations between 5-hmC levels and general demographic characteristics/routine clinicopathological parameters in the GC patients. The TNM stages (P = 0.012), neural invasion (P = 0.008), age (P = 0.008)

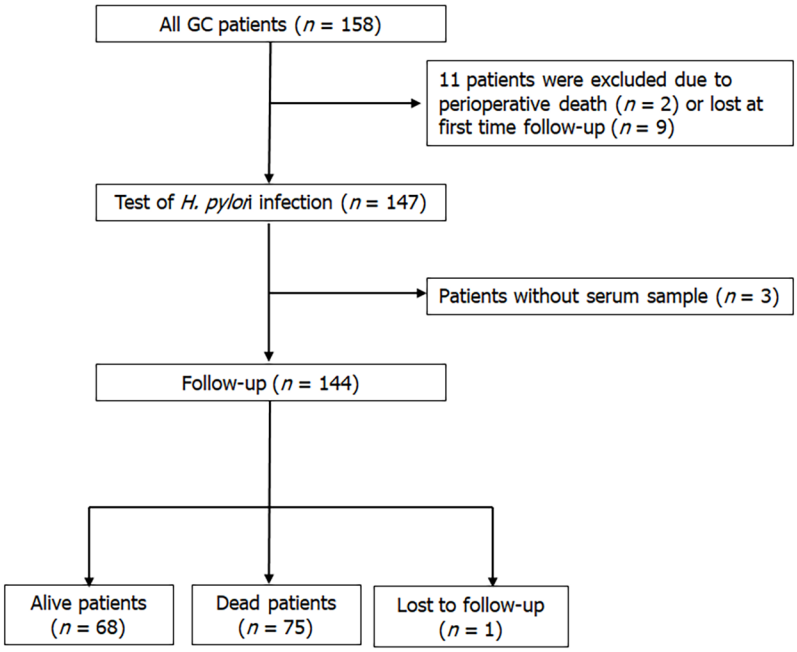

DOI: 10.4251/wjgo.v14.i7.1295 **Copyright** ©The Author(s) 2022.

Figure 1 Flow chart of the subjects enrolled. GC: Gastric cancer; *H. pylori*: *Helicobacter pylori*.

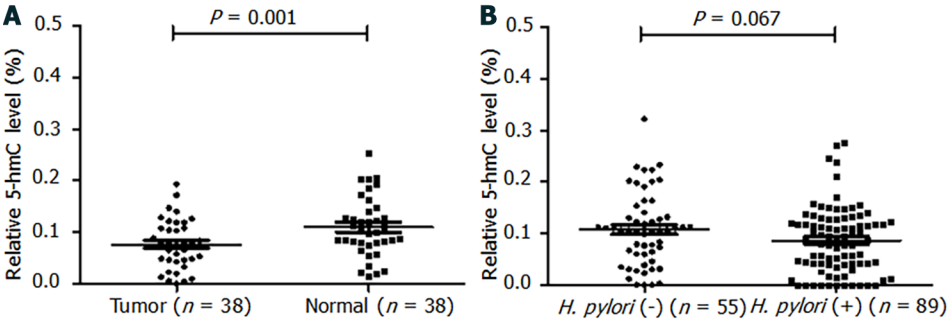

DOI: 10.4251/wjgo.v14.i7.1295 **Copyright** ©The Author(s) 2022.

Figure 2 5-hydroxymethylcytosine level measurement compared between tumor *vs* control tissues and *Helicobacter pylori*-negative *vs* positive subgroups. A: Tumor *vs* control tissues; B: *Helicobacter pylori* -negative *vs* positive subgroups. 5-hmC: 5-hydroxymethylcytosine.

and *H. pylori* infection (P = 0.049) were associated with 5-hmC level. Details were shown in Table 1.

For the 144 GC patients, the results of *H. pylori* infection examination showed that 89 (61.8%) subjects were positive and 55 (38.2%) subjects were negative. We compared the 5-hmC level between *H. pylori*-positive infection and *H. pylori*-negative infection groups. It showed that the 5-hmC level was reduced in the *H. pylori*-positive group, but the P value was at the boundary of significance (P = 0.067, Figure 2B).

We further investigated the association between 5-hmC level and characteristics stratified by *H. pylori* infection status. We found that 5-hmC levels were higher in patients aged more than 60 years (P = 0.009), with neural invasion positive (P = 0.002), with low histological grade (P = 0.042) or with later TNM stage (P = 0.012) in the *H. pylori*-positive subset, but no significant associations were observed in the *H. pylori*-negative subset except sex (Table 2).

Overall survival analyses were performed in total patients and patient stratification by *H. pylori* infection status or TNM stage. The results of the Kaplan-Meier analysis showed that the 5-hmC level was not associated with overall survival in total patients or *H. pylori*-negative or positive groups (log rank P values were 0.406, 0.094 and 0.763, respectively, Figure 3A-C). Furthermore, the 5hmC high level was associated with longer overall survival time compared with the 5hmC low group in the TNM stage I and II subgroup, and log rank test showed the survival curves were significantly different (log rank P = 0.037, Figure 3D), but the association was not significant in the TNM stage III subgroup (log rank P = 0.547, Figure 3E).

In the full patient set, 5-hmC high level was a significant favorable predictor of overall survival in multivariate Cox regression analysis (HR = 0.61, 95%CI: 0.38-0.98, P = 0.040) after adjustment for tumor size, histological grade and TNM stage (Table 3).

Table 1 5-hydroxymethylcytosine levels between different characteristics, *n* = 144

Characteristics	Total, *n* (%)	5-hmC low, *n* (%)	5-hmC high, *n* (%)	*P* value
Sex				
Male	45 (31.3)	17 (24.3)	28 (37.8)	0.079
Female	99 (68.7)	53 (75.7)	46 (62.2)	
Age in yr				
< 60	56 (38.9)	35 (50.0)	21 (28.4)	0.008
≥ 60	88 (61.1)	35 (50.0)	53 (71.6)	
Histological grade				
Low	106 (73.6)	47 (67.1)	59 (79.7)	0.087
High	38 (26.4)	23 (32.9)	15 (20.3)	
WHO Classification				
Tubular adenocarcinoma	115 (79.9)	55 (78.6)	60 (81.1)	0.707
Others	29 (20.1)	15 (21.4)	14 (18.9)	
Tumor size in cm				
< 5	62 (43.1)	32 (45.7)	30 (40.5)	0.531
≥ 5	82 (56.9)	38 (54.3)	44 (59.5)	
Vascular invasion				
Negative	39 (27.1)	23 (32.9)	16 (21.6)	0.129
Positive	105 (72.9)	47 (67.1)	58 (78.4)	
Neural invasion				
Negative	64 (44.4)	39 (55.7)	25 (33.8)	0.008
Positive	80 (55.6)	31 (44.3)	49 (66.2)	
Depth of invasion				
T1/T2	54 (37.5)	30 (42.9)	24 (32.4)	0.197
T3/T4	90 (62.5)	40 (57.1)	50 (67.6)	
Lymph metastasis				
N0	41 (28.5)	24 (34.3)	17 (23.0)	0.133
N1/N2/N3	103 (71.5)	46 (65.7)	57 (77.0)	
TNM stage				
I + II	73 (50.7)	43 (61.4)	30 (40.5)	0.012
III	71 (49.3)	27 (38.6)	44 (59.5)	
Chemotherapy				
No	75 (52.1)	33 (47.1)	42 (56.8)	0.248
Yes	69 (47.9)	37 (52.9)	32 (43.2)	
H. pylori				
Negative	55 (38.2)	21 (30.0)	34 (45.9)	0.049
Positive	89 (61.8)	49 (70.0)	40 (54.1)	

5-hmC: 5-hydroxymethylcytosine; *H. pylori*: *Helicobacter pylori*; WHO: World Health Organization.

Multivariate Cox regression analysis for overall survival was also performed in GC patients stratified by *H. pylori* infection status or TNM stage. In the *H. pylori*-negative GC subgroup, increased 5-hmC level was a favorable prognostic factor in the multivariate Cox regression analysis (HR = 0.30, 95%CI: 0.13-0.68, *P* = 0.004) (Table 4), which indicated that higher 5-hmC level was an independent significant

Table 2 5-hydroxymethylcytosine level stratified by different characteristics according to *Helicobacter pylori* infection condition

Characteristics	*H. pylori* (-), *n* = 55		*H. pylori* (+), *n* = 89	
	5-hmC high, *n* (%)	*P* value	5-hmC high, *n* (%)	*P* value
Sex				
Male	18 (50.0)	0.013	28 (44.4)	0.883
Female	16 (84.2)		12 (46.2)	
Age in yr				
< 60	10 (55.6)	0.505	11 (28.9)	0.009
≥ 60	24 (64.9)		29 (56.9)	
Histological grade				
High	10 (55.6)	0.505	5 (25.0)	0.042
Low	24 (64.9)		35 (50.7)	
WHO classification				
Tubular adenocarcinoma	31 (60.8)	1[1]	29 (45.3)	0.911
Others	3 (75.0)		11 (44.0)	
Tumor size in cm				
< 5	13 (61.9)	0.992	17 (41.5)	0.542
≥ 5	21 (61.8)		23 (47.9)	
Vascular invasion				
Negative	10 (52.6)	0.308	6 (30.0)	0.127
Positive	24 (66.7)		34 (49.3)	
Neural invasion				
Negative	16 (57.1)	0.467	9 (25.0)	0.002
Positive	18 (66.7)		31 (58.5)	
Depth of invasion				
T1/T2	12 (50.0)	0.112	12 (40.0)	0.504
T3/T4	22 (71.0)		28 (47.5)	
Lymph metastasis				
N0	9 (50.0)	0.208	8 (34.8)	0.255
N1/N2/N3	25 (67.6)		32 (48.5)	
TNM stage				
I + II	17 (54.8)	0.226	13 (31.0)	0.012
III	17 (70.8)		27 (57.4)	
Chemotherapy				
No	19 (61.3)	0.927	23 (52.3)	0.169
Yes	15 (62.5)		17 (37.8)	

[1]*P* value of Fisher' exact test. 5-hmC: 5-hydroxymethylcytosine; *H. pylori*: *Helicobacter pylori*; WHO: World Health Organization.

protective factor of overall survival time in patients without *H. pylori* infection. However, within the *H. pylori*-positive group, we did not observe any significant association between 5-hmC level and GC patient prognosis.

Among patients with TNM stage I or II, increased 5-hmC level was associated with favorable prognosis after adjustment for sex in the multivariate Cox regression analysis (HR = 0.32, 95%CI: 0.13-0.77, *P* = 0.011). However, no significant association was observed between 5-hmC level and the prognosis in patients with TNM stage III (Table 5).

Table 3 Multivariate analyses of risk factors affecting overall survival in total patients, *n* = 144

Characteristics		HR (95%CI)	*P* value
Tumor size in cm	< 5	1	0.027
	≥ 5	1.78 (1.07-2.95)	
Histological grade	High	1	0.011
	Low	2.25 (1.21-4.18)	
TNM stage	I + II	1	< 0.001
	III	2.84 (1.72-4.70)	
5-hmC	Low	1	0.040
	High	0.61 (0.38-0.98)	

5-hmC: 5-hydroxymethylcytosine; CI: Confidence interval; HR: Hazard ratio.

Table 4 Multivariate analysis of risk factors affecting overall survival in the *Helicobacter pylori*-negative subgroup, *n* = 55

Characteristics		HR (95%CI)	*P* value
Neural invasion	Negative	1	< 0.001
	Positive	5.45 (2.28-13.07)	
Tumor size in cm	< 5	1	0.031
	≥ 5	2.63 (1.09-6.32)	
5-hmC	Low	1	0.004
	High	0.30 (0.13-0.68)	

5-hmC: 5-hydroxymethylcytosine; CI: Confidence interval; HR: Hazard ratio.

Table 5 Multivariate analyses of risk factors affecting overall survival in the TNM stage I + II subgroup, *n* = 73

Characteristics		HR (95%CI)	*P* value
Sex	Female	1	0.047
	Male	0.43 (0.19-0.99)	
5-hmC	Low	1	0.011
	High	0.32 (0.13-0.77)	

5-hmC: 5-hydroxymethylcytosine; CI: Confidence interval; HR: Hazard ratio.

DISCUSSION

Long-time *H. pylori* infection leads to chronic inflammation and further aberrant DNA methylation, which plays an important role in tumorigenesis of GC. The global prevalence of *H. pylori* reported by a meta-analysis across individual countries varied from 18.9% to 87.7%, and the prevalence in China was 55.8% (95%CI: 51.8%-59.9%)[13]. Among our 144 GC patients, 89 (61.8%) patients were defined as *H. pylori*-positive by ELISA. The infection rate was slightly higher than the prevalence in the general Chinese population but was similar to the previously reported prevalence in GC patients[14,15], indicating that our study cohort was representative.

DNA methylation/hydroxymethylation is one of the most widely studied epigenetic modifications and has been shown to play significant roles in tumorigenesis and prognosis[16]. Previous studies have shown that aberrant DNA methylation is a common event and a strong candidate mechanism for early nongenetic alterations in GC[17]. Nevertheless, the reports of DNA hydroxymethylation and GC are limited to several small studies.

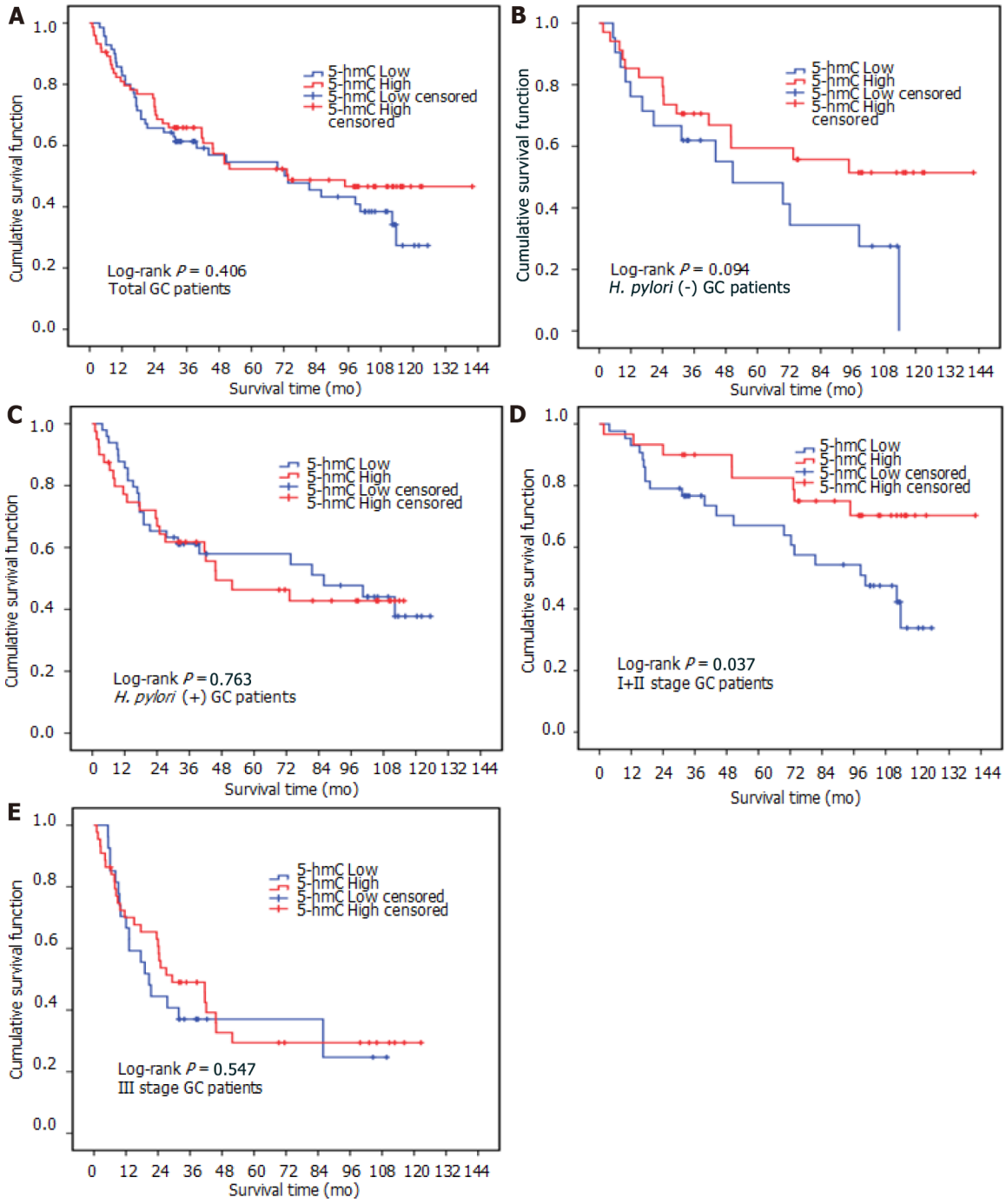

DOI: 10.4251/wjgo.v14.i7.1295

Figure 3 Kaplan–Meier estimates of overall survival in gastric cancer patients. A: Total gastric cancer (GC) patients; B: GC patients with negative *Helicobacter pylori* (*H. pylori*) infection; C: GC patients with positive *H. pylori* infection; D: GC patients with I or II TNM stage; E: GC patients with III TNM stage. 5-hmC: 5-hydroxymethylation.

We estimated the 5-hmC level with an absolutely quantitative method ELISA, which is more objective than the semi-quantitative evaluation system of immunohistochemistry. The results showed that the 5-hmC level was downregulated in GC tissues compared with matched control tissues, which revealed that it was associated with the occurrence of GC and is consistent with previous reports[18]. Although some evidence has emerged about the potential progression and prognostic implications of 5-hmC level in GC[12], very few studies have evaluated the association stratified by *H. pylori* infection status. The present study was performed on a well-characterized cohort to simultaneously evaluate the level of 5-hmC in GC patients and subsets stratified by *H. pylori* infection to assess the association between 5-hmC levels and the susceptibility or prognosis of GC in order to provide more evidence for the effect of *H. pylori*-infection DNA hydroxymethylation on GC.

The 5-hmC level was slightly decreased in the *H. pylori*-positive subset compared to the *H. pylori*-negative group in our study. It is hypothesized that *H. pylori* infection affects *TET1* expression in normal

gastric epithelial cells and reduces the genome hydroxymethylation level[19]. Interestingly, higher global 5-hmC levels were associated with GC progression in the *H. pylori*-positive subset. A similar phenomenon was reported that the 5-hmC level in *ERG*- prostate cancer patients was lower than *ERG*+ patients, but a higher 5hmC level was associated with tumor progression in *ERG*- prostate cancer patients[20]. This could be explained by cells responding to hypoxia inducing a transcriptional program regulated by the *TET* family. Hypoxia together with reactive oxygen species increase global 5-hmC levels by transcriptional activation of *TET1*[21,22]. *H. pylori* infection induced the expression of hypoxia-inducible factor[23], which is required for hypoxic induction of *TET1* and global increase of 5-hmC. The proliferation rate of *H. pylori* under aerobic conditions was 3-fold higher than under microaerophilic conditions, and the bacterial growth was more dependent on carbon dioxide than on oxygen[24].

This interesting phenomenon and potential mechanism suggested to us that the 5-hmC level changed due to *H. pylori* infection and was not simply one direction but complicated. Therefore, it was essential to assess the association between 5-hmC and the prognosis of GC patients in negative or positive *H. pylori* infection. Our results first showed that reduced 5-hmC was associated with poor prognosis in all GC patients, which was consistent with previous studies[11,12]. Furthermore, in *H. pylori*-negative GC patients, the 5-hmC level was a significant predictor of prognosis, independent of routine clinicopathological factors. But in contrast, 5-hmC had no prediction value of prognosis in *H. pylori*-positive GC patients. These results highlight the importance of *H. pylori* stratification in GC biomarker studies. Similarly to our results, the study conducted in prostate cancer patients also showed that the prognostic predictor value of 5-hmC was discrepant in *ERG*- and *ERG*+ prostate cancer patients[20]. Together with our results, it supports potential prognostic implications of 5-hmC as cancer subtype-specific.

In this study, the association between 5-hmC level and the prognosis of GC patients was not significant in the Kaplan-Meier analysis, which could not be adjusted for potential confounders. However, it showed significant association in the multivariate Cox regression after the confounders such as TNM stage were adjusted. This indicated that the clinical characteristics such as TNM stage (which is strongly associated with the prognosis of GC patients) confused the relationship between 5-hmC level and the prognosis. This conclusion was further supported by the Cox regression results of TNM stage stratified analysis.

Several limitations should be mentioned of the present study. First, our study was based at a single center. The prognostic value of 5-hmC in *H. pylori*-negative but not positive GC patients' needs to be validated in larger and multicenter GC patient cohorts. Another limitation of our study is the lack of data of 5-methylcytosine and enzymes related to 5-hmC regulation for our sample set. Thus, we have not investigated the correlation between them, which should be investigated in future studies.

CONCLUSION

5-hmC level was a significant predictor of the prognosis of GC patients without *H. pylori* infection, independent of routine clinicopathological factors.

ARTICLE HIGHLIGHTS

Research background

Most gastric cancer (GC) patients are diagnosed at middle or late stage because the symptoms in early stage are obscure, which causes higher mortality rates of GC. Analyses show that aberrant DNA methylation is highly correlated with GC risk. *Helicobacter pylori* (*H. pylori*) was identified as a class I carcinogen leading to gastric adenocarcinoma, and *H. pylori*-induced chronic inflammation plays a direct role in the induction of aberrant DNA methylation. The median demethylation product 5-hydroxymethylcytosine (5-hmC) is considered as an activating epigenetic marker, and it plays complex roles in gene regulation of tumorigenesis.

Research motivation

A few small studies analyzed the association between 5-hmC levels and GC, but the evidence is lacking, especially for *H. pylori*-induced GC.

Research objectives

Exploring the association between 5-hmC level and the progression and prognosis of GC patients with or without *H. pylori* infection.

Research methods

This was a retrospective cohort study to estimate the predicted value of 5-hmC level in the progression and prognosis of GC patients with different *H. pylori* infection status.

Research results

A high level of 5-hmC was an independent significant favorable predictor of overall survival in the entire GC patient cohort (hazard ratio = 0.61, 95% confidence interval: 0.38-0.98, P = 0.040), the *H. pylori*-negative GC subgroup (hazard ratio = 0.30, 95% confidence interval: 0.13-0.68, P = 0.004) and GC patients with early TNM stage (hazard ratio = 0.32, 95% confidence interval: 0.13-0.77, P = 0.011).

Research conclusions

5-hmC level was a significant predictor of the prognosis of GC patients without *H. pylori* infection.

Research perspectives

A large-scale GC patient cohort to assess the association between the level of 5-hmC and the prognosis of GC patients, especially for different *H. pylori* infection status, should be conducted.

ACKNOWLEDGEMENTS

We are grateful to all sample donors and the research assistants who helped with sample collection.

FOOTNOTES

Author contributions: Cao XY conceived and designed the study; Fu YL and Wu YH conducted data analysis and drafted the manuscript, and they contributed equally to this work; Cao DH, Jia ZF and Shen A collected data and biospecimens on gastric cancer patients; Jiang J measured the level of 5-hmC; All authors approved the final version for submission.

Supported by National Natural Science Foundation of China, No. 81874279; Scientific and Technological Development Program of Jilin Province, No. 20190201093JC and No. 20200201326JC; Jilin Province Department of Finance, No. JLSWSRCZX2020-010; and Youth Development Fund from First Hospital of Jilin University, No. JDYY11202021.

Institutional review board statement: This study was approved by the First Hospital of Jilin University Institutional Review Board (Approval No.2021-493).

Informed consent statement: Patients were not required to give informed consent to the study because the analysis used anonymous clinical data that were obtained after each patient agreed to treatment by written consent.

Conflict-of-interest statement: All authors declared no competing financial interests.

Data sharing statement: Technical appendix, statistical code, and dataset available from the corresponding author at email jd3d2ub@jlu.edu.cn.

STROBE statement: The authors have read the STROBE Statement—checklist of items, and the manuscript was prepared and revised according to the STROBE Statement—checklist of items.

Country/Territory of origin: China

ORCID number: Ying-Li Fu 0000-0003-0455-5962; Yan-Hua Wu 0000-0002-9920-3486; Dong-Hui Cao 0000-0002-6795-6395; Zhi-Fang Jia 0000-0001-9838-1726; Ao Shen 0000-0002-3169-0062; Jing Jiang 0000-0001-9714-9255; Xue-Yuan Cao 0000-0002-1982-1672.

S-Editor: Ma YJ
L-Editor: Filipodia
P-Editor: Ma YJ

REFERENCES

1 **Sung H**, Ferlay J, Siegel RL, Laversanne M, Soerjomataram I, Jemal A, Bray F. Global Cancer Statistics 2020: GLOBOCAN Estimates of Incidence and Mortality Worldwide for 36 Cancers in 185 Countries. *CA Cancer J Clin* 2021; **71**: 209-249 [PMID: 33538338 DOI: 10.3322/caac.21660]

2 **Wang K**, Yuen ST, Xu J, Lee SP, Yan HH, Shi ST, Siu HC, Deng S, Chu KM, Law S, Chan KH, Chan AS, Tsui WY, Ho SL, Chan AK, Man JL, Foglizzo V, Ng MK, Ching YP, Cheng GH, Xie T, Fernandez J, Li VS, Clevers H, Rejto PA, Mao M, Leung SY. Whole-genome sequencing and comprehensive molecular profiling identify new driver mutations in gastric cancer. *Nat Genet* 2014; **46**: 573-582 [PMID: 24816253 DOI: 10.1038/ng.2983]

3 **Nakajima T**, Maekita T, Oda I, Gotoda T, Yamamoto S, Umemura S, Ichinose M, Sugimura T, Ushijima T, Saito D. Higher methylation levels in gastric mucosae significantly correlate with higher risk of gastric cancers. *Cancer Epidemiol Biomarkers Prev* 2006; **15**: 2317-2321 [PMID: 17119066 DOI: 10.1158/1055-9965.epi-06-0436]

4 **Maekita T**, Nakazawa K, Mihara M, Nakajima T, Yanaoka K, Iguchi M, Arii K, Kaneda A, Tsukamoto T, Tatematsu M, Tamura G, Saito D, Sugimura T, Ichinose M, Ushijima T. High levels of aberrant DNA methylation in Helicobacter pylori-infected gastric mucosae and its possible association with gastric cancer risk. *Clin Cancer Res* 2006; **12**: 989-995 [PMID: 16467114 DOI: 10.1158/1078-0432.ccr-05-2096]

5 **Parsonnet J**, Friedman GD, Vandersteen DP, Chang Y, Vogelman JH, Orentreich N, Sibley RK. Helicobacter pylori infection and the risk of gastric carcinoma. *N Engl J Med* 1991; **325**: 1127-1131 [PMID: 1891020 DOI: 10.1056/nejm199110173251603]

6 **Shimazu T**, Asada K, Charvat H, Kusano C, Otake Y, Kakugawa Y, Watanabe H, Gotoda T, Ushijima T, Tsugane S. Association of gastric cancer risk factors with DNA methylation levels in gastric mucosa of healthy Japanese: a cross-sectional study. *Carcinogenesis* 2015; **36**: 1291-1298 [PMID: 26354778 DOI: 10.1093/carcin/bgv125]

7 **Nakajima T**, Enomoto S, Yamashita S, Ando T, Nakanishi Y, Nakazawa K, Oda I, Gotoda T, Ushijima T. Persistence of a component of DNA methylation in gastric mucosae after Helicobacter pylori eradication. *J Gastroenterol* 2010; **45**: 37-44 [PMID: 19821005 DOI: 10.1007/s00535-009-0142-7]

8 **Song CX**, Yi C, He C. Mapping recently identified nucleotide variants in the genome and transcriptome. *Nat Biotechnol* 2012; **30**: 1107-1116 [PMID: 23138310 DOI: 10.1038/nbt.2398]

9 **Mellén M**, Ayata P, Dewell S, Kriaucionis S, Heintz N. MeCP2 binds to 5hmC enriched within active genes and accessible chromatin in the nervous system. *Cell* 2012; **151**: 1417-1430 [PMID: 23260135 DOI: 10.1016/j.cell.2012.11.022]

10 **Thomson JP**, Lempiäinen H, Hackett JA, Nestor CE, Müller A, Bolognani F, Oakeley EJ, Schübeler D, Terranova R, Reinhardt D, Moggs JG, Meehan RR. Non-genotoxic carcinogen exposure induces defined changes in the 5-hydroxymethylome. *Genome Biol* 2012; **13**: R93 [PMID: 23034186 DOI: 10.1186/gb-2012-13-10-r93]

11 **Park JL**, Kim HJ, Seo EH, Kwon OH, Lim B, Kim M, Kim SY, Song KS, Kang GH, Choi BY, Kim YS. Decrease of 5hmC in gastric cancers is associated with TET1 silencing due to with DNA methylation and bivalent histone marks at TET1 CpG island 3'-shore. *Oncotarget* 2015; **6**: 37647-37662 [PMID: 26462176 DOI: 10.18632/oncotarget.6069]

12 **Yang Q**, Wu K, Ji M, Jin W, He N, Shi B, Hou P. Decreased 5-hydroxymethylcytosine (5-hmC) is an independent poor prognostic factor in gastric cancer patients. *J Biomed Nanotechnol* 2013; **9**: 1607-1616 [PMID: 23980508 DOI: 10.1166/jbn.2013.1713]

13 **Hooi JKY**, Lai WY, Ng WK, Suen MMY, Underwood FE, Tanyingoh D, Malfertheiner P, Graham DY, Wong VWS, Wu JCY, Chan FKL, Sung JJY, Kaplan GG, Ng SC. Global Prevalence of Helicobacter pylori Infection: Systematic Review and Meta-Analysis. *Gastroenterology* 2017; **153**: 420-429 [PMID: 28456631 DOI: 10.1053/j.gastro.2017.04.022]

14 **Alipour M**. Molecular Mechanism of Helicobacter pylori-Induced Gastric Cancer. *J Gastrointest Cancer* 2021; **52**: 23-30 [PMID: 32926335 DOI: 10.1007/s12029-020-00518-5]

15 **Elzouki AN**, Buhjab SI, Alkialani A, Habel S, Sasco AJ. Gastric cancer and Helicobacter pylori infection in the eastern Libya: a descriptive epidemiological study. *Arab J Gastroenterol* 2012; **13**: 85-88 [PMID: 22980598 DOI: 10.1016/j.ajg.2012.06.002]

16 **Flavahan WA**, Gaskell E, Bernstein BE. Epigenetic plasticity and the hallmarks of cancer. *Science* 2017; **357** [PMID: 28729483 DOI: 10.1126/science.aal2380]

17 **Do C**, Shearer A, Suzuki M, Terry MB, Gelernter J, Greally JM, Tycko B. Genetic-epigenetic interactions in cis: a major focus in the post-GWAS era. *Genome Biol* 2017; **18**: 120 [PMID: 28629478 DOI: 10.1186/s13059-017-1250-y]

18 **Liu H**, Xu T, Cheng Y, Jin MH, Chang MY, Shu Q, Allen EG, Jin P, Wang X. Altered 5-Hydroxymethylcytosine Landscape in Primary Gastric Adenocarcinoma. *DNA Cell Biol* 2019; **38**: 1460-1469 [PMID: 31657619 DOI: 10.1089/dna.2019.4965]

19 **Zhao R**, Liu Z, Xu W, Song L, Ren H, Ou Y, Liu Y, Wang S. Helicobacter pylori infection leads to KLF4 inactivation in gastric cancer through a TET1-mediated DNA methylation mechanism. *Cancer Med* 2020; **9**: 2551-2563 [PMID: 32017451 DOI: 10.1002/cam4.2892]

20 **Strand SH**, Hoyer S, Lynnerup AS, Haldrup C, Storebjerg TM, Borre M, Orntoft TF, Sorensen KD. High levels of 5-hydroxymethylcytosine (5hmC) is an adverse predictor of biochemical recurrence after prostatectomy in ERG-negative prostate cancer. *Clin Epigenetics* 2015; **7**: 111 [PMID: 26478752 DOI: 10.1186/s13148-015-0146-5]

21 **Mariani CJ**, Vasanthakumar A, Madzo J, Yesilkanal A, Bhagat T, Yu Y, Bhattacharyya S, Wenger RH, Cohn SL, Nanduri J, Verma A, Prabhakar NR, Godley LA. TET1-mediated hydroxymethylation facilitates hypoxic gene induction in neuroblastoma. *Cell Rep* 2014; **7**: 1343-1352 [PMID: 24835990 DOI: 10.1016/j.celrep.2014.04.040]

22 **Tsai YP**, Chen HF, Chen SY, Cheng WC, Wang HW, Shen ZJ, Song C, Teng SC, He C, Wu KJ. TET1 regulates hypoxia-induced epithelial-mesenchymal transition by acting as a co-activator. *Genome Biol* 2014; **15**: 513 [PMID: 25517638 DOI: 10.1186/s13059-014-0513-0]

23 **Valenzuela-Valderrama M**, Cerda-Opazo P, Backert S, González MF, Carrasco-Véliz N, Jorquera-Cordero C, Wehinger S, Canales J, Bravo D, Quest AFG. The *Helicobacter pylori* Urease Virulence Factor Is Required for the Induction of Hypoxia-Induced Factor-1α in Gastric Cells. *Cancers (Basel)* 2019; **11** [PMID: 31185594 DOI: 10.3390/cancers11060799]

24 **Abass A**, Okano T, Boonyaleka K, Kinoshita-Daitoku R, Yamaoka S, Ashida H, Suzuki T. Effect of low oxygen

concentration on activation of inflammation by Helicobacter pylori. *Biochem Biophys Res Commun* 2021; **560**: 179-185 [PMID: 34000467 DOI: 10.1016/j.bbrc.2021.04.123]

World Journal of Gastrointestinal Oncology

Submit a Manuscript: https://www.f6publishing.com

World J Gastrointest Oncol 2022 July 15; 14(7): 1307-1323

DOI: 10.4251/wjgo.v14.i7.1307

ISSN 1948-5204 (online)

ORIGINAL ARTICLE

Retrospective Study

Neutrophile-to-lymphocyte, lymphocyte-to-monocyte, and platelet-to-lymphocyte ratios as prognostic and response biomarkers for resectable locally advanced gastric cancer

Tiago Cruz Tomás, Inês Eiriz, Marina Vitorino, Rodrigo Vicente, João Gramaça, Alicia Guadalupe Oliveira, Paulo Luz, Mafalda Baleiras, Ana Sofia Spencer, Luísa Leal Costa, Patrícia Liu, Joana Mendonça, Magno Dinis, Teresa Padrão, Marisol Correia, Gonçalo Atalaia, Michelle Silva, Teresa Fiúza

Specialty type: Oncology

Provenance and peer review: Unsolicited article; Externally peer reviewed.

Peer-review model: Single blind

Peer-review report's scientific quality classification

Grade A (Excellent): A
Grade B (Very good): 0
Grade C (Good): 0
Grade D (Fair): 0
Grade E (Poor): 0

P-Reviewer: An T, China

Received: August 2, 2021
Peer-review started: August 2, 2021
First decision: September 5, 2021
Revised: September 19, 2021
Accepted: June 23, 2022
Article in press: June 23, 2022
Published online: July 15, 2022

Tiago Cruz Tomás, Inês Eiriz, Marina Vitorino, Rodrigo Vicente, Gonçalo Atalaia, Michelle Silva, Teresa Fiúza, Department of Medical Oncology, Hospital Professor Doutor Fernando Fonseca EPE, Amadora 2720-276, Portugal

João Gramaça, Department of Medical Oncology, Centro Hospitalar Barreiro-Montijo EPE, Barreiro 2830-003, Portugal

Alicia Guadalupe Oliveira, Department of Medical Oncology, Hospital do Espírito Santo de Évora EPE, Évora 7000-811, Portugal

Paulo Luz, Department of Medical Oncology, Centro Hospitalar Universitário do Algarve EPE, Algarve 8000-386, Portugal

Mafalda Baleiras, Department of Medical Oncology, Hospital São Francisco Xavier, Centro Hospitalar Lisboa Ocidental EPE, Lisboa 1449-005, Portugal

Ana Sofia Spencer, Department of Medical Oncology, Hospital Santo António dos Capuchos, Centro Hospital Lisboa Central EPE, Lisboa 1169-050, Portugal

Luísa Leal Costa, Department of Medical Oncology, Hospital Beatriz Ângelo, Loures 2674-514, Portugal

Patrícia Liu, Department of Medical Oncology, Centro Hospitalar de Trás-os-Montes e Alto Douro EPE, Vila Real 5000-508, Portugal

Joana Mendonça, Department of Medical Oncology, Hospital da Senhora da Oliveira EPE, Guimarães 4835-044, Portugal

Magno Dinis, Department of Medical Oncology, Hospital Garcia de Orta EPE, Almada 2805-267, Portugal

Teresa Padrão, Department of Medical Oncology, Hospital da Luz, Lisboa 1500-650, Portugal

Marisol Correia, Department of Medical Oncology, Hospital Distrital de Santarém EPE, Santaré m 2005-177, Portugal

Corresponding author: Tiago Cruz Tomás, MD, Doctor, Department of Medical Oncology, Hospital Professor Doutor Fernando Fonseca EPE, IC 19, Amadora 2720-276, Portugal. tiago.tomas@campus.ul.pt

Abstract

BACKGROUND

Perioperative fluorouracil plus leucovorin, oxaliplatin, and docetaxel (FLOT) improves prognosis in locally advanced gastric cancer (LAGC). Neutrophil-to-lymphocyte (NLR), lymphocyte-to-monocyte (LMR), and platelet-to-lymphocyte (PLR) ratios are prognostic biomarkers but not predictive factors.

AIM

To assess blood ratios' (NLR, LMR and PLR) potential predictive response to FLOT and survival outcomes in resectable LAGC patients.

METHODS

This was a multicentric retrospective study investigating the clinical potential of NLR, LMR, and PLR in resectable LAGC patients, treated with at least one preoperative FLOT cycle, from 12 Portuguese hospitals. Means were compared through non-parametric Mann-Whitney tests. Receiver operating characteristic curve analysis defined the cut-off values as: High PLR > 141 for progression and > 144 for mortality; high LMR > 3.56 for T stage regression (TSR). Poisson and Cox regression models the calculated relative risks/hazard ratios, using NLR, pathologic complete response, TSR, and tumor regression grade (TRG) as independent variables, and overall survival (OS) as the dependent variable.

RESULTS

This study included 295 patients (mean age, 63.7 years; 59.7% males). NLR was correlated with survival time (r = 0.143, P = 0.014). PLR was associated with systemic progression during FLOT (P = 0.022) and mortality (P = 0.013), with high PLR patients having a 2.2-times higher risk of progression [95% confidence interval (CI): 0.89-5.26] and 1.5-times higher risk of mortality (95%CI: 0.92-2.55). LMR was associated with TSR, and high LMR patients had a 1.4-times higher risk of achieving TSR (95%CI: 1.01-1.99). OS benefit was found with TSR (P = 0.015) and partial/complete TRG (P < 0.001). Patients without TSR and with no evidence of pathological response had 2.1-times (95%CI: 1.14-3.96) and 2.8-times (95%CI: 1.6-5) higher risk of death.

CONCLUSION

Higher NLR is correlated with longer survival time. High LMR patients have a higher risk of decreasing T stage, whereas high PLR patients have higher odds of progressing under FLOT and dying. Patients with TSR and a pathological response have better OS and lower risk of dying.

Key Words: Gastric cancer; Perioperative fluorouracil plus leucovorin, oxaliplatin, and docetaxel; Neutrophil-to-lymphocyte; Lymphocyte-to-monocyte; Platelet-to-lymphocyte; Tumor regression grade

Core Tip: Fluorouracil plus leucovorin, oxaliplatin, and docetaxel (FLOT) perioperative regimen has become the standard of care for resectable locally advanced gastric cancer, but there is a need for prognostic and predictive biomarkers. Neutrophil-to-lymphocyte (NLR), lymphocyte-to-monocyte (LMR), and platelet-to-lymphocyte (PLR) ratios are useful in solid tumors. We performed exploratory analyses regarding pathological response prediction and survival outcomes. NLR is weakly correlated with overall survival, high LMR patients have higher risk of T stage regression, high PLR patients have higher odds of progressing under FLOT and higher risk of mortality, and patients without T stage or pathological regression have higher risk of dying.

Citation: Tomás TC, Eiriz I, Vitorino M, Vicente R, Gramaça J, Oliveira AG, Luz P, Baleiras M, Spencer AS, Costa LL, Liu P, Mendonça J, Dinis M, Padrão T, Correia M, Atalaia G, Silva M, Fiúza T. Neutrophile-to-lymphocyte, lymphocyte-to-monocyte, and platelet-to-lymphocyte ratios as prognostic and response biomarkers for resectable locally advanced gastric cancer. *World J Gastrointest Oncol* 2022; 14(7): 1307-1323
URL: https://www.wjgnet.com/1948-5204/full/v14/i7/1307.htm
DOI: https://dx.doi.org/10.4251/wjgo.v14.i7.1307

INTRODUCTION

Locally advanced gastric cancer (LAGC) are common gastrointestinal malignancies and are the third leading cause of cancer-related mortality worldwide[1]. Patients with stage IIC and IV gastric cancer have 5-year survival rates of 20.2% and 8.8%, respectively, with most patients diagnosed in the advanced stage due to the absence of signs and symptoms in early-stage disease[2]. Recent developments in chemotherapy (CT) have improved prognosis, even in patients with advanced gastric cancer. There has been a focus on neoadjuvant CT and, despite lacking prognostic and treatment response biomarkers, fluorouracil plus leucovorin, oxaliplatin, and docetaxel (FLOT) perioperative CT has led to improved prognosis in patients with LAGC[3-6]. Available evidence suggests that a favorable histopathological response to treatment may be a useful positive predictive marker in LAGC. Nonetheless, tumor response and prognosis are still difficult to predict before treatment initiation, making potential biomarkers crucial to predict patient prognosis and individualize treatment and follow-up. Many serum biomarkers for early and advanced gastric cancer have been reported: Carcinoembryonic antigen is a frequently used biomarker, as well as carbohydrate antigen 19-9 (CA 19-9), CA 72-4, CA 125, and alpha-fetoprotein, which are also helpful for prognosis and monitoring gastric cancer recurrence[7-9]. However, these biomarkers do not predict responses and survival outcomes because of their limited specificity and sensitivity in LAGC. Although many other serum biomarkers are under investigation (*e.g.*, small noncoding microRNAs; fibroblast growth factor 2 amplification; e-cadherin, phosphatidylinositol-4,5-bisphosphate 3-kinase, catalytic subunit alpha, and phosphatase and tensin homolog mutations; mesenchymal epithelial transition gene amplification/overexpression; tumor protein p53 mutation; microsatellite instability), their cost-effectiveness ratio is also high, making them expensive to routinely use in clinical practice[10]. Recently, there has been an effort to validate blood ratios [neutrophil-to-lymphocyte (NLR), lymphocyte-to-monocyte (LMR), and platelet-to-lymphocyte (PLR)] as possible biomarkers, as they are routinely analyzed, cheap, and have known pathophysiological mechanisms associated with cancer development. Inflammation impacts carcinogenesis including tumor initiation, promotion, and metastization of solid and hematological malignancies. Blood immune and inflammatory cells (neutrophils, lymphocytes, platelets, and monocytes), as well as cytokines, play important roles in the tumor microenvironment, invasion, and metastization and are potential biomarkers worth being explored in the context of LAGC[11-14].

Lymphocytes seem to reflect the systemic inflammatory status, and some parameters using these cells predict survival outcomes in cancer patients[15-19]. With lymphocytes playing an important role in cancer immune monitoring and prevention, it appears that a pro-inflammatory microenvironment leads to impaired T-cell responses, mediated by cytokines, compromising cell-mediated immunity[20]. Depending on the inflammatory cytokine mediating the environment, neutrophils may exert either antitumoral or protumoral activities[21]. Under acute inflammatory stimulus, activated neutrophils can undertake antitumoral activity, while under chronic inflammation, these neutrophiles can induce a tumor growth and metastization process. Cytokines such as interleukin-6, which is elevated in gastric cancer patients, can induce protumoral neutrophil activity[22]. This behavior might explain why there is a correlation between neutrophil count and prognosis. The effects of inflammatory responses mediated by cytokines also influence tumor-associated monocytes, another main regulator of cancer inflammation. Tumor cells induce monocyte differentiation into tumor-associated macrophages, weakening antitumor immune responses and stimulating migration and metastatic spread[23-26]. Peripheral monocyte serum levels are negatively associated with prognosis in different cancer types[27-29].

NLR, LMR, and PLR are inflammatory biomarkers that are independent prognostic factors of survival in several solid tumors, as their assessment is inexpensive[30,31]. Preoperative assessment of the NLR has the clinical potential to predict tumor progression and prognosis in patients with resectable gastric cancer and esophageal squamous cell carcinoma[32,33]. In recent studies, high PLR has been associated with tumor aggressiveness in patients with several malignancies, as well as poor overall survival (OS) and disease-free survival (DFS)[34-38]. Combined NLR and PLR also predicts CT response and prognosis in patients with advanced gastric cancer[39]. Lower LMR is independently associated with worse OS of several malignancies in the advanced setting and more aggressive tumor behavior[40-42]. However, NLR, LMR, and PLR as predictors of response to CT have not been assessed in patients with resectable LAGC cancer.

Tumor regression grade (TRG) is a system used to evaluate residual tumor in patients administered preoperative therapies. TRG focuses on the quantity rather than location of the tumor, providing information on the response to therapies and predicting prognosis[43]. There are many different grading systems without global consensus[44-47]. Among various scores, the College of American Pathology (CAP) TRG score system, based on the relative amount between fibrosis and residual tumor, is widely applied in gastrointestinal cancers[48]. Some studies have suggested that patients with a lower TRG score (1-2 or 1-3) have better survival than those with a higher TRG score (3-5 or 4-5)[44,49,50]. Based on the MAGIC trial, Smyth *et al*[51] found that patients in the TRG 3-5 and node-positive group had worse OS than others, whereas patients with TRG 1-2 and node-negative had better OS.

This goal of this exploratory study was to assess NLR, LMR, and PLR as potential biomarkers for predicting response and survival outcomes in resectable LAGC patients, determined before preoperative CT. To the best of our knowledge, this is the first study to analyze the clinical potential of these ratios in a Portuguese population in a preoperative setting.

MATERIALS AND METHODS

Study design

This was a multicentric retrospective study including 295 patients from 12 Portuguese oncological centers, diagnosed with resectable LAGC [histologically confirmed advanced clinical stage cT2 or higher, or nodal-positive stage (cN+), or both], who underwent curative intent surgery after at least one preoperative FLOT (preFLOT) cycle, since its initial use in institutions until December 31, 2020. Data collection ended in April 2021, with a minimum follow-up time of 1 mo after surgery.

Participant oncological centers by region were as follows: South & Centre Region - Hospital Professor Doutor Fernando Fonseca, Centro Hospitalar Barreiro-Montijo, Centro Hospitalar Lisboa Ocidental, Centro Hospitalar Lisboa Central, Hospital da Luz de Lisboa, Hospital Beatriz Ângelo, Hospital Garcia de Orta, Hospital Distrital de Santarém, Hospital do Espírito Santo de Évora, Centro Hospitalar Universitário do Algarve; North Region - Centro Hospitalar de Trás-Os-Montes e Alto Douro, and Hospital da Senhora da Oliveira de Guimarães. The exclusion criteria were: Age < 18 years, synchronous or metachronous cancer in other organs, and absence of detailed therapeutic information and unknown laboratory values for NLR, LMR, or PLR.

Variables

The database included demographic, histological, clinical, surgical, and pathological variables. Regarding age, patients were divided into elder (≥ 75 years) and non-elder (< 75 years) groups. This division was made due to the growing aging society in western countries, where frailty risk increases above 75 years of age[52]. Neutrophils, lymphocytes, monocytes, and platelets were considered absolute cell counts, based on the last blood sample drawn prior to initiation of preFLOT. NLR was determined by dividing neutrophil absolute count by lymphocyte absolute count, LMR was determined by dividing lymphocyte absolute count by monocyte absolute count, and PLR was determined by dividing platelet absolute count by lymphocyte absolute count[15-20]. Histological diagnosis and grade were considered, as well as tumor site and tumor-node-metastasis (TNM) stage, which was evaluated according to the 8th edition of the American Joint Committee on Cancer staging manual. Patients were staged before the initiation of preoperative therapy. All patients were clinically staged with thorax, abdomen, and pelvic computerized tomography scans; upper endoscopic ultrasound was not requested for additional staging, but if the information was available, it was considered for local staging. Patients were submitted to exploratory laparoscopy for staging purposes, where they were considered for local staging and exclusion of macroscopic peritoneal metastization. Surgical variables included type of resection, type of lymphadenectomy, and margins. Regarding systemic treatment, number of cycles, toxicity, and time until surgery were considered. Pathological tumor response was assessed considering TRG. As previously stated, several grade scoring systems are used, with CAP score being the most used in the participating institutions. To standardize the analysis, we simplified the scores into three categories: Complete tumor regression (pathological complete response), partial/incomplete tumor regression (pathological partial/incomplete response), and no evidence of regression (absence of pathological response). Complete tumor regression was also considered a pathological complete response (pCR). Clinical responses were compared to pathological response obtained with surgery, and tumor downstaging was considered comparing clinical and pathological staging, as at least one of the following: T stage reduction and/or N stage reduction (downstaging). Patients with maintenance or increase in either T or N were considered as not having downstaged. Patients' period of survival was considered as time since histological diagnosis until death or last time seen alive, in months.

Statistical analyses

Data are represented as the relative and absolute frequencies, central tendency measures, and dispersion. Means regarding all ratios were compared using *t*-tests, and in case of non-normality through non-parametric Mann-Whitney tests, specifically for sex, age group (< 75 years *vs* ≥ 75 years),

preFLOT suspension, progression under preFLOT, tumor downstaging, T and N regression, TRG, OS and mortality. Analysis of receiver operating characteristics (ROC) curve defined a cut-off value for group stratification, to facilitate patient stratification in the clinical practice. The areas under the curves were calculated to evaluate the predictive abilities of PLR to discriminate patients' progressive systemic disease and mortality and of LMR to discriminate patients with T downstaging. High PLR was defined as > 141 for progression and > 144 for mortality; high LMR was defined as > 3.56 for T stage regression (TSR). Relative risk was calculated using Poisson regression, with the progression under preFLOT, mortality and TSR the dependent variables and PLR and LMR groups the independent variables. Pearson's correlation coefficient was used to assess the association between NLR and OS. Kaplan-Meier estimator was used to compare survival curves considering several variables (pCR, TSR, and TRG) and log-rank tests were used to assess statistical significance. Cox regression was used to calculate hazard ratios, with NLR, pCR, TSR, and TRG being the independent variables, and OS the dependent variable. Significance level was established at 0.05. All statistical analyses were performed using SPSS software (version 26.0; IBM Corp. Released 2019. IBM SPSS Statistics for Windows; Armonk, NY, United states). This retrospective observational study was approved on May 19, 2021 by the Ethics Committee of Hospital Professor Doutor Fernando Fonseca (Approval No. 045/2021).

RESULTS

Patients' demographics are described in Table 1. Two-hundred and ninety-five patients were included, with a mean age of 63.7 years (range: 31-84 years), and 59.7% males (n = 176). Mostly adenocarcinomas (98.3%), while only 3 patients had non-specified carcinoma and 1 patient had squamous cell carcinoma. Poorly differentiated histology was identified in 40.9% (n = 121), while 25.3% (n = 75) were moderately differentiated and 8.8% (n = 26) well differentiated. Regarding Lauren classification, 51.4% (n = 152) were intestinal or mixed subtypes and 20.6% (n = 61) were diffuse subtype. Most were located in the stomach (n = 272; body: 47%; antrum: 33.8%; cardia: 11.1%), 6.8% (n = 20) in the gastroesophageal junction and only 1% (n = 3) in the lower esophagus. Peritoneal lavage cytology was performed, prior to therapy initiation, in 253 patients (85.8%), with 42 missing data; of these, 6 patients had a suspicious cytology for neoplastic cells and 3 patients had a positive cytology, but all were considered for surgery in the absence of macroscopic peritoneal metastasis.

Among the 295 patients, the descriptive analysis revealed: Absolute neutrophile counts ranged from 1170 to 21290, with a mean ± SD of 6103 ± 3354; absolute lymphocyte count ranged from 200 to 9110, with a mean ± SD of 1890 ± 1014; absolute monocytes count ranged from 600 to 4440, with a mean ± SD of 585 ± 407; and absolute platelets count ranged from 25600 to 658000, with a mean ± SD of 268658 ± 92373. NLR ranged from 0.48 to 99.5 and mean ± SD was 4.66 ± 7.1; LMR ranged from 0.33 to 143.33 and mean ± SD was 5.29 ± 9.2; and PLR ranged from 15.79 to 1260 and mean ± SD was 182.91 ± 148.19.

Median number of preFLOT cycles was 4 (range: 1-12). Suspension of treatment due to toxicity occurred in 22 patients (7.5%). Twenty-four patients (8.1%) progressed systemically under preFLOT. Median waiting time to surgery was 12 wk (range: 6-33). Regarding patients with curative intent (n = 271, 8 missing data): Total gastrectomy was performed in 49% of patients (n = 129), while 46% (n = 121) had subtotal gastrectomy, 4.1% (n = 11) had Ivory-Lewis esophagectomy and 0.8% (n = 2) had distal gastrectomy; complete standard lymphadenectomies were performed in 96% (D2: 85.4%, n = 193; D1+: 10.6%, n = 24), with 45 missing data; R0 resection was achieved in 91.9% patients (n = 249), with 9 missing data. TSR occurred in 46.5% (n = 126; 17 missing data), and N stage regression occurred in 57.6% (n = 156; 9 missing data). Tumor downstaging (TD) defined as TSR and/or N stage regression in comparison of imagiological/clinical *vs* pathological staging, was observed in 61% patients (n = 161), while 39% didn't respond (n = 53) or progressed (n = 50), with 7 missing data.

Of the 239 surgical specimens evaluated for TRG, using our standardized classification, 46.4% (n = 111) showed partial/incomplete response, 33.5% (n = 80) no response, and 20.1% (n = 48) pCR. Mean OS of general population was 35.1 ± 1.2 mo, with a mean follow-up time of 19.4 ± 0.7 mo. At the end of study time, 233 patients (79%) were alive.

NLR, LMR, and PLR analyses

A statistically significant association between NLR and age group (< 75 years *vs* ≥ 75 years) and sex was not found. However, the difference in means was considerable for both variables (NLR mean in male patients = 4.18 *vs* female patients = 5.37, P = 0.073; mean in patients ≥ 75 years = 4.21 *vs* patients < 75 years = 4.72, P = 0.37) in Table 2. No association was found between NLR and early suspension of treatment due to toxicity. However, difference in means was clinically significant (NLR mean in patients with suspension = 5.32 *vs* without suspension = 4.61; P = 0.336). Although TD was not associated with any ratio, difference in means regarding NLR was considerable (mean in patients with TD = 4.93 *vs* without TD = 3.57; P = 0.081). NLR was not associated with T or N stage regression, although difference in means was considerable regarding N stage regression (NLR mean in patients with N regression = 5.02 *vs* without N regression = 4.06; P = 0.119).

Table 1 Patients' demographics

	All, *n* = 295
Age at diagnosis in yr, mean (min-max)	63.7 (31-84)
Male, *n* (%)	176 (59.7%)
Primary tumor site, *n* (%)	
Stomach	
Body	139 (47.1%)
Antrum	100 (33.9%)
Cardia	33 (11.2%)
Lower esophagus	3 (1%)
Gastroesophageal junction	20 (6.8%)
Lauren classification[1], *n* (%)	
Diffuse	61 (21.6%)
Intestinal or mixed	152 (53.9%)
NOS	69 (24.5%)
Differentiation degree[2], *n* (%)	
Well differentiated	26 (11.7%)
Moderately differentiated	75 (33.8%)
Poorly differentiated	121 (54.5%)
Blood cell count and blood ratios serum quantification, mean ± SD	
Neutrophiles	6103 ± 3354
Lymphocytes	1890 ± 1014
Platelets	268658 ± 92373
Monocytes	585 ± 407
NLR	4.66 ± 7.1
LMR	5.29 ± 9.2
PLR	182.91 ± 148.19
Clinical/imagiological T stage[3], *n* (%)	
T1	12 (4.3%)
T2	67 (23.8%)
T3	130 (46.3%)
T4	72 (25.6%)
Clinical/imagiological N stage[4], *n* (%)	
Nx	14 (4.8%)
N0	43 (14.7%)
N1	66 (22.5%)
N2	62 (21.2%)
N3	7 (2.4%)
N+	101 34.5%)
PreFLOT cycles, median (min-max)	4 (1-12)
Progressive disease under preFLOT, *n* (%)	24 (8.1%)
Suspension of preFLOT due to toxicity, *n* (%)	22 (7.5%)
Waiting time to surgery in wk, median (min-max)	12 (6-33)

Patients submitted to surgery[5], *n* (%)	271 (91.9%)
Total gastrectomy	129 (49%)
Subtotal gastrectomy	121 (46%)
Distal gastrectomy	2 (0.8%)
Esophagectomy	11 (4.1%)
Lymphadenectomy[6], *n* (%)	
D1	9 (4%)
D1+	24 (10.6%)
D2	193 (85.4%)
Resection margin[7], *n* (%)	
0	249 (95%)
1	13 (5%)
Pathological T stage[4], *n* (%)	
T0	40 (14.7%)
Tis	2 (0.7%)
T1	52 (19%)
T2	39 (14.3%)
T3	96 (35.2%)
T4	44 (16.1%)
Pathological N stage[4], *n* (%)	
N0	147 (53.8%)
N1	36 (13.2)
N2	48 (17.6%)
N3	42 (15.4%)
Pathological stage regression, *n* (%)	
T stage regression[8]	126 (46.5%)
N stage regression[9]	156 (57.6%)
Post-surgery tumor staging status, *n* (%)	
Tumor downstaging	161 (61%)
No response	53 (20.1%)
Tumor upstaging	50 (18.9%)
TRG[10], *n* (%)	
Complete tumor regression	48 (20.1%)
Partial/incomplete tumor regression	111 (46.4%)
No evidence of regression	80 (33.5%)
Mortality status at the end of study time, *n* (%)	
Dead	62 (21%)
Alive	233 (79%)

[1]13 missing data.
[2]73 missing data.
[3]14 missing data.
[4]22 missing data.
[5]8 missing data.
[6]45 missing data.

[7]9 missing data.
[8]17 missing data.
[9]9 missing data.
[10]56 missing data.
FLOT: Fluorouracil plus leucovorin, oxaliplatin, and docetaxel; LMR: Lymphocyte-to-monocyte ratio; NLR: Neutrophile-to-lymphocyte ratio; NOS: Nitric oxide synthase; PLR: Platelet-to-lymphocyte ratio; preFLOT: Preoperative fluorouracil plus leucovorin, oxaliplatin, and docetaxel; SD: Standard deviation; TRG: Tumor regression grade.

Table 2 Relationship between neutrophil-to-lymphocyte, lymphocyte-to-monocyte, and platelet-to-lymphocyte ratios and clinicopathological variables in patients with resectable locally advanced gastroesophageal cancer

	NLR, mean ± SD	*P* value	LMR, mean ± SD	*P* value	PLR, mean ± SD	*P* value
Age		0.37		0.323		0.335
< 75 yr (*n* = 262)	4.72 ± 7.24		5.37 ± 9.66		178.88 ± 129.45	
≥ 75 yr (*n* = 33)	4.21 ± 5.94		4.69 ± 4.06		214.98 ± 252.77	
Sex		0.073		0.435		0.177
Male (*n* = 176)	4.19 ± 4.33		5.12 ± 4.9		169.61 ± 120.07	
Female (*n* = 119)	5.37 ± 9.84		5.55 ± 13.24		202.6 ± 146.38	
Treatment suspension due to toxicity		0.336		0.818		0.144
Yes (*n* = 22)	5.32 ± 5.5		5.05 ± 3.89		208.26 ± 136.91	
No (*n* = 273)	4.61 ± 7.22		5.31 ± 9.5		180.87 ± 149.11	
Systemic progression under preFLOT		0.935		0.287		0.022
Yes (*n* = 24)	4.66 ± 4.48		3.78 ± 2.9		251.94 ± 173.3	
No (*n* = 271)	4.66 ± 7.29		5.43 ± 9.55		176.8 ± 144.54	
T stage regression		0.743		0.021		0.62
Yes (*n* = 126)	4.14 ± 3.94		4.38 ± 3.64		168.23 ± 117.2	
No (*n* = 138)	4.73 ± 8.97		6.5 ± 12.84		177.73 ± 145.62	
N stage regression		0.119		0.635		0.157
Yes (*n* = 156)	5.04 ± 8.81		5.76 ± 12.04		184.45 ± 140.76	
No (*n* = 115)	4.06 ± 4.56		4.91 ± 4.29		166.13 ± 150.31	
Tumor downstaging		0.081		0.873		0.82
Yes (*n* = 161)	5.07 ± 8.58		4.7 ± 4.27		180.13 ± 139.93	
No (*n* = 103)	4.02 ± 4.74		6.58 ± 14.42		197.79 ± 154.23	
TRG		0.9		0.99		0.305
Partial/incomplete or complete regression (*n* = 161)	4.87 ± 8.45		5.17 ± 11.49		180.4 ± 139.45	
No evidence of regression (*n* = 86)	4.77 ± 5.3		4.45 ± 3.63		189.73 ± 157.16	
Pathological complete response		0.511		0.472		0.832
Yes (*n* = 48)	4.32 ± 3.73		4.62 ± 4.1		177 ± 138.81	
No (*n* = 191)	5 ± 8.23		5.09 ± 10.54		183.87 ± 151.46	
Mortality status at the end of study time		0.082		0.14		0.013
Alive (*n* = 233)	4.47 ± 7.45		5.6 ± 10.18		175.64 ± 149.02	
Dead (*n* = 62)	5.38 ± 5.57		4.15 ± 3.45		210.27 ± 142.87	

FLOT: Fluorouracil plus leucovorin, oxaliplatin, and docetaxel; LMR: Lymphocyte-to-monocyte ratio; NLR: Neutrophile-to-lymphocyte ratio; PLR: Platelet-to-lymphocyte ratio; preFLOT: Preoperative fluorouracil plus leucovorin, oxaliplatin, and docetaxel; SD: Standard deviation; TRG: Tumor regression grade.

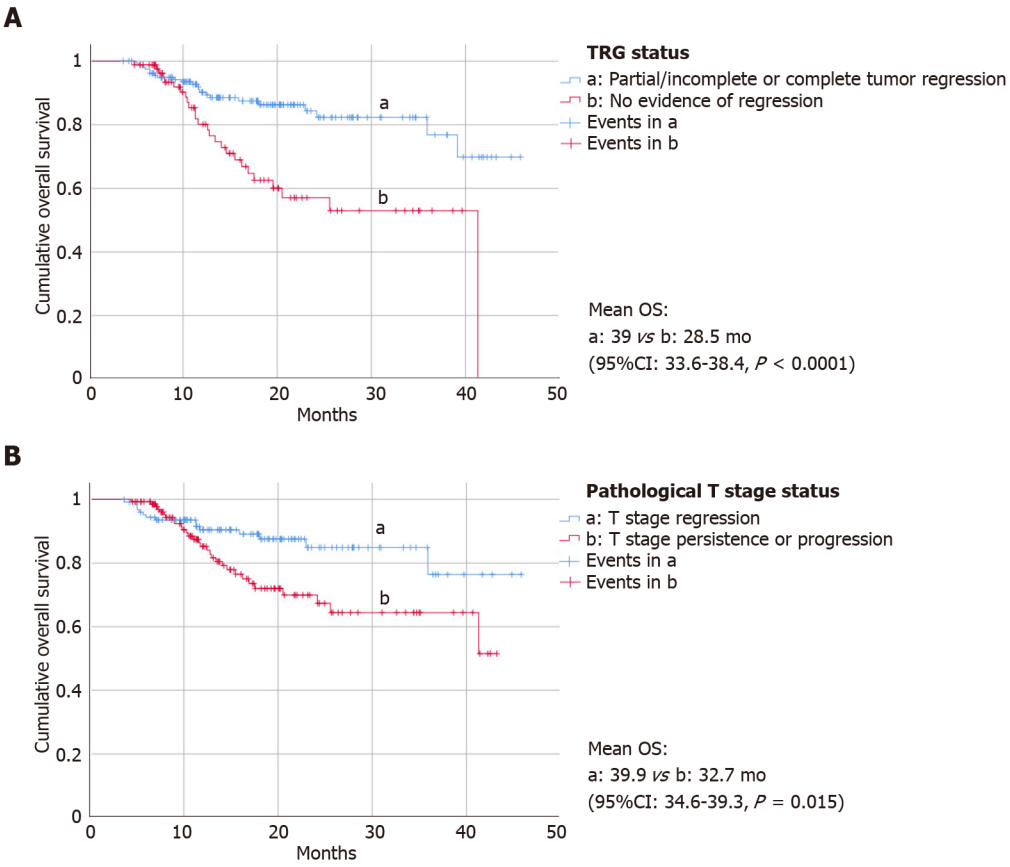

DOI: 10.4251/wjgo.v14.i7.1307

Figure 1 Overall Survival curves of resectable locally advanced gastroesophageal cancer patients. A: Stratified by tumor regression grade status, a: Partial/incomplete or complete tumor regression; b: No evidence of regression; B: Stratified by pathological T stage regression status, a: T stage regression; b: T stage persistence or progression. OS: Overall survival; TRG: Tumor regression grade; CI: Confidence interval.

LMR was not associated with sex and age group, but showed a considerable difference between age groups (LMR mean in patients ≥ 75 years = 4.68 *vs* patients < 75 years = 5.37, $P = 0.335$). An association between LMR and TSR was found ($P = 0.021$). Among the 264 patients, LMR ranged from 0.33 to 143.33, with mean ± SD LMR value in patients with T regression ($n = 126$) of 4.38 ± 3.64 and patients without TSR ($n = 138$) of 6.5 ± 12.84. According to ROC analysis, optimal cut-off of LMR was established at 3.56, with a sensitivity/specificity of 0.594 and 0.421. Patients were divided into the following groups according to the cut-off values for LMR: High (> 3.56; $n = 134$) and low LMR (≤ 3.56; $n = 130$). High LMR patients have 1.4-times higher relative risk of achieving TSR than low LMR patients [95% confidence interval (CI): 1.01-1.99; $P = 0.043$] in Table 3.

PLR did not reveal a statistically significant association between sex and age groups, but showed a considerable difference between age groups (PLR mean in patients ≥ 75 years = 214.98 *vs* patients < 75 years = 178.88; $P = 0.323$). Considering early suspension of treatment due to toxicity, PLR did not show to be associated, although difference in means was considerable (PLR mean in patients with suspension = 208.26 *vs* without suspension = 180.87; $P = 0.144$). We also found PLR to be associated with systemic progression during preFLOT ($P = 0.022$). PLR ranged from 15.79 to 1260, with a mean ± SD PLR value in patients with systemic progression during preFLOT ($n = 24$) of 251.94 ± 173.3 and in patients without progression ($n = 271$) of 176.8 ± 144.54. According to ROC analysis, optimal cut-off of PLR was established at 141 for progression, with a sensitivity/specificity for the PLR of 0.667/0.5. Patients were divided into the following groups according to the cut-off values for PLR: High (> 141; $n = 152$) and low PLR (≤ 141; $n = 143$). High PLR patients have 2.2-times higher relative risk of progressing under preFLOT (95%CI: 0.89-5.26; $P = 0.088$).

PLR was not associated with T and/or N stage regression, although difference in means was considerable regarding N stage regression (PLR mean in patients with N regression = 184.45 *vs* without N regression = 166.13; $P = 0.157$). Even though this ratio was not associated with TRG evaluation, difference in means regarding PLR was considerable (PLR mean in patients with partial/incomplete or complete tumor regression to treatment = 180.4 *vs* no evidence of regression to treatment = 189.73; $P = 0.305$). This ratio was also associated with mortality ($P = 0.013$), regardless of surgery. The mean ± SD PLR value in patients dead at the end of the study time analysis ($n = 62$) was 210.27 ± 142.87 and in patients alive at the end of the study time ($n = 233$) was 175.64 ± 149.48. According to ROC analysis, optimal cut-off of PLR was established at 144 for survival status, with a sensitivity/specificity of

Table 3 Univariate regressions of significant predictive or prognostic factors in resectable locally advanced gastroesophageal cancer patients

Poisson regression	Relative risk (95%CI)	Hazard ratio (95%CI)	*P* value
T stage regression between LMR groups			
> 3.56/≤ 3.56	1.42 (1.01-1.99)		0.043
Progression between PLR groups			
> 141/≤ 141	2.17 (0.89-5.26)		0.088
Mortality between PLR groups			
> 144/≤ 144	1.53 (0.92-2.55)		0.103
Cox regression			
NLR		1 (0.97-1.0)	0.972
Patients without pCR		2.1 (0.8-5.2)	0.129
Patients without (pathological) tumor regression		2.8 (1.6-5)	< 0.001
Patients without T stage regression		2.1 (1.1-3.9)	0.017

CI: Confidence interval; FLOT: Fluorouracil plus leucovorin, oxaliplatin, and docetaxel; LMR: Lymphocyte-to-monocyte ratio; NLR: Neutrophile-to-lymphocyte ratio; pCR: Pathological complete response; PLR: Platelet-to-lymphocyte ratio; preFLOT: Preoperative fluorouracil plus leucovorin, oxaliplatin, and docetaxel; TRG: Tumor regression grade.

0.613/0.481. Patients were divided into the following groups according to the cut-off values for PLR: High (> 144; n = 152) and low PLR (≤ 144; n = 143). High PLR patients have 1.5 times higher relative risk of dying than low PLR patients, although not statistically significant but the 95%CI lower limit is near 1 (95%CI: 0.92-2.55; P = 0.103).

Survival outcomes

NLR was found to be associated with OS time, with a weak positive correlation (r = 0.143; P = 0.014): For every one unit increase in NLR, there was a 0.1 mo increase in mean OS. Nevertheless, through Cox regression, there was no evidence of survival benefit between OS and NLR in Table 3. Neither LMR or PLR were associated with OS. Regarding pCR, the three ratios did not show a statistically significant association nor reveal considerable difference in means. We also did not find an association between pCR and OS; however, difference of means was considerable (mean OS without pCR of 14.9 mo *vs* 18.4 mo with pCR; P = 0.428). Although not statistically significant, patients without pCR seem to have higher risk (2.1 times) of dying than patients with pCR (95%CI: 0.8-5.2; P = 0.129) in Table 3. With TRG categories as partial/incomplete or complete tumor regression *vs* no evidence of regression to treatment, there was an association with OS (P = 0.009), with a survival of 39 mo *vs* 28.5 mo, respectively (95%CI: 33.6-38.4; P < 0.001) in Figure 1A. The univariate Cox regression revealed that patients without evidence of tumor regression had 2.8-times higher risk of dying than patients with partial or complete tumor regression (95%CI: 1.6-5, P < 0.001). OS was found to be associated with TSR (P = 0.03). Patients with T regression had better OS than those without T regression (39.9 mo *vs* 32.7 mo, respectively; P = 0.015) in Figure 1B. Univariate Cox regression revealed that patients without TSR had 2.1 times higher risk of dying than patients with TSR (95%CI: 1.14-3.96; P = 0.017).

DISCUSSION

In summary, our statistically significant results showed that: NLR was weakly (positive) correlated with OS time, but there was no evidence of survival benefit; LMR was associated with TSR; high LMR patients had 1.42-times relative risk of TSR; PLR was associated with systemic progression under preFLOT, as well as mortality; patients without TSR had 2.1-times risk of dying; and patients without pathological tumor regression had 2.8-times higher risk of dying.

Regarding cancer-related mortality and morbidity, gastric cancer is still one of the main causes, despite the development of new approaches, surgery, and systemic treatment-wise[53]. Survival outcomes vary considering patients in different conditions, degrees of invasion and differentiation, as well as TNM stages. The importance of searching for new treatment strategies and their validation, with the objective of improving survival outcomes, relies on the considerable number of patients with advanced disease at diagnosis. The perioperative FLOT strategy, studied by Al-Batran *et al*[3]

demonstrated a palpable benefit providing better outcomes. Nonetheless, it is still difficult to predict tumor response to systemic treatment and identify predictive factors to stratify patients into risk groups, which would be important to optimize individualized treatment and follow-up.

Several studies have described a correlation between elevated neutrophil count or high NLR and worse prognosis, as well as progression of disease[39,54]. Our findings seemed to slightly contradict the literature, as we found NLR had a weak positive correlation with OS, revealing that the higher the calculated NLR is, a better OS is expected, but Cox regression did not find an association between NLR and death status. Some studies have published reference values and prognostic correlations for NLR. However, these studies were conducted using small cohort of patients with different races, mainly Asian patients. It is possible differences could be found regarding other populations, specifically European patients. Also, it seems that in the literature there is a consistent difference in sex and age group, which our study supports despite not reaching statistical significance (women and younger patients have a higher NLR mean than men and older patients), but this needs to be replicated in further investigation[55]. This reveals the need for more validation studies in the European population.

LMR has been suggested to be an important factor for predicting prognosis in patients with hematologic and solid malignancies, such as lung and colon cancers[41,42,56-58]. Lower LMR is independently associated with poor OS in gastric cancer patients undergoing radical gastrectomy, and low LMR patients have a higher hazard ratio for both OS and DFS than high LMR[58]. This suggests that lower LMR might be associated with a more aggressive tumor behavior, higher surgical mortality rates, and worse long-term survival[59,60].

Although we did not find evidence of an association between LMR and prognosis, we showed an association between LMR and TSR, with high LMR patients having higher risk of achieving T stage reduction than low LMR patients. Also, our data showed an association between OS and TSR, documenting that patients without TSR had 2.1-times risk of dying, which we could indirectly interpret that patients with high LMR could have a better prognosis. We know that higher TNM staging, specifically T staging, is associated with less survival probability, crosswise solid and hematological tumors, so we could indirectly interpret that patients with low LMR are less likely to have TSR and, consequently, lower survival odds, but this needs to be further investigated.

N stage regression was not found to be associated with the three ratios, but NLR and PLR values seem to be clinically considerable, as patients with N reduction present higher ratio values. Further studies are needed to understand whether advanced TNM staging is associated with higher NLR and PLR ratio values[15,61]. Combining T and N stages to assess TD did not reveal a statistically significant association, despite patients that achieved TD tend to have higher NLR values.

PLR has been widely associated with different stages of tumor development, systemic treatment response and prognostic survival outcomes of cancer patients, namely in LAGC[61-63]. Nonetheless, specific physiopathology is complex and remains unclear. One plausible hypothesis is that a decreased PLR could reflect tumor disadvantage status, such as inflammatory status, immune disorders, malnutrition and thrombosis[64-66]. Low PLR has been associated with less aggressive clinicopathological features, including decreased depth of invasion, less lymph node metastasis, and early tumor stage, while higher risk of lymph node metastasis, increased serosa invasion risk, and advanced stage disease is associated with elevated PLR in patients with gastric cancer[15,61]. It has also been considered a prognostic factor, with high PLR patients being associated with worse OS[39].

Our study found an association between PLR and disease progression during preFLOT, showing that patients with high PLR have higher risk of progressing under CT. We also found a correlation between death and PLR, with high PLR patients having higher risk of dying than low PLR patients. Regarding tumoral response to CT, none of the ratios was associated with pCR achievement, albeit in TRG evaluation, PLR showed a considerable difference in means despite not being statistically significant, with patients without pathological response to CT presenting higher PLR values. Despite not finding an association between pCR and OS, TRG evaluation revealed an association with OS, documenting that patients without pathological tumor regression had 2.8 times higher risk of dying. Although not statistically significant, we could infer that patients with high PLR did not respond so well to CT and could have worse prognosis, despite further analysis is needed. We can extrapolate that these data show a more biologically aggressive tumor and that this might be a reasonable motive for a more active surveillance in these higher risk patients, to detect early progression.

Finally, treatment-associated toxicity is an important clinical factor to be considered in patients, with more emphasis in the elderly population. Although we did not find a correlation between the three ratios and early suspension of treatment due to toxicity, we demonstrate that patients in need of treatment suspension tend to have higher NLR and PLR values. The association with treatment toxicity could be an aspect worthy of future investigation.

This study gathered information suggesting that these biomarkers could be suited to stratify patients by risk to preoperative CT. Knowing the difficulty to predict tumor response before initiation of systemic treatment using clinical and pathological data, we focused on the potential of NLR, LMR and PLR, already reported as systemic inflammatory and immune cancer environment important pieces. Our study stands out from others due to the analysis of these already known blood ratios in a curative setting of gastric cancer, with an approach to the CT response prediction. It has a good representation of Portugal population, being also one of the few studies undergone in a European population: We should

keep in mind that possible genetic differences regarding gastric cancer and also inflammation/immune mechanisms should be considered as influencers of the blood ratios analysis (*vs* Asian or Latino-American patients). Due to lack of information regarding treatment prediction in resectable gastric cancer (even less information regarding the European population in this setting), it would be interesting to retrospectively analyze these blood ratios in the phase II/III FLOT4-AIO trial.

The present study had several limitations. First, this exploratory study involved a retrospective analysis in a relatively small population (n = 295); consequently, larger validation studies are needed to confirm the potential of these ratios. Second, with NLR, LMR and PLR associated with the inflammatory response, patients under anti-inflammatory effects from other medications could potentially bias the results. Third, we did not control the process and timing of blood collection and analysis; expectedly, blood analysis were undertaken before initiation of systemic treatment, but the period of time since blood results until treatment initiation can widely vary, and patients inflammatory state can be also volatile; depending on the length of time between blood collection and analysis, the composition of blood cells could be altered or destroyed, compromising correct estimation of the different ratios. Fourth, clinical and pathological staging were observational dependent: Every participant hospital was responsible for the evaluation process of its patients, and even different gastroenterologists, radiologists and pathologists evaluated these patients, with possible subjective assessments that could bias the results. Fifth, our median waiting time to surgery was 12 wk, being the recommended interval 4-6 wk (used in the FLOT4-AIO trial); this could possibly be a confounding variable and our results should be replicated prospectively for confirmation.

CONCLUSION

We believe that the NLR, LMR, and PLR could be important biomarkers, and that further prospective investigation is needed to validate these ratios and possibly develop a score that could help in the decision-making process in the clinical management of patients with resectable LAGC.

ARTICLE HIGHLIGHTS

Research background

Fluorouracil plus leucovorin, oxaliplatin, and docetaxel (FLOT) perioperative regimen became the standard of care in resectable locally advanced gastric cancer (LAGC), but there is still a need for prognostic and predictive response biomarkers. Blood ratios, such as neutrophil-to-lymphocyte (NLR), lymphocyte-to-monocyte (LMR) and platelet-to-lymphocyte (PLR) ratios are known prognostic biomarkers in several solid tumors. Tumor regression grade (TRG) is a system used to evaluate residual tumor in patients submitted to preoperative therapies, providing information on the response to therapies and predicting prognosis.

Research motivation

This study investigated the prognostic and predictive significance of pre-treatment blood ratios in resectable LAGC.

Research objectives

This study assessed the potential value of NLR, LMR, and PLR in predicting survival outcomes and response to preoperative FLOT (preFLOT) regimen in resectable LAGC.

Research methods

We retrospectively analyzed patients with resectable LAGC treated with at least one preFLOT cycle, from 12 Portuguese hospitals. NLR, LMR, and PLR pre-treatment values were exploratory correlated with different variables, and with those statistically significant pre-treatment values were divided according to into high or low groups, determined by receiver operating characteristic curve, and evaluated regarding association to survival outcomes and response prediction. Relative risks and hazard ratios were calculated, with NLR, pathological complete response, T stage regression (TSR) and TRG as independent variables, and overall survival (OS) the dependent variable.

Research results

We included 295 patients in this study. NLR was correlated with time of survival (r = 0.143; P = 0.014). High PLR was defined as > 141 for progression and > 144 for mortality; high LMR was defined as > 3.56 for TSR. PLR was associated with systemic progression during FLOT (P = 0.022) and mortality (P = 0.013), with high PLR patients having 2.2 times higher risk of progression [95% confidence interval (CI): 0.89-5.26] and 1.5 times higher risk of mortality (95%CI: 0.92-2.55). LMR was associated with TSR and

high LMR patients have 1.4 times higher risk of achieving TSR (95%CI: 1.01-1.99). OS benefit was found with TSR (P = 0.015) and partial/complete TRG (P < 0.001). Patients without TSR as well as no evidence of pathological response have 2.1 (95%CI: 1.14-3.96) and 2.8-times (95%CI: 1.6-5) higher risk of death.

Research conclusions

NLR, LMR, and PLR are significant biomarkers that are potential indicators for prognosis and treatment response prediction.

Research perspectives

In further investigation, validation of these blood ratios is important, as well as integration into risk scores that could help clinicians in the decision-making strategy in the clinical management of patients with resectable LAGC.

ACKNOWLEDGEMENTS

We would like to express our gratitude to Dr. Patrícia Soares, from Escola Nacional de Saúde Pública, for all the help and guidance in the statistical analysis of this study.

FOOTNOTES

Author contributions: Tomás TC designed and conducted the research, formally processed the statistical data, and wrote the paper; Vitorino M, Vicente R, Gramaça J, Oliveira AG, Luz P, Spencer AS, Eiriz I, Liu P, Mendonça J, Costa LL, Baleiras M, Dinis M, Correia M, and Padrão T performed the investigation and data collection; Atalaia G, Silva M, and Fiúza T supervised and validated the report.

Institutional review board statement: The study was reviewed and approved by the Ethical Committee for Health of Hospital Professor Doutor Fernando Fonseca (approval No. 045/2021).

Informed consent statement: The informed consent statement was waived.

Conflict-of-interest statement: All the authors report no relevant conflicts of interest for this article.

Data sharing statement: No data are available.

Country/Territory of origin: Portugal

ORCID number: Tiago Cruz Tomás 0000-0002-9535-8931; Inês Eiriz 0000-0002-1760-3436; Marina Vitorino 000-0002-8058-1495; Rodrigo Vicente 0000-0001-6780-4271; João Gramaça 0000-0001-6968-0436; Alicia Guadalupe Oliveira 000-0003-0833-0736; Paulo Luz 0000-0002-3905-0238; Mafalda Baleiras 0000-0003-2830-4287; Ana Sofia Spencer 0000-0002-1413-702X; Luísa Leal Costa 0000-0002-2966-9192; Patrícia Liu 0000-0002-2180-9779; Joana Mendonça 0000-0002-3188-5767; Magno Dinis 0000-0001-7433-2460; Teresa Padrão 0000-0002-4199-7252; Marisol Correia 0000-0002-2554-8254; Gonçalo Atalaia 0000-0002-0868-3622; Michelle Silva 0000-0002-2242-1223; Teresa Fiúza 0000-0002-6139-6550.

S-Editor: Wang JJ
L-Editor: Filipodia
P-Editor: Wang JJ

REFERENCES

1 **Global Burden of Disease Cancer Collaboration**, Fitzmaurice C, Dicker D, Pain A, Hamavid H, Moradi-Lakeh M, MacIntyre MF, Allen C, Hansen G, Woodbrook R, Wolfe C, Hamadeh RR, Moore A, Werdecker A, Gessner BD, Te Ao B, McMahon B, Karimkhani C, Yu C, Cooke GS, Schwebel DC, Carpenter DO, Pereira DM, Nash D, Kazi DS, De Leo D, Plass D, Ukwaja KN, Thurston GD, Yun Jin K, Simard EP, Mills E, Park EK, Catalá-López F, deVeber G, Gotay C, Khan G, Hosgood HD 3rd, Santos IS, Leasher JL, Singh J, Leigh J, Jonas JB, Sanabria J, Beardsley J, Jacobsen KH, Takahashi K, Franklin RC, Ronfani L, Montico M, Naldi L, Tonelli M, Geleijnse J, Petzold M, Shrime MG, Younis M, Yonemoto N, Breitborde N, Yip P, Pourmalek F, Lotufo PA, Esteghamati A, Hankey GJ, Ali R, Lunevicius R, Malekzadeh R, Dellavalle

R, Weintraub R, Lucas R, Hay R, Rojas-Rueda D, Westerman R, Sepanlou SG, Nolte S, Patten S, Weichenthal S, Abera SF, Fereshtehnejad SM, Shiue I, Driscoll T, Vasankari T, Alsharif U, Rahimi-Movaghar V, Vlassov VV, Marcenes WS, Mekonnen W, Melaku YA, Yano Y, Artaman A, Campos I, MacLachlan J, Mueller U, Kim D, Trillini M, Eshrati B, Williams HC, Shibuya K, Dandona R, Murthy K, Cowie B, Amare AT, Antonio CA, Castañeda-Orjuela C, van Gool CH, Violante F, Oh IH, Deribe K, Soreide K, Knibbs L, Kereselidze M, Green M, Cardenas R, Roy N, Tillmann T, Li Y, Krueger H, Monasta L, Dey S, Sheikhbahaei S, Hafezi-Nejad N, Kumar GA, Sreeramareddy CT, Dandona L, Wang H, Vollset SE, Mokdad A, Salomon JA, Lozano R, Vos T, Forouzanfar M, Lopez A, Murray C, Naghavi M. The Global Burden of Cancer 2013. *JAMA Oncol* 2015; **1**: 505-527 [PMID: 26181261 DOI: 10.1001/jamaoncol.2015.0735]

2 **Kim SG**, Seo HS, Lee HH, Song KY, Park CH. Comparison of the Differences in Survival Rates between the 7th and 8th Editions of the AJCC TNM Staging System for Gastric Adenocarcinoma: a Single-Institution Study of 5,507 Patients in Korea. *J Gastric Cancer* 2017; **17**: 212-219 [PMID: 28970951 DOI: 10.5230/jgc.2017.17.e23]

3 **Al-Batran SE**, Homann N, Pauligk C, Goetze TO, Meiler J, Kasper S, Kopp HG, Mayer F, Haag GM, Luley K, Lindig U, Schmiegel W, Pohl M, Stoehlmacher J, Folprecht G, Probst S, Prasnikar N, Fischbach W, Mahlberg R, Trojan J, Koenigsmann M, Martens UM, Thuss-Patience P, Egger M, Block A, Heinemann V, Illerhaus G, Moehler M, Schenk M, Kullmann F, Behringer DM, Heike M, Pink D, Teschendorf C, Löhr C, Bernhard H, Schuch G, Rethwisch V, von Weikersthal LF, Hartmann JT, Kneba M, Daum S, Schulmann K, Weniger J, Belle S, Gaiser T, Oduncu FS, Güntner M, Hozaeel W, Reichart A, Jäger E, Kraus T, Mönig S, Bechstein WO, Schuler M, Schmalenberg H, Hofheinz RD; FLOT4-AIO Investigators. Perioperative chemotherapy with fluorouracil plus leucovorin, oxaliplatin, and docetaxel versus fluorouracil or capecitabine plus cisplatin and epirubicin for locally advanced, resectable gastric or gastro-oesophageal junction adenocarcinoma (FLOT4): a randomised, phase 2/3 trial. *Lancet* 2019; **393**: 1948-1957 [PMID: 30982686 DOI: 10.1016/S0140-6736(18)32557-1]

4 **Al-Batran SE**, Homann N, Pauligk C, Illerhaus G, Martens UM, Stoehlmacher J, Schmalenberg H, Luley KB, Prasnikar N, Egger M, Probst S, Messmann H, Moehler M, Fischbach W, Hartmann JT, Mayer F, Höffkes HG, Koenigsmann M, Arnold D, Kraus TW, Grimm K, Berkhoff S, Post S, Jäger E, Bechstein W, Ronellenfitsch U, Mönig S, Hofheinz RD. Effect of Neoadjuvant Chemotherapy Followed by Surgical Resection on Survival in Patients With Limited Metastatic Gastric or Gastroesophageal Junction Cancer: The AIO-FLOT3 Trial. *JAMA Oncol* 2017; **3**: 1237-1244 [PMID: 28448662 DOI: 10.1001/jamaoncol.2017.0515]

5 **Fitzgerald TL**, Efird JT, Bellamy N, Russo SM, Jindal C, Mosquera C, Holliday EG, Biswas T. Perioperative chemotherapy versus postoperative chemoradiotherapy in patients with resectable gastric/gastroesophageal junction adenocarcinomas: A survival analysis of 5058 patients. *Cancer* 2017; **123**: 2909-2917 [PMID: 28386965 DOI: 10.1002/cncr.30692]

6 **Li Y**, Chen J, He Q, Ji X, Wang X, Fan C, Li G. Clinical efficacy of neoadjuvant chemotherapy regimens FLEEOX vs. XELOX in patients with initially unresectable advanced gastric cancer: a propensity score analysis. *Oncotarget* 2017; **8**: 86886-86896 [PMID: 29156843 DOI: 10.18632/oncotarget.19004]

7 **Li Y**, Yang Y, Lu M, Shen L. Predictive value of serum CEA, CA19-9 and CA72.4 in early diagnosis of recurrence after radical resection of gastric cancer. *Hepatogastroenterology* 2011; **58**: 2166-2170 [PMID: 22024091 DOI: 10.5754/hge11753]

8 **Emoto S**, Ishigami H, Yamashita H, Yamaguchi H, Kaisaki S, Kitayama J. Clinical significance of CA125 and CA72-4 in gastric cancer with peritoneal dissemination. *Gastric Cancer* 2012; **15**: 154-161 [PMID: 21892754 DOI: 10.1007/s10120-011-0091-8]

9 **Wu HH**, Lin WC, Tsai KW. Advances in molecular biomarkers for gastric cancer: miRNAs as emerging novel cancer markers. *Expert Rev Mol Med* 2014; **16**: e1 [PMID: 24456939 DOI: 10.1017/erm.2013.16]

10 **Lauren B**, Ostvar S, Silver E, Ingram M, Oh A, Kumble L, Laszkowska M, Chu JN, Hershman DL, Manji G, Neugut AI, Hur C. Cost-Effectiveness Analysis of Biomarker-Guided Treatment for Metastatic Gastric Cancer in the Second-Line Setting. *J Oncol* 2020; **2020**: 2198960 [PMID: 32148492 DOI: 10.1155/2020/2198960]

11 **Hainaut P**, Plymoth A. Targeting the hallmarks of cancer: towards a rational approach to next-generation cancer therapy. *Curr Opin Oncol* 2013; **25**: 50-51 [PMID: 23150341 DOI: 10.1097/CCO.0b013e32835b651e]

12 **Brigati C**, Noonan DM, Albini A, Benelli R. Tumors and inflammatory infiltrates: friends or foes? *Clin Exp Metastasis* 2002; **19**: 247-258 [PMID: 12067205 DOI: 10.1023/a:1015587423262]

13 **Balkwill F**, Mantovani A. Inflammation and cancer: back to Virchow? *Lancet* 2001; **357**: 539-545 [PMID: 11229684 DOI: 10.1016/S0140-6736(00)04046-0]

14 **Coussens LM**, Werb Z. Inflammation and cancer. *Nature* 2002; **420**: 860-867 [PMID: 12490959 DOI: 10.1038/nature01322]

15 **Lian L**, Xia YY, Zhou C, Shen XM, Li XL, Han SG, Zheng Y, Mao ZQ, Gong FR, Wu MY, Chen K, Tao M, Li W. Application of platelet/lymphocyte and neutrophil/lymphocyte ratios in early diagnosis and prognostic prediction in patients with resectable gastric cancer. *Cancer Biomark* 2015; **15**: 899-907 [PMID: 26444485 DOI: 10.3233/CBM-150534]

16 **Wang H**, Ding Y, Li N, Wu L, Gao Y, Xiao C, Jiang H, Zheng Y, Mao C, Deng J, Wang H, Xu N. Prognostic Value of Neutrophil-Lymphocyte Ratio, Platelet-Lymphocyte Ratio, and Combined Neutrophil-Lymphocyte Ratio and Platelet-Lymphocyte Ratio in Stage IV Advanced Gastric Cancer. *Front Oncol* 2020; **10**: 841 [PMID: 32637353 DOI: 10.3389/fonc.2020.00841]

17 **Feng JF**, Huang Y, Chen QX. Preoperative platelet lymphocyte ratio (PLR) is superior to neutrophil lymphocyte ratio (NLR) as a predictive factor in patients with esophageal squamous cell carcinoma. *World J Surg Oncol* 2014; **12**: 58 [PMID: 24641770 DOI: 10.1186/1477-7819-12-58]

18 **Hu B**, Yang XR, Xu Y, Sun YF, Sun C, Guo W, Zhang X, Wang WM, Qiu SJ, Zhou J, Fan J. Systemic immune-inflammation index predicts prognosis of patients after curative resection for hepatocellular carcinoma. *Clin Cancer Res* 2014; **20**: 6212-6222 [PMID: 25271081 DOI: 10.1158/1078-0432.CCR-14-0442]

19 **Hong X**, Cui B, Wang M, Yang Z, Wang L, Xu Q. Systemic Immune-inflammation Index, Based on Platelet Counts and Neutrophil-Lymphocyte Ratio, Is Useful for Predicting Prognosis in Small Cell Lung Cancer. *Tohoku J Exp Med* 2015; **236**: 297-304 [PMID: 26250537 DOI: 10.1620/tjem.236.297]

20 **Liu H**, Wu Y, Wang Z, Yao Y, Chen F, Zhang H, Wang Y, Song Y. Pretreatment platelet-to-lymphocyte ratio (PLR) as a predictor of response to first-line platinum-based chemotherapy and prognosis for patients with non-small cell lung cancer. *J Thorac Dis* 2013; **5**: 783-789 [PMID: 24409356 DOI: 10.3978/j.issn.2072-1439.2013.12.34]

21 **Stanec Z**, Ivrlac R, Hulina D, Dzepina I, Unusić J, Montani D, Prpić I. [An anatomic study of the septofascial layer in the forearm]. *Chir Maxillofac Plast* 1989; **19**: 1-8 [PMID: 2489516 DOI: 10.1007/s12307-014-0147-5]

22 **Ikeguchi M**, Hatada T, Yamamoto M, Miyake T, Matsunaga T, Fukumoto Y, Yamada Y, Fukuda K, Saito H, Tatebe S. Serum interleukin-6 and -10 levels in patients with gastric cancer. *Gastric Cancer* 2009; **12**: 95-100 [PMID: 19562463 DOI: 10.1007/s10120-009-0509-8]

23 **Wilcox RA**, Wada DA, Ziesmer SC, Elsawa SF, Comfere NI, Dietz AB, Novak AJ, Witzig TE, Feldman AL, Pittelkow MR, Ansell SM. Monocytes promote tumor cell survival in T-cell lymphoproliferative disorders and are impaired in their ability to differentiate into mature dendritic cells. *Blood* 2009; **114**: 2936-2944 [PMID: 19671921 DOI: 10.1182/blood-2009-05-220111]

24 **Peng LS**, Zhang JY, Teng YS, Zhao YL, Wang TT, Mao FY, Lv YP, Cheng P, Li WH, Chen N, Duan M, Chen W, Guo G, Zou QM, Zhuang Y. Tumor-Associated Monocytes/Macrophages Impair NK-Cell Function *via* TGFβ1 in Human Gastric Cancer. *Cancer Immunol Res* 2017; **5**: 248-256 [PMID: 28148545 DOI: 10.1158/2326-6066.CIR-16-0152]

25 **Mantovani A**, Schioppa T, Porta C, Allavena P, Sica A. Role of tumor-associated macrophages in tumor progression and invasion. *Cancer Metastasis Rev* 2006; **25**: 315-322 [PMID: 16967326 DOI: 10.1007/s10555-006-9001-7]

26 **Mantovani A**, Allavena P, Sica A, Balkwill F. Cancer-related inflammation. *Nature* 2008; **454**: 436-444 [PMID: 18650914 DOI: 10.1038/nature07205]

27 **Wang YQ**, Zhu YJ, Pan JH, Xu F, Shao XG, Sha JJ, Liu Q, Huang YR, Dong BJ, Xue W. Peripheral monocyte count: an independent diagnostic and prognostic biomarker for prostate cancer - a large Chinese cohort study. *Asian J Androl* 2017; **19**: 579-585 [PMID: 27569002 DOI: 10.4103/1008-682X.186185]

28 **Valero C**, Pardo L, López M, García J, Camacho M, Quer M, León X. Pretreatment count of peripheral neutrophils, monocytes, and lymphocytes as independent prognostic factor in patients with head and neck cancer. *Head Neck* 2017; **39**: 219-226 [PMID: 27534525 DOI: 10.1002/hed.24561]

29 **Han L**, Jia Y, Song Q, Wang N, Wang J, Bai B, Chen X, Wang C, Cheng Y. Prognostic significance of preoperative absolute peripheral monocyte count in esophageal squamous cell carcinoma. *Dis Esophagus* 2016; **29**: 740-746 [PMID: 26316375 DOI: 10.1111/dote.12401]

30 **Diakos CI**, Charles KA, McMillan DC, Clarke SJ. Cancer-related inflammation and treatment effectiveness. *Lancet Oncol* 2014; **15**: e493-e503 [PMID: 25281468 DOI: 10.1016/S1470-2045(14)70263-3]

31 **Roxburgh CS**, McMillan DC. Cancer and systemic inflammation: treat the tumour and treat the host. *Br J Cancer* 2014; **110**: 1409-1412 [PMID: 24548867 DOI: 10.1038/bjc.2014.90]

32 **Arigami T**, Okumura H, Matsumoto M, Uchikado Y, Uenosono Y, Kita Y, Owaki T, Mori S, Kurahara H, Kijima Y, Ishigami S, Natsugoe S. Analysis of the Fibrinogen and Neutrophil-Lymphocyte Ratio in Esophageal Squamous Cell Carcinoma: A Promising Blood Marker of Tumor Progression and Prognosis. *Medicine (Baltimore)* 2015; **94**: e1702 [PMID: 26496280 DOI: 10.1097/MD.0000000000001702]

33 **Arigami T**, Uenosono Y, Matsushita D, Yanagita S, Uchikado Y, Kita Y, Mori S, Kijima Y, Okumura H, Maemura K, Ishigami S, Natsugoe S. Combined fibrinogen concentration and neutrophil-lymphocyte ratio as a prognostic marker of gastric cancer. *Oncol Lett* 2016; **11**: 1537-1544 [PMID: 26893776 DOI: 10.3892/ol.2015.4049]

34 **Kim EY**, Lee JW, Yoo HM, Park CH, Song KY. The Platelet-to-Lymphocyte Ratio Versus Neutrophil-to-Lymphocyte Ratio: Which is Better as a Prognostic Factor in Gastric Cancer? *Ann Surg Oncol* 2015; **22**: 4363-4370 [PMID: 25805235 DOI: 10.1245/s10434-015-4518-z]

35 **Templeton AJ**, Ace O, McNamara MG, Al-Mubarak M, Vera-Badillo FE, Hermanns T, Seruga B, Ocaña A, Tannock IF, Amir E. Prognostic role of platelet to lymphocyte ratio in solid tumors: a systematic review and meta-analysis. *Cancer Epidemiol Biomarkers Prev* 2014; **23**: 1204-1212 [PMID: 24793958 DOI: 10.1158/1055-9965.EPI-14-0146]

36 **Yodying H**, Matsuda A, Miyashita M, Matsumoto S, Sakurazawa N, Yamada M, Uchida E. Prognostic Significance of Neutrophil-to-Lymphocyte Ratio and Platelet-to-Lymphocyte Ratio in Oncologic Outcomes of Esophageal Cancer: A Systematic Review and Meta-analysis. *Ann Surg Oncol* 2016; **23**: 646-654 [PMID: 26416715 DOI: 10.1245/s10434-015-4869-5]

37 **Zhao QT**, Yuan Z, Zhang H, Zhang XP, Wang HE, Wang ZK, Duan GC. Prognostic role of platelet to lymphocyte ratio in non-small cell lung cancers: A meta-analysis including 3,720 patients. *Int J Cancer* 2016; **139**: 164-170 [PMID: 26915723 DOI: 10.1002/ijc.30060]

38 **Lu C**, Gao P, Yang Y, Chen X, Wang L, Yu D, Song Y, Xu Q, Wang Z. Prognostic evaluation of platelet to lymphocyte ratio in patients with colorectal cancer. *Oncotarget* 2017; **8**: 86287-86295 [PMID: 29156795 DOI: 10.18632/oncotarget.21141]

39 **Hirahara T**, Arigami T, Yanagita S, Matsushita D, Uchikado Y, Kita Y, Mori S, Sasaki K, Omoto I, Kurahara H, Maemura K, Okubo K, Uenosono Y, Ishigami S, Natsugoe S. Combined neutrophil-lymphocyte ratio and platelet-lymphocyte ratio predicts chemotherapy response and prognosis in patients with advanced gastric cancer. *BMC Cancer* 2019; **19**: 672 [PMID: 31286873 DOI: 10.1186/s12885-019-5903-y]

40 **Pan YC**, Jia ZF, Cao DH, Wu YH, Jiang J, Wen SM, Zhao D, Zhang SL, Cao XY. Preoperative lymphocyte-to-monocyte ratio (LMR) could independently predict overall survival of resectable gastric cancer patients. *Medicine (Baltimore)* 2018; **97**: e13896 [PMID: 30593200 DOI: 10.1097/MD.0000000000013896]

41 **Toyokawa T**, Kubo N, Tamura T, Sakurai K, Amano R, Tanaka H, Muguruma K, Yashiro M, Hirakawa K, Ohira M. The pretreatment Controlling Nutritional Status (CONUT) score is an independent prognostic factor in patients with resectable thoracic esophageal squamous cell carcinoma: results from a retrospective study. *BMC Cancer* 2016; **16**: 722 [PMID: 27599460 DOI: 10.1186/s12885-016-2696-0]

42 **Chan JC**, Chan DL, Diakos CI, Engel A, Pavlakis N, Gill A, Clarke SJ. The Lymphocyte-to-Monocyte Ratio is a Superior Predictor of Overall Survival in Comparison to Established Biomarkers of Resectable Colorectal Cancer. *Ann Surg* 2017; **265**: 539-546 [PMID: 27070934 DOI: 10.1097/SLA.0000000000001743]

43 **Davies AR**, Gossage JA, Zylstra J, Mattsson F, Lagergren J, Maisey N, Smyth EC, Cunningham D, Allum WH, Mason RC. Tumor stage after neoadjuvant chemotherapy determines survival after surgery for adenocarcinoma of the esophagus and esophagogastric junction. *J Clin Oncol* 2014; **32**: 2983-2990 [PMID: 25071104 DOI: 10.1200/JCO.2014.55.9070]

44 **Mandard AM**, Dalibard F, Mandard JC, Marnay J, Henry-Amar M, Petiot JF, Roussel A, Jacob JH, Segol P, Samama G. Pathologic assessment of tumor regression after preoperative chemoradiotherapy of esophageal carcinoma. Clinicopathologic correlations. *Cancer* 1994; **73**: 2680-2686 [PMID: 8194005 DOI: 10.1002/1097-0142(19940601)73:11<2680::aid-cncr2820731105>3.0.co;2-c]

45 **Ryan R**, Gibbons D, Hyland JM, Treanor D, White A, Mulcahy HE, O'Donoghue DP, Moriarty M, Fennelly D, Sheahan K. Pathological response following long-course neoadjuvant chemoradiotherapy for locally advanced rectal cancer. *Histopathology* 2005; **47**: 141-146 [PMID: 16045774 DOI: 10.1111/j.1365-2559.2005.02176.x]

46 **Becker K**, Mueller JD, Schulmacher C, Ott K, Fink U, Busch R, Böttcher K, Siewert JR, Höfler H. Histomorphology and grading of regression in gastric carcinoma treated with neoadjuvant chemotherapy. *Cancer* 2003; **98**: 1521-1530 [PMID: 14508841 DOI: 10.1002/cncr.11660]

47 **Rödel C**, Martus P, Papadoupolos T, Füzesi L, Klimpfinger M, Fietkau R, Liersch T, Hohenberger W, Raab R, Sauer R, Wittekind C. Prognostic significance of tumor regression after preoperative chemoradiotherapy for rectal cancer. *J Clin Oncol* 2005; **23**: 8688-8696 [PMID: 16246976 DOI: 10.1200/JCO.2005.02.1329]

48 **Burgart LJ**, Chopp WV, Jain D. Protocol for the Examination of Specimens From Patients With Carcinoma of the Stomach. College of American Pathologists, 2021

49 **Noble F**, Lloyd MA, Turkington R, Griffiths E, O'Donovan M, O'Neill JR, Mercer S, Parsons SL, Fitzgerald RC, Underwood TJ; OCCAMS consortium. Multicentre cohort study to define and validate pathological assessment of response to neoadjuvant therapy in oesophagogastric adenocarcinoma. *Br J Surg* 2017; **104**: 1816-1828 [PMID: 28944954 DOI: 10.1002/bjs.10627]

50 **Mokadem I**, Dijksterhuis WPM, van Putten M, Heuthorst L, de Vos-Geelen JM, Haj Mohammad N, Nieuwenhuijzen GAP, van Laarhoven HWM, Verhoeven RHA. Recurrence after preoperative chemotherapy and surgery for gastric adenocarcinoma: a multicenter study. *Gastric Cancer* 2019; **22**: 1263-1273 [PMID: 30949777 DOI: 10.1007/s10120-019-00956-6]

51 **Smyth EC**, Fassan M, Cunningham D, Allum WH, Okines AF, Lampis A, Hahne JC, Rugge M, Peckitt C, Nankivell M, Langley R, Ghidini M, Braconi C, Wotherspoon A, Grabsch HI, Valeri N. Effect of Pathologic Tumor Response and Nodal Status on Survival in the Medical Research Council Adjuvant Gastric Infusional Chemotherapy Trial. *J Clin Oncol* 2016; **34**: 2721-2727 [PMID: 27298411 DOI: 10.1200/JCO.2015.65.7692]

52 **Torpy JM**, Lynm C, Glass RM. JAMA patient page. Frailty in older adults. *JAMA* 2006; **296**: 2280 [PMID: 17090776 DOI: 10.1001/jama.296.18.2280]

53 **Miller KD**, Nogueira L, Mariotto AB, Rowland JH, Yabroff KR, Alfano CM, Jemal A, Kramer JL, Siegel RL. Cancer treatment and survivorship statistics, 2019. *CA Cancer J Clin* 2019; **69**: 363-385 [PMID: 31184787 DOI: 10.3322/caac.21565]

54 **Murakami Y**, Saito H, Shimizu S, Kono Y, Shishido Y, Miyatani K, Matsunaga T, Fukumoto Y, Fujiwara Y. Neutrophil-to-Lymphocyte Ratio as a Prognostic Indicator in Patients With Unresectable Gastric Cancer. *Anticancer Res* 2019; **39**: 2583-2589 [PMID: 31092456 DOI: 10.21873/anticanres.13381]

55 **Lee JS**, Kim NY, Na SH, Youn YH, Shin CS. Reference values of neutrophil-lymphocyte ratio, lymphocyte-monocyte ratio, platelet-lymphocyte ratio, and mean platelet volume in healthy adults in South Korea. *Medicine (Baltimore)* 2018; **97**: e11138 [PMID: 29952958 DOI: 10.1097/MD.0000000000011138]

56 **Hu P**, Shen H, Wang G, Zhang P, Liu Q, Du J. Prognostic significance of systemic inflammation-based lymphocyte-monocyte ratio in patients with lung cancer: based on a large cohort study. *PLoS One* 2014; **9**: e108062 [PMID: 25275631 DOI: 10.1371/journal.pone.0108062]

57 **Stotz M**, Pichler M, Absenger G, Szkandera J, Arminger F, Schaberl-Moser R, Samonigg H, Stojakovic T, Gerger A. The preoperative lymphocyte to monocyte ratio predicts clinical outcome in patients with stage III colon cancer. *Br J Cancer* 2014; **110**: 435-440 [PMID: 24357796 DOI: 10.1038/bjc.2013.785]

58 **Lieto E**, Galizia G, Auricchio A, Cardella F, Mabilia A, Basile N, Del Sorbo G, Castellano P, Romano C, Orditura M, Napolitano V. Preoperative Neutrophil to Lymphocyte Ratio and Lymphocyte to Monocyte Ratio are Prognostic Factors in Gastric Cancers Undergoing Surgery. *J Gastrointest Surg* 2017; **21**: 1764-1774 [PMID: 28752404 DOI: 10.1007/s11605-017-3515-x]

59 **Hsu JT**, Wang CC, Le PH, Chen TH, Kuo CJ, Lin CJ, Chou WC, Yeh TS. Lymphocyte-to-monocyte ratios predict gastric cancer surgical outcomes. *J Surg Res* 2016; **202**: 284-290 [PMID: 27229102 DOI: 10.1016/j.jss.2016.01.005]

60 **Cong X**, Li S, Xue Y. [Impact of preoperative lymphocyte to monocyte ratio on the prognosis of the elderly patients with stage II(-III(gastric cancer]. *Zhonghua Wei Chang Wai Ke Za Zhi* 2016; **19**: 1144-1148 [PMID: 27781252]

61 **Zhang X**, Zhao W, Yu Y, Qi X, Song L, Zhang C, Li G, Yang L. Clinicopathological and prognostic significance of platelet-lymphocyte ratio (PLR) in gastric cancer: an updated meta-analysis. *World J Surg Oncol* 2020; **18**: 191 [PMID: 32731872 DOI: 10.1186/s12957-020-01952-2]

62 **Zhou X**, Xu L, Huang Z, Zhang L, Zhang H, Zhu W, Liu P. The hematologic markers as prognostic factors in patients with resectable gastric cancer. *Cancer Biomark* 2016; **17**: 359-367 [PMID: 27434296 DOI: 10.3233/CBM-160648]

63 **Deng J**, Zhang P, Sun Y, Peng P, Huang Y. Prognostic and clinicopathological significance of platelet to lymphocyte ratio in esophageal cancer: a meta-analysis. *J Thorac Dis* 2018; **10**: 1522-1531 [PMID: 29707302 DOI: 10.21037/jtd.2018.02.58]

64 **Cruz-Ramos M**, Del Puerto-Nevado L, Zheng B, López-Bajo R, Cebrian A, Rodríguez-Remirez M, García-García L, Solanes-Casado S, García-Foncillas J. Prognostic significance of neutrophil-to lymphocyte ratio and platelet-to lymphocyte ratio in older patients with metastatic colorectal cancer. *J Geriatr Oncol* 2019; **10**: 742-748 [PMID: 30327283 DOI: 10.1016/j.jgo.2018.10.002]

65 **Pang W**, Lou N, Jin C, Hu C, Arvine C, Zhu G, Shen X. Combination of preoperative platelet/lymphocyte and neutrophil/lymphocyte rates and tumor-related factors to predict lymph node metastasis in patients with gastric cancer. *Eur*

J Gastroenterol Hepatol 2016; **28**: 493-502 [PMID: 26854795 DOI: 10.1097/MEG.0000000000000563]

66 **Moyes LH**, Leitch EF, McKee RF, Anderson JH, Horgan PG, McMillan DC. Preoperative systemic inflammation predicts postoperative infectious complications in patients undergoing curative resection for colorectal cancer. *Br J Cancer* 2009; **100**: 1236-1239 [PMID: 19319134 DOI: 10.1038/sj.bjc.6604997]

World Journal of Gastrointestinal Oncology

Submit a Manuscript: https://www.f6publishing.com

World J Gastrointest Oncol 2022 July 15; 14(7): 1324-1336

DOI: 10.4251/wjgo.v14.i7.1324

ISSN 1948-5204 (online)

ORIGINAL ARTICLE

Retrospective Study

Effect of obesity on post-operative outcomes following colorectal cancer surgery

Derek Mao, David E Flynn, Stephanie Yerkovich, Kayla Tran, Usha Gurunathan, Manju D Chandrasegaram

Specialty type: Oncology

Provenance and peer review: Invited article; Externally peer reviewed.

Peer-review model: Single blind

Peer-review report's scientific quality classification
Grade A (Excellent): 0
Grade B (Very good): B, B
Grade C (Good): C
Grade D (Fair): 0
Grade E (Poor): 0

P-Reviewer: Díez M, Spain; Liu F, China

Received: November 22, 2021
Peer-review started: November 22, 2021
First decision: December 27, 2021
Revised: January 10, 2022
Accepted: June 18, 2022
Article in press: June 18, 2022
Published online: July 15, 2022

Derek Mao, Faculty of Medicine and Health, The University of Sydney, Sydney 2050, New South Wales, Australia

David E Flynn, Manju D Chandrasegaram, Department of General Surgery, The Prince Charles Hospital, Brisbane 4032, Queensland, Australia

Stephanie Yerkovich, Usha Gurunathan, Manju D Chandrasegaram, Faculty of Medicine, The University of Queensland, Brisbane 4006, Queensland, Australia

Kayla Tran, Department of Pathology, The Prince Charles Hospital, Brisbane 4032, Queensland, Australia

Usha Gurunathan, Department of Anaesthesia, The Prince Charles Hospital, Brisbane 4032, Queensland, Australia

Corresponding author: Manju D Chandrasegaram, FRCS, MBChB, Attending Doctor, Senior Lecturer, Surgeon, Department of General Surgery, The Prince Charles Hospital, Rode Road, Brisbane 4032, Queensland, Australia. m.chandrasegaram@uq.edu.au

Abstract

BACKGROUND

Colorectal cancer (CRC) resection is currently being undertaken in an increasing number of obese patients. Existing studies have yet to reach a consensus as to whether obesity affects post-operative outcomes following CRC surgery.

AIM

To evaluate the post-operative outcomes of obese patients following CRC resection, as well as to determine the post-operative outcomes of obese patients in the subgroup undergoing laparoscopic surgery.

METHODS

Six-hundred and fifteen CRC patients who underwent surgery at the Prince Charles Hospital between January 2010 and December 2020 were categorized into two groups based on body mass index (BMI): Obese [BMI ≥ 30, n = 182 (29.6%)] and non-obese [BMI < 30, n = 433 (70.4%)]. Demographics, comorbidities, surgical features, and post-operative outcomes were compared between both groups. Post-operative outcomes were also compared between both groups in the subgroup of patients undergoing laparoscopic surgery [n = 472: BMI ≥ 30, n = 136 (28.8%); BMI

< 30, *n* = 336 (71.2%)].

RESULTS

Obese patients had a higher burden of cardiac (73.1% *vs* 56.8%; *P* < 0.001) and respiratory comorbidities (37.4% *vs* 26.8%; *P* = 0.01). Obese patients were also more likely to undergo conversion to an open procedure (12.8% *vs* 5.1%; *P* = 0.002), but did not experience more post-operative complications (51.6% *vs* 44.1%; *P* = 0.06) or high-grade complications (19.2% *vs* 14.1%; *P* = 0.11). In the laparoscopic subgroup, however, obesity was associated with a higher prevalence of post-operative complications (47.8% *vs* 39.3%; *P* = 0.05) but not high-grade complications (17.6% *vs* 11.0%; *P* = 0.07).

CONCLUSION

Surgical resection of CRC in obese individuals is safe. A higher prevalence of post-operative complications in obese patients appears to only be in the context of laparoscopic surgery.

Key Words: Colorectal cancer; Obesity; Body mass index; Post-operative outcomes; Clavien-Dindo

Core Tip: This retrospective study assessed the post-operative outcomes of obese patients undergoing colorectal cancer (CRC) resection. Despite having a greater burden of cardiovascular and respiratory comorbidities and increased rate of conversion to open surgery, obese patients had equitable post-operative outcomes as those with a normal body mass index. There were no differences in severity of complications, length of stay, or mortality rates. Comparisons of obese and non-obese patients undergoing laparoscopic surgery showed that obese patients had a higher prevalence of post-operative complications but not high-grade complications. CRC surgery in obese individuals is generally safe, with caution advised if a laparoscopic approach is planned.

Citation: Mao D, Flynn DE, Yerkovich S, Tran K, Gurunathan U, Chandrasegaram MD. Effect of obesity on post-operative outcomes following colorectal cancer surgery. *World J Gastrointest Oncol* 2022; 14(7): 1324-1336
URL: https://www.wjgnet.com/1948-5204/full/v14/i7/1324.htm
DOI: https://dx.doi.org/10.4251/wjgo.v14.i7.1324

INTRODUCTION

Colorectal cancer (CRC) contributes substantially to the healthcare burden worldwide[1], and is the fourth most commonly diagnosed malignancy and second most common cause of cancer-related death in Australia[2]. Obesity is a rising global pandemic associated with systemic disease and poor health outcomes[3]. Body mass index (BMI) is an overall measure of total body fat, and is an easily calculable and accepted surrogate marker of obesity[4]. The World Health Organization (WHO) defines obesity in adults as a BMI of ≥ 30 kg/cm^2[5].

The increasing prevalence of obesity is of particular concern to colorectal surgeons, as it is not only implicated in the pathogenesis of CRC but also may have an impact on post-operative outcomes[6]. However, with several studies reporting inconsistent findings[7-9], there remains no consensus. The Clavien-Dindo Classification is a standardized system of grading post-operative complications, ranging from grade I (minor events) to grade V (death)[10]. With objective criteria, it is a highly reproducible method of grading post-operative complications, and is validated across several surgical disciplines including colorectal surgery[11].

In this study, we conducted a retrospective cohort study to outline and compare the clinical characteristics of obese and non-obese patients undergoing surgical resection of CRC at our institution, as well as to evaluate the impact of obesity on post-operative outcomes using the Clavien-Dindo Classification of Surgical Complications. The secondary aim was to determine the impact of obesity on post-operative outcomes in the subgroup of patients undergoing laparoscopic CRC resection.

MATERIALS AND METHODS

Study design

The Prince Charles Hospital (TPCH) CRC Database includes all patients who have undergone CRC

Table 1 Demographic and co-morbidity characteristics of patients undergoing colorectal cancer surgery

		BMI < 30 (% of group)	BMI ≥ 30 (% of group)	Total	*P* value
Patients		433	182	615	
Age		71 (58.0-79.0)	70 (60.0-77.0)		0.45
Sex	Male	232 (53.6)	83 (45.6)	315	0.08
	Female	201 (46.4)	99 (54.4)	300	
ASA grade	Low (ASA 1-2)	198 (45.7)	54 (29.7)	252	< 0.001
	High (ASA ≥ 3)	235 (54.3)	128 (70.3)	363	
Any cardiac comorbidity		246 (56.8)	133 (73.1)	379	< 0.001
Specified cardiac comorbidity	Ischemic heart disease	79 (18.2)	37 (20.3)	116	0.57
	Coronary artery bypass graft	25 (5.8)	16 (8.8)	41	0.21
	Coronary stents	25 (5.8)	15 (8.2)	40	0.28
	Pacemaker	8 (1.8)	5 (2.7)	13	0.54
	Valve replacement	19 (4.4)	4 (2.2)	23	0.25
	Heart failure	19 (4.4)	9 (4.9)	28	0.83
	Hypertension	186 (43.0)	117 (64.3)	303	< 0.001
	Atrial fibrillation	54 (12.5)	29 (15.9)	83	0.25
Any respiratory comorbidity		116 (26.8)	68 (37.4)	184	0.01
Specified respiratory comorbidity	Asthma	41 (9.5)	27 (14.8)	68	0.07
	Chronic obstructive pulmonary disease	52 (12.0)	20 (11.0)	72	0.78
	Bronchiectasis	6 (1.4)	3 (1.6)	9	0.73
	Obstructive sleep apnea	10 (2.3)	26 (14.3)	36	< 0.001
Any metabolic comorbidity		158 (36.5)	182 (100.0)	340	< 0.001
Specified metabolic comorbidity	Type 1 diabetes mellitus	3 (0.7)	0 (0.0)	3	0.56
	Type 2 diabetes mellitus	55 (12.7)	52 (28.6)	107	< 0.001
	Hyperlipidemia	116 (26.8)	59 (32.4)	175	0.17
Current smoker		67 (15.5)	25 (13.8)	92	0.71
Alcohol > 2 standard drinks/d		44 (10.2)	13 (7.1)	57	0.29

ASA: American Society of Anesthesiologists; BMI: Body mass index.

resection at our institution. The criteria for inclusion in TPCH CRC Database were all patients who had histologically confirmed CRC (including appendiceal cancers as per the International Classification of Diseases-10 classification) and underwent an operation at TPCH between January 2010 and December 2020. As per the WHO definition, patients were grouped into an obese group (BMI ≥ 30) or non-obese group (BMI < 30), and the demographic features, comorbidities, and surgical features in each group were reported and compared. In addition, the post-operative outcomes of patients in each group were also compared.

Ethics approval

Approval for the TPCH Colorectal Cancer Database was granted by TPCH Human Research Ethics Committee (HREC/17/QPCH/295).

Demographics and comorbidities

Demographic data documented in this study included age, sex, BMI, smoking, and alcohol status. Patient comorbidities were categorized into cardiac, respiratory and metabolic etiologies, with specific diseases recorded in each category if present. The American Society of Anesthesiologists (ASA) grade was also recorded (Table 1).

Table 2 Surgical features of patients undergoing colorectal cancer surgery

		BMI < 30 (% of group)	BMI ≥ 30 (% of group)	Total	*P* value
Patients		433	182	615	
Cancer location	Appendix	37 (8.5)	9 (4.9)	46	0.47
	Cecum to transverse colon	205 (47.3)	92 (50.5)	297	
	Splenic flexure to sigmoid colon	143 (33.0)	61 (33.5)	204	
	Rectum	48 (11.1)	20 (11.0)	68	
Operative urgency	Elective	359 (82.9)	161 (88.5)	519	0.09
	Emergency	74 (17.1)	21 (11.5)	95	
Operative approach	Laparoscopic	265 (61.5)	96 (53.3)	361	0.002
	Open	72 (16.7)	20 (11.1)	92	
	Laparoscopic-assisted	71 (16.5)	40 (22.2)	111	
	Laparoscopic converted to open	22 (5.1)	23 (12.8)	45	
	Transanal excision	1 (0.2)	1 (0.2)	2	
Operation performed	Appendicectomy	31 (7.2)	8 (4.4)	39	0.18
	Right hemicolectomy	170 (39.3)	74 (40.7)	244	
	Extended right hemicolectomy	34 (7.9)	18 (9.9)	52	
	Left hemicolectomy	18 (4.2)	11 (6.0)	29	
	Hartmann's procedure	20 (4.6)	5 (2.7)	25	
	High anterior resection	76 (17.6)	37 (20.3)	113	
	Low anterior resection	27 (6.2)	9 (4.9)	36	
	Ultra-low anterior resection	28 (6.5)	5 (2.7)	33	
	Other	29 (6.7)	15 (8.2)	44	
Stoma requirement		65 (15.0)	18 (9.9)	83	0.09
Peri-operative transfusion requirement		65 (15.0)	28 (15.4)	93	0.90

BMI: Body mass index.

Surgical features

Surgical features recorded included cancer location, operative urgency, operative approach, colorectal operation performed, requirement for stoma, and peri-operative requirement for transfusion (Table 2).

Post-operative outcomes

Post-operative outcomes recorded included the occurrence of any post-operative complication, which were each graded by the Clavien-Dindo Classification of Surgical Complications (Supplementary material). Complications were also classified as either no complication/low-grade and high-grade, defined as Clavien-Dindo grades I-II and III-V respectively. In addition, complications were attributed to either a surgical or medical cause, with specific surgical and medical complications also recorded if they occurred (Table 3).

The outcomes as above were also undertaken in the subgroup of patients undergoing laparoscopic surgery (Table 4). Patients who underwent laparoscopic surgery who were converted to an open procedure intra-operatively were excluded from this subgroup. Furthermore, post-operative outcomes of obese *vs* non-obese patients were compared in subgroups divided by cancer location. Patients were divided into a right sided colon cancer (caecum to transverse colon) subgroup (Table 5), left sided colon cancer (splenic flexure to sigmoid colon) subgroup (Table 6) and a rectal cancer subgroup (Table 7).

Statistical analysis

Statistical analysis was performed using Stata v17 (StataCorp, La Jolla, CA, United States). Categorial variables are presented as frequencies, and continuous variables are presented as medians and interquartile ranges. Groups were assessed using the *t*-test, χ^2 test or Fisher's exact test as appropriate. Statistically significant results were defined as $P \leq 0.05$.

Table 3 Post-operative outcomes of patients undergoing colorectal cancer surgery

		BMI < 30 (% of group)	BMI ≥ 30 (% of group)	Total	*P* value
Patients		433	182	615	
Post-operative complication (CD grade)	No complication	242 (55.9)	88 (48.4)	330	0.06
	Complication	191 (44.1)	94 (51.6)	285	
	I	31 (7.2)	17 (9.3)	48	
	II	99 (22.9)	42 (23.1)	141	
	IIIa	27 (6.2)	15 (8.2)	42	
	IIIb	13 (3.0)	6 (3.3)	19	
	IVa	13 (3.0)	10 (5.5)	23	
	IVb	0 (0.0)	3 (1.6)	3	
	V	8 (1.8)	1 (0.5)	9	
	No complication or low-grade complication (CD I-II)	372 (85.9)	147 (80.8)	519	0.11
	High-grade complication (CD IIIa-V)	61 (14.1)	35 (19.2)	96	
Any surgical complication		99 (22.9)	48 (26.4)	147	0.35
Specified surgical complications	Abdomino-pelvic collection	16 (3.7)	3 (1.6)	19	0.21
	Anastomotic leak	12 (2.8)	7 (3.8)	19	0.46
	Wound infection	19 (4.4)	7 (3.8)	26	0.83
	Prolonged ileus	49 (11.3)	27 (14.8)	76	0.23
	Post-operative hemorrhage	3 (0.7)	2 (1.1)	5	0.64
	Return to theatre	13 (3.0)	7 (3.8)	20	0.62
	Post-operative sepsis	16 (8.3)	8 (8.6)	24	1.00
Any medical complication		96 (22.2)	37 (20.3)	133	0.67
Specified medical complications	VTE (DVT/PE)	4 (0.9)	2 (1.1)	6	1.00
	Pneumonia	19 (4.4)	8 (4.4)	27	1.00
	Ischemic cardiac event	5 (1.2)	5 (2.7)	10	0.17
	Cardiac arrhythmia	30 (6.9)	9 (4.9)	39	0.47
	Respiratory failure	10 (2.3)	8 (4.4)	18	0.19
	Renal failure	12 (2.8)	7 (3.8)	19	0.46
	Unplanned ICU admission	16 (3.7)	6 (3.3)	22	1.00
Post-operative length of stay (d)		6 (IQR 5-11)	7 (IQR 5-11)		0.42

BMI: Body mass index; CD: Clavien-Dindo; DVT: Deep vein thrombosis; ICU: Intensive care unit; IQR: Interquartile range; PE: Pulmonary embolism; VTE: Venous thrombo-embolism.

RESULTS

Patient demographics and comorbidities

From January 2010 to December 2020, 615 patients at our institution fulfilled the inclusion criteria and were included in the database. In all, 182 patients (29.6%) had a BMI ≥ 30 (obese group), and 433 patients (70.4%) had a BMI < 30 (non-obese group). Table 1 outlines and compares the demographic features and comorbidities in both groups.

Patients in both groups were of similar age (obese group, 70 years *vs* non-obese group, 71 years; P = 0.45) and sex (45.6% male *vs* 53.6% male; P = 0.08). By contrast, the obese group had a greater proportion of patients graded at a higher ASA grade (ASA I-II: 29.7% *vs* 45.7%, ASA ≥ III: 70.3% *vs* 54.3%; P < 0.001), and also had a higher prevalence of cardiac comorbidities (73.1% *vs* 56.8%; P < 0.001) and respiratory comorbidities (37.4% *vs* 26.8%; P = 0.01) compared to patients in the non-obese group. Obese

Table 4 Post-operative outcomes in the subgroup of patients undergoing laparoscopic colorectal cancer surgery

		BMI < 30 (% of group)	BMI ≥ 30 (% of group)	Total	*P* value
Patients		336	136	472	
Post-operative complication (CD grade)	No complication	204 (60.7)	71 (52.2)	275	0.05
	Complication	132 (39.3)	65 (47.8)	197	
	I	24 (7.1)	12 (8.8)	36	
	II	71 (21.1)	29 (21.3)	100	
	IIIa	20 (6.0)	10 (7.4)	30	
	IIIb	6 (1.8)	6 (4.4)	12	
	IVa	6 (1.8)	6 (4.4)	12	
	IVb	0 (0.0)	2 (1.5)	2	
	V	5 (1.5)	0 (0.0)	5	
	No complication or low-grade complication (CD I-II)	299 (89.0)	112 (82.4)	411	0.07
	High-grade complication (CD IIIa-V)	37 (11.0)	24 (17.6)	61	
Any surgical complication		68 (20.2)	37 (27.2)	105	0.11
Specified surgical complications	Abdomino-pelvic collection	9 (2.7)	3 (2.2)	12	1.00
	Anastomotic leak	7 (2.1)	5 (3.7)	12	0.34
	Wound infection	13 (3.9)	6 (4.4)	19	0.80
	Prolonged ileus	33 (9.8)	21 (15.4)	54	0.11
	Post-operative hemorrhage	2 (0.6)	1 (0.7)	3	1.00
	Return to theatre	6 (1.8)	6 (4.4)	12	0.11
	Post-operative sepsis	12 (9.0)	4 (6.2)	16	0.59
Any medical complication		66 (19.6)	21 (15.4)	87	0.36
Specified medical complications	VTE (DVT/PE)	3 (0.9)	1 (0.7)	4	1.00
	Pneumonia	13 (3.9)	2 (1.5)	15	0.25
	Ischemic cardiac event	3 (0.9)	3 (2.2)	6	0.36
	Cardiac arrhythmia	23 (6.8)	7 (5.1)	30	0.68
	Respiratory failure	7 (2.1)	6 (4.4)	13	0.21
	Renal failure	7 (2.1)	4 (2.9)	11	0.52
	Unplanned ICU admission	6 (1.8)	3 (2.2)	9	0.72
Post-operative length of stay (d)		6 (IQR 4-9)	6 (IQR 5-10)		0.15

BMI: Body mass index; CD: Clavien-Dindo; DVT: Deep vein thrombosis; ICU: Intensive care unit; IQR: Interquartile range; PE: Pulmonary embolism; VTE: Venous thrombo-embolism.

patients were more likely to have type II diabetes mellitus (28.6% *vs* 12.7%; $P < 0.001$).

Surgical features

Table 2 outlines and compares the surgical features between the obese and non-obese groups. Both groups had a similar proportion of elective and emergency procedures (88.5% *vs* 82.9% and 11.5% *vs* 17.1% respectively; $P = 0.09$). The obese group had a higher proportion of patients requiring conversion to an open procedure (12.8% *vs* 5.1%; $P = 0.002$). Both groups had a similar percentage of patients requiring peri-operative blood transfusion (15.4% *vs* 15.0%; $P = 0.90$).

Post-operative outcomes

Table 3 outlines and compares the post-operative outcomes and complications between the obese and non-obese groups. There were no significant differences between groups in terms of the prevalence of

Table 5 Post-operative outcomes in the subgroup of patients with right sided colon cancer

		BMI < 30 (% of group)	BMI ≥ 30 (% of group)	Total	*P* value
Patients		205	92	297	
Post-operative complication (CD grade)	No complication	94 (45.9)	44 (47.8)	138	0.61
	Complication	111 (54.1)	48 (52.2)	159	
	I	21 (10.2)	9 (9.8)	30	
	II	58 (28.3)	23 (25.0)	81	
	IIIa	19 (9.3)	7 (7.6)	26	
	IIIb	3 (1.5)	1 (1.1)	4	
	IVa	8 (3.9)	5 (5.4)	13	
	IVb	0 (0.0)	2 (2.2)	2	
	V	2 (1.0)	1 (1.1)	3	
	No complication or low-grade complication (CD I-II)	173 (84.4)	76 (82.6)	249	0.73
	High-grade complication (CD IIIa-V)	32 (15.6)	16 (17.4)	48	
Any surgical complication		52 (25.4)	22 (23.9)	74	0.88
Specified surgical complications	Abdomino-pelvic collection	7 (3.4)	3 (0.0)	10	0.10
	Anastomotic leak	7 (3.4)	0 (0.0)	7	1.00
	Wound infection	10 (4.9)	3 (3.3)	13	0.76
	Prolonged ileus	26 (12.7)	14 (15.2)	40	0.58
	Post-operative hemorrhage	1 (0.5)	2 (2.2)	3	0.23
	Return to theatre	3 (1.5)	1 (1.1)	4	1.00
	Post-operative sepsis	2 (1.0)	1 (1.1)	3	1.00
Any medical complication		55 (26.8)	25 (27.2)	80	1.00
Specified medical complications	VTE (DVT/PE)	2 (1.0)	1 (1.1)	3	1.00
	Pneumonia	14 (6.8)	6 (6.5)	20	1.00
	Ischemic cardiac event	2 (1.0)	3 (3.3)	5	0.17
	Cardiac arrhythmia	20 (9.8)	6 (6.5)	26	0.51
	Respiratory failure	4 (2.0)	5 (5.4)	9	0.14
	Renal failure	7 (3.4)	6 (6.5)	13	0.23
	Unplanned ICU admission	8 (3.9)	4 (4.3)	12	1.00
Post-operative length of stay (d)		7 (IQR 5-11)	6 (IQR 5-11)		0.91

BMI: Body mass index; CD: Clavien-Dindo; DVT: Deep vein thrombosis; IQR: Interquartile range; PE: Pulmonary embolism; VTE: Venous thromboembolism.

post-operative complications (51.6% *vs* 44.1%; *P* = 0.06) or high-grade complications (19.2% *vs* 14.1%; *P* = 0.11). In-hospital mortality (Clavien-Dindo V) occurred in 1 obese patient (0.5%) and 8 non-obese patients (1.8%). There were no differences between both groups in the incidence of surgical complications (26.4% *vs* 22.9%; *P* = 0.35), including, but not limited to, anastomotic leak (3.8% *vs* 2.8%; *P* = 0.46), wound infection (3.8% *vs* 4.4%; *P* = 0.83) and return to theatre (3.8% *vs* 3.0%; *P* = 0.62). The prevalence of post-operative medical complications was also similar between both groups (20.3% *vs* 22.2%; *P* = 0.67), and there were no differences in the prevalence of specific medical complications. The median post-operative length of stay was also similar between both groups (7 d *vs* 6 d; *P* = 0.42).

Post-operative outcomes in patients undergoing laparoscopic surgery

A total of 472 patients (76.7%) underwent laparoscopic and laparoscopic-assisted surgery; among them, 336 (71.2%) had a BMI < 30, and 136 (28.8%) had a BMI ≥ 30. Obese patients in the laparoscopic surgery

Table 6 Post-operative outcomes in the subgroup of patients with left sided colon cancer

		BMI < 30 (% of group)	BMI ≥ 30 (% of group)	Total	*P* value
Patients		143	61	204	
Post-operative complication (CD grade)	No complication	90 (62.9)	32 (52.5)	122	0.09
	Complication	53 (37.1)	29 (47.5)	82	
	I	7 (4.9)	6 (9.8)	13	
	II	32 (22.4)	12 (19.7)	44	
	IIIa	3 (2.1)	6 (9.8)	9	
	IIIb	5 (3.5)	2 (3.3)	7	
	IVa	3 (2.1)	2 (3.3)	5	
	IVb	0 (0.0)	1 (1.6)	1	
	V	3 (2.1)	0 (0.0)	3	
	No complication or low-grade complication (CD I-II)	129 (90.2)	50 (82.0)	179	0.11
	High-grade complication (CD IIIa-V)	14 (9.8)	11 (18.0)	25	
Any surgical complication		29 (20.3)	17 (27.9)	46	0.27
Specified surgical complications	Abdomino-pelvic collection	7 (4.9)	2 (3.3)	9	0.73
	Anastomotic leak	4 (2.8)	2 (3.3)	6	1.00
	Wound infection	4 (2.8)	3 (4.9)	7	0.43
	Prolonged ileus	17 (11.9)	9 (14.8)	26	0.65
	Post-operative hemorrhage	1 (0.7)	0 (0.0)	1	1.00
	Return to theatre	5 (3.5)	3 (4.9)	8	0.70
	Post-operative sepsis	3 (2.1)	0 (0.0)	3	0.56
Any medical complication		28 (19.6)	6 (9.8)	34	0.10
Specified medical complications	VTE (DVT/PE)	1 (0.7)	1 (1.6)	2	0.51
	Pneumonia	5 (3.5)	2 (3.3)	7	1.00
	Ischemic cardiac event	1 (0.7)	0 (0.0)	1	1.00
	Cardiac arrhythmia	6 (4.2)	0 (0.0)	6	1.00
	Respiratory failure	4 (2.8)	2 (3.3)	6	1.00
	Renal failure	4 (2.8)	0 (0.0)	4	0.32
	Unplanned ICU admission	5 (3.5)	2 (3.3)	7	1.00
Post-operative length of stay (d)		7 (IQR 5-10)	7 (IQR 5-10)		0.89

BMI: Body mass index; CD: Clavien-Dindo; DVT: Deep vein thrombosis; IQR: Interquartile range; PE: Pulmonary embolism; VTE: Venous thromboembolism.

subgroup similarly had a higher ASA grade (ASA I-II: 36.8% *vs* 48.1%, ASA ≥ III: 63.2% *vs* 51.9%; $P = 0.03$), and a higher prevalence of pre-existing cardiac comorbidities (72.8% *vs* 56.3%; $P < 0.001$) and respiratory comorbidities (38.2% *vs* 26.9%; $P = 0.02$) compared to non-obese patients.

Post-operative outcomes of the patients in the cohort undergoing laparoscopic surgery are shown in Table 4. Obese patients were more likely to experience a post-operative complication (47.8% *vs* 39.3%; $P = 0.05$); however, there was no differences between both groups in the incidence of high-grade complications (17.6% *vs* 11.0%; $P = 0.07$). There were similarly no major differences between both groups in the percentage of patients who experienced a surgical complication (27.2% *vs* 20.2%; $P = 0.11$) or medical complication (15.4% *vs* 19.6%; $P = 0.36$). The median post-operative length of stay was equivalent between both groups (6 d *vs* 6 d; $P = 0.15$).

Table 7 Post-operative outcomes in the subgroup of patients with rectal cancer

		BMI < 30 (% of group)	BMI ≥ 30 (% of group)	Total	*P* value
Patients		48	20	68	
Post-operative complication (CD grade)	No complication	22 (45.8)	6 (30.0)	28	0.68
	Complication	26 (54.2)	14 (70.0)	40	
	I	3 (6.3)	2 (10.0)	5	
	II	8 (16.7)	5 (25.0)	13	
	IIIa	5 (10.4)	2 (10.0)	7	
	IIIb	5 (10.4)	3 (15.0)	8	
	IVa	2 (4.2)	2 (10.0)	4	
	IVb	0 (0.0)	0 (0.0)	0	
	V	3 (6.3)	0 (0.0)	3	
	No complication or low-grade complication (CD I-II)	33 (68.8)	13 (65.0)	46	0.78
	High-grade complication (CD IIIa-V)	15 (31.2)	7 (35.0)	22	
Any surgical complication		18 (37.5)	7 (35.0)	25	1.00
Specified surgical complications	Abdomino-pelvic collection	2 (4.2)	1 (5.0)	3	1.00
	Anastomotic leak	1 (2.1)	2 (10.0)	3	0.20
	Wound infection	5 (10.4)	0 (0.0)	5	0.31
	Prolonged ileus	6 (12.5)	3 (15.0)	9	1.00
	Post-operative hemorrhage	1 (2.1)	0 (0.0)	1	1.00
	Return to theatre	5 (10.4)	3 (15.0)	8	0.68
	Post-operative sepsis	1 (2.1)	0 (0.0)	1	1.00
Any medical complication		13 (27.1)	5 (25.0)	18	1.00
Specified medical complications	VTE (DVT/PE)	1 (2.1)	0 (0.0)	1	1.00
	Pneumonia	0 (0.0)	0 (0.0)	0	
	Ischemic cardiac event	2 (4.2)	2 (10.0)	4	0.58
	Cardiac arrhythmia	4 (8.3)	2 (10.0)	6	1.00
	Respiratory failure	2 (4.2)	1 (5.0)	3	1.00
	Renal failure	1 (2.1)	1 (5.0)	2	0.50
	Unplanned ICU admission	3 (6.3)	0 (0.0)	3	0.55
Post-operative length of stay (d)		9 (IQR 6-14)	10 (IQR 5-21)		0.91

BMI: Body mass index; CD: Clavien-Dindo; DVT: Deep vein thrombosis; IQR: Interquartile range; PE: Pulmonary embolism; VTE: Venous thrombo-embolism.

Post-operative outcomes of obese vs non-obese patients based on cancer location

Obese and non-obese patients in the right-sided colon cancer subgroup had equivalent outcomes, with no differences in the incidence of post-operative complications (52.2% *vs* 54.1%; $P = 0.61$), high-grade complications (17.4% *vs* 15.6%; $P = 0.73$), surgical complications (23.9% *vs* 25.4%; $P = 0.88$), or medical complications (27.2% *vs* 26.8%; $P = 1.00$). Similarly in the left-sided colon cancer subgroup there were no differences between obese and non-obese patients in the percentage of post-operative complications (47.5% *vs* 37.1%; $P = 0.09$), high-grade complications (18.0% *vs* 9.8%; $P = 0.11$), surgical complications (27.9% *vs* 20.3%; $P = 0.27$), or medical complications (9.8% *vs* 19.6%; $P = 0.10$). In the rectal cancer subgroup, there were also no differences between obese and non-obese patients in the prevalence of post-operative complications (70.0% *vs* 54.2%; $P = 0.68$), high-grade complications (35.0% *vs* 31.2%; $P = 0.78$), surgical complications (35.0% *vs* 37.5%; $P = 1.00$), or medical complications (25.0% *vs* 27.1%; $P = 1.00$).

DISCUSSION

We found that despite patients with an obese BMI having significantly higher rates of cardiac comorbidities, respiratory comorbidities, type II diabetes mellitus, and conversion to open surgery compared to patients with a non-obese BMI, there was no increased prevalence of post-operative complications (51.6% *vs* 44.1%; $P = 0.06$) or high-grade complications (19.2% *vs* 14.1%; $P = 0.11$) following CRC surgery. Our findings are concordant with Genser *et al*[12], who reported that in patients undergoing emergency colon cancer surgery, obese patients did not experience a higher proportion of post-operative complications (54% *vs* 52%; $P = 0.86$) or high-grade complications (20% *vs* 17%; $P = 0.47$). Despite our obese cohort having a higher burden of medical comorbidities, we did not observe an increased rate of specific post-operative medical complications. Smith *et al*[13] also showed that obese patients are not at an increased risk of post-operative pneumonia or renal failure, and Merkow *et al*[14] showed that obese patients are similarly not at increased risk of post-operative pneumonia, cardiac arrest, myocardial infarction, or stroke. Obesity may not be an independent predictor of peri-operative cardiac complications, with the latter more accurately related to functional status rather than traditional cardiovascular risk factors[15].

Importantly, we determined that the impact of obesity on post-operative outcomes may only manifest in patients undergoing laparoscopic resection, with obese patients in this subgroup having a significantly increased prevalence of post-operative complications (47.8% *vs* 39.3%; $P = 0.05$). It should be noted that these findings were not influenced by patients who underwent laparoscopic converted to open surgery given that they were excluded from this subgroup.

In contrast to our findings, a Chinese study by Xia *et al*[16] reported that following laparoscopic CRC resection, patients with a BMI ≥ 30 had a higher but non-significant incidence of Clavien-Dindo grade III complications compared to patients with a BMI of < 25 (14.3% *vs* 5.1%; $P = 0.178$). Similarly, a Korean study on laparoscopic CRC outcomes by Park *et al*[17] also showed that obesity was not associated with an increased rate of major post-operative complications including ileus, bleeding and anastomotic leak (7.4% *vs* 5.3%; $P = 0.889$). Non-significant results in both these studies may be related to the lower prevalence of obesity in Asian countries, which is reflected by both studies having only 2.7% of their cohorts categorized as BMI ≥ 30. Two systematic reviews of laparoscopic CRC surgery outcomes in the obese by Fung *et al*[18] and He *et al*[19] have both reported obesity to be associated with increased overall post-operative morbidity [odds ratio (OR) = 1.54, 95% confidence interval (CI): 1.21-1.97 and OR = 1.40, 95%CI: 1.18-1.66 respectively].

It is widely recognized that visceral obesity is associated with increased intra-operative technical difficulty by reducing access and visualization from thickened omentum and mesentery, distorting surgical planes, and increasing the risk of bleeding from both difficult mobilization of vessels and friable fatty tissue[20]. Our finding of poorer post-operative outcomes in obese patients undergoing laparoscopic surgery and not the obese cohort in general may be due to the fact that these aforementioned issues are aggravated in a laparoscopic approach, where increased intra-abdominal adiposity may severely restrict the already small working space available during a minimally-invasive resection. In addition, obese patients are pre-disposed to having a reduced physiologic reserve, and are thus at a greater risk of hemodynamic compromise during pneumoperitoneum from both increased intra-abdominal pressure and systemic acidosis secondary to carbon dioxide absorption[21].

In the modern era, laparoscopic surgery has been established as the standard of care in CRC surgery [22]. Although we have shown that utilizing this approach is associated with an increased prevalence of general post-operative complications in obese patients, we acknowledge that there are circumstances where the well-recognized benefits of laparoscopic surgery such as earlier restoration of gut motility, reduced post-operative pain and shorter length of stay may outweigh the perceived risks[23,24]. Martin and Stocchi[25] have proposed several practical strategies during laparoscopic colectomy in the obese such as the use of a 30-degree laparoscope to facilitate exposure and 10 mm instruments to allow for greater leverage during retraction, as well as the use of intra-corporeal vessel ligation given potential difficulties in exteriorizing thickened omentum. Surgeons attempting a laparoscopic approach in obese patients should be adequately experienced and aware that the benefits of laparoscopic surgery likely diminish if meaningful progress in the operation is not made.

We recognize that as an anthropometric measure, BMI has its limitations in the ability to identify visceral obesity, and also is distributed differently among ethnic groups[26]. Our rationale for using BMI as opposed to more specific volumetric measures of intra-abdominal adiposity such as visceral fat area, is that BMI is a much more commonly used definition of obesity in the literature. This enabled us to compare our outcomes directly against a larger number of studies. In addition, given that BMI is indicative of whole-body fat, it also allows for the analysis of general adipose-associated pathophysiological processes[19].

We found that despite patients with an obese BMI having significantly higher rates of cardiac comorbidities, respiratory comorbidities, type II diabetes mellitus, and conversion to open surgery compared to patients with a non-obese BMI, there was no increased prevalence of post-operative complications (51.6% *vs* 44.1%; $P = 0.06$) or high-grade complications (19.2% *vs* 14.1%; $P = 0.11$) following CRC surgery.

CONCLUSION

Surgical resection of CRC in obese individuals is safe. A higher prevalence of post-operative complications in obese patients appears to only be in the context of laparoscopic surgery.

ARTICLE HIGHLIGHTS

Research background

Obesity is a worldwide epidemic of increasing significance. Although the colorectal surgeons of today manage a greater number of obese patients with colorectal cancer (CRC), the current literature reports inconsistent findings on whether this phenomenon impacts post-operative outcomes following CRC surgery.

Research motivation

This research was conducted to determine whether obese patients had equivalent outcomes compared to non-obese patients following CRC surgery. This is an important issue, as there is no consensus on whether obesity truly impacts post-operative outcomes, yet obese patients are at risk of having their surgery withheld or delayed based on this factor alone.

Research objectives

The primary aim of this study was to compare the post-operative outcomes of obese *vs* non-obese patients following CRC surgery. With laparoscopic surgery now recognized as the standard of care in CRC management, post-operative outcomes between obese and non-obese patients were also analyzed in the subgroup of patients undergoing laparoscopic CRC surgery.

Research methods

Patients who underwent CRC resection between January 2010 and December 2020 at the Prince Charles Hospital, Queensland, Australia were included in this study. As per the World Health Organization definition, this study defined obesity as a body mass index (BMI) ≥ 30 mg/kg^2. Patients were divided into an obese and non-obese group, and post-operative outcomes were compared between these two groups using parametric and non-parametric tests. This study also analyzed the post-operative outcomes of obese *vs* non-obese patients in the subgroup undergoing laparoscopic CRC surgery.

Research results

This research has demonstrated that although obese patients were more likely to experience conversion to an open procedure (P = 0.002), they did not experience more post-operative complications (P = 0.06) or high-grade complications (P = 0.11). There were also no differences in in-hospital mortality (P = 0.06) or length of stay (P = 0.42). In the laparoscopic subgroup however, patients were more likely to experience a post-operative complication (P = 0.05), but did not experience more high-grade complications (P = 0.07).

Research conclusions

Our study has determined that obesity is no barrier to adequate post-operative outcomes following CRC surgery, with obese patients having equivalent post-operative outcomes compared to their non-obese counterparts. Caution is advised however, when attempting a laparoscopic approach in obese patients.

Research perspectives

Although BMI is a well-recognized and accepted surrogate marker of obesity, further studies in this area should analyze post-operative outcomes using other markers of visceral obesity. In addition, the effect of nutritional status and body composition on post-operative outcomes can be explored.

FOOTNOTES

Author contributions: Mao D designed the study, performed the research, and wrote the manuscript; Flynn DE designed the study methodology and helped perform the research; Yerkovich S helped with data collection, statistical analysis, and manuscript review; Tran K and Gurunathan U helped with data collection, clinical advice, data analysis, and manuscript review; Chandrasegaram MD helped with design methodology and conceptualization, study supervision, manuscript editing and finalization.

Institutional review board statement: Ethics approval for this database was granted by the Prince Charles Hospital Human Research Ethics Committee (Approval No. HREC/17/QPCH/295).

Informed consent statement: I certify that patients were not required to give informed consent to the study because the analysis used anonymous clinical data that was obtained after each patient agreed to treatment by written consent.

Conflict-of-interest statement: All the authors report no relevant conflicts of interest for this article.

Data sharing statement: No additional data are available.

Country/Territory of origin: Australia

ORCID number: Derek Mao 0000-0002-3979-734X; David E Flynn 0000-0003-2150-3849; Stephanie Yerkovich 0000-0003-4163-4782; Kayla Tran 0000-0002-9216-6774; Usha Gurunathan 0000-0002-0336-872X; Manju D Chandrasegaram 0000-0002-4826-5038.

S-Editor: Wang JJ
L-Editor: Filipodia
P-Editor: Wang JJ

REFERENCES

1 **Ferlay J**, Soerjomataram I, Dikshit R, Eser S, Mathers C, Rebelo M, Parkin DM, Forman D, Bray F. Cancer incidence and mortality worldwide: sources, methods and major patterns in GLOBOCAN 2012. *Int J Cancer* 2015; **136**: E359-E386 [PMID: 25220842 DOI: 10.1002/ijc.29210]
2 **Australian Institute of Health and Welfare**. Cancer data in Australia. [cited 15 May 2021]. Available from: https://www.aihw.gov.au/reports/cancer/cancer-data-in-australia
3 **Pi-Sunyer X**. The medical risks of obesity. *Postgrad Med* 2009; **121**: 21-33 [PMID: 19940414 DOI: 10.3810/pgm.2009.11.2074]
4 **Borruel S**, Moltó JF, Alpañés M, Fernández-Durán E, Álvarez-Blasco F, Luque-Ramírez M, Escobar-Morreale HF. Surrogate markers of visceral adiposity in young adults: waist circumference and body mass index are more accurate than waist hip ratio, model of adipose distribution and visceral adiposity index. *PLoS One* 2014; **9**: e114112 [PMID: 25479351 DOI: 10.1371/journal.pone.0114112]
5 Obesity: preventing and managing the global epidemic. Report of a WHO consultation. *World Health Organ Tech Rep Ser* 2000; **894**: i-xii, 1 [PMID: 11234459]
6 **Yehuda-Shnaidman E**, Schwartz B. Mechanisms linking obesity, inflammation and altered metabolism to colon carcinogenesis. *Obes Rev* 2012; **13**: 1083-1095 [PMID: 22937964 DOI: 10.1111/j.1467-789X.2012.01024.x]
7 **Govaert JA**, Lijftogt N, van Dijk WA, Tseng LN, Liem RS, Tollenaar RA, Fiocco M, Wouters MW; Dutch Value Based Healthcare Study Group. Colorectal cancer surgery for obese patients: Financial and clinical outcomes of a Dutch population-based registry. *J Surg Oncol* 2016; **113**: 489-495 [PMID: 26843323 DOI: 10.1002/jso.24187]
8 **Poelemeijer YQM**, Lijftogt N, Detering R, Fiocco M, Tollenaar RAEM, Wouters MWJM. Obesity as a determinant of perioperative and postoperative outcome in patients following colorectal cancer surgery: A population-based study (2009-2016). *Eur J Surg Oncol* 2018; **44**: 1849-1857 [PMID: 29937416 DOI: 10.1016/j.ejso.2018.05.027]
9 **Healy LA**, Ryan AM, Sutton E, Younger K, Mehigan B, Stephens R, Reynolds JV. Impact of obesity on surgical and oncological outcomes in the management of colorectal cancer. *Int J Colorectal Dis* 2010; **25**: 1293-1299 [PMID: 20563875 DOI: 10.1007/s00384-010-0963-0]
10 **Dindo D**, Demartines N, Clavien PA. Classification of surgical complications: a new proposal with evaluation in a cohort of 6336 patients and results of a survey. *Ann Surg* 2004; **240**: 205-213 [PMID: 15273542 DOI: 10.1097/01.sla.0000133083.54934.ae]
11 **Widmar M**, Keskin M, Strombom PD, Gennarelli RL, Szeglin BC, Smith JJ, Nash GM, Weiser MR, Paty PB, Russell D, Garcia-Aguilar J. Evaluating the Validity of the Clavien-Dindo Classification in Colectomy Studies: A 90-Day Cost of Care Analysis. *Dis Colon Rectum* 2021; **64**: 1426-1434 [PMID: 34623350 DOI: 10.1097/DCR.0000000000001966]
12 **Genser L**, Manceau G, Mege D, Bridoux V, Lakkis Z, Venara A, Voron T, Bege T, Sielezneff I, Karoui M; on behalf of the AFC (French Surgical Association) Working Group. 30-Day Postoperative Morbidity of Emergency Surgery for Obstructive Right- and Left-Sided Colon Cancer in Obese Patients: A Multicenter Cohort Study of the French Surgical Association. *Dig Surg* 2020; **37**: 111-118 [PMID: 30939470 DOI: 10.1159/000497450]
13 **Smith RK**, Broach RB, Hedrick TL, Mahmoud NN, Paulson EC. Impact of BMI on postoperative outcomes in patients undergoing proctectomy for rectal cancer: a national surgical quality improvement program analysis. *Dis Colon Rectum* 2014; **57**: 687-693 [PMID: 24807592 DOI: 10.1097/DCR.0000000000000097]
14 **Merkow RP**, Bilimoria KY, McCarter MD, Bentrem DJ. Effect of body mass index on short-term outcomes after colectomy for cancer. *J Am Coll Surg* 2009; **208**: 53-61 [PMID: 19228503 DOI: 10.1016/j.jamcollsurg.2008.08.032]

15 **Fleisher LA**, Fleischmann KE, Auerbach AD, Barnason SA, Beckman JA, Bozkurt B, Davila-Roman VG, Gerhard-Herman MD, Holly TA, Kane GC, Marine JE, Nelson MT, Spencer CC, Thompson A, Ting HH, Uretsky BF, Wijeysundera DN. 2014 ACC/AHA guideline on perioperative cardiovascular evaluation and management of patients undergoing noncardiac surgery: executive summary: a report of the American College of Cardiology/American Heart Association Task Force on Practice Guidelines. *Circulation* 2014; **130**: 2215-2245 [PMID: 25085962 DOI: 10.1161/CIR.0000000000000105]

16 **Xia X**, Huang C, Jiang T, Cen G, Cao J, Huang K, Qiu Z. Is laparoscopic colorectal cancer surgery associated with an increased risk in obese patients? *World J Surg Oncol* 2014; **12**: 184 [PMID: 24919472 DOI: 10.1186/1477-7819-12-184]

17 **Park JW**, Lim SW, Choi HS, Jeong SY, Oh JH, Lim SB. The impact of obesity on outcomes of laparoscopic surgery for colorectal cancer in Asians. *Surg Endosc* 2010; **24**: 1679-1685 [PMID: 20039065 DOI: 10.1007/s00464-009-0829-0]

18 **Fung A**, Trabulsi N, Morris M, Garfinkle R, Saleem A, Wexner SD, Vasilevsky CA, Boutros M. Laparoscopic colorectal cancer resections in the obese: a systematic review. *Surg Endosc* 2017; **31**: 2072-2088 [PMID: 27778169 DOI: 10.1007/s00464-016-5209-y]

19 **He Y**, Wang J, Bian H, Deng X, Wang Z. BMI as a Predictor for Perioperative Outcome of Laparoscopic Colorectal Surgery: a Pooled Analysis of Comparative Studies. *Dis Colon Rectum* 2017; **60**: 433-445 [PMID: 28267012 DOI: 10.1097/DCR.0000000000000760]

20 **Lascano CA**, Kaidar-Person O, Szomstein S, Rosenthal R, Wexner SD. Challenges of laparoscopic colectomy in the obese patient: a review. *Am J Surg* 2006; **192**: 357-365 [PMID: 16920431 DOI: 10.1016/j.amjsurg.2006.04.011]

21 **Nguyen NT**, Wolfe BM. The physiologic effects of pneumoperitoneum in the morbidly obese. *Ann Surg* 2005; **241**: 219-226 [PMID: 15650630 DOI: 10.1097/01.sla.0000151791.93571.70]

22 **Mamidanna R**, Burns EM, Bottle A, Aylin P, Stonell C, Hanna GB, Faiz O. Reduced risk of medical morbidity and mortality in patients selected for laparoscopic colorectal resection in England: a population-based study. *Arch Surg* 2012; **147**: 219-227 [PMID: 22106248 DOI: 10.1001/archsurg.2011.311]

23 **Zhuang CL**, Huang DD, Chen FF, Zhou CJ, Zheng BS, Chen BC, Shen X, Yu Z. Laparoscopic *versus* open colorectal surgery within enhanced recovery after surgery programs: a systematic review and meta-analysis of randomized controlled trials. *Surg Endosc* 2015; **29**: 2091-2100 [PMID: 25414064 DOI: 10.1007/s00464-014-3922-y]

24 **Fujii S**, Tsukamoto M, Fukushima Y, Shimada R, Okamoto K, Tsuchiya T, Nozawa K, Matsuda K, Hashiguchi Y. Systematic review of laparoscopic *vs* open surgery for colorectal cancer in elderly patients. *World J Gastrointest Oncol* 2016; **8**: 573-582 [PMID: 27559437 DOI: 10.4251/wjgo.v8.i7.573]

25 **Martin ST**, Stocchi L. Laparoscopic colorectal resection in the obese patient. *Clin Colon Rectal Surg* 2011; **24**: 263-273 [PMID: 23204942 DOI: 10.1055/s-0031-1295690]

26 **Tsujinaka S**, Konishi F, Kawamura YJ, Saito M, Tajima N, Tanaka O, Lefor AT. Visceral obesity predicts surgical outcomes after laparoscopic colectomy for sigmoid colon cancer. *Dis Colon Rectum* 2008; **51**: 1757-65; discussion 1765 [PMID: 18600376 DOI: 10.1007/s10350-008-9395-0]

World Journal of Gastrointestinal Oncology

Submit a Manuscript: https://www.f6publishing.com

World J Gastrointest Oncol 2022 July 15; 14(7): 1337-1347

DOI: 10.4251/wjgo.v14.i7.1337

ISSN 1948-5204 (online)

ORIGINAL ARTICLE

Retrospective Study

Predictors for malignant potential and deep submucosal invasion in colorectal laterally spreading tumors

Xiao-Wen Hao, Peng Li, Yong-Jun Wang, Ming Ji, Shu-Tian Zhang, Hai-Yun Shi

Specialty type: Oncology

Provenance and peer review: Unsolicited article; Externally peer reviewed.

Peer-review model: Single blind

Peer-review report's scientific quality classification

Grade A (Excellent): 0
Grade B (Very good): B, B
Grade C (Good): C
Grade D (Fair): 0
Grade E (Poor): 0

P-Reviewer: Chandrasegaram MD, Australia; Paik HJ, South Korea; Talaat IM, United Arab Emirates

Received: March 15, 2022
Peer-review started: March 15, 2022
First decision: May 10, 2022
Revised: May 24, 2022
Accepted: June 22, 2022
Article in press: June 22, 2022
Published online: July 15, 2022

Xiao-Wen Hao, Peng Li, Yong-Jun Wang, Ming Ji, Shu-Tian Zhang, Hai-Yun Shi, National Clinical Research Centre for Digestive Disease, Beijing Digestive Disease Centre, Beijing Key Laboratory for Precancerous Lesion of Digestive Disease, Beijing Friendship Hospital, Capital Medical University, Beijing 100050, China

Corresponding author: Hai-Yun Shi, MD, PhD, Associate Professor, National Clinical Research Centre for Digestive Disease, Beijing Digestive Disease Centre, Beijing Key Laboratory for Precancerous Lesion of Digestive Disease, Beijing Friendship Hospital, Capital Medical University, No. 95 Yong'an Road, Xicheng District, Beijing 100050, China.
shihaiyun1016@gmail.com

Abstract

BACKGROUND

Colorectal laterally spreading tumors (LSTs) with malignant potential require *en bloc* resection by endoscopic submucosal dissection (ESD), but lesions with deep submucosal invasion (SMI) are endoscopically unresectable.

AIM

To investigate the factors associated with high-grade dysplasia (HGD)/carcinoma and deep SMI in colorectal LSTs.

METHODS

The endoscopic and histological results of consecutive patients who underwent ESD for colorectal LSTs in our hospital from June 2013 to March 2019 were retrospectively analyzed. The characteristics of LST subtypes were compared. Risk factors for HGD/carcinoma and deep SMI (invasion depth ≥ 1000 μm) were determined using multivariate logistic regression.

RESULTS

A total of 323 patients with 341 colorectal LSTs were enrolled. Among the four subtypes, non-granular pseudodepressed (NG-PD) LSTs (85.5%) had the highest rate of HGD/carcinoma, followed by the granular nodular mixed (G-NM) (77.0%), granular homogenous (29.5%), and non-granular flat elevated (24.2%) subtypes. Deep SMI occurred commonly in NG-PD LSTs (12.9%). In the adjusted multivariate analysis, NG-PD [odds ratio (OR) = 16.8, $P < 0.001$) and G-NM (OR = 7.8, $P < 0.001$) subtypes, size ≥ 2 cm (OR = 2.2, $P = 0.005$), and positive non-lifting sign (OR = 3.3, $P = 0.024$) were independently associated with HGD/carcinoma. The NG-PD subtype (OR = 13.3, $P < 0.001$) and rectosigmoid location (OR = 8.7, P

= 0.007) were independent risk factors for deep SMI.

CONCLUSION
Because of their increased risk for malignancy, it is highly recommended that NG-PD and G-NM LSTs are removed *en bloc* through ESD. Given their substantial risk for deep SMI, surgery needs to be considered for NG-PD LSTs located in the rectosigmoid, especially those with positive non-lifting signs.

Key Words: Colorectal laterally spreading tumors; Subtype; Deep submucosal invasion; Endoscopic submucosal dissection

Core Tip: The incidence of laterally spreading tumors (LSTs) is continually increasing; however, the optimal strategy for resecting large colorectal LSTs is still under debate. Endoscopic submucosal dissection (ESD) and surgery each have their pros and cons. In this work, we demonstrated that it is highly recommend that non-granular pseudodepressed (NG-PD) and granular nodular mixed LSTs are removed through ESD, and given their substantial risk for deep submucosal invasion, surgery needs to be considered in NG-PD LSTs located in the rectosigmoid, especially those with positive non-lifting signs.

Citation: Hao XW, Li P, Wang YJ, Ji M, Zhang ST, Shi HY. Predictors for malignant potential and deep submucosal invasion in colorectal laterally spreading tumors. *World J Gastrointest Oncol* 2022; 14(7): 1337-1347
URL: https://www.wjgnet.com/1948-5204/full/v14/i7/1337.htm
DOI: https://dx.doi.org/10.4251/wjgo.v14.i7.1337

INTRODUCTION

Colorectal laterally spreading tumors (LSTs) are lesions 10 mm or greater in diameter characterized by lateral and circumferential extension with a low vertical axis along the colorectal wall[1]. LSTs are easily missed during colonoscopy and constitute an important contributor to post-colonoscopy colorectal cancer[2,3]. LSTs are morphologically categorized into the granular type (LST-G), which has a nodular surface, and non-granular type (LST-NG), which has a smooth surface[1,3]. The LST-G type can be divided into a granular nodular mixed subtype (G-NM) and homogeneous subtype (G-H), according to the existence of irregular and large nodules. The LST-NG type can be further subclassified into the non-granular pseudodepressed (NG-PD), presenting a gently sloping central depression, and the flat elevated subtype (NG-FE), characterized by a flat and smooth surface[1,3]. Although some studies have reported that the four subtypes of LSTs have varying clinicopathological features, previous analyses have not been adjusted for confounding factors, and the risk of deep submucosal invasion (SMI) and endoscopic resectability have not been evaluated[4-7].

Endoscopic resection is widely used to treat colorectal neoplasms with a negligible risk of lymph node metastasis. *En bloc* resection is indicated for early colorectal cancer[8]. In Eastern countries, early colorectal cancer includes carcinoma *in situ*, tumors with a SMI depth less than 1000 μm (superficial SMI or T1a), and tumors with a SMI depth greater than 1000 μm (deep SMI or T1b)[9]. Given their high risk of lymph node metastasis, lesions with deep SMI are endoscopically unresectable and require surgery [10]. Endoscopic methods for achieving *en bloc* resection includes endoscopic mucosal resection (EMR) (for lesions < 2 cm) and endoscopic submucosal dissection (ESD) (for larger lesions)[9,11]. ESD is also indicated when the likelihood of superficial SMI is high[8].

LSTs are good candidates for endoscopic resection owing to their low overall rate of SMI[3]. However, each morphologic subtype of LSTs is associated with a distinct risk of SMI. Tumor size is known to have various additional effects on SMI among the four subtypes[1,3]. Therefore, morphologic subtype is the initial consideration when selecting treatments for LSTs. Risk stratification of carcinogenesis and invasiveness according to morphologic subtype in combination with other factors remains to be fully elucidated. The aim of our study was to determine the predictors for carcinoma, invasion depth and endoscopically unresectable lesions for colorectal LSTs and to perform risk assessments for each morphologic subtype.

MATERIALS AND METHODS

The endoscopic and histological results of consecutive patients who underwent ESD for colorectal LSTs at Beijing Friendship Hospital between June 2013 and March 2019 were retrospectively reviewed. In our centre, ESD is the standard treatment for LSTs. Patients with familial adenomatous polyposis or inflammatory bowel disease were excluded. This study was approved by the Ethics Committee of Beijing Friendship Hospital, Capital Medical University.

Because of the retrospective nature of this study, decisions regarding study inclusion were made by two endoscopists after reviewing all colonoscopy findings. LSTs were defined as lesions ≥ 1 cm in diameter that extended laterally and circumferentially along the colorectal wall rather than perpendicular to it. All lesions were reviewed and classified by two endoscopists (Shi HY and Hao XW) using Kudo's classification. All lesions were subclassified as follows: (1) G-NM subtype, which had a granular surface with giant nodules; (2) G-H subtype, which had an even granular surface; (3) NG-PD subtype, characterized by a mixture of elevated and depressed flat regions in each lesion; or (4) NG-FE subtype, exhibited an elevated flat and smooth surface[1].

In pathological evaluations, high-grade dysplasia was regarded as carcinoma *in situ*, according to the Japanese classification[9]. Carcinomas included carcinoma *in situ* and tumors with SMI. Lesions with a SMI depth ≥ 1000 μm were defined as having deep SMI. If the pathologic diagnosis was adenocarcinoma, in addition to invasion depth, the degree of carcinoma differentiation and tumor budding, as well as the presence of lymphovascular invasion, were evaluated. Endoscopically resectable lesions were defined as those without any of the following features: Poorly differentiated, deep SMI invasion, lymphovascular invasion, and high-grade tumor budding. Demographic and clinicopathologic data, including sex, age, LST subtype (G-NM, G-H, NG-PD, NG-FE), location, size, and pathological features, were recorded.

Statistical analysis

Categorical variables were analysed using the χ^2 test or Fisher's exact test where appropriate. Continuous data were analysed using Student's *t* test if they were normally distributed or the Mann-Whitney *U* test if they followed a skewed distribution. Variables found to be significant in univariate analysis were entered into multivariate logistic regression to determine the independent factors for carcinoma, SMI, deep SMI and endoscopically unresectable lesions. Two-sided *P* values < 0.05 were considered significant. Statistical analyses were performed with IBM SPSS Statistics 20.0.

RESULTS

Characteristics of the patients and lesions

A total of 323 patients with 341 LSTs were included. The mean age was 64.7 years (range 26-88 years), and 56.0% were men. The median size of the lesions was 20 (range 10-100) mm. Most (52.5%) LSTs were located in the right colon, and 41.1% of the lesions were located in the rectosigmoid region. G-NM was the predominant subtype (44.6%). Up to 59.8% of the LSTs were carcinoma, among which 84.4% (173/204) were carcinoma *in situ*. The proportions of SMI, deep SMI and endoscopic unresectable lesions were 9.1%, 3.5% and 4.7%, respectively (Table 1).

Comparisons among LST subtypes

Table 2 shows that the four LST subtypes had distinct clinicopathological features. G-NM [median 25 mm, interquartile range (IQR) 18-40 mm] was the largest subtype (*vs* any of the other three subtypes, *P* < 0.001), and NG-FE (median 15 mm, IQR 13-19 mm) was the smallest subtype (*vs* NG-PD subtype, *P* = 0.009; *vs* G-H subtype, *P* = 0.002). A higher percentage of the G-H (68.9%), NG-PD (51.6%) and NG-FE (66.7%) subtypes were located in the right colon, whereas the majority (56.6%) of the G-NM LSTs were located in the rectosigmoid region. The carcinoma rates of the G-NM and NG-PD LSTs were 77.0% and 85.5%, respectively, and both were significantly higher than those of the G-H (*vs* 29.5%, *P* < 0.001) and NG-FE (*vs* 24.2%, *P* < 0.001) LSTs. Of the tumors that were carcinoma, carcinoma *in situ* accounted for 90.6% (106/117), 100% (18/18), 66.0% (35/53) and 87.5% (14/16) of G-NM, G-H, NG-PD and NG-FE lesions, respectively. Among the four subtypes, the NG-PD subtype had the highest risk for having SMI (*vs* any of the other three subtypes, *P* < 0.001), having deep SMI (12.9% *vs* 2.6% of the G-NM subtype, *P* = 0.004; 12.9% *vs* 0% of the G-H/NG-FE subtype, *P* = 0.002), and being endoscopically unresectable (14.5% *vs* 4.6% of the G-NM subtype, *P* = 0.016; 14.5% *vs* 0% of the G-H/NG-FE subtype, *P* = 0.001).

Predictors for carcinoma

As shown in Table 3, in univariate analysis, the G-NM subtype, NG-PD subtype, rectosigmoid location, size ≥ 2 cm, and positive non-lifting sign were associated with a higher risk for carcinoma. In the adjusted multivariate analysis, the G-NM subtype [odds ratio (OR) = 7.8, 95% confidence interval (CI): 3.8-16.1, *P* < 0.001)], NG-PD subtype (OR = 16.8, 95%CI: 6.5-43.5, *P* < 0.001), size ≥ 2 cm (OR = 2.2,

Table 1 Characteristics of the patients and lesions

	Total
Number of patients	323
Male sex, *n* (%)	181 (56.0)
Age, mean ± SD, yr	64.7 ± 10.5
Number of lesions	341
Size, median (IQR), cm	2.0 (1.5-3.0)
Location, *n* (%)	
Caecum and ascending colon	137 (40.2)
Transverse colon	42 (12.3)
Descending colon	22 (6.5)
Sigmoid	45 (13.2)
Rectum	95 (27.9)
LST subtype, *n* (%)	
G-NM	152 (44.6)
G-H	61 (17.9)
NG-PD	62 (18.2)
NG-FE	66 (19.4)
HGD/carcinoma, *n* (%)	204 (59.8)
Carcinoma *in situ*, *n* (%)	173 (50.7)
SMI, *n* (%)	31 (9.1)
Deep SMI, *n* (%)	12 (3.5)
Endoscopically unresectable, *n* (%)	16 (4.7)

LST: Laterally spreading tumor; G-NM: Granular nodular mixed; G-H: Granular homogenous; NG-FE: Non-granular flat elevated; NG-PD: Non-granular pseudodepressed; IQR: Interquartile range; SMI: Submucosal invasion.

95%CI: 1.3-3.9, P = 0.005), and positive non-lifting sign (OR = 3.3, 95%CI: 1.2-9.2, P = 0.024) remained independent predictors. We further performed subgroup analysis according to LST subtype. For the G-NM subtype, a larger size was associated with a higher risk of carcinoma (85.1% of lesions ≥ 3 cm *vs* 70.6% of those < 3 cm, P = 0.035). Almost all (96.0%) of the NG-PD lesions located in the rectosigmoid region were carcinoma.

Predictors for SMI and deep SMI

The NG-PD subtype (OR = 9.1, 95%CI: 3.9-21.0, P < 0.001), rectosigmoid location (OR = 3.2, 95%CI: 1.4-7.6, P = 0.007), and positive non-lifting sign (OR = 3.0, 95%CI: 1.2-8.0, P = 0.023) were independent predictive factors for SMI in the adjusted multivariate analysis (Table 4). The NG-PD subtype, rectosigmoid location and positive non-lifting sign were associated with an increased risk for deep SMI. In the adjusted multivariate analysis, the NG-PD subtype (OR = 13.3, 95%CI: 3.7-47.9, P < 0.001) and rectosigmoid location (OR = 8.7, 95%CI: 1.8-42.3, P = 0.007) were independent predictors for deep SMI (Table 4).

In the subgroup analysis by LST subtype, for the G-NM subtype, lesions located in the rectum were more likely to have SMI than those located in the colon (13.8% *vs* 2.3%, P = 0.009). None of the G-H lesions in our study invaded the submucosal layer. For the NG-PD subtype, 61.5% of LSTs with a positive non-lifting sign (*vs* 22.7% of those without a positive non-lifting sign, P = 0.015) had SMI. Deep SMI occurred in 44.4% of NG-PD lesions with a positive non-lifting sign (*vs* 9.3% of lesions without a non-lifting sign, P = 0.023) and 30.4% of those located in the rectosigmoid region (*vs* 3.0% of lesions located proximal to the sigmoid colon, P = 0.006). Kudo's pit pattern type V (60.0% *vs* 0% of those with type I-IV pit patterns, P = 0.027) and JNET type 2B/3 (75.0% *vs* 0% of those with JNET type 1/2A, P = 0.033) were associated with a significantly higher risk for deep SMI. For NG-FE lesions, a rectosigmoid location was associated with a higher risk of SMI (15.4% *vs* 0%, P = 0.036). None of the NG-FE LSTs in our study invaded the deep submucosal layer.

Table 2 Characteristics of laterally spreading tumor subtypes

	G-NM (*n* = 152)	G-H (*n* = 61)	NG-PD (*n* = 62)	NG-FE (*n* = 66)
Size, median (IQR), cm	2.5 (1.8-4.0)	1.8 (1.5-2.4)	1.8 (1.5-2.5)	1.5 (1.3-1.9)
Location, *n* (%)				
Right-sided colon	61 (40.1)	42 (68.9)	32 (51.6)	44 (66.7)
Caecum	25 (16.4)	16 (26.2)	4 (6.4)	4 (6.1)
Ascending colon	31 (20.4)	19 (31.1)	12 (19.4)	26 (39.4)
Transverse colon	5 (3.3)	7 (11.5)	16 (25.8)	14 (21.2)
Descending colon	5 (3.3)	3 (4.9)	5 (8.1)	9 (13.6)
Rectosigmoid	86 (56.6)	16 (26.2)	25 (40.3)	13 (19.7)
Sigmoid	21 (13.8)	4 (6.6)	11 (17.7)	9 (13.6)
Rectum	65 (42.8)	12 (19.7)	14 (22.6)	4 (6.1)
HGD/carcinoma rate, *n* (%)	117 (77.0)	18 (29.5)	53 (85.5)	16 (24.2)
Carcinoma in situ, *n* (%)	106 (69.7)	18 (29.5)	35 (56.4)	14 (21.2)
SMI rate, *n* (%)	11 (7.2)	0 (0)	18 (29.0)	2 (3.0)
Deep SMI rate, *n* (%)	4 (2.6)	0 (0)	8 (12.9)	0 (0)
Endoscopically unresectable, *n* (%)	7 (4.6)	0 (0)	9 (14.5)	0 (0)

LST: Laterally spreading tumor; G-NM: Granular nodular mixed; G-H: Granular homogenous; NG-FE: Non-granular flat elevated; NG-PD: Non-granular pseudodepressed; IQR: Interquartile range; HGD: High-grade dysplasia; SMI: Submucosal invasion.

Predictors for endoscopically unresectable lesions

The NG-PD subtype (OR = 7.1, 95%CI: 2.3-22.0, P = 0.001), rectosigmoid location (OR = 10.5, 95%CI: 2.2-49.0, P = 0.003), and positive non-lifting sign (OR = 3.5, 95%CI: 1.0-12.0, P = 0.045) were independent predictors for endoscopically unresectable lesions (Table 5). For the NG-PD subtype, 33.3% of the lesions in the rectosigmoid region (*vs* 3.0% of those located proximal to the sigmoid colon, P = 0.003) and 50.0% of the lesions with positive non-lifting signs (*vs* 9.3% of those without non-lifting signs, P = 0.008) were endoscopically unresectable. The risk for being endoscopically unresectable was low in G-NM LSTs. All of the G-H or NG-FE LSTs in our study were endoscopically resectable.

DISCUSSION

Our study revealed that the G-NM subtype, NG-PD subtype, size ≥ 2 cm and positive non-lifting sign were independent predictors for carcinoma. The NG-PD subtype, rectosigmoid location and positive non-lifting sign were independently associated with SMI and endoscopically unresectable lesions. We comprehensively compared the clinicopathological characteristics among the four subtypes of LSTs. G-NM lesions had the largest tumor size among the four subtypes and most commonly occurred in the rectosigmoid region. Although a substantial proportion of carcinomas (77%) were found among G-NM LSTs, over 90% of the carcinomas were carcinomas *in situ*. Approximately 30% of the G-H LSTs were carcinomas, and all were carcinoma *in situ*. The NG-PD subtype was associated with the highest risks for being malignant (86%), having SMI (29%), having deep invasion (12.9%) and being endoscopically unresectable (16%) among the four subtypes. NG-FE LSTs had the smallest tumor size and a malignancy rate of approximately 25%. None of the malignant lesions considered the NG-FE subtype invaded the deep submucosal layer.

Large non-pedunculated colorectal lesions are traditionally managed by surgical resection[12]. Over the past decade, with the evolution of endoscopic techniques, endoscopic resection has become the first-line therapy for colorectal tumors without deep invasion[13,14]. Compared to surgery, endoscopic resection is associated with significantly lower rates of complications and a much quicker recovery[15-17]. Long-term outcomes including recurrence and survival rates are comparable between endoscopic and surgical treatment[8,18]. Furthermore, endoscopic resection has been shown to be more cost-effective than surgery for the management of superficial colorectal neoplasms[19,20]. *En bloc* resection is indicated for carcinomatous lesions because of its superiority over piecemeal resection in reducing recurrence rates[8,9,21-23]. If superficial SMI is suspected, ESD is recommended to provide complete resection for accurate histological staging and reduced recurrence[8]. LSTs are good candidates for

Table 3 Univariate and multivariate analyses of predictors for high-grade dysplasia /carcinoma

	Univariate		Multivariate	
	OR (95%CI)	*P* value	OR (95%CI)	*P* value
LST subtype				
NG-FE	1	-	1	-
NG-PD	18.4 (7.4-45.4)	< 0.001	16.8 (6.5-43.5)	< 0.001
G-NM	10.4 (5.3-20.6)	< 0.001	7.8 (3.8-16.1)	< 0.001
G-H	1.3 (0.6-2.9)	0.504	1.1 (0.5-2.4)	0.871
Location				
Non-rectosigmoid	1	-		
Rectosigmoid	2.3 (1.5-3.7)	< 0.001		
Size, cm				
< 2	1	-	1	-
≥ 2	2.6 (1.6-4.0)	< 0.001	2.2 (1.3-3.9)	0.005
Non-lifting sign				
Negative	1	-	1	-
Positive	4.0 (1.6-9.8)	0.003	3.3 (1.2-9.2)	0.024

LST: Laterally spreading tumor; G-NM: Granular nodular mixed; G-H: Granular homogenous; NG-FE: Non-granular flat elevated; NG-PD: Non-granular pseudodepressed; OR: Odds ratio; CI: Confidence interval.

endoscopic resection due to their low risk for deep invasion[24,25]. In our study, approximately 60% of the LSTs were carcinomas, and the majority (approximately 85%) were carcinoma *in situ*.

An accurate preoperative diagnosis to identify carcinoma and determine the depth of invasion is essential for selecting an appropriate therapeutic strategy. We investigated independent factors for carcinoma, SMI, deep SMI and endoscopically unresectable lesions. The G-NM subtype, NG-PD subtype, large lesion size and positive non-lifting sign were predictors for carcinoma in our study, which was in line with previous studies[5-8,26]. For SMI, we found that the NG-PD subtype, positive non-lifting sign and rectosigmoid location were predictive factors. Although the NG-PD subtype and positive non-lifting sign are well acknowledged markers for SMI[5-8,21,26], the rectosigmoid location is a newly identified predictor for SMI. A large prospective multicentre study from Australia reported that rectosigmoid location was an independent factor for SMI, and the significance of this parameter remained among lesions without obvious high-risk features for SMI (type V Kudo pit pattern and Paris 0-IIc components)[27]. Rectal lesions accounted for a greater proportion of lesions with SMI in a few previous studies[4,28]. This may suggest different pathways of carcinogenesis between distal and proximal LSTs. Endoscopic resection of lesions located in the distal colorectum, particularly in the rectum, is technically easier and is associated with a lower risk of complications than that of lesions located in the proximal colon[29]. Endoscopically assessing the depth of SMI is extremely important in deciding whether to perform ESD or refer the patient to surgery. However, research investigating predictors for deep SMI is limited. Yamada *et al*[30] reported that a depressed component was strongly associated with deep SMI both in LST-G and LST-NG. In our study, the NG-PD subtype and rectosigmoid location were also independent factors for deep SMI. We also confirmed that NG-PD, rectosigmoid location and positive non-lifting sign were independent factors for endoscopic unresectability. In addition to deep SMI, factors including lymphovascular invasion also determine endoscopic resectability. There were 4 cases of lymphovascular invasion on pathological examination without deep SMI in our study. The other risk factors for being endoscopically unresectable are very large lesion size (size > 40 mm), special location (lesions involving the ileocaecal valve, appendix, diverticulum), prior failed attempt at resection or recurrence at site of previous resection, and non-lifting sign after submucosal injection[31].

The risk of carcinoma, invasion depth and endoscopic unrespectability in each LST subtypes was further assessed. G-H LSTs are good candidates for EMR due to their relatively small tumor size and very low risk for SMI. For G-NM lesions, the overall rate of carcinoma was high, and this rate increased with as lesion size increased. A rectal location was associated with a high risk for SMI. Therefore, *en bloc* resection is desirable for the G-NM subtype, whereas ESD is preferred for large lesions and those located in the rectum. NG-FE LSTs had a small tumor size and low overall risk for SMI. However, the risk for SMI increased significantly if the lesions were located in the rectosigmoid region, suggesting

Table 4 Univariate and multivariate analyses of predictors for submucosal invasion and deep submucosal invasion

	Univariate		Multivariate	
	OR (95%CI)	*P* value	OR (95%CI)	*P* value
Risk factors for SMI				
LST subtype				
Non-NG-PD	1	-	1	-
NG-PD	8.6 (3.9-18.7)	< 0.001	9.1 (3.9-21.0)	< 0.001
Location				
Non-rectosigmoid	1	-	1	-
Rectosigmoid	2.9 (1.3-6.3)	0.007	3.2 (1.4-7.6)	0.007
Non-lifting sign				
Negative	1	-	1	-
Positive	4.8 (2.0-11.3)	< 0.001	3.0 (1.2-8.0)	0.023
Risk factors for deep SMI				
LST subtype				
Non-NG-PD	1		1	
NG-PD	11.3 (3.3-39.1)	< 0.001	13.3 (3.7-47.9)	< 0.001
Location				
Non-rectosigmoid	1		1	
Rectosigmoid	7.8 (1.7-36.2)	0.009	8.7 (1.8-42.3)	0.007
Non-lifting sign				
Negative	1			
Positive	5.2 (1.5-18.6)	0.010		

LST: Laterally spreading tumor; NG-PD: Non-granular pseudodepressed; OR: Odds ratio; CI: Confidence interval; SMI: Submucosal invasion.

ESD in such cases. A consensus has been reached that the NG-PD subtype is an indicator for ESD[8,11,32]. The high rate of SMI in our study supported this consensus. However, the NG-PD subtype is also associated with a high risk of being endoscopically unresectable. The decision between performing ESD and referring the patient to surgical treatment should be cautiously considered in this scenario. Our results showed that a rectosigmoid location, positive non-lifting sign and type V Kudo pit pattern were associated with a significantly higher risk for having deep SMI and being endoscopically unresectable. Before treating lesions with these risk features, the endoscopists' experience and patients' preferences should be cautiously considered. Despite improvements in endoscopic diagnosis, the sensitivity of endoscopic techniques for identifying SMI remains unsatisfactory[27]. In recent years, *en bloc* ESD prior to surgery as a total excisional biopsy for early colorectal carcinoma has been introduced in clinical practice[33]. A recent multicentre study on the influence of preoperative ESD on the prognosis of patients with early colorectal carcinomas (T1) found that *en bloc* ESD did not adversely affect the long-term clinical outcomes[34]. As a more cost-effective method than surgery, ESD is a reasonable first option for early colorectal carcinomas without obvious features of deep invasion.

To the best of our knowledge, the present work is one of the largest studies comprehensively comparing the clinicopathological features, including risk of carcinoma, depth of invasion and endoscopic resectability, among the four subtypes of LSTs. With a relatively large number of cases involved, we were able to perform multivariate analyses and determine the independent predictors for carcinoma, SMI, deep SMI and endoscopic unresectability. Subgroup analyses were also conducted to identify distinct risks for the four subtypes of LSTs. We also proposed a treatment strategy for each subtype of LST, according to the risks of carcinoma and deep SMI based on our findings. Additionally, ESD is the standard therapy for LSTs in our centre and enables accurate pathological evaluation with detailed information on the depth of invasion and other risk factors for lymph node metastasis.

Several limitations of our study should be acknowledged. First, as this was a single-centre retrospective study based on clinical records, regional or institutional bias may exist. Second, because ESD was the commonly used treatment for LSTs in our centre and to allow for accurate histopathological assessment, only lesions that were resected *en bloc* by ESD were included in this study; thus,

Table 5 Univariate and multivariate analyses of predictors for endoscopically unresectable laterally spreading tumors

	Univariate		Multivariate	
	OR (95%CI)	*P* value	OR (95%CI)	*P* value
LST subtype				
Non-NG-PD	1	-	1	-
NG-PD	7.2 (2.6-20.3)	< 0.001	7.1 (2.3-22.0)	0.001
Location				
Non-rectosigmoid	1	-	1	-
Rectosigmoid	11.1 (2.5-49.7)	0.002	10.5 (2.2-49.0)	0.003
Non-lifting sign				
Negative	1	-	1	-
Positive	6.3 (2.1-18.6)	0.001	3.5 (1.0-12.0)	0.045

LST: Laterally spreading tumor; NG-PD: Non-granular pseudodepressed; OR: Odds ratio; CI: Confidence interval.

there were no data on LSTs resected by EMR and surgery. However, the number of these lesions was relatively small. Third, it has previously been reported that magnifying observation (pit pattern diagnosis) and image-enhancement technology (*e.g.*, narrow band imaging) are reliable and effective methods for predicting the depth of tumor invasion; however, due to the inherent limitations of retrospective studies, some lesion records on JNET and Kudo pit pattern type were missing.

CONCLUSION

In conclusion, the clinicopathological characteristics of LSTs varied according to subtypes in terms of size, distribution, malignant potential, depth of invasion and endoscopic resectability. Because of their increased risk for malignancy, it is highly recommended that NG-PD and G-NM LSTs are removed *en bloc* through ESD. Given their substantial risk for deep SMI, surgery needs to be considered in NG-PD subtype LSTs located in the rectosigmoid, especially those with a positive non-lifting sign.

ARTICLE HIGHLIGHTS

Research background

The incidence of laterally spreading tumors (LSTs) is continually increasing; however, the optimal strategy for resecting large colorectal LSTs is still under debate. Endoscopic submucosal dissection (ESD) is associated with a high *en bloc* resection rate, low risk of recurrence and perfect pathological analysis. However, the possibility of a positive postoperative pathological resection margin exists, which would require additional surgical procedures. Surgery has a high complication rate, high mortality and prolonged hospital stays.

Research motivation

Accurate preoperative assessment based on various risk factors to identify carcinoma and invasion depth is essential for selecting an appropriate therapeutic strategy.

Research objectives

This study aimed to identify the predictors of carcinoma, invasion depth and endoscopically unresectable lesions for colorectal LSTs and to facilitate appropriate preoperative selection.

Research methods

This retrospective study analysed the endoscopic and histological results of consecutive patients who underwent ESD for colorectal LSTs in our hospital during a six-year period. The characteristics of the LSTs were compared by subtypes. Risk factors for high-grade dysplasia (HGD)/carcinoma and deep submucosal invasion (SMI) (invasion depth ≥ 1000 μm) were determined for each morphologic subtype.

Research results

Among the four subtypes, non-granular pseudodepressed (NG-PD) LSTs had the highest rate of HGD/carcinoma and deep SMI (invasion depth ≥ 1000 μm). NG-PD subtype and rectosigmoid location were the independent risk factors for deep SMI in adjusted multivariate analysis.

Research conclusions

We demonstrated that it is highly recommend that NG-PD and granular nodular mixed (G-NM) LSTs are removed through ESD; given their substantial risk for deep SMI, surgery needs to be considered in NG-PD LSTs located in the rectosigmoid, especially those with positive non-lifting signs.

Research perspectives

A risk score chart, which can determine the risk for carcinoma, invasion depth and endoscopically unresectable lesions for colorectal LSTs should be developed. It can help endoscopists in selective use of different types of endo-resection or to proceed to surgery instead of endoscopy.

FOOTNOTES

Author contributions: Shi HY designed the research study and performed the data collection; Hao XW analyzed the data and wrote the first draft of the manuscript; Li P, Wang YJ, Ji M and Zhang ST performed the endoscopic therapies; Shi HY reviewed and edited the manuscript; and all authors read and approved the final manuscript.

Supported by Beijing Nova Program, No. Z201100006820147; and Beijing Municipal Administration of Hospitals' Youth Program, No. QML20180102.

Institutional review board statement: This study was approved by the Ethics Committee of Beijing Friendship Hospital (2020-P2-047-01) and was performed in accordance with the ethical guidelines of the 1975 Declaration of Helsinki.

Informed consent statement: All study participants, or their legal guardian, provided informed written consent prior to study enrollment.

Conflict-of-interest statement: All the authors report no relevant conflicts of interest for this article.

Data sharing statement: No additional data are available.

Country/Territory of origin: China

ORCID number: Xiao-Wen Hao 0000-0003-1955-9325; Peng Li 0000-0003-2927-2758; Yong-Jun Wang 0000-0002-9584-7196; Ming Ji 0000-0002-2666-7423; Shu-Tian Zhang 0000-0003-2356-4397; Hai-Yun Shi 0000-0002-2084-8370.

S-Editor: Wang JJ
L-Editor: A
P-Editor: Wang JJ

REFERENCES

1 **Kudo Se**, Lambert R, Allen JI, Fujii H, Fujii T, Kashida H, Matsuda T, Mori M, Saito H, Shimoda T, Tanaka S, Watanabe H, Sung JJ, Feld AD, Inadomi JM, O'Brien MJ, Lieberman DA, Ransohoff DF, Soetikno RM, Triadafilopoulos G, Zauber A, Teixeira CR, Rey JF, Jaramillo E, Rubio CA, Van Gossum A, Jung M, Vieth M, Jass JR, Hurlstone PD. Nonpolypoid neoplastic lesions of the colorectal mucosa. *Gastrointest Endosc* 2008; **68**: S3-47 [PMID: 18805238 DOI: 10.1016/j.gie.2008.07.052]

2 **Sanduleanu S**, Masclee AM, Meijer GA. Interval cancers after colonoscopy-insights and recommendations. *Nat Rev Gastroenterol Hepatol* 2012; **9**: 550-554 [PMID: 22907162 DOI: 10.1038/nrgastro.2012.136]

3 **Kudo SE**, Takemura O, Ohtsuka K. Flat and depressed types of early colorectal cancers: from East to West. *Gastrointest Endosc Clin N Am* 2008; **18**: 581-593, xi [PMID: 18674705 DOI: 10.1016/j.giec.2008.05.013]

4 **Kim BC**, Chang HJ, Han KS, Sohn DK, Hong CW, Park JW, Park SC, Choi HS, Oh JH. Clinicopathological differences of laterally spreading tumors of the colorectum according to gross appearance. *Endoscopy* 2011; **43**: 100-107 [PMID:

21165823 DOI: 10.1055/s-0030-1256027]
5 **Zhao X**, Zhan Q, Xiang L, Wang Y, Wang X, Li A, Liu S. Clinicopathological characteristics of laterally spreading colorectal tumor. *PLoS One* 2014; **9**: e94552 [PMID: 24751926 DOI: 10.1371/journal.pone.0094552]
6 **Cong ZJ**, Hu LH, Ji JT, Xing JJ, Shan YQ, Li ZS, Yu ED. A long-term follow-up study on the prognosis of endoscopic submucosal dissection for colorectal laterally spreading tumors. *Gastrointest Endosc* 2016; **83**: 800-807 [PMID: 26341853 DOI: 10.1016/j.gie.2015.08.043]
7 **Myung DS**, Kweon SS, Lee J, Shin IS, Kim SW, Seo GS, Kim HS, Joo YE. Clinicopathological features of laterally spreading colorectal tumors and their association with advanced histology and invasiveness: An experience from Honam province of South Korea: A Honam Association for the Study of Intestinal Diseases (HASID). *PLoS One* 2017; **12**: e0184205 [PMID: 28977010 DOI: 10.1371/journal.pone.0184205]
8 **Tanaka S**, Kashida H, Saito Y, Yahagi N, Yamano H, Saito S, Hisabe T, Yao T, Watanabe M, Yoshida M, Saitoh Y, Tsuruta O, Sugihara KI, Igarashi M, Toyonaga T, Ajioka Y, Kusunoki M, Koike K, Fujimoto K, Tajiri H. Japan Gastroenterological Endoscopy Society guidelines for colorectal endoscopic submucosal dissection/endoscopic mucosal resection. *Dig Endosc* 2020; **32**: 219-239 [PMID: 31566804 DOI: 10.1111/den.13545]
9 **Nishimura M**, Saito Y, Nakanishi Y, Shia J, Lauwers GY, Wallace MB. Pathology definitions and resection strategies for early colorectal neoplasia: Eastern *versus* Western approaches in the post-Vienna era. *Gastrointest Endosc* 2020; **91**: 983-988 [PMID: 31874160 DOI: 10.1016/j.gie.2019.12.021]
10 **Bosch SL**, Teerenstra S, de Wilt JH, Cunningham C, Nagtegaal ID. Predicting lymph node metastasis in pT1 colorectal cancer: a systematic review of risk factors providing rationale for therapy decisions. *Endoscopy* 2013; **45**: 827-834 [PMID: 23884793 DOI: 10.1055/s-0033-1344238]
11 **Draganov PV**, Wang AY, Othman MO, Fukami N. AGA Institute Clinical Practice Update: Endoscopic Submucosal Dissection in the United States. *Clin Gastroenterol Hepatol* 2019; **17**: 16-25.e1 [PMID: 30077787 DOI: 10.1016/j.cgh.2018.07.041]
12 **Bronzwaer MES**, Koens L, Bemelman WA, Dekker E, Fockens P; COPOS study group. Volume of surgery for benign colorectal polyps in the last 11 years. *Gastrointest Endosc* 2018; **87**: 552-561.e1 [PMID: 29108978 DOI: 10.1016/j.gie.2017.10.032]
13 **Hassan C**, Repici A, Sharma P, Correale L, Zullo A, Bretthauer M, Senore C, Spada C, Bellisario C, Bhandari P, Rex DK. Efficacy and safety of endoscopic resection of large colorectal polyps: a systematic review and meta-analysis. *Gut* 2016; **65**: 806-820 [PMID: 25681402 DOI: 10.1136/gutjnl-2014-308481]
14 **Fukami N**. Surgery Versus Endoscopic Mucosal Resection Versus Endoscopic Submucosal Dissection for Large Polyps: Making Sense of When to Use Which Approach. *Gastrointest Endosc Clin N Am* 2019; **29**: 675-685 [PMID: 31445690 DOI: 10.1016/j.giec.2019.06.007]
15 **Kiriyama S**, Saito Y, Yamamoto S, Soetikno R, Matsuda T, Nakajima T, Kuwano H. Comparison of endoscopic submucosal dissection with laparoscopic-assisted colorectal surgery for early-stage colorectal cancer: a retrospective analysis. *Endoscopy* 2012; **44**: 1024-1030 [PMID: 23012216 DOI: 10.1055/s-0032-1310259]
16 **Ahlenstiel G**, Hourigan LF, Brown G, Zanati S, Williams SJ, Singh R, Moss A, Sonson R, Bourke MJ; Australian Colonic Endoscopic Mucosal Resection (ACE) Study Group. Actual endoscopic *versus* predicted surgical mortality for treatment of advanced mucosal neoplasia of the colon. *Gastrointest Endosc* 2014; **80**: 668-676 [PMID: 24916925 DOI: 10.1016/j.gie.2014.04.015]
17 **Dang H**, de Vos Tot Nederveen Cappel WH, van der Zwaan SMS, van den Akker-van Marle ME, van Westreenen HL, Backes Y, Moons LMG, Holman FA, Peeters KCMJ, van der Kraan J, Langers AMJ, Lijfering WM, Hardwick JCH, Boonstra JJ. Quality of life and fear of cancer recurrence in T1 colorectal cancer patients treated with endoscopic or surgical tumor resection. *Gastrointest Endosc* 2019; **89**: 533-544 [PMID: 30273589 DOI: 10.1016/j.gie.2018.09.026]
18 **Heo J**, Jeon SW, Jung MK, Kim SK, Kim J, Kim S. Endoscopic resection as the first-line treatment for early colorectal cancer: comparison with surgery. *Surg Endosc* 2014; **28**: 3435-3442 [PMID: 24962854 DOI: 10.1007/s00464-014-3618-3]
19 **Jayanna M**, Burgess NG, Singh R, Hourigan LF, Brown GJ, Zanati SA, Moss A, Lim J, Sonson R, Williams SJ, Bourke MJ. Cost Analysis of Endoscopic Mucosal Resection *vs* Surgery for Large Laterally Spreading Colorectal Lesions. *Clin Gastroenterol Hepatol* 2016; **14**: 271-8.e1 [PMID: 26364679 DOI: 10.1016/j.cgh.2015.08.037]
20 **Law R**, Das A, Gregory D, Komanduri S, Muthusamy R, Rastogi A, Vargo J, Wallace MB, Raju GS, Mounzer R, Klapman J, Shah J, Watson R, Wilson R, Edmundowicz SA, Wani S. Endoscopic resection is cost-effective compared with laparoscopic resection in the management of complex colon polyps: an economic analysis. *Gastrointest Endosc* 2016; **83**: 1248-1257 [PMID: 26608129 DOI: 10.1016/j.gie.2015.11.014]
21 **Chen T**, Qin WZ, Yao LQ, Zhong YS, Zhang YQ, Chen WF, Hu JW, Ooi M, Chen LL, Hou YY, Xu MD, Zhou PH. Long-term outcomes of endoscopic submucosal dissection for high-grade dysplasia and early-stage carcinoma in the colorectum. *Cancer Commun (Lond)* 2018; **38**: 3 [PMID: 29764504 DOI: 10.1186/s40880-018-0273-4]
22 **Belderbos TD**, Leenders M, Moons LM, Siersema PD. Local recurrence after endoscopic mucosal resection of nonpedunculated colorectal lesions: systematic review and meta-analysis. *Endoscopy* 2014; **46**: 388-402 [PMID: 24671869 DOI: 10.1055/s-0034-1364970]
23 **Saunders BP**, Tsiamoulos ZP. Endoscopic mucosal resection and endoscopic submucosal dissection of large colonic polyps. *Nat Rev Gastroenterol Hepatol* 2016; **13**: 486-496 [PMID: 27353401 DOI: 10.1038/nrgastro.2016.96]
24 **Bogie RMM**, Veldman MHJ, Snijders LARS, Winkens B, Kaltenbach T, Masclee AAM, Matsuda T, Rondagh EJA, Soetikno R, Tanaka S, Chiu HM, Sanduleanu-Dascalescu S. Endoscopic subtypes of colorectal laterally spreading tumors (LSTs) and the risk of submucosal invasion: a meta-analysis. *Endoscopy* 2018; **50**: 263-282 [PMID: 29179230 DOI: 10.1055/s-0043-121144]
25 **Bae JH**, Yang DH, Lee JY, Soh JS, Lee S, Lee HS, Lee HJ, Park SH, Kim KJ, Ye BD, Myung SJ, Yang SK, Kim JH, Byeon JS. Clinical outcomes of endoscopic submucosal dissection for large colorectal neoplasms: a comparison of protruding and laterally spreading tumors. *Surg Endosc* 2016; **30**: 1619-1628 [PMID: 26169642 DOI: 10.1007/s00464-015-4392-6]
26 **Kim KO**, Jang BI, Jang WJ, Lee SH. Laterally spreading tumors of the colorectum: clinicopathologic features and

malignant potential by macroscopic morphology. *Int J Colorectal Dis* 2013; **28**: 1661-1666 [PMID: 23934010 DOI: 10.1007/s00384-013-1741-6]

27 **Burgess NG**, Hourigan LF, Zanati SA, Brown GJ, Singh R, Williams SJ, Raftopoulos SC, Ormonde D, Moss A, Byth K, Mahajan H, McLeod D, Bourke MJ. Risk Stratification for Covert Invasive Cancer Among Patients Referred for Colonic Endoscopic Mucosal Resection: A Large Multicenter Cohort. *Gastroenterology* 2017; **153**: 732-742.e1 [PMID: 28583826 DOI: 10.1053/j.gastro.2017.05.047]

28 **Miyamoto H**, Ikematsu H, Fujii S, Osera S, Odagaki T, Oono Y, Yano T, Ochiai A, Sasaki Y, Kaneko K. Clinicopathological differences of laterally spreading tumors arising in the colon and rectum. *Int J Colorectal Dis* 2014; **29**: 1069-1075 [PMID: 24986136 DOI: 10.1007/s00384-014-1931-x]

29 **Ma MX**, Bourke MJ. Complications of endoscopic polypectomy, endoscopic mucosal resection and endoscopic submucosal dissection in the colon. *Best Pract Res Clin Gastroenterol* 2016; **30**: 749-767 [PMID: 27931634 DOI: 10.1016/j.bpg.2016.09.009]

30 **Yamada M**, Saito Y, Sakamoto T, Nakajima T, Kushima R, Parra-Blanco A, Matsuda T. Endoscopic predictors of deep submucosal invasion in colorectal laterally spreading tumors. *Endoscopy* 2016; **48**: 456-464 [PMID: 26919264 DOI: 10.1055/s-0042-100453]

31 **Rutter MD**, Chattree A, Barbour JA, Thomas-Gibson S, Bhandari P, Saunders BP, Veitch AM, Anderson J, Rembacken BJ, Loughrey MB, Pullan R, Garrett WV, Lewis G, Dolwani S. British Society of Gastroenterology/Association of Coloproctologists of Great Britain and Ireland guidelines for the management of large non-pedunculated colorectal polyps. *Gut* 2015; **64**: 1847-1873 [PMID: 26104751 DOI: 10.1136/gutjnl-2015-309576]

32 **Pimentel-Nunes P**, Dinis-Ribeiro M, Ponchon T, Repici A, Vieth M, De Ceglie A, Amato A, Berr F, Bhandari P, Bialek A, Conio M, Haringsma J, Langner C, Meisner S, Messmann H, Morino M, Neuhaus H, Piessevaux H, Rugge M, Saunders BP, Robaszkiewicz M, Seewald S, Kashin S, Dumonceau JM, Hassan C, Deprez PH. Endoscopic submucosal dissection: European Society of Gastrointestinal Endoscopy (ESGE) Guideline. *Endoscopy* 2015; **47**: 829-854 [PMID: 26317585 DOI: 10.1055/s-0034-1392882]

33 **Asayama N**, Oka S, Tanaka S, Hayashi N, Arihiro K, Chayama K. Endoscopic submucosal dissection as total excisional biopsy for clinical T1 colorectal carcinoma. *Digestion* 2015; **91**: 64-69 [PMID: 25632920 DOI: 10.1159/000368866]

34 **Yamashita K**, Oka S, Tanaka S, Nagata S, Hiraga Y, Kuwai T, Furudoi A, Tamura T, Kunihiro M, Okanobu H, Nakadoi K, Kanao H, Higashiyama M, Kuraoka K, Shimamoto F, Chayama K. Preceding endoscopic submucosal dissection for T1 colorectal carcinoma does not affect the prognosis of patients who underwent additional surgery: a large multicenter propensity score-matched analysis. *J Gastroenterol* 2019; **54**: 897-906 [PMID: 31104172 DOI: 10.1007/s00535-019-01590-w]

World Journal of Gastrointestinal Oncology

Submit a Manuscript: https://www.f6publishing.com

World J Gastrointest Oncol 2022 July 15; 14(7): 1348-1355

DOI: 10.4251/wjgo.v14.i7.1348

ISSN 1948-5204 (online)

CASE REPORT

Pediatric case of colonic perivascular epithelioid cell tumor complicated with intussusception and anal incarceration: A case report

Luan Kou, Wen-Wen Zheng, Li Jia, Xiao-Li Wang, Ji-Hai Zhou, Jiao-Rong Hao, Zhu Liu, Feng-Yu Gao

Specialty type: Gastroenterology and hepatology

Provenance and peer review: Unsolicited article; Externally peer reviewed.

Peer-review model: Single blind

Peer-review report's scientific quality classification

Grade A (Excellent): 0
Grade B (Very good): B
Grade C (Good): 0
Grade D (Fair): D
Grade E (Poor): 0

P-Reviewer: Akbulut S, Turkey; Kim YW, South Korea

Received: December 15, 2021
Peer-review started: December 15, 2021
First decision: April 17, 2022
Revised: April 28, 2022
Accepted: June 27, 2022
Article in press: June 27, 2022
Published online: July 15, 2022

Luan Kou, Wen-Wen Zheng, Li Jia, Xiao-Li Wang, Ji-Hai Zhou, Jiao-Rong Hao, Zhu Liu, Feng-Yu Gao, Department of Gastroenterology, Shandong Provincial Maternal and Child Health Care Hospital, Jinan 250014, Shandong Province, China

Corresponding author: Feng-Yu Gao, MD, Doctor, Department of Gastroenterology, Shandong Provincial Maternal and Child Health Care Hospital, No. 238 Jingshi East Road, Jinan 250014, Shandong Province, China. gaofengyu2000@163.com

Abstract

BACKGROUND

Perivascular epithelioid cell tumor (PEComa) represents a group of rare mesenchymal tumors. PEComa can occur in many organs but is rare in the colorectum, especially in children. Furthermore, PEComa is a rare cause of intussusception, the telescoping of a segment of the gastrointestinal tract into an adjacent one. We describe a rare case of pediatric PEComa complicated with intussusception and anal incarceration, and conduct a review of the current literature.

CASE SUMMARY

A 12-year-old girl presented with abdominal pain and abdominal ultrasound suggested intussusception. Endoscopic direct-vision intussusception treatment and colonoscopy was performed. A spherical tumor was discovered in the transverse colon and removed by surgery. Postoperative pathologic analyses revealed that the tumor volume was 5.0 cm × 4.5 cm × 3.0 cm and the tumor tissue was located in the submucosa of the colon, arranged in an alveolar pattern. The cell morphology was regular, no neoplastic necrosis was observed, and nuclear fission was rare. The immunohistochemical staining results were as follows: Human melanoma black 45 (HMB 45) (+), cluster of differentiation 31 (CD31) (+), cytokeratin (-), melanoma-associated antigen recognized by T cells (-), smooth muscle actin (-), molleya (-), desmin (-), S-100 (-), CD117 (-), and Ki67 (positive rate in hot spot < 5%). Combined with the results of pathology and immunohisto-chemistry, we diagnosed the tumor as PEComa. Postoperative recovery was good at the 4 mo follow-up.

CONCLUSION

The diagnosis of PEComa mainly depends on pathology and immunohisto-

chemistry. Radical resection is the preferred treatment method.

Key Words: Perivascular epithelioid cell tumor; Colonic; Intussusception; Anal incarceration; Endoscopic direct-vision intussusception treatment; Case report

Core Tip: Perivascular epithelioid cell tumor (PEComa) of the colon is rarely encountered in the clinic, especially in pediatric patients. We describe a rare case of PEComa complicated with intussusception and anal incarceration in a 12-year-old female. We performed endoscopic direct-vision intussusception treatment and surgical removal. The diagnosis of PEComa mainly depends on pathology and immunohistochemistry. Radical resection is the preferred treatment method.

Citation: Kou L, Zheng WW, Jia L, Wang XL, Zhou JH, Hao JR, Liu Z, Gao FY. Pediatric case of colonic perivascular epithelioid cell tumor complicated with intussusception and anal incarceration: A case report. *World J Gastrointest Oncol* 2022; 14(7): 1348-1355
URL: https://www.wjgnet.com/1948-5204/full/v14/i7/1348.htm
DOI: https://dx.doi.org/10.4251/wjgo.v14.i7.1348

INTRODUCTION

Colonic perivascular epithelioid cell tumor (PEComa) is rare in clinical practice, especially in children. Intussusception caused by PEComa is even rarer. This report describes a pediatric case of colonic PEComa with intussusception and anal incarceration treated with endoscopic intussusception reduction. This is the first report of such a case. Furthermore, we review the studies on colorectal PEComa indexed in the PubMed database and accessed with the keywords "Colonic PEComa" and "Rectal PEComa". A total of 30 cases were retrieved, and we provide a detailed analysis and summarization of these cases here.

CASE PRESENTATION

Chief complaints

A 12-year-old girl presented with abdominal pain as the first manifestation.

History of present illness

The patient had developed paroxysmal angina pectoris around the umbilicus and lower abdomen 17 d prior, accompanied by nausea and vomiting. Intussusception was diagnosed in a local hospital by ultrasound, and was reduced by air enema. Contrast-enhanced computed tomography (CT) scan showed abnormal enhancement on the left side of the transverse colon with intussusception, which was considered as polyps (Figure 1). Supplementary colonoscopy showed a spherical protuberance of 5 cm in diameter in the transverse colon (Figure 2). The patient was transferred to our hospital for further diagnosis and treatment.

History of past illness

The patient had no previous medical history.

Personal and family history

There was no relevant personal or family history of colon tumor.

Physical examination

The patient's vital signs were stable, the abdomen was flat and soft, the left lower abdomen was tender, and there was mild rebound pain.

Laboratory examinations

Results of routine blood, liver function, and coagulation and tumor marker tests were within the normal ranges.

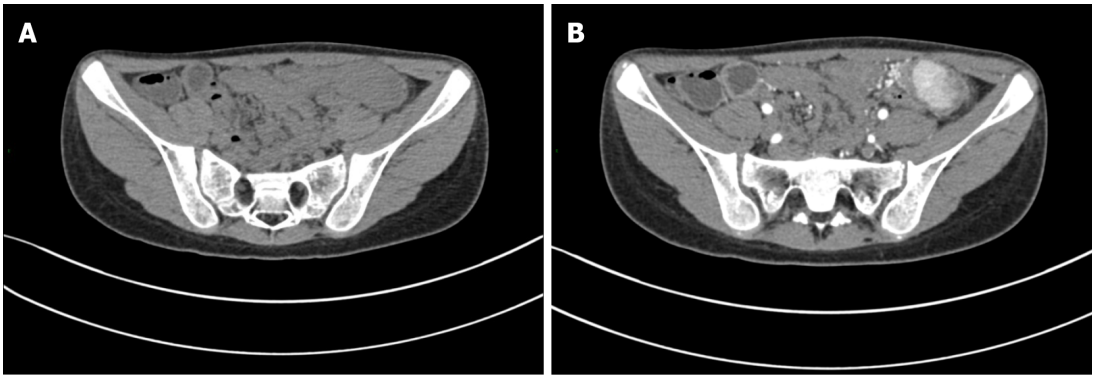

DOI: 10.4251/wjgo.v14.i7.1348

Figure 1 Abdominal computed tomography results. A: Plain scan showed a transverse colonic mass; B: Space-occupying lesion showed obvious enhancement.

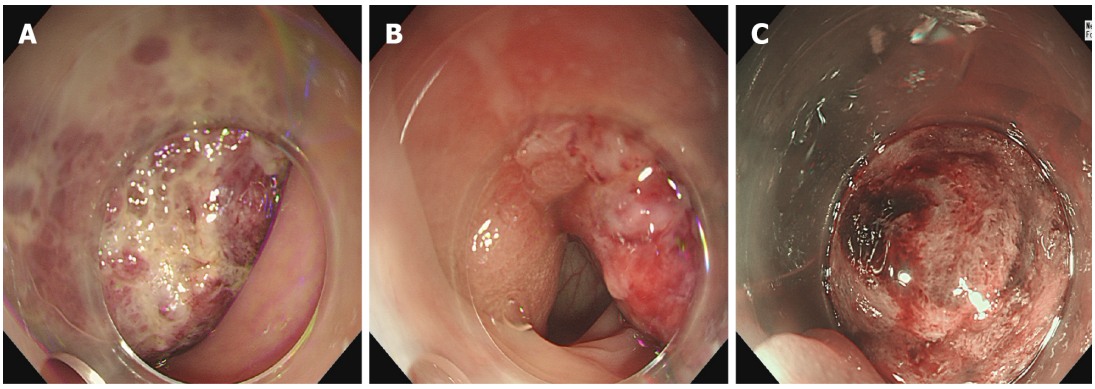

DOI: 10.4251/wjgo.v14.i7.1348

Figure 2 Colonoscopy results. A: The tumor is spherical, with a diameter of about 5 cm, a surface that is congested and eroded, and with formation of local ulcers; B The root of the tumor has a thick pedicle, with rough surface mucosa and covered with leukoplakia; C: Narrow band imaging showed that the glandular ducts had disappeared and the presence of vasodilation.

Imaging examinations

Contrast-enhanced CT scan showed abnormal enhancement on the left side of the transverse colon with intussusception, which was considered as polyps (Figure 1). Supplementary colonoscopy showed a spherical protuberance of 5 cm in diameter in the transverse colon (Figure 2).

MULTIDISCIPLINARY EXPERT CONSULTATION

Combined with the microscopy findings and considering the high risk associated with endoscopy, after discussion with the pediatric surgeons, pediatricians, pathologists, and ultrasonographers, we decided to remove the tumor *via* general surgery.

FINAL DIAGNOSIS

PEComa was diagnosed by immunohistochemistry.

TREATMENT

We performed surgery on the patient, a tumor was found in the transverse colon near the spleen, of about 6 cm × 4 cm × 3 cm in size, with a wide pedicle connected to the bowel. It had good mobility, a hard texture, and a rich blood supply. Edema of the surrounding bowel wall and mesentery was found, separating the mesentery in turn and being ligated to the affected mesenteric vessels. We completely

removed the tumor, in addition to about 3 cm of the affected bowel (Figure 3).

Postoperative pathology showed that the tumor volume was 5.0 cm × 4.5 cm × 3.0 cm and the tumor tissue was located in the submucosa of colon, arranged in an acinar shape with mild cell morphology, no tumor necrosis, and rare instances of mitosis. The immunohistochemical staining results were as follows: Human melanoma black 45 (HMB-45) (+), cluster of differentiation 31 (CD31) (+), cytokeratin (-), melanoma-associated antigen recognized by T cells (-), smooth muscle actin (-), molleya (-), desmin (-), S-100 (-), CD117 (-), and Ki67 (hot spot positive rate < 5%) (Figure 4).

OUTCOME AND FOLLOW-UP

The patient recovered well after the operation, and no abnormalities were found at the 6 mo follow-up.

DISCUSSION

PEComa represents a group of mesenchymal tumors characterized by perivascular epithelioid cells[1]. The etiology is still unclear, and some scholars consider it to be related to the gene mutation of the tuberous sclerosis complex[2]. Histologically, it is mainly composed of blood vessels, spindle cells or epithelioid cells, and fat. The proportion of the three components varies, which leads to large differences in imaging manifestations; it can manifest as poorly differentiated soft tissue tumors or as sclerosing tumors. Its density or signal performance is also closely related to the tumor cell components, but most of these tumors are characterized by a soft tissue mass with a regular shape, clear boundary, high density, and low signal intensity[3].

PEComa diagnosis depends on the pathology and immunohistochemistry findings. According to the World Health Organization classification of digestive system tumors published in 2019, the basic and ideal diagnostic criteria of PEComa are: epithelioid cells and (or) spindle cells in tissues, eosinophilic granular or transparent cytoplasm; nestlike, trabecular or lamellar structure; and co-expression of melanocytes and smooth muscle markers[4]. At present, there is no definitive standard for the diagnosis of benign and malignant PEComa. Folpe *et al*[5] divided the tumors into benign, malignant, and undetermined malignant potential. The malignant features included: tumor size > 5 cm, marginal infiltration, atypical nuclear, mitotic image ≥ 1/50 high-power field, tumor necrosis, and vascular invasion. Benign tumors are considered malignant when they have more than two of the aforementioned features; cases where the diagnosis of malignant potential is uncertain and there is tumor necrosis, including obvious nuclear atypia and high proliferation index, need close follow-up[4]. Considering the pathological results of this case, we considered the tumor to be benign; however, due to the patient's young age and large tumor volume, close follow-up is still needed.

PEComa is rarely reported. Cecal PEComa was first reported by Birkhaeuser *et al*[6] in 2004. Since then, a total of 30 cases (Table 1)[6-32] of colorectal PEComa have been reported (as determined upon performance of a detailed PubMed search), including 18 females and 12 males, of ages ranging from 5.5-years-old to 69-years-old; most of these patients were adults, and only 7 (23%) were younger than 15-years-old. There was a significant sex difference among the adults but no significant sex difference among the children, consistent with the findings reported by Fadare[33], who proposed that PEComa may be a hormone-dependent tumor. PEComa can occur in all parts of the colon, although they occur more often in the left colon (9 cases in the sigmoid colon[11,12,15,16,18,21,22,26,31], 5 in the rectum[6,7,13,28,29], 3 in the descending colon[9,16,27], 4 in the ascending colon[16,19,30], 7 in the cecum[8,14,20,23-25,32], 1 in the transverse colon[10], and 1 in the right colon[17]).

The diameter of the reported tumors have ranged from 0.8 cm to 8.0 cm. There are no specific symptoms. The tumor can manifest abdominal pain, diarrhea, abdominal distension, hematochezia, or other symptoms of gastrointestinal tumors[19]. The most common clinical manifestation is abdominal pain (44%). Two intussusception cases have been reported. Among the 30 cases, 23 patients underwent surgery and 4 of them given postoperative adjuvant chemotherapy[14,19,26,31]. In total, 5 underwent endoscopic mucosal resection[10,20,24,25,30], and 1 patient underwent endoscopic mucosal dissection after pathological diagnosis. No recurrence was found during follow-up. There have been 10 malignant PEComa cases reported[8,9,11,14,15,19,23,26,28,31]; among them, 2 patients died[9,23] and 2 were lost to follow-up but involving the pancreas and liver metastasis respectively[28,31]. Combined with limited case analysis, the prognosis of malignant PEComa is poor.

Ileocolic intussusception is one of the most common abdominal emergencies involving children who are less than 3-years-old[34]. The pathophysiology underlying the majority of pediatric intussusception cases is thought to be secondary to a transient viral illness[35]. In adults, 70%-90% of intussusception can be found to have a clear cause, and about 40% are caused by a primary or secondary malignant tumor[36]. Here, we have reported the first pediatric case of benign PEComa in the transverse colon with intussusception, tumor prolapse, and incarceration outside the anus.

Table 1 Review of case reports of colorectal perivascular epithelioid cell tumor

Ref.	Age (yr)	Sex	Symptom	Location	Size (mm)	Metastasis	Treatment	Follow-up
1 Birkhaeuser *et al* [6]	35	F	Bleeding	Cecum	35	No	SR	NER at 5 yr
2 Genevay *et al*[7]	36	F	Anemia and rectorrhagia	Cecum	35	No	SR	NA
3 Evert *et al*[8]	56	F	Rectal obstruction loss	Rectum	80 × 50	Lung metastasis	NA	NA
4 Yamamoto *et al* [9]	43	F	Abdominal pain	Descending	80	No	SR	DOD at 38 mo
5 Baek *et al*[10]	16	F	NA	Transverse	25	No	ER	NER at 24 mo
6 Pisharody *et al* [11]	11	M	Bleeding	Sigmoid	30	Lymph node metastasis	SR	NER at 5 mo
7 Righi *et al*[12]	11	M	NA	Sigmoid	35	NA	SR	NA
8 Qu *et al*[13]	43	F	NA	Cecum	20	No	SR	NER at 25 mo
9 Ryan *et al*[14]	15	F	Bleeding	Rectum	37	Lymph node metastasis	SR and AC	NER at 5 mo
10 Tanaka *et al* [15]	14	F	Physical examination	Sigmoid	40	No	SR	NA
11 Shi *et al*[16]	38	F	Abdominal pain	Ascending	60	No	SR	NER at 8 mo
12 Shi *et al*[16]	42	M	Abdominal pain	Sigmoid	45	No	SR	NER at 15 mo
13 Shi *et al*[16]	36	M	Abdominal pain	Descending	48	No	SR	NER at 32 mo
14 Shi *et al*[16]	45	F	Abdominal pain	Ascending	35	No	SR	NER at 36 mo
15 Gross *et al*[17]	5.5	M	Abdominal pain and fever	Right	50	No	SR	NER at 15 yr
16 Freeman *et al* [18]	17	F	Bleeding	Sigmoid	NA	No	SR	NA
17 Park *et al*[19]	7	M	Abdominal pain and bleeding	Ascending	37	No	SR and IFN therapy	NER at 26 mo
18 Mar *et al*[20]	11	F	Prolapsed mass	Rectum	20	No	ER	NA
19 Lee *et al*[21]	62	F	Abdominal pain and melena	Sigmoid	50	NA	NA	NA
20 Cho *et al*[22]	62	F	Bleeding	Sigmoid	50	No	SR	NER at 16 mo
21 Scheppach *et al* [23]	23	M	Abdominal pain and bleeding	Rectum	NA	Lymph node and liver metastasis	SR and AC	DOD at 23 mo
22 Im *et al*[24]	17	M	Bleeding	Rectum	30	No	ER	NER at 10 mo
23 Kanazawa *et al* [25]	55	F	Physical examination	Rectum	25	No	ER	NER at 12 mo
24 Cheng *et al*[26]	40	M	Dyschezia	Sigmoid	70 × 60	No	SR	Pancreatic metastasis at 27 mo
25 Iwamoto *et al* [27]	42	F	Physical examination	Descending	NA	No	SR	NA
26 Lin *et al*[28]	28	M	Abdominal pain and bleeding	Cecum	88	No	SR	Liver metastasis at 49 mo
27 Iwa *et al*[29]	69	M	Physical examination	Cecum	41 × 32	No	SR	NA
28 Bennett *et al* [30]	67	F	Physical examination	Ascending	80	No	ER	NA
29 Cheng *et al*[31]	17	M	Bleeding	Sigmoid	NA	Lymph node metastasis	SR and AC	NER at 24 mo
30 Yeon *et al*[32]	45	F	Physical examination	Rectum	20	No	SR	NA

AC: Adjuvant chemotherapy; DOD: Died of disease; ER: Endoscopic resection; F: Female; M: Male; NA: Not available; NER: No evidence of recurrence; SR: Surgical resection.

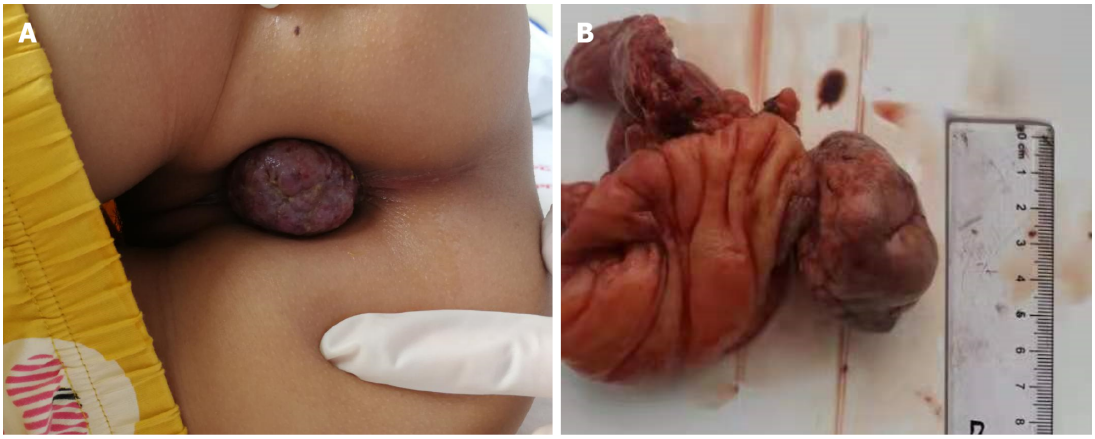

DOI: 10.4251/wjgo.v14.i7.1348

Figure 3 Tumor. A: The tumor was outside the anus; B: The tumor was removed surgically, in addition to about 3 cm of the affected bowel.

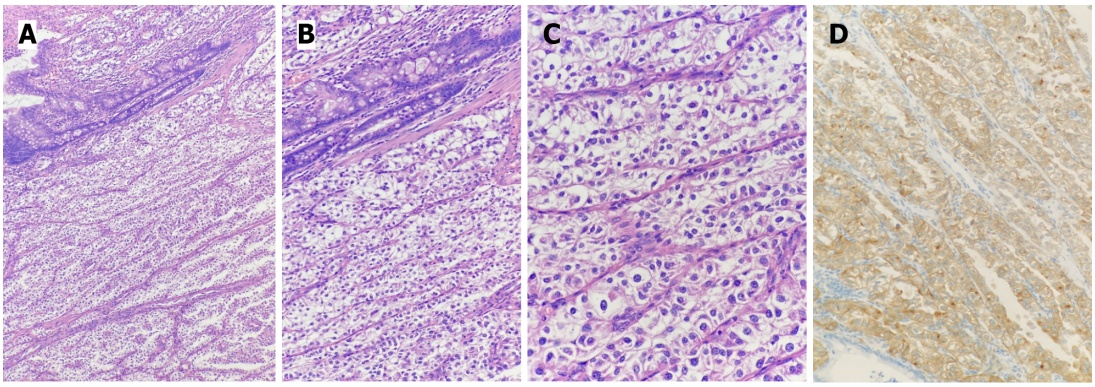

DOI: 10.4251/wjgo.v14.i7.1348

Figure 4 Pathology and immunohistochemistry results. A: 40 × magnification showing that the tumor was located in the intestinal wall, and the tumor cells were arranged in nests or acini; B: 100 × magnification showing that the tumor cells were transparent or eosinophilic granular; C: 200 × magnification showing abundant capillaries in the interstitium; D: Human melanoma black 45 (+) detected by the EnVision method.

At present, benign PEComa has no adjuvant drug treatment. The main treatment for colon PEComa is radical resection, with a good prognosis. Long-term clinical and CT follow-up is recommended. Scheppach *et al*[23] administered sirolimus, doxorubicin, ifosfamide, citabine and docetaxel successively after surgery, which had no obvious effect. Park *et al*[19] reported on a 7-year-old boy with poorly differentiated PEComa in the ascending colon, who received adjuvant interferon-alpha for 1 year after surgery. There was no recurrence after 26 mo of follow-up. That was the first report of interferon-alpha for the treatment of PEComa in the colon. In recent years, an increasing number of targeted drugs have been used in PEComa. Studies have shown that mechanistic target of rapamycin inhibitors are the most effective drugs for the treatment of advanced/metastatic PEComa[37].

CONCLUSION

PEComa is a special type of mesenchymal tissue tumor, which is rarely encountered in the clinic and lacks specific clinical manifestations. The diagnosis depends on pathology and immunohistochemistry findings. Radical resection is the preferred treatment method, and there is no standardized treatment for postoperative adjuvant therapy. Targeted drug application is gradually increasing and has achieved certain results but still needs further research.

FOOTNOTES

Author contributions: Kou L analyzed the data and wrote the paper; Zheng WW, Jia L, and Gao FY revised the paper; Wang XL, Zhou JH, Hao JR, and Liu Z collected the patient's clinical data; Gao FY designed the report.

Informed consent statement: Informed written consent was obtained from the patients for the publication of this report and any accompanying images.

Conflict-of-interest statement: The authors declare that they have no conflict of interest.

CARE Checklist (2016) statement: The authors have read the CARE Checklist (2016), and the manuscript was prepared and revised according to the CARE Checklist (2016).

Country/Territory of origin: China

ORCID number: Luan Kou 0000-0001-6728-7956; Wen-Wen Zheng 0000-0003-0524-3549; Li Jia 0000-0002-2541-4723; Xiao-Li Wang 0000-0002-8947-4645; Ji-Hai Zhou 0000-0002-4760-6494; Jiao-Rong Hao 0000-0003-0260-8805; Zhu Liu 0000-0002-6785-3820; Feng-Yu Gao 0000-0002-7226-7842.

S-Editor: Chen YL
L-Editor: A
P-Editor: Chen YL

REFERENCES

1 **Hornick JL**, Fletcher CD. PEComa: what do we know so far? *Histopathology* 2006; **48**: 75-82 [PMID: 16359539 DOI: 10.1111/j.1365-2559.2005.02316.x]
2 **Thway K**, Fisher C. PEComa: morphology and genetics of a complex tumor family. *Ann Diagn Pathol* 2015; **19**: 359-368 [PMID: 26144278 DOI: 10.1016/j.anndiagpath.2015.06.003]
3 **Tan Y**, Zhang H, Xiao EH. Perivascular epithelioid cell tumour: dynamic CT, MRI and clinicopathological characteristics--analysis of 32 cases and review of the literature. *Clin Radiol* 2013; **68**: 555-561 [PMID: 23245276 DOI: 10.1016/j.crad.2012.10.021]
4 **WHO Classification of tumours Editorial Board**. WHO Classification of tumours of the digestive system. 5th ed. Lyon: IARC Press, 2019: 485-488
5 **Folpe AL**, Mentzel T, Lehr HA, Fisher C, Balzer BL, Weiss SW. Perivascular epithelioid cell neoplasms of soft tissue and gynecologic origin: a clinicopathologic study of 26 cases and review of the literature. *Am J Surg Pathol* 2005; **29**: 1558-1575 [PMID: 16327428 DOI: 10.1097/01.pas.0000173232.22117.37]
6 **Birkhaeuser F**, Ackermann C, Flueckiger T, Guenin MO, Kern B, Tondelli P, Peterli R. First description of a PEComa (perivascular epithelioid cell tumor) of the colon: report of a case and review of the literature. *Dis Colon Rectum* 2004; **47**: 1734-1737 [PMID: 15540307 DOI: 10.1007/s10350-004-0637-5]
7 **Genevay M**, Mc Kee T, Zimmer G, Cathomas G, Guillou L. Digestive PEComas: a solution when the diagnosis fails to "fit". *Ann Diagn Pathol* 2004; **8**: 367-372 [PMID: 15614743 DOI: 10.1053/j.anndiagpath.2004.08.008]
8 **Evert M**, Wardelmann E, Nestler G, Schulz HU, Roessner A, Röcken C. Abdominopelvic perivascular epithelioid cell sarcoma (malignant PEComa) mimicking gastrointestinal stromal tumour of the rectum. *Histopathology* 2005; **46**: 115-117 [PMID: 15656899 DOI: 10.1111/j.1365-2559.2005.01991.x]
9 **Yamamoto H**, Oda Y, Yao T, Oiwa T, Kobayashi C, Tamiya S, Kawaguchi K, Hino O, Tsuneyoshi M. Malignant perivascular epithelioid cell tumor of the colon: report of a case with molecular analysis. *Pathol Int* 2006; **56**: 46-50 [PMID: 16398680 DOI: 10.1111/j.1440-1827.2006.01917.x]
10 **Baek JH**, Chung MG, Jung DH, Oh JH. Perivascular epithelioid cell tumor (PEComa) in the transverse colon of an adolescent: a case report. *Tumori* 2007; **93**: 106-108 [PMID: 17455882]
11 **Pisharody U**, Craver RD, Brown RF, Gardner R, Schmidt-Sommerfeld E. Metastatic perivascular epithelioid cell tumor of the colon in a child. *J Pediatr Gastroenterol Nutr* 2008; **46**: 598-601 [PMID: 18493218 DOI: 10.1097/MPG.0b013e318148b65c]
12 **Righi A**, Dimosthenous K, Rosai J. PEComa: another member of the MiT tumor family? *Int J Surg Pathol* 2008; **16**: 16-20 [PMID: 18203778 DOI: 10.1177/1066896907309733]
13 **Qu GM**, Hu JC, Cai L, Lang ZQ. Perivascular epithelioid cell tumor of the cecum: a case report and review of literatures. *Chin Med J (Engl)* 2009; **122**: 1713-1715 [PMID: 19719977]
14 **Ryan P**, Nguyen VH, Gholoum S, Carpineta L, Abish S, Ahmed NN, Laberge JM, Riddell RH. Polypoid PEComa in the rectum of a 15-year-old girl: case report and review of PEComa in the gastrointestinal tract. *Am J Surg Pathol* 2009; **33**: 475-482 [PMID: 19092636 DOI: 10.1097/PAS.0b013e31819003d1]
15 **Tanaka M**, Kato K, Gomi K, Matsumoto M, Kudo H, Shinkai M, Ohama Y, Kigasawa H, Tanaka Y. Perivascular epithelioid cell tumor with SFPQ/PSF-TFE3 gene fusion in a patient with advanced neuroblastoma. *Am J Surg Pathol* 2009; **33**: 1416-1420 [PMID: 19606011 DOI: 10.1097/PAS.0b013e3181a9cd6c]
16 **Shi HY**, Wei LX, Sun L, Guo AT. Clinicopathologic analysis of 4 perivascular epithelioid cell tumors (PEComas) of the

gastrointestinal tract. *Int J Surg Pathol* 2010; **18**: 243-247 [PMID: 19124450 DOI: 10.1177/1066896908330481]
17 **Gross E**, Vernea F, Weintraub M, Koplewitz BZ. Perivascular epithelioid cell tumor of the ascending colon mesentery in a child: case report and review of the literature. *J Pediatr Surg* 2010; **45**: 830-833 [PMID: 20385296 DOI: 10.1016/j.jpedsurg.2010.01.015]
18 **Freeman HJ**, Webber DL. Perivascular epithelioid cell neoplasm of the colon. *World J Gastrointest Oncol* 2010; **2**: 205-208 [PMID: 21160599 DOI: 10.4251/wjgo.v2.i4.205]
19 **Park SJ**, Han DK, Baek HJ, Chung SY, Nam JH, Kook H, Hwang TJ. Perivascular epithelioid cell tumor (PEComa) of the ascending colon: the implication of IFN-α2b treatment. *Korean J Pediatr* 2010; **53**: 975-978 [PMID: 21218021 DOI: 10.3345/kjp.2010.53.11.975]
20 **Maran-Gonzalez A**, Baldet P, Costes V. [Polypoid PEComa: case report and literature review]. *Ann Pathol* 2011; **31**: 102-107 [PMID: 21601115 DOI: 10.1016/j.annpat.2010.07.005]
21 **Lee M**, Cho KJ, Yu C, Park Y, Kim JC, Kim J, Yu E, Kim MJ. Perivascular epithelioid cell tumor of the sigmoid colon with transcription factor E3 expression. *Ann Diagn Pathol* 2012; **16**: 306-311 [PMID: 21546294 DOI: 10.1016/j.anndiagpath.2011.01.007]
22 **Cho YW**, Kim KJ, Ye BD, Byeon JS, Myung SJ, Yang SK, Kim JH. [A case of a perivascular epithelioid cell tumor mimicking colon cancer]. *Korean J Gastroenterol* 2012; **60**: 377-381 [PMID: 23242022 DOI: 10.4166/kjg.2012.60.6.377]
23 **Scheppach W**, Reissmann N, Sprinz T, Schippers E, Schoettker B, Mueller JG. PEComa of the colon resistant to sirolimus but responsive to doxorubicin/ifosfamide. *World J Gastroenterol* 2013; **19**: 1657-1660 [PMID: 23539498 DOI: 10.3748/wjg.v19.i10.1657]
24 **Im S**, Yoo C, Jung JH, Choi HJ, Yoo J, Kang CS. Primary perivascular epithelioid cell tumor in the rectum: a case report and review of the literature. *Pathol Res Pract* 2013; **209**: 244-248 [PMID: 23484779 DOI: 10.1016/j.prp.2013.01.001]
25 **Kanazawa A**, Fujii S, Godai TI, Ishibe A, Oshima T, Fukushima T, Ota M, Yukawa N, Rino Y, Imada T, Ito J, Nozawa A, Masuda M, Kunisaki C. Perivascular epithelioid cell tumor of the rectum: report of a case and review of the literature. *World J Surg Oncol* 2014; **12**: 12 [PMID: 24410788 DOI: 10.1186/1477-7819-12-12]
26 **Cheng J**, Deng M, Gao J, Tao K. A recurrent perivascular epithelioid cell tumor of sigmoid colon with pancreatic metastasis: an extremely rare case report and review of the literature. *Int J Colorectal Dis* 2016; **31**: 1237-1240 [PMID: 26567117 DOI: 10.1007/s00384-015-2443-z]
27 **Iwamoto R**, Kataoka TR, Furuhata A, Ono K, Hirota S, Kawada K, Sakai Y, Haga H. Perivascular epithelioid cell tumor of the descending colon mimicking a gastrointestinal stromal tumor: a case report. *World J Surg Oncol* 2016; **14**: 285 [PMID: 27842558 DOI: 10.1186/s12957-016-1046-7]
28 **Lin KH**, Chang NJ, Liou LR, Su MS, Tsao MJ, Huang ML. Successful management of perivascular epithelioid cell tumor of the rectum with recurrent liver metastases: A case report. *Medicine (Baltimore)* 2018; **97**: e11679 [PMID: 30075560 DOI: 10.1097/MD.0000000000011679]
29 **Iwa N**, Yutani C, Kobayashi TK. Presence of eosinophilic intracytoplasmic inclusions diagnosed by fine needle aspiration cytology in perivascular epithelioid cell tumor (PEComa) arising from the cecum. *Diagn Cytopathol* 2019; **47**: 359-361 [PMID: 30499191 DOI: 10.1002/dc.24086]
30 **Bennett J**, Laury R, Dai H, Walde C, Kasi A. A Curious Case of Colonic Perivascular Epithelioid Cell Tumor: A Unique Diagnosis With Variable Presentations. *Cureus* 2020; **12**: e11164 [PMID: 33251071 DOI: 10.7759/cureus.11164]
31 **Cheng HC**, Kuo CY, Huang CW, Shih HH, Lin CH, Wang JY. Unusual paediatric sigmoid perivascular epithelioid cell tumour with regional lymph node metastasis treated using gemcitabine and docetaxel: a case report and literature review. *J Int Med Res* 2021; **49**: 3000605211041509 [PMID: 34510959 DOI: 10.1177/03000605211041509]
32 **Yeon HJ**, Sung NS, Roh SJ, Choi WJ, Park YW. PEComa in the rectum: A case report and review of the literature on epithelioid angiomyolipoma. *Int J Surg Case Rep* 2021; **86**: 106301 [PMID: 34392019 DOI: 10.1016/j.ijscr.2021.106301]
33 **Fadare O**. Perivascular epithelioid cell tumor (PEComa) of the uterus: an outcome-based clinicopathologic analysis of 41 reported cases. *Adv Anat Pathol* 2008; **15**: 63-75 [PMID: 18418088 DOI: 10.1097/PAP.0b013e31816613b0]
34 **Applegate KE**. Intussusception in children: evidence-based diagnosis and treatment. *Pediatr Radiol* 2009; **39** Suppl 2: S140-S143 [PMID: 19308373 DOI: 10.1007/s00247-009-1178-9]
35 **Burnett E**, Kabir F, Van Trang N, Rayamajhi A, Satter SM, Liu J, Yousafzai MT, Anh DD, Basnet AT, Flora MS, Houpt E, Qazi SH, Canh TM, Rayamajhi AK, Saha BK, Saddal NS, Muneer S, Hung PH, Islam T, Ali SA, Tate JE, Yen C, Parashar UD. Infectious Etiologies of Intussusception Among Children <2 Years Old in 4 Asian Countries. *J Infect Dis* 2020; **221**: 1499-1505 [PMID: 31754717 DOI: 10.1093/infdis/jiz621]
36 **Akbulut S**. Unusual cause of adult intussusception: diffuse large B-cell non-Hodgkin's lymphoma: a case report and review. *Eur Rev Med Pharmacol Sci* 2012; **16**: 1938-1946 [PMID: 23242720]
37 **Unluoglu S**, Bayol U, Korkmaz N, Ozenen B, Ipekci F, Pala EE. Perivascular epithelioid cell tumor of the ileum presenting as diverticulitis. *Case Rep Pathol* 2012; **2012**: 476941 [PMID: 22953133 DOI: 10.1155/2012/476941]

World Journal of Gastrointestinal Oncology

Submit a Manuscript: https://www.f6publishing.com

World J Gastrointest Oncol 2022 July 15; 14(7): 1356-1362

DOI: 10.4251/wjgo.v14.i7.1356

ISSN 1948-5204 (online)

CASE REPORT

Primary signet-ring cell carcinoma of the extrahepatic bile duct: A case report

Chao-Bang Xie, Yang Wu, Feng Li, Kai-Fei Zhao, Rong-Shu Shi, Qiong Huang, Jin Ao, Di Ke

Specialty type: Gastroenterology and hepatology

Provenance and peer review: Unsolicited article; Externally peer reviewed.

Peer-review model: Single blind

Peer-review report's scientific quality classification

Grade A (Excellent): 0
Grade B (Very good): B
Grade C (Good): C
Grade D (Fair): 0
Grade E (Poor): 0

P-Reviewer: Kitagawa Y, Japan; Singh I, United States

Received: January 23, 2022
Peer-review started: January 23, 2022
First decision: April 17, 2022
Revised: April 30, 2022
Accepted: June 21, 2022
Article in press: June 21, 2022
Published online: July 15, 2022

Chao-Bang Xie, Yang Wu, Feng Li, Kai-Fei Zhao, Rong-Shu Shi, Jin Ao, Di Ke, Department of Radiology, The Affiliated Hospital of Zunyi Medical University, Zunyi 563000, Guizhou Province, China

Qiong Huang, Department of Pathology, The Affiliated Hospital of Zunyi Medical University, Zunyi 563000, Guizhou Province, China

Corresponding author: Kai-Fei Zhao, Doctor, Associate Professor, Deputy Director, Department of Radiology, The Affiliated Hospital of Zunyi Medical University, No. 149 Dalian Road, Zunyi 563000, Guizhou Province, China. zhaokaifei8943@sina.com

Abstract

BACKGROUND

Signet ring cell carcinoma (SRCC) is a specific type of mucinous secretory adenocarcinoma, which contains abundant mucus in the cytoplasm and pushes the nucleus to one side of the cell membrane, forming a round or oval, and the nuclear deviations give the cells a signet ring-like appearance. SRCC often originates in the gastrointestinal tract, especially in the stomach. However, primary SRCC of the extrahepatic bile duct is extremely rare. Therefore, little is known about its epidemiology, treatment, and prognosis.

CASE SUMMARY

An 82-year-old female was admitted with abdominal pain, jaundice, and skin pruritus for 2 mo. She had no specific family history. Physical examination presented normal vital signs, icteric sclera, visible jaundice, and mild tenderness in the right upper abdominal quadrant. Tumor-related cell markers were within normal values. Contrast-enhanced computed tomography revealed a thickened wall of the common bile duct, strengthened with intrahepatic bile duct dilation and multiple round-like lesions in the liver. In addition, the lymph nodes in the hepatic hilum area, the pancreatic head area, and around the abdominal aorta were enlarged. Thus, a preoperative diagnosis of cholangiocarcinoma was established. To alleviate jaundice and prolong the overall survival, percutaneous transhepatic cholangiopancreatic drainage (PTCD) was performed. During the operation, segmental stenosis of the extrahepatic bile duct and a vine-like expansion of the intrahepatic bile duct was observed. Furthermore, a biliary biopsy was performed under fluoroscopy to determine the nature and origin of the lesion. The pathological diagnosis of the biopsy was SRCC. Finally, a diagnosis of primary SRCC of extrahepatic bile duct with distant lymph node

metastasis and multiple liver metastases was made based on the radiographic, PTCD, and pathological characteristics. The tumor was diagnosed as T3N1M1 stage IV. Despite our aggressive approach, the patient died of liver failure after 1 mo.

CONCLUSION
This is the only case report on primary SRCC of the extrahepatic bile duct with distant organ metastasis to date.

Key Words: Cholangiocarcinoma; Adenocarcinoma; Signet ring cell carcinoma; Extrahepatic bile duct; Case report

Core Tip: We report a case where an 82-year-old female was admitted with abdominal pain, jaundice, and skin pruritus for 2 mo. The radiological diagnosis was a cholangiocarcinoma. To alleviate jaundice and prolong the overall survival, percutaneous transhepatic cholangiopancreatic drainage (PTCD) was performed. During the operation, in order to determine the nature and origin of the lesion, a biliary biopsy was performed under fluoroscopy. Finally, a diagnosis of primary signet ring cell carcinoma of extrahepatic bile duct with distant lymph node metastasis and multiple liver metastases was made based on the radiographic, PTCD, and pathological characteristics. However, despite active treatment, the disease progressed rapidly, and the patient died after 1 mo due to liver failure.

Citation: Xie CB, Wu Y, Li F, Zhao KF, Shi RS, Huang Q, Ao J, Ke D. Primary signet-ring cell carcinoma of the extrahepatic bile duct: A case report. *World J Gastrointest Oncol* 2022; 14(7): 1356-1362
URL: https://www.wjgnet.com/1948-5204/full/v14/i7/1356.htm
DOI: https://dx.doi.org/10.4251/wjgo.v14.i7.1356

INTRODUCTION

Cholangiocarcinoma (CCA) is a common malignant tumor of the biliary system, and 90%-95% of the pathologic types of CCA are adenocarcinomas[1]. Signet ring cell carcinoma (SRCC) is a subtype of poorly differentiated adenocarcinoma with strong invasion and poor prognosis[2]. Although it can occur in various organs, including the stomach, colon, esophagus, bladder, prostate, pancreas, and breast[2], it mainly arises in the stomach[3], where > 96% of SRCCs occur[4]. However, the occurrence of the extrahepatic bile duct is extremely rare.

Previously, only a few studies have reported cases of primary SRCC of the extrahepatic bile duct due to the rarity this disease . Herein, we report that a case of primary SRCC of the extrahepatic bile duct diagnosed *via* a biopsy of the biliary tree. Additionally, we conducted a literature review to describe the epidemiology and explore the treatment and prognosis of the disease.

CASE PRESENTATION

Chief complaints

Abdominal pain, jaundice, and skin pruritus for 2 mo.

History of present illness

The patient was admitted with abdominal pain, jaundice, and skin pruritus for 2 mo.

History of past illness

The patient was previously healthy and had no specific medical history.

Personal and family history

She had no specific family history.

Physical examination

Physical examination presented normal vital signs, icteric sclera, visible jaundice, and mild tenderness in the upper right abdominal quadrant.

Laboratory examinations

Tumor-related cell markers were as follows: carbohydrate antigen 19-9, > 2 044 U/mL (reference range: < 35 U/mL); cancer antigen 125, 146 U/mL (reference range: < 35 U/mL); human chorionic gonadotropin, 23.38 IU/L (reference range: < 5 IU/L); alpha-fetoprotein and carcinoembryonic antigen (CEA), within normal range. Laboratory tests: total bilirubin, 446 μmol/L (reference range: 5-21 μmol/L); direct bilirubin, 232.9 μmol/L (reference range: 0-3.4 μmol/L); indirect bilirubin, 213.1 μmol/L (reference range: 1.7-13.6 μmol/L).

Imaging examinations

Contrast-enhanced computed tomography revealed that the wall of the common bile duct was thickened and strengthened (Figure 1A and B, arrows) with intrahepatic bile duct dilation (Figure 1C, arrows), and numerous hypodense lesions in the liver showed slight annular enhancement (Figure 1C, asterisks). In addition, the lymph nodes in the hepatic hilum area, the pancreatic head area, and around the abdominal aorta were enlarged (diameter 1.5-2.5 cm) with mild enhancement (Figure 1A and B, asterisks).

Diagnostic work-up

To alleviate jaundice and prolong the overall survival, percutaneous transhepatic cholangiopancreatic drainage (PTCD) was performed. During the operation, segmental stenosis of the extrahepatic bile duct (Figure 1E, arrows) and a vine-like expansion of the intrahepatic bile duct (Figure 1D, arrows) were observed. To determine the nature and origin of the lesion, a biliary biopsy was performed under fluoroscopy (Figure 1F, arrows). Hematoxylin and eosin (H&E) staining revealed abundant mucin in the cytoplasm pushed the nuclei aside, giving the cells the characteristic signet ring morphology (Figure 2A). The pathological diagnosis of the biopsy was SRCC. Immunohistochemistry (IHC) showed the following indicators: CK19 (++), CAM5.2 (+), CK7 (++), CK broad-spectrum (++), CEA (++), Ki-67 (10%), CK20 (-), CDX2 (-), glypican-3 (-), hepatocyte (-), vimentin (-), and special staining for PAS (+) (Figure 2B-F). The IHC of biopsy materials showed that the tumor cells were positive for CK19 (Figure 2B) and CK7 (Figure 2D) but negative for both CK20 and CDX2, suggesting the biliary tract origin of carcinoma. In addition, the gastroscopy and colonoscopy of the common primary site of SRCC did not show any abnormality.

FINAL DIAGNOSIS

Finally, a diagnosis of primary SRCC of extrahepatic bile duct with distant lymph node metastasis and multiple liver metastases was made based on the radiographic, PTCD, and pathological characteristics. The tumor was diagnosed as T3N1M1 stage IV according to the 8th edition of the American Joint Committee on Cancer (AJCC) cancer staging system[5]. Further imaging, such as positron emission tomography-computed tomography (PET-CT), was essential to determine any other sites of distant metastasis. Nonetheless, due to rapidly deteriorating condition in a short period, the patient died before the PET-CT was completed.

TREATMENT

This patient was treated with S-adenosylmethionine (intravenous infusion, 1.5 g once a day) to protect the liver and relieve jaundice. PTCD was performed simultaneously to alleviate obstructive jaundice.

OUTCOME AND FOLLOW-UP

The patient died after 1 mo due to liver failure. The timeline can be seen in Figure 3.

DISCUSSION

Herein, we present a rare case of primary SRCC of extrahepatic bile duct with distant lymph node metastasis and multiple intrahepatic metastases. To the best of our knowledge, this is the second case confirmed by direct forceps biopsy under fluoroscopy and the first case of primary SRCC of the extrahepatic bile duct with distant organ metastasis. Distant organ metastasis is a critical factor influencing prognosis. Therefore, our case had a worse prognosis compared to those reported previously. Moreover, surgical resection was not a reasonable treatment due to the patient's old age and poor liver function; hence, she received only palliative treatment, including liver protection and PTCD.

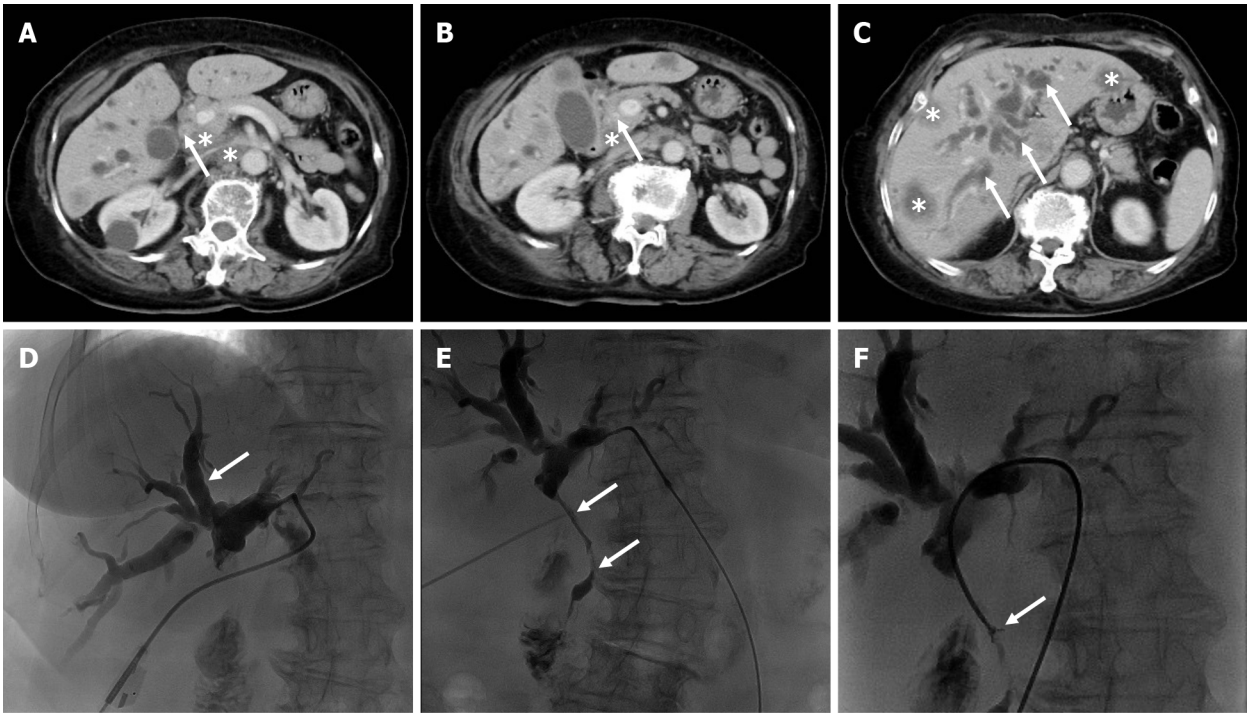

DOI: 10.4251/wjgo.v14.i7.1356

Figure 1 Contrast-enhanced computed tomography and percutaneous transhepatic cholangiopancreatic drainage images. A and B: Contrast-enhanced computed tomography (CECT) of the abdomen shows that the common bile duct wall is thickened and strengthened (arrows) with enlarged lymph nodes (asterisks); C: CECT shows intrahepatic bile duct dilation (arrows) and multiple liver metastases (asterisks); D and E: Percutaneous transhepatic cholangiopancreatic drainage shows a vine-like expansion of the intrahepatic bile duct (D, arrows) and segmental stenosis of the extrahepatic bile duct (E, arrows); F: A biliary biopsy was performed under fluoroscopy (arrows).

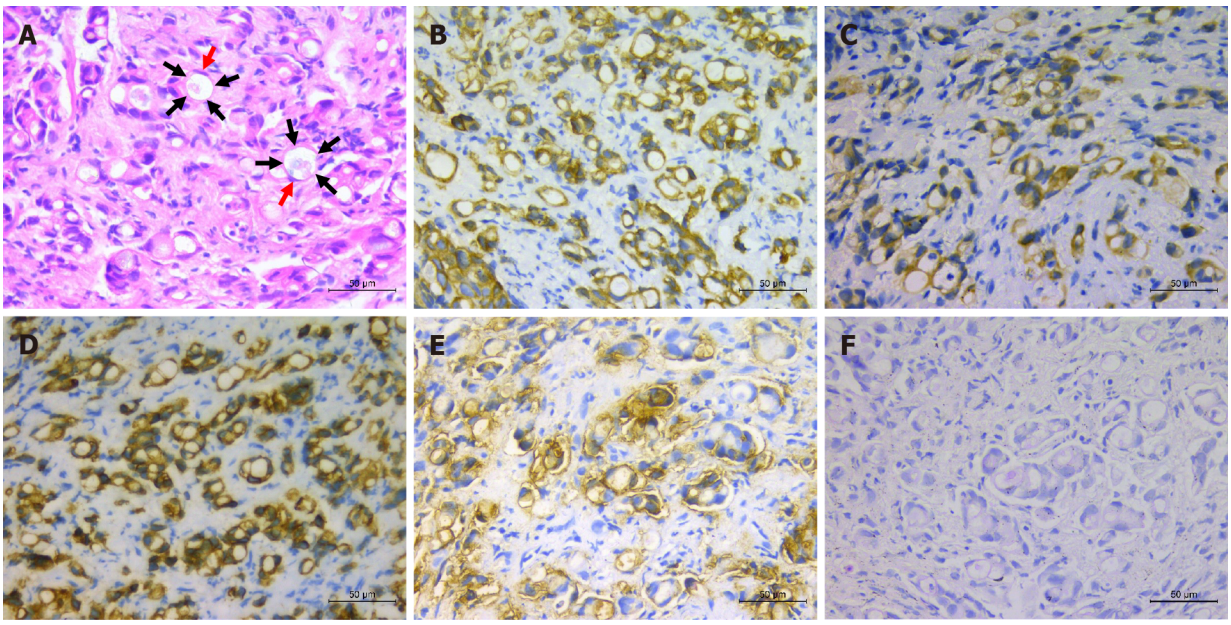

DOI: 10.4251/wjgo.v14.i7.1356

Figure 2 Primary signet ring cell carcinoma of the extrahepatic bile duct. A: Hematoxylin and eosin staining (× 400), showing signet ring cells (arrows) with abundant intracytoplasmic vacuoles and peripherally displaced nuclei (red arrows); B-F: Immunohistochemistry staining (× 400), CK19, CAM5.2, CK7, CEA, and PAS-positive staining, respectively.

However, despite active treatment, the disease progressed rapidly, and the patient died after 1 mo due to liver failure. Therefore, we concluded that primary SRCC of the extrahepatic bile duct is not prone to distant organ metastasis, and if accompanied by distant organ metastasis, it grows rapidly and has a strong invasion and poor prognosis.

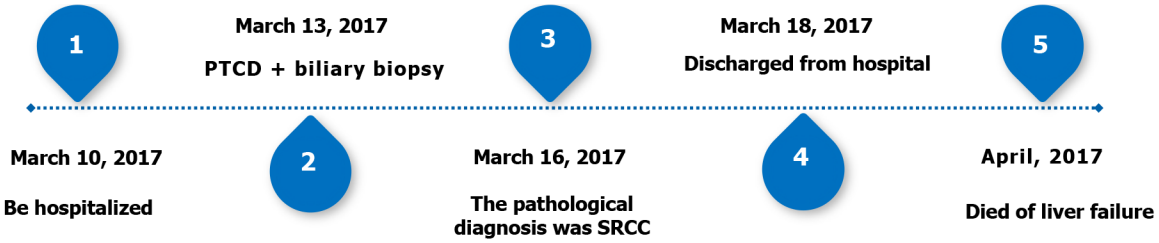

DOI: 10.4251/wjgo.v14.i7.1356

Figure 3 Timeline. SRCC: Signet ring cell carcinoma; PTCD: Percutaneous transhepatic cholangiopancreatic drainage.

Primary SRCC of the extrahepatic bile duct is an extremely rare subtype of bile duct adenocarcinoma of unknown origin. Presently, there are two theories regarding its origin. One is that the tumors may arise from ectopic gastric mucosa, while the other is that SRCCs may develop from gastric-type epithelial metaplasia[6]. In our case, no ectopic gastric mucosa and epithelial metaplasia were detected in the biliary biopsy. Thus, the origin of primary SRCC in the extrahepatic bile duct needs to be evaluated in future studies[14].

For the literature review, relevant articles in English were retrieved from the PubMed, Ovid database, and Web of Science from 1949 to January 10, 2022. The keywords used for the search were "signet ring cell cholangiocarcinoma" OR "signet ring cell carcinoma of bile duct". These words were used individually or with the Boolean operator "AND". A total of 129 articles were analyzed from 1949 to 2022. The flow chart of the literature screening process is illustrated in Figure 4. Finally, 11 cases were included in this meta-analysis. The following data were collected: the name of the first author, year of publication, patient's age, sex, location, TNM staging, treatment, and follow-up results (Table 1).

In the current study, we included 3 males[7,10,12] and 8 females[8,9,11,13-17] with an average age of 58.5 years (range: 32-73 years). This phenomenon suggested that primary SRCC of the extrahepatic bile duct occurs in elderly patients, which was similar to previous reports[9]. However, due to the small number of patients, the correlation between the incidence of primary SRCC of the extrahepatic bile duct and gender needs to be investigated further. The analysis of 11 patients revealed that primary SRCC of the extrahepatic bile duct occurred in the distal bile duct in 8 cases[7,8,10-12,14-16] and the perihilar bile duct in only 3 cases[9,13,17]. This showed that primary SRCC of the extrahepatic bile duct occurs in the distal bile duct compared to the perihilar bile duct. The mechanism of occurrence may be that the distal bile duct is prone to the ectopic gastric mucosa and gastric-type epithelial metaplasia; however, it needs to be evaluated further[14]. According to the 8th edition of the AJCC cancer staging system, 9 cases[7-15] had an obvious invasion of the extrahepatic bile duct, of which 3[8,12,13] showed infiltration of the adjacent tissue structures. Peritoneum and retroperitoneal lymph node metastasis were observed in 5 cases[7,8,12,14,15] without distant metastasis. This phenomenon indicated that primary SRCC of the extrahepatic bile duct mainly grows along the wall, often with lymph node metastasis, but distant organ metastasis is extremely rare. The treatment for primary SRCC of extrahepatic bile duct includes resection, such as pancreaticoduodenectomy or resection of the biliary tree, followed by radiotherapy and chemotherapy. Also, integrative treatments that combine two or three have been applied[7-17]. 7/11 cases[8-10,12-14,16] received only surgical resection, 1/11 case[17] received chemotherapy alone, 1/11 case[11] received surgical resection followed by chemotherapy, 1/11 case[15] received chemoradiotherapy, and 1/11 case[7] received combined treatment of surgical resection, radiotherapy, and chemotherapy. Currently, surgical treatment is the gold standard for patients with cancer without distant metastasis. However, no standardized protocol and guidelines for treating primary SRCC of the extrahepatic bile duct are currently available because of the limited number of cases and studies. Yang *et al*[2] proposed that the primary SRCC location can be used as an independent prognostic factor of survival and that compared to stomach SRCC, the primary gallbladder, the ampulla of Vater, and pancreatic SRCCs have a worse prognosis. Therefore, an optimal treatment strategy is essential. Based on the results of this study, active surgical treatment may improve the prognosis in the event of surgical conditions in patients. Nonetheless, cases with poor prognosis even after radical resection are apparent. However, a standard recommendation of whether to perform adjuvant radiotherapy or chemotherapy cannot be established because of the small number of patients who received radiotherapy or chemotherapy in this study. Thus, to improve the survival and quality of life of patients, a multidisciplinary treatment such as concomitant use of chemotherapy is necessary.

CONCLUSION

Overall, primary SRCC of the extrahepatic bile duct is extremely rare, and cases with distant organ metastases have never been reported. Currently, surgical treatment is the gold standard for patients

Table 1 Summary of reported cases of signet ring cell carcinoma of extrahepatic bile duct

Ref.	Age	Sex	Location	TNM[1]	Treatment	Outcome
Lee *et al*[7], 2010	55	M	Distal	T3N1M0	Resection; Chemoradiation	Alive at 24 mo
Ogata *et al*[8], 2010	42	F	Distal	T4N1M0	Resection	Alive at 6 mo
Somer *et al*[9], 2012	66	F	Perihilar	T3N0M0	Resection	No described
Kita *et al*[10], 2014	73	F	Distal	T3N0M0	Resection; Gemcitabine/cisplatin	Alive at 12 mo
Kwon *et al*[11], 2014	63	M	Distal	T3N0M0	Resection	Dead at 15 mo
Hua *et al*[12], 2015	52	M	Distal	T4N1M0	Resection	Dead at 6 mo
Chedid *et al*[13], 2015	66	F	Perihilar	T4N0M0	Resection	Dead at 15 mo
Zhang *et al*[14], 2018	32	F	Distal	T3N1M0	Resection	Dead at 5 mo
Welsh *et al*[15], 2018	55	F	Distal	T3N1M0	Chemoradiation	Dead at 4 mo
Hameed *et al*[16], 2019	72	F	Distal	T1N0M0	Resection	No described
Ghoddoosi *et al*[17], 2021	68	F	Perihilar	T1N0M0	Gemcitabine/cisplatin	Alive at 9 mo
Present case	82	F	Distal	T3N1M1	PTCD	Dead at 1 mo

[1]AJCC Cancer Staging Manual, 8th edition.
PTCD: Percutaneous transhepatic cholangiopancreatic drainage.

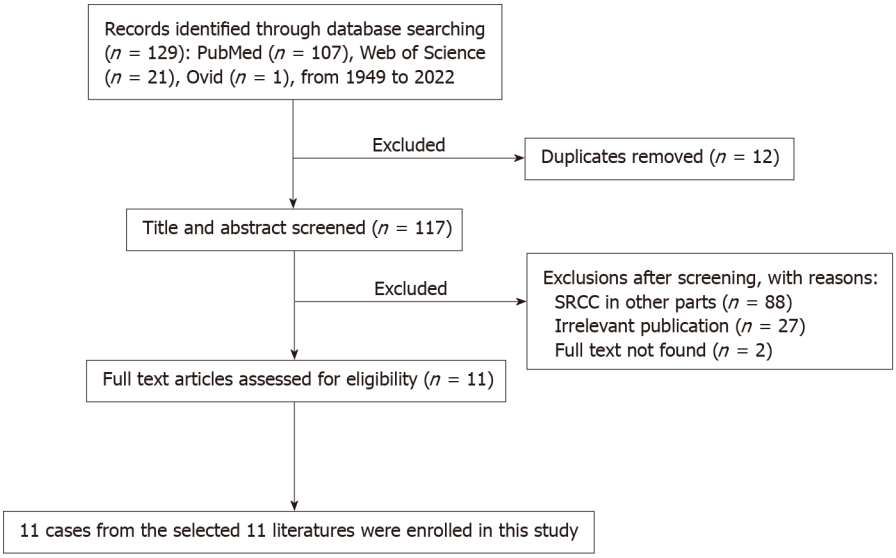

DOI: 10.4251/wjgo.v14.i7.1356

Figure 4 Flowchart of the literature screening process for primary signet ring cell carcinoma of the extrahepatic bile duct. SRCC: Signet ring cell carcinoma.

with primary SRCC of the extrahepatic bile duct without distant metastasis. However, aggressive multidisciplinary treatment is essential when surgical resection is not feasible or metastasis is observed.

FOOTNOTES

Author contributions: Xie CB, Wu Y, Li F, and Zhao KF reviewed the literature and contributed to manuscript drafting; Shi RS analyzed and interpreted the patient data; Huang Q provided pathological images; Ao J and Ke D managed the patient; all authors read and approved the final manuscript.

Supported by the Zunyi City Science and Technology Department, No. HZ-2021-44.

Informed consent statement: Informed consent was obtained from the patient' family for the publication of this case as the patient has deceased.

Conflict-of-interest statement: We have no conflict of interest.

CARE Checklist (2016) statement: The authors have read the CARE Checklist (2016), and the manuscript was prepared and revised according to the CARE Checklist (2016).

Country/Territory of origin: China

ORCID number: Chao-Bang Xie 0000-0001-6976-4357; Yang Wu 0000-0003-1976-7968; Feng Li 0000-0001-5350-4040; Kai-Fei Zhao 0000-0002-8274-2600; Rong-Shu Shi 0000-0002-4052-1308; Qiong Huang 0000-0001-7178-9027; Jin Ao 0000-0003-2774-8812.

S-Editor: Yan JP
L-Editor: Filipodia
P-Editor: Yan JP

REFERENCES

1 **Brindley PJ**, Bachini M, Ilyas SI, Khan SA, Loukas A, Sirica AE, Teh BT, Wongkham S, Gores GJ. Cholangiocarcinoma. *Nat Rev Dis Primers* 2021; **7**: 65 [PMID: 34504109 DOI: 10.1038/s41572-021-00300-2]
2 **Yang M**, Yang Y, Chen J, Stella GM, Um SW, Tandon YK, Liu H. A case report of primary signet ring cell carcinoma of the lung: imaging study and literature review. *Transl Lung Cancer Res* 2021; **10**: 3840-3849 [PMID: 34733632 DOI: 10.21037/tlcr-21-654]
3 **el-Zimaity HM**, Itani K, Graham DY. Early diagnosis of signet ring cell carcinoma of the stomach: role of the Genta stain. *J Clin Pathol* 1997; **50**: 867-868 [PMID: 9462273 DOI: 10.1136/jcp.50.10.867]
4 **Wang S**, Li J, You J, Zhou Y. Clinicopathological characteristics and prognosis of signet ring cell carcinoma of the gallbladder. *BMC Gastroenterol* 2021; **21**: 248 [PMID: 34090347 DOI: 10.1186/s12876-021-01831-4]
5 **Amin M**. AJCC Cancer Staging Manual. 8th ed. American Joint Committee on Cancer; 2017 [DOI: 10.1007/978-0-387-88441-7]
6 **Hoedemaeker PJ**. Heterotopic gastric mucosa in the duodenum. *Digestion* 1970; **3**: 165-173 [PMID: 4915587 DOI: 10.1159/000197027]
7 **Lee EY**, Kim C, Kim MJ, Park JY, Park SW, Song SY, Chung JB, Kim H, Bang S. Signet ring cell carcinoma of the extrahepatic bile- duct. *Gut Liver* 2010; **4**: 402-406 [PMID: 20981222 DOI: 10.5009/gnl.2010.4.3.402]
8 **Ogata S**, Kimura A, Hatsuse K, Yamamoto J, Shimazaki H, Nakanishi K, Kawai T. Poorly differentiated adenocarcinoma with signet-ring cell carcinoma of the extrahepatic bile duct in a 42-year-old Japanese female: a case report. *Acta Med Okayama* 2010; **64**: 63-65 [PMID: 20200586 DOI: 10.18926/AMO/32860]
9 **Somer L**, Andrejić B, Milošević P. Origin and pathological characteristics of Klatskin tumor: a case report and literature review. *Pol J Pathol* 2012; **63**: 65-70 [PMID: 22535609]
10 **Kita E**, Tsujimoto A, Nakamura K, Sudo K, Hara T, Kainuma O, Yamamoto H, Itami M, Yamaguchi Y. Signet ring cell carcinoma of the extrahepatic bile duct diagnosed by preoperative biopsy: a case report. *Case Rep Gastroenterol* 2014; **8**: 353-357 [PMID: 25520605 DOI: 10.1159/000369249]
11 **Kwon HJ**, Yoon GS, Kwon YC, Kim SG, Jeong JY. Signet-ring cell carcinoma of the distal common bile duct: report of a case. *Korean J Pathol* 2014; **48**: 315-318 [PMID: 25214866 DOI: 10.4132/KoreanJPathol.2014.48.4.315]
12 **Hua R**, Zhang JF, Liu W, Huo YM, Sun YW. Signet-ring cell carcinoma coexisting with adenocarcinoma arising in a choledochal cyst: report of a case. *Surg Today* 2015; **45**: 1049-1052 [PMID: 25352010 DOI: 10.1007/s00595-014-1049-3]
13 **Chedid MF**, Lucas ET, Cerski CT, Lopes MF, Amaral OB, Chedid AD. Signet-ring cell hilar cholangiocarcinoma: case report. *Arq Bras Cir Dig* 2015; **28**: 148-149 [PMID: 26176256 DOI: 10.1590/S0102-67202015000200016]
14 **Zhang C**, Zhou J, Kou K, Liu S, We F, Wang G. Occurrence of signet-ring cell carcinoma with cholangiocarcinoma 25 years after choledochal cyst excision: A case report. *Medicine (Baltimore)* 2018; **97**: e9956 [PMID: 29465585 DOI: 10.1097/MD.0000000000009956]
15 **Welsh JL**, Jaber O, Ivanovic M, Johlin FC, El Abiad RG, Clamon GH, Smith MC, Chan CHF. Rapidly Progressing Primary Extrahepatic Bile Duct Signet-Ring Cell Carcinoma in a Caucasian Woman. *J Gastrointest Cancer* 2018; **49**: 63-66 [PMID: 27270710 DOI: 10.1007/s12029-016-9843-3]
16 **Hameed N**, Stephen M. Signet Ring Cell Carcinoma of the Extrahepatic Bile Duct: A Case Report. *Am J Clin Pathol* 2019; **152**: S68-S69 [DOI: 10.1093/ajcp/aqz113.077]
17 **Ghoddoosi M**, Hormati A, Ouladdameshghi D, Ahmadpour S. Signet ring cell hilar cholangiocarcinoma diagnosed *via* direct transpapillary cold forceps biopsy under fluoroscopy. *Gastroenterol Hepatol* 2021 [PMID: 33647345 DOI: 10.1016/j.gastrohep.2021.01.005]

World Journal of Gastrointestinal Oncology

Submit a Manuscript: https://www.f6publishing.com

World J Gastrointest Oncol 2022 July 15; 14(7): 1363-1371

DOI: 10.4251/wjgo.v14.i7.1363

ISSN 1948-5204 (online)

CASE REPORT

Da Vinci robot-assisted pancreato-duodenectomy in a patient with situs inversus totalis: A case report and review of literature

Bai-Bei Li, Shi-Liu Lu, Xiang He, Biao Lei, Jian-Ni Yao, Si-Chen Feng, Shui-Ping Yu

Specialty type: Gastroenterology and hepatology

Provenance and peer review: Unsolicited article; Externally peer reviewed.

Peer-review model: Single blind

Peer-review report's scientific quality classification

Grade A (Excellent): 0
Grade B (Very good): B, B
Grade C (Good): C
Grade D (Fair): 0
Grade E (Poor): 0

P-Reviewer: Chang A, Thailand; Isac S, Romania; Telkes G, Hungary

Received: March 20, 2022
Peer-review started: March 20, 2022
First decision: April 17, 2022
Revised: April 30, 2022
Accepted: June 26, 2022
Article in press: June 26, 2022
Published online: July 15, 2022

Bai-Bei Li, Shi-Liu Lu, Xiang He, Biao Lei, Jian-Ni Yao, Si-Chen Feng, Shui-Ping Yu, Department of Hepatobiliary Surgery, The First Affiliated Hospital of Guangxi Medical University, Nanning 530021, Guangxi Zhuang Autonomous Region, China

Corresponding author: Shui-Ping Yu, PhD, Doctor, Department of Hepatobiliary Surgery, The First Affiliated Hospital of Guangxi Medical University, No. 6 Shuangyong Road, Nanning 530021, Guangxi Zhuang Autonomous Region, China. 478517575@qq.com

Abstract

BACKGROUND

Situs inversus totalis (SIT) is an extremely rare congenital malformation characterized by mirror displacement of the thoracoabdominal organs such as the heart, liver, spleen, and stomach. Herein, we describe a patient with SIT complicated with cholangiocarcinoma who underwent successful pancreaticoduodenectomy with the assistance of a da Vinci robot.

CASE SUMMARY

A 58-year-old female presented to the hospital with paroxysmal pain in her left upper abdomen, accompanied by jaundice and staining of the sclera as chief complaints. Imaging examination detected a mass at the distal end of the common bile duct, with inverted thoracic and abdominal organs. Endoscopic retrograde cholangiopancreatography forceps biopsy revealed the presence of a well-differentiated adenocarcinoma. The patient successfully underwent robotic-assisted pancreaticoduodenectomy; the operation lasted 300 min, the intraoperative blood loss was 500 mL, and there were no intraoperative and postoperative complications.

CONCLUSION

SIT is not directly related to the formation of cholangiocarcinoma. Detailed preoperative imaging examination is conducive to disease diagnosis and also convenient for determining the feasibility of tumor resection. Robot-assisted pancreaticoduodenectomy for SIT complicated with cholangiocarcinoma provides a safe, feasible, minimally invasive, and complication-free alternative with adequate preoperative planning combined with meticulous intraoperative procedures.

Key Words: Situs inversus totalis; Cholangiocarcinoma; Da Vinci robot; Whipple; Surgery; Case report

Core Tip: Situs inversus totalis (SIT) is an extremely rare congenital malformation characterized by a mirror image displacement of the thoracoabdominal organs such as the heart, liver, spleen and stomach. SIT combined with choledochal cancer is even rarer, and da Vinci robot-assisted pancreaticoduodenectomy in patients with SIT combined with choledochal cancer has not been reported. This case demonstrates that preoperative thorough planning, intraoperative precise anatomical knowledge, effective teamwork, meticulous treatment, and postoperative care are feasible with the aid of the da Vinci robot for pancreaticoduodenectomy in patients with SIT.

Citation: Li BB, Lu SL, He X, Lei B, Yao JN, Feng SC, Yu SP. Da Vinci robot-assisted pancreato-duodenectomy in a patient with situs inversus totalis: A case report and review of literature. *World J Gastrointest Oncol* 2022; 14(7): 1363-1371
URL: https://www.wjgnet.com/1948-5204/full/v14/i7/1363.htm
DOI: https://dx.doi.org/10.4251/wjgo.v14.i7.1363

INTRODUCTION

Situs inversus totalis (SIT) is characterized by complete mirror displacement of the anatomical positions of organs in the thoracoabdominal cavity. It has been reported that its incidence is 1/8000-1/25000 with a male to female ratio of 3:2[1-3]. Although the exact cause of SIT remains unknown, it is generally accepted that it is caused by autosomal abnormalities[4]. In addition, some mutations, such as Dynein Axonemal Heavy Chain 11 and NME7, have been shown to be closely related to SIT[5,6]. Patients with SIT typically exhibit no obvious symptoms, and their health and life expectancy appear to be unaffected [7]. Cholangiocarcinoma is a rare malignant tumor originating from bile duct epithelial cells, accounting for merely 3% of digestive tract malignant tumors[8]. It has an insidious onset, a high degree of malignancy, and a poor prognosis[9]. The da Vinci surgical robot system appeared at the end of the 20th century, and the fourth generation of the robot was launched in 2014, with qualitative improvements in flexibility, accuracy, and imaging clarity. Notably, a remote observation and guidance system was developed in the second half of 2014[10,11]. According to reports, the da Vinci robot has evolved into its fifth generation[12]. To date, several cases of complete visceral choledochal carcinoma have been reported[7,13-18], but da Vinci robot-assisted pancreatoduodenectomy in a patient with SIT has not been reported so far. This is the case report of a patient with SIT complicated with cholangiocarcinoma who underwent pancreaticoduodenectomy assisted by a da Vinci surgical robot. We detailed the diagnosis and management of this case, as well as a thorough evaluation of the associated literature.

CASE PRESENTATION

Chief complaints

A 58-year-old female patient presented to our hospital in November 2021 with jaundice, yellow sclera, paroxysmal pain in the left upper abdomen, itching, fatigue, tea-like urine, and weight loss of 1.5 kg.

History of present illness

The patient developed symptoms 2 mo ago with recurrent upper left abdominal pain.

History of past illness

The patient underwent surgery for cholecystolithiasis 10 years ago.

Personal and family history

The patient had no similar family history or genetic history of the disease.

Physical examination

Physical examination on admission revealed yellow discoloration of the skin and sclera, no chest deformity, and cardiac sound in the right chest. The abdomen was soft, while the upper abdomen was tender. There was no rebound tenderness or muscle tension. The liver and spleen were not palpable under the rib edge, and the activities of both lower limbs were unremarkable.

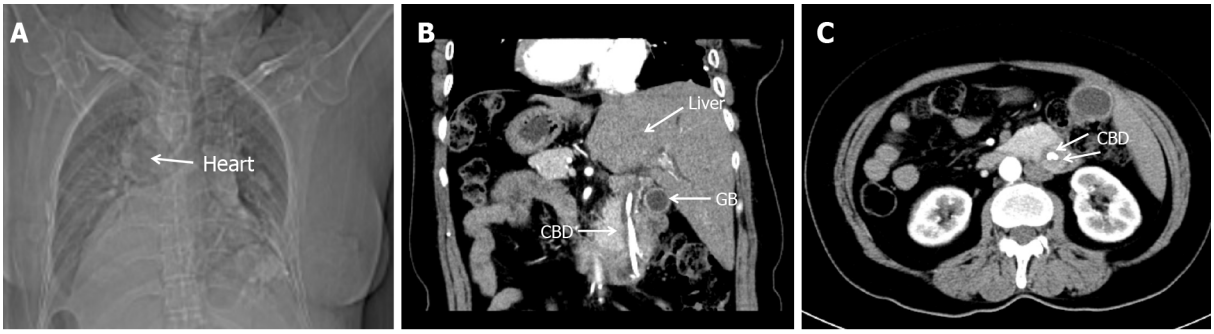

DOI: 10.4251/wjgo.v14.i7.1363

Figure 1 Preoperative imaging of the patient. A: Chest X-ray illustrated that the right heart was mirrored; B and C: Multi-slice spiral computed tomography displayed complete transposition of thoracic and abdominal organs and a mass in the lower common bile duct. CBD: Common bile duct; GB: Gallbladder.

Laboratory examinations

Preoperative auxiliary examinations were as follows: Total bilirubin 126.2 μmol/L (normal range: 3.4-20.5 μmol/L); Direct bilirubin 97.2 μmol/L (normal range: 0-6.8 μmol/L); Indirect bilirubin 29.2 μmol/L (normal range: 3.1-14.3 μmol/L); Aspartate aminotransferase 19.0 U/L (normal range: 13-40 U/L); Alanine aminotransferase (ALT) 28.0 U/L (normal range: 7-45 U/L); Alkaline phosphatase 255 U/L (normal range: 50-135 U/L); Abnormal prothrombin 76.60 ng/mL (normal range: 0-40 ng/mL); Carbohydrate antigen 19-9 197.96 U/mL (normal range: 0-37.00 ng/mL). Other blood biochemical indexes were within the normal range.

Imaging examinations

The chest X-ray exposed that the right heart was mirrored (Figure 1A). Multi-slice spiral computed tomography CT (MSCT) revealed complete transposition of the thoracic and abdominal viscera, as well as a tumor in the lower segment of the common bile duct, with minimal intestinal obstruction. The intrahepatic bile duct, extrahepatic bile duct, and pancreatic duct were dilated, and cholecystolithiasis with chronic cholecystitis was diagnosed (Figure 1B and C). Endoscopic retrograde cholangiopancreatography (ERCP) was performed, and the tissue was taken for pathological biopsy; the results showed a well-differentiated adenocarcinoma. Magnetic resonance imaging (MRI) showed intraluminal growth of cholangiocarcinoma in the lower part of the common bile duct with dilatation of the bile duct and pancreatic duct.

Further diagnostic work-up

Postoperative histological results were as follows: (1) Well-differentiated adenocarcinoma of the common bile duct with invasion of the duodenal wall. No vascular tumor thrombus and nerve invasion were identified; (2) There were no signs of malignancy in the gastric, duodenal, and pancreatic margins; (3) Each of the 6 Lymph nodes manifested reactive hyperplasia; and (4) Cholecystolithiasis with chronic cholecystitis.5. Immunohistochemical staining was positive for CDX-2, cytokeratin (CK) 7 and CK19 (Figure 2).

FINAL DIAGNOSIS

According to the American Joint Committee on Cancer/International Alliance for Cancer Control TNM staging system, the patient's tumor stage was IIB stage[19]. The pathological stage of the patient was pT3N0M0.

TREATMENT

Prior to surgery, the anesthesiologist assessed the patient's perioperative risk score. According to the American Society of Anesthesiologists Physical Status classification system (ASA PS)[20], the ASA score of the patient was P2.

The detailed procedure of the operation is as follows: (1) The surgery was prepared in accordance with the specifications of the da Vinci System. The layout of the operation window and the instrument arm are illustrated in Figure 3; (2) Upon entering the abdominal cavity, it was observed that the abdominal organs were fully inverted (Figure 4A); (3) The gallbladder was anterogradely dissected while the cystic duct was retained. Then, the common hepatic artery was exposed (Figure 4B). Following this, the right gastric artery, the left hepatic artery, and the right hepatic artery were exposed.

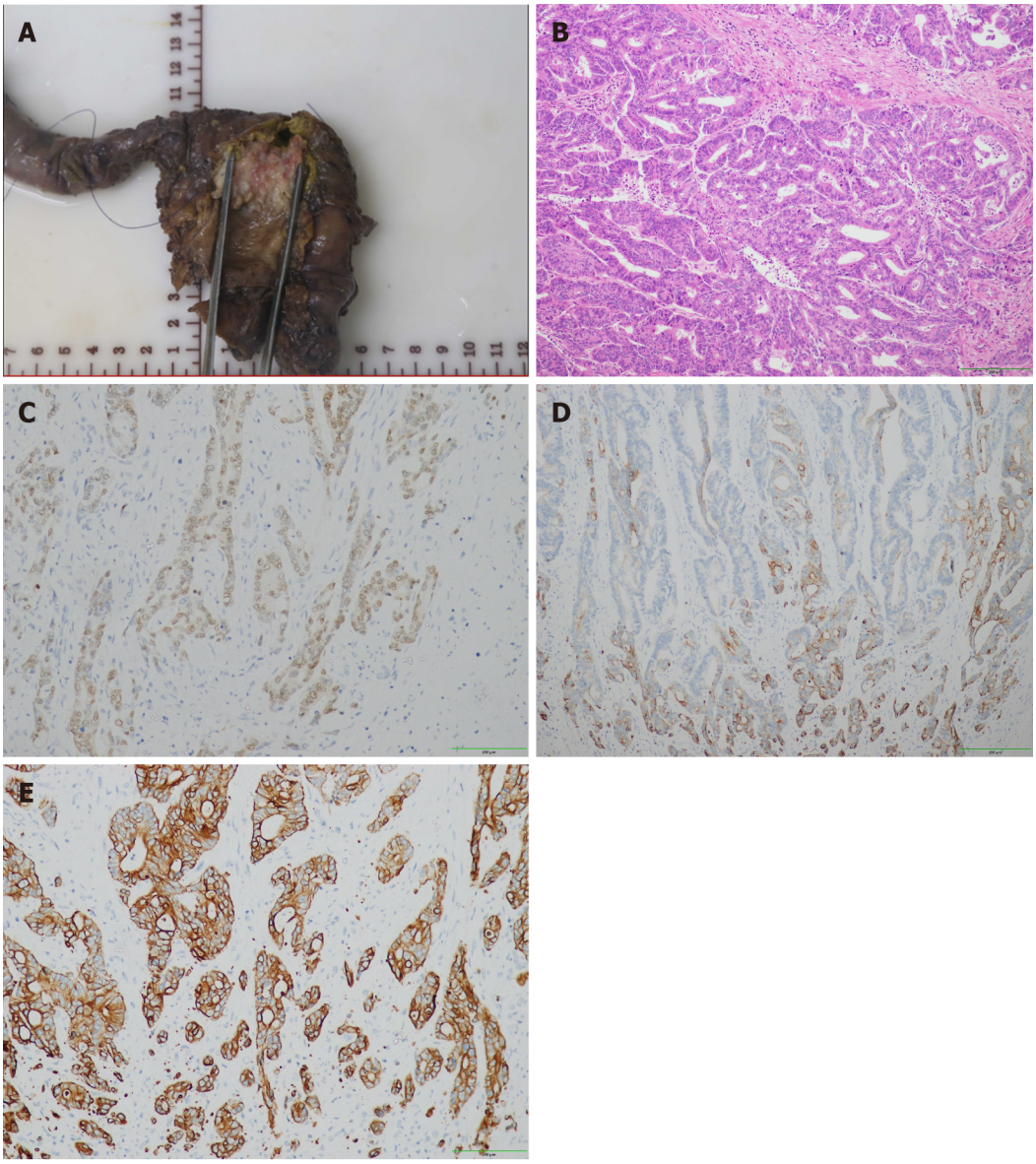

DOI: 10.4251/wjgo.v14.i7.1363

Figure 2 Postoperative pathological picture. A: The mass in the distal common bile duct infiltrated the duodenal wall; B: Well-differentiated adenocarcinoma; C: Immunohistochemical CDX-2 positive; D: Immunohistochemical cytokeratin (CK)7 positive; E: Immunohistochemical CK19 positive.

Next, the suprapyloric lymph node (NO. 5), anterosuperior lymph node of common hepatic artery (NO. 8a), and hepatoduodenal ligament lymph nodes (along the hepatic artery) (NO. 12a) were dissected, and the portal vein and its left and right branches were exposed. Afterward, hepatoduodenal ligament lymph nodes (along the portal vein) (NO. 12p) were dissected, the common hepatic duct and common bile duct were exposed, and hepatoduodenal ligament lymph nodes (along the bile duct) (NO. 12b) were dissected (Figure 4C). Finally, the hepatic portal vein was skeletonized, and the common bile duct was excised; (4) The gastrocolic and hepatogastric ligaments were dissected. Thereafter, the right blood vessels of the gastric reticulum were clamped and cut off, and the subpyloric lymph nodes (NO. 6) were dissected. A Kocher incision was made to expose the inferior vena cava (Figure 4D). Most of the pancreatic head covered the descending and horizontal part of the duodenum, making it difficult to expose the superior mesenteric artery (Figure 4E). The superior mesenteric vein was subsequently exposed along the lower margin of the pancreas, following which the posterior space of the pancreas was separated. Next, the pancreas was cut off, and the location of the pancreatic duct was determined (Figure 4F). The superior mesenteric artery was protected under direct vision. The uncinate process was subsequently cut off along the right side of the superior mesenteric vein. Lastly, the pancreaticoduodenum was resected (Figure 4G); (5) Pancreaticojejunostomy and choledochojejunostomy were performed. The specimens were removed from the abdominal cavity *via* a median 8 cm incision in the upper abdomen, and gastrojejunostomy was executed through this incision; and (6) A total of 3 drainage tubes were placed in Wen's foramen, behind the pancreaticojejunostomy, and in the pelvic cavity. The operation lasted 300 min, and the intraoperative bleeding was only 500 mL.

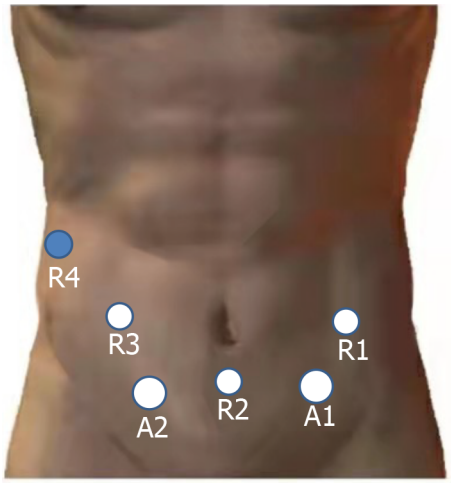

DOI: 10.4251/wjgo.v14.i7.1363

Figure 3 Operation hole layout and device arm placement. A1 and A2: Assistant; R1, R3, and R4: Robotic arms; R2: Camera.

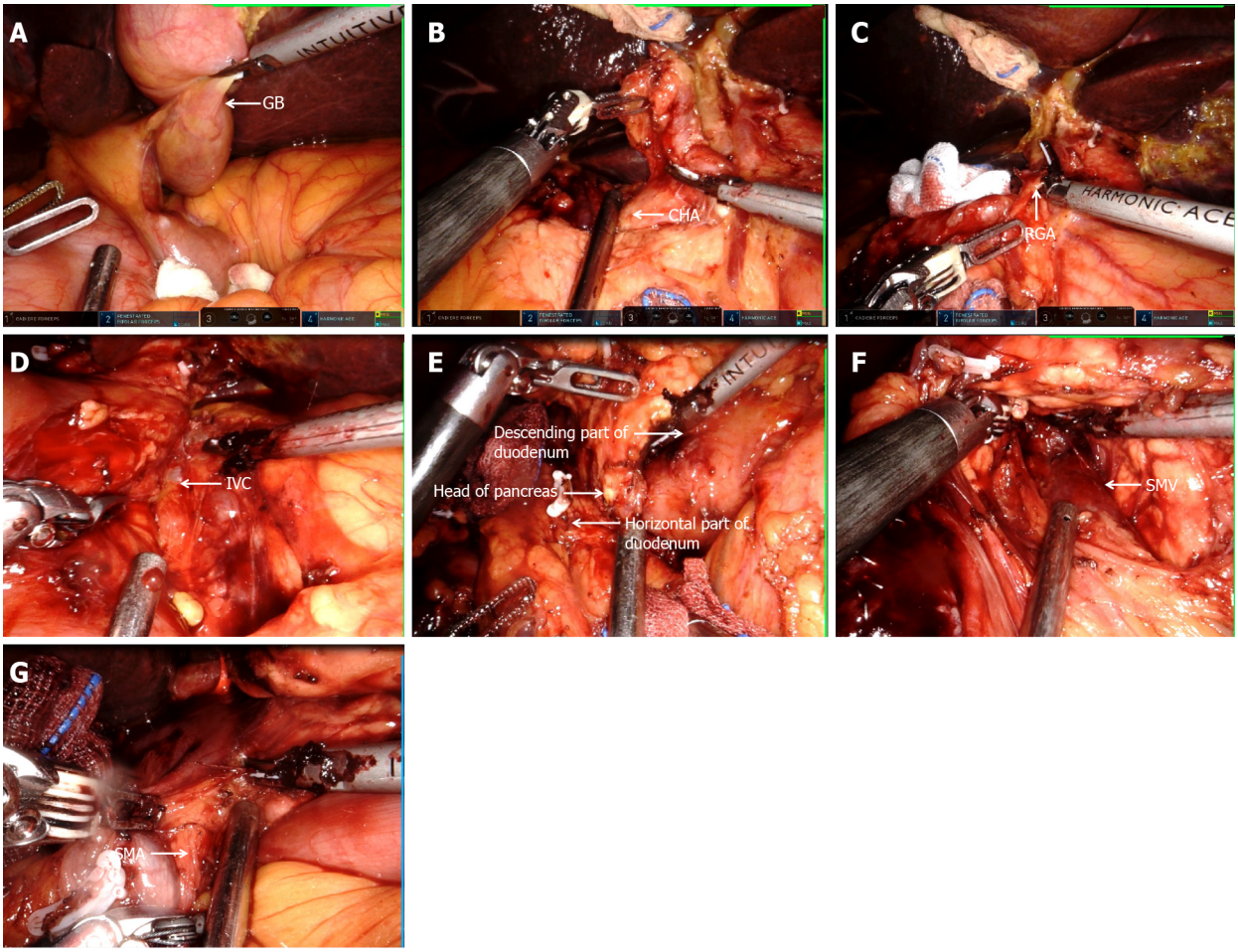

DOI: 10.4251/wjgo.v14.i7.1363

Figure 4 Detailed surgical procedure. A: Abdominal examination revealed that the abdominal organs were in reverse positions; B: The common hepatic artery was exposed; C: Separation revealed the right gastric artery; D: A Kocher incision was made to expose the inferior vena cava; E: The head of the pancreas covered the descending and horizontal parts of the duodenum; F: Exposing the superior mesenteric vein; G: The uncinate process of the pancreas was amputated along the right side of the superior mesenteric vein. CHA: Common hepatic artery; GB: Gallbladder; IVC: Inferior vena cava; RGA: Right gastric artery; SMA: Superior mesenteric artery; SMV: Superior mesenteric vein.

OUTCOME AND FOLLOW-UP

There were no severe complications during or after the operation. The patient stayed in the hospital for

a total of 30 d and was discharged 22 d following surgery. At the last follow-up (March 15, 2022), there was no evidence of recurrence, and tumor markers had fallen within the normal range. After treatment, he lived completely independently and is still alive.

DISCUSSION

At present, it is generally acknowledged that SIT with malignancies is a rare coincidence, although SIT with gastric cancer, rectal cancer, pancreatic cancer, liver cancer, and other tumors have been reported [21-24]. Indeed, only 8 cases of SIT complicated with choledochal carcinoma have been reported so far[7, 13-18]. The clinicopathological features of the 8 previously reported cases and our case are summarized in Table 1. The cohort consisted of 6 men and 3 women, ranging from 33-years-old to 74-years-old, including 3 from Japan, 2 from China, 2 from the United States, 1 from Italy, and 1 from Morocco. Eight out of the 9 patients underwent the Whipple procedure, and 1 patient underwent choledochectomy and Roux-en-Y hepaticojejunostomy. Histopathological results determined that there were 4 cases of well-differentiated adenocarcinoma, 1 case of medium-differentiated adenocarcinoma, 1 case of poorly-differentiated adenocarcinoma, and 1 case of high-grade intraepithelial neoplasia.

Most of the early clinical manifestations of cholangiocarcinoma are atypical, and patients seek medical treatment owing to epigastric discomfort, abdominal pain, abdominal distension, loss of appetite, and other symptoms[25]. A minority of patients with cholangiocarcinoma caused by the tumor may develop symptoms of typical obstructive jaundice with severe colic[26]. However, SIT generally lacks specific clinical manifestations, considering it is frequently accompanied by other diseases or discovered during physical examination[27]. By reviewing the literature, it was noted that the reported clinical manifestations of SIT complicated with cholangiocarcinoma include jaundice, abdominal pain, weight loss, and other symptoms. Among the cohort, 5 cases developed jaundice, as was the case in our patient. Thus, jaundice can be considered the primary clinical manifestation of SIT complicated with cholangiocarcinoma. Earlier studies have reported that MSCT, MRI, endoscopic ultrasound, and ERCP are of tremendous value in the diagnosis and preoperative evaluation of SIT complicated with cholangiocarcinoma[7,18].

The following points need to be considered when performing robot-assisted pancreaticoduodenectomy in SIT patients. Compared to healthy individuals, the gall bladder, bile duct, and gastrointestinal tract form a symmetric structure in SIT patients. Therefore, surgeons must be accustomed to preoperative images of SIT patients to avoid prolonged operation time due to unfamiliarity with the anatomy of SIT patients. Additionally, we uncovered for the first time that the thoracic and abdominal organs of SIT patients with cholangiocarcinoma have not only left and right reverse positions but also anterior and posterior reverse positions. During the operation, the pancreatic head of the patient covered the descending and horizontal parts of the duodenum, which was inverted from its normal anatomical structure. Considering the atypical anatomy of this patient, there was no reference for the preoperative procedure. In addition to the conventional operation with three mechanical arms, two auxiliary operation holes were used to improve operability and safety. Due to the atypical anatomy of SIT, routine thinking should be avoided during the operation, and the operation should be initiated with familiarity and a clear anatomical position to avoid accidental injury. During the operation, with the help of a da Vinci robot 3D and a highly clear magnified view, the method of small steps was used to dissect and separate; for the bleeding or blurred parts of the visual field, different from normal anatomy, one should try to avoid blind anatomical separation. For example, when the Kocher technique is used to dissociate the descending part of the duodenum and other parts, the anatomy is not forced to follow the conventional technique, but in the da Vinci robot high-definition field of vision, from shallow to deep, rapid, initial resection of tiny tissue, abnormal bleeding, and other cases in a timely and effective manner. The humanoid wrist function of the da Vinci robot also highlights its superiority to laparoscopic surgeries in narrow spaces and unconventional suture operation, as well as the effect of open surgery. The patient recovered well following surgery, without developing complications such as biliary fistula, pancreatic leakage, gastric emptying dysfunction, pseudocolinestherasis deficits, and airway obstruction[28-31]. Furthermore, incision healing was also significantly better than open surgery.

CONCLUSION

SIT is a rare genetic disease, and da Vinci robotic surgery is the current poster child for minimally invasive surgery. We believe that with thorough preoperative planning, precise intraoperative anatomical knowledge, effective teamwork, meticulous treatment, and postoperative care, da Vinci robotic-assisted pancreaticoduodenectomy in patients with SIT is feasible and developmental.

Table 1 Characteristics of patients who had situs inversus totalis with biliary tumor

Case	Ref.	Country	Age/sex	Size	Jaundice	Alkaline phosphatase	Treatment	Histological type	Stage	Postoperative complication
1	Organ *et al* [15], 1991	United States	68/F	2 cm	Yes	905 U/L	Whipple	m	IIIB	NA
2	Tsunoda *et al* [17], 2006	Japan	65/M	NA	NA	NA	Whipple	NA	NA	None
3	Benhammane *et al*[14], 2012	Morocco	33/M	15 mm	Yes	NA	Whipple	w	IIB	None
4	Kyuno *et al*[7], 2013	Japan	74/M	NA	NA	NA	Whipple	w	IIB	Pancreatic fistula
5	Kyuno *et al*[7], 2013	Japan	67/M	NA	NA	NA	Whipple	w	IA	Pancreatic fistula
6	Togliani *et al* [13], 2013	Italy	67/M	2 cm	Yes	NA	Whipple	NA	NA	NA
7	Zhang *et al* [16], 2019	China	61/M	1.8 cm × 1.5 cm × 1.5 cm	Yes	1011 U/L	Choledochectomy + Roux-en-Y hepaticojejunostomy	l	IIB	None
8	Coronel *et al* [18], 2020	United States	67/F	11 mm	Yes	570 U/L	Whiple	h	0	NA
9	The present case	China	58/F	3 cm × 1.9 cm × 0.7 cm	Yes	255 U/L	Whiple	w	IIB	None

h: High grade biliary intraepithelial neoplasia; l: Low differentiation adenocarcinoma; m: Medium differentiated adenocarcinoma; M: Male; F: Female; NA: Not available; W: Well differentiated adenocarcinoma.

ACKNOWLEDGEMENTS

I would like to express my gratitude to all those who helped me during the writing of this thesis and their efforts in the management of this patient.

FOOTNOTES

Author contributions: Li BB and Lu SL reviewed the literature, designed the case report presentation, and wrote the manuscript; He X and Lei B participated in manuscript preparation, revision, patient investigation and treatment; Yao JN and Feng SC participated in patient investigation and treatment and provided the gross and pathology images; Yu SP designed the case report presentation and revised the manuscript; all authors have read and approved the final manuscript.

Informed consent statement: Informed written consent was obtained from the patient for publication of this report and any accompanying images.

Conflict-of-interest statement: The authors declare that they have no conflicts of interest.

CARE Checklist (2016) statement: The authors have read the CARE Checklist (2016), and the manuscript was prepared and revised according to the CARE Checklist (2016).

Country/Territory of origin: China

ORCID number: Bai-Bei Li 0000-0002-6133-9361; Shi-Liu Lu 0000-0002-8020-0488; Xiang He 0000-0002-1132-070X; Biao Lei 0000-0002-3010-0972; Jian-Ni Yao 0000-0002-0461-3408; Si-Chen Feng 0000-0001-9015-1336; Shui-Ping Yu 0000-0002-1581-7342.

S-Editor: Yan JP
L-Editor: Filipodia
P-Editor: Yan JP

REFERENCES

1 **Gentile BA**, Tighe DA. Situs Inversus Totalis. *N Engl J Med* 2019; **380**: e45 [PMID: 31189040 DOI: 10.1056/NEJMicm1811002]
2 **Chen W**, Guo Z, Qian L, Wang L. Comorbidities in situs inversus totalis: A hospital-based study. *Birth Defects Res* 2020; **112**: 418-426 [PMID: 31994846 DOI: 10.1002/bdr2.1652]
3 **Chen LJ**, Qiu X, Sun H, Xu PF, Yin FM, Xu LJ. Two types of lung cancer with situs inversus totalis: a case report and review of the literature. *J Int Med Res* 2020; **48**: 300060520944107 [PMID: 33106071 DOI: 10.1177/0300060520944107]
4 **Burvill A**, Blackham R, Hamdorf J. Laparoscopic sleeve gastrectomy in a patient with *situs inversus totalis* and Kartagener syndrome: an unusual surgical conundrum. *BMJ Case Rep* 2019; **12** [PMID: 31345831 DOI: 10.1136/bcr-2019-229550]
5 **Bartoloni L**, Blouin JL, Pan Y, Gehrig C, Maiti AK, Scamuffa N, Rossier C, Jorissen M, Armengot M, Meeks M, Mitchison HM, Chung EM, Delozier-Blanchet CD, Craigen WJ, Antonarakis SE. Mutations in the DNAH11 (axonemal heavy chain dynein type 11) gene cause one form of situs inversus totalis and most likely primary ciliary dyskinesia. *Proc Natl Acad Sci U S A* 2002; **99**: 10282-10286 [PMID: 12142464 DOI: 10.1073/pnas.152337699]
6 **Reish O**, Aspit L, Zouella A, Roth Y, Polak-Charcon S, Baboushkin T, Benyamini L, Scheetz TE, Mussaffi H, Sheffield VC, Parvari R. A Homozygous Nme7 Mutation Is Associated with Situs Inversus Totalis. *Hum Mutat* 2016; **37**: 727-731 [PMID: 27060491 DOI: 10.1002/humu.22998]
7 **Kyuno D**, Kimura Y, Imamura M, Uchiyama M, Ishii M, Meguro M, Kawamoto M, Mizuguchi T, Hirata K. Pancreaticoduodenectomy for biliary tract carcinoma with situs inversus totalis: difficulties and technical notes based on two cases. *World J Surg Oncol* 2013; **11**: 312 [PMID: 24341840 DOI: 10.1186/1477-7819-11-312]
8 **Krasinskas AM**. Cholangiocarcinoma. *Surg Pathol Clin* 2018; **11**: 403-429 [PMID: 29751883 DOI: 10.1016/j.path.2018.02.005]
9 **Labib PL**, Goodchild G, Pereira SP. Molecular Pathogenesis of Cholangiocarcinoma. *BMC Cancer* 2019; **19**: 185 [PMID: 30819129 DOI: 10.1186/s12885-019-5391-0]
10 **Aldousari SA**, Buabbas AJ, Yaiesh SM, Alyousef RJ, Alenezi AN. Multiple perceptions of robotic-assisted surgery among surgeons and patients: a cross-sectional study. *J Robot Surg* 2021; **15**: 529-538 [PMID: 32776285 DOI: 10.1007/s11701-020-01136-w]
11 **Ferguson JM**, Pitt B, Kuntz A, Granna J, Kavoussi NL, Nimmagadda N, Barth EJ, Herrell SD 3rd, Webster RJ 3rd. Comparing the accuracy of the da Vinci Xi and da Vinci Si for image guidance and automation. *Int J Med Robot* 2020; **16**: 1-10 [PMID: 32808429 DOI: 10.1002/rcs.2149]
12 **Shin HR**, Lee K, Yu HW, Kim SJ, Chai YJ, Choi JY, Lee KE. Comparison of Perioperative Outcomes Using the da Vinci S, Si, X, and Xi Robotic Platforms for BABA Robotic Thyroidectomy. *Medicina (Kaunas)* 2021; **57** [PMID: 34684167 DOI: 10.3390/medicina57101130]
13 **Togliani T**, Pilati S, Mantovani N, Savioli A, Gaetti L, Negri S, Fusaroli P. Extrahepatic cholangiocarcinoma in a patient with situs inversus totalis diagnosed by endoscopic ultrasound. *Endoscopy* 2013; **45** Suppl 2 UCTN: E229-E230 [PMID: 23945923 DOI: 10.1055/s-0033-1344327]
14 **Benhammane H**, Kharmoum S, Terraz S, Berney T, Nguyen-Tang T, Genevay M, El Mesbahi O, Roth A. Common bile duct adenocarcinoma in a patient with situs inversus totalis: report of a rare case. *BMC Res Notes* 2012; **5**: 681 [PMID: 23234596 DOI: 10.1186/1756-0500-5-681]
15 **Organ BC**, Skandalakis LJ, Gray SW, Skandalakis JE. Cancer of bile duct with situs inversus. *Arch Surg* 1991; **126**: 1150-1153 [PMID: 1929848 DOI: 10.1001/archsurg.1991.01410330112017]
16 **Zhang SM**, Chen ZG, Ma LL, Wu XA, Hua SH. Common bile duct adenocarcinoma in a patient with situs inversus totalis:a case report. *Anhui Med Pharm J* 2019; **23** [DOI: 10.3969/j.issn.1009-6469]
17 **Tsunoda S**, Miyashita T, Murata M. Pancreaticoduodenectomy for common bile duct cancer in a patient with situs inversus totalis: a case report. *Int Surg* 2006; **91**: 24-27 [PMID: 16706098]
18 **Coronel M**, Lanke G, Cambell D, Coronel E, Tzeng CD, Foo W, Lee JH. Performing Endoscopic Retrograde Cholagiopancreatpgraphy and Endoscopic Ultrasound for Management of Malignant Bile Duct Obstruction in a Patient With a Situs Inversus Totalis. *ACG Case Rep J* 2020; **7**: e00483 [PMID: 33324708 DOI: 10.14309/crj.0000000000000483]
19 **Adsay NV**, Bagci P, Tajiri T, Oliva I, Ohike N, Balci S, Gonzalez RS, Basturk O, Jang KT, Roa JC. Pathologic staging of pancreatic, ampullary, biliary, and gallbladder cancers: pitfalls and practical limitations of the current AJCC/UICC TNM staging system and opportunities for improvement. *Semin Diagn Pathol* 2012; **29**: 127-141 [PMID: 23062420 DOI: 10.1053/j.semdp.2012.08.010]
20 **Horvath B**, Kloesel B, Todd MM, Cole DJ, Prielipp RC. The Evolution, Current Value, and Future of the American Society of Anesthesiologists Physical Status Classification System. *Anesthesiology* 2021; **135**: 904-919 [PMID: 34491303 DOI: 10.1097/ALN.0000000000003947]
21 **Suh BJ**. A Case of Gastric Cancer with Situs Inversus Totalis. *Case Rep Oncol* 2017; **10**: 130-135 [PMID: 28203176 DOI: 10.1159/000456539]
22 **Kasai S**, Hino H, Shiomi A, Kagawa H, Manabe S, Yamaoka Y, Kato S, Hanaoka M, Kinugasa Y. Robotic-assisted surgery for rectal cancer with situs inversus totalis: A case report. *Asian J Endosc Surg* 2021; **14**: 803-806 [PMID: 33797194 DOI: 10.1111/ases.12937]
23 **Hussan MA**, Yang Z, Dong X, Yang H, Li N, Qiao S. A laparoscopic pancreaticoduodenectomy for pancreatic adenocarcinoma in a patient with situs inversus totalis. *J Surg Case Rep* 2021; **2021**: rjab316 [PMID: 34316352 DOI:

10.1093/jscr/rjab316]
24 **Liao KX**, Li JW. ASO Author Reflections: A New Minimally Invasive Procedure for Hepatocellular Carcinoma with Situs Inversus Totalis. *Ann Surg Oncol* 2021; **28**: 6832-6833 [PMID: 33620618 DOI: 10.1245/s10434-021-09736-y]
25 **Fong ZV**, Brownlee SA, Qadan M, Tanabe KK. The Clinical Management of Cholangiocarcinoma in the United States and Europe: A Comprehensive and Evidence-Based Comparison of Guidelines. *Ann Surg Oncol* 2021; **28**: 2660-2674 [PMID: 33646431 DOI: 10.1245/s10434-021-09671-y]
26 **Turgeon MK**, Maithel SK. Cholangiocarcinoma: a site-specific update on the current state of surgical management and multi-modality therapy. *Chin Clin Oncol* 2020; **9**: 4 [PMID: 31500433 DOI: 10.21037/cco.2019.08.09]
27 **Téllez-Beltrán D**, González-Muñoz A, Barón-Cifuentes V, Pradilla-Gómez JM. Abdominal aortic aneurysm in a patient with situs inversus totalis. *Cir Cir* 2020; **88**: 79-82 [PMID: 32963397 DOI: 10.24875/CIRU.20001581]
28 **El Nakeeb A**, El Sorogy M, Hamed H, Said R, Elrefai M, Ezzat H, Askar W, Elsabbagh AM. Biliary leakage following pancreaticoduodenectomy: Prevalence, risk factors and management. *Hepatobiliary Pancreat Dis Int* 2019; **18**: 67-72 [PMID: 30413347 DOI: 10.1016/j.hbpd.2018.10.005]
29 **Ebata T**, Yokoyama Y, Igami T, Sugawara G, Takahashi Y, Nimura Y, Nagino M. Hepatopancreatoduodenectomy for cholangiocarcinoma: a single-center review of 85 consecutive patients. *Ann Surg* 2012; **256**: 297-305 [PMID: 22750757 DOI: 10.1097/SLA.0b013e31826029ca]
30 **Hogg C**. Primary ciliary dyskinesia: when to suspect the diagnosis and how to confirm it. *Paediatr Respir Rev* 2009; **10**: 44-50 [PMID: 19410200 DOI: 10.1016/j.prrv.2008.10.001]
31 **Ferkol T**, Leigh M. Primary ciliary dyskinesia and newborn respiratory distress. *Semin Perinatol* 2006; **30**: 335-340 [PMID: 17142159 DOI: 10.1053/j.semperi.2005.11.001]

World Journal of Gastrointestinal Oncology

Submit a Manuscript: https://www.f6publishing.com

World J Gastrointest Oncol 2022 July 15; 14(7): 1372-1374

DOI: 10.4251/wjgo.v14.i7.1372

ISSN 1948-5204 (online)

CORRECTION

Correction to "Novel long non-coding RNA LINC02532 promotes gastric cancer cell proliferation, migration, and invasion *in vitro*"

Cheng Zhang, Ming-Hui Ma, Yu Liang, Kun-Zhe Wu, Dong-Qiu Dai

Specialty type: Oncology

Provenance and peer review: Unsolicited article; Externally peer reviewed.

Peer-review model: Single blind

Peer-review report's scientific quality classification

Grade A (Excellent): A
Grade B (Very good): B
Grade C (Good): C, C
Grade D (Fair): 0
Grade E (Poor): 0

P-Reviewer: Chiba T, Japan; Morozov S, Russia; Preda SD, Romania; Ribeiro IB, Brazil
A-Editor: Liu X, China

Received: October 21, 2021
Peer-review started: October 21, 2021
First decision: April 17, 2022
Revised: April 21, 2022
Accepted: June 4, 2022
Article in press: June 4, 2022
Published online: July 15, 2022

Cheng Zhang, Ming-Hui Ma, Yu Liang, Dong-Qiu Dai, Department of Gastrointestinal Surgery, The Fourth Affiliated Hospital of China Medical University, Shenyang 110032, Liaoning Province, China

Kun-Zhe Wu, Scientific Research Center, China-Japan Union Hospital of Jilin University, Changchun 130000, Jilin province, China

Corresponding author: Dong-Qiu Dai, PhD, Chief Doctor, Department of Gastrointestinal Surgery, The Fourth Affiliated Hospital of China Medical University, No. 4 Chongshan Road, Shenyang 110032, Liaoning Province, China. daidq63@163.com

Abstract

We have replaced the misapplied images and the revised Figure 3 is provided.

Key Words: Correction; Gastric cancer; LINC02532; Prognosis; Bioinformatics

Core Tip: This is a correction to "Novel long non-coding RNA LINC02532 promotes gastric cancer cell proliferation, migration, and invasion *in vitro*". We found that the result of Si-LINC02532 #2 group in the MGC-803 cell invasion assay was displayed by a mistake in Figure 3A. The revised Figure 3 was uploaded.

Citation: Zhang C, Ma MH, Liang Y, Wu KZ, Dai DQ. Correction to "Novel long non-coding RNA LINC02532 promotes gastric cancer cell proliferation, migration, and invasion *in vitro*". *World J Gastrointest Oncol* 2022; 14(7): 1372-1374
URL: https://www.wjgnet.com/1948-5204/full/v14/i7/1372.htm
DOI: https://dx.doi.org/10.4251/wjgo.v14.i7.1372

TO THE EDITOR

We recently read our manuscript[1] published in the *World Journal of Gastrointestinal Oncology* (manuscript No. 43472, DOI: 10.4251/wjgo.v11.i2.91), and we found that the result of Si-LINC02532 #2 group in the MGC-803 cell invasion assay was displayed by

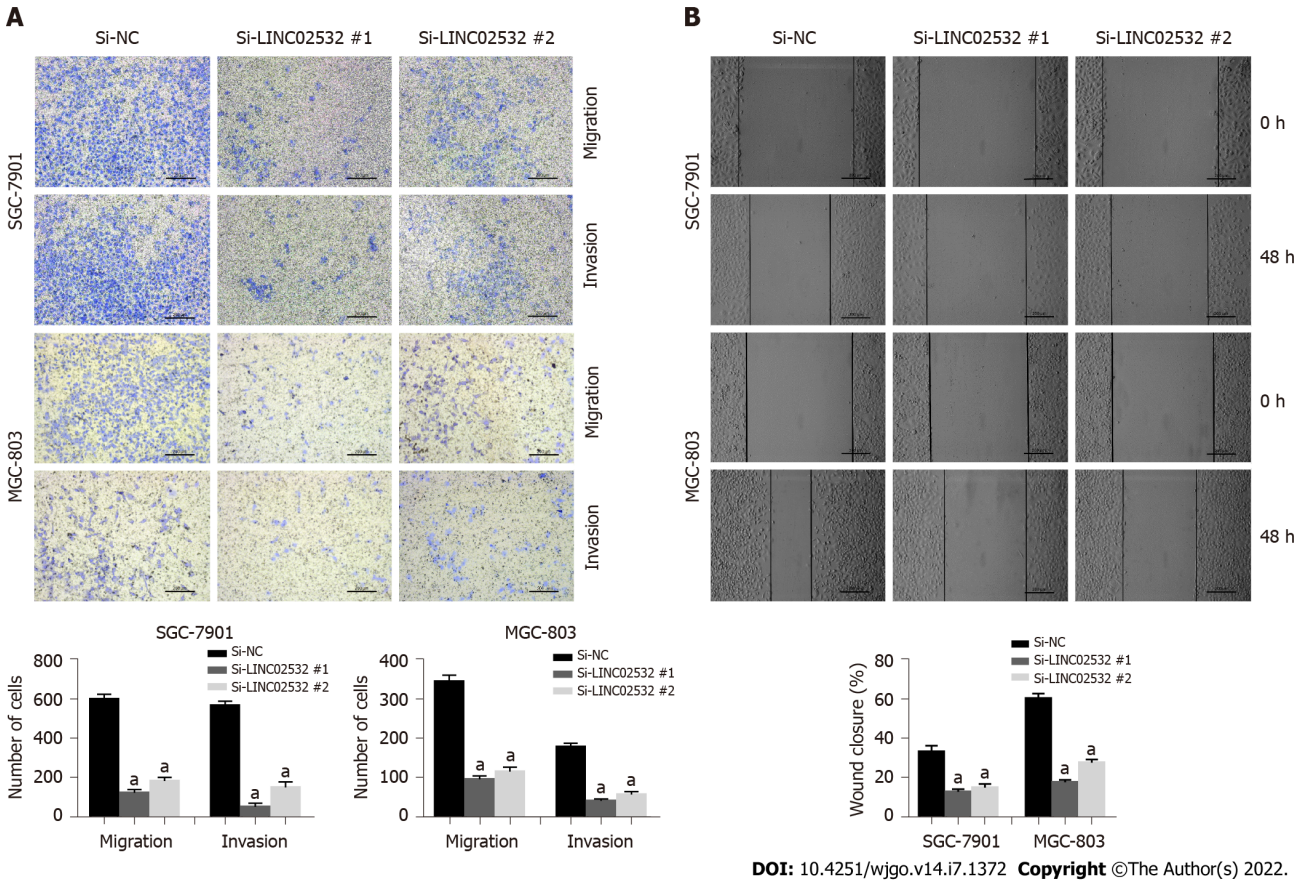

DOI: 10.4251/wjgo.v14.i7.1372

Figure 1 Transwell assays with or without Matrigel were performed to assess the capacity of cell invasion and migration, respectively. A: Transwell assays with or without Matrigel were performed to assess the capacity of cell invasion and migration, respectively. The results revealed that LINC02532 knockdown promoted gastric cancer cell migration and invasion; B: The wound healing assay further displayed that LINC02532 knockdown promoted gastric cancer cell migration. $^{a}P < 0.05$ was considered statistically significant.

a mistake in Figure 3A. Therefore, we are writing to apply for the modification of Figure 3A. The revised Figure 3 was uploaded in the attachment (Figure 1). This mistake has no influence on the interpretation of the results or conclusion in this study.

FOOTNOTES

Author contributions: Dai DQ contributed to this correction; all authors have read and approve the final manuscript.

Conflict-of-interest statement: All the authors report no relevant conflicts of interest for this article.

Country/Territory of origin: China

ORCID number: Cheng Zhang 0000-0001-5317-8775; Ming-Hui Ma 0000-0002-2566-0932; Yu Liang 0000-0001-9136-7139; Kun-Zhe Wu 0000-0003-4258-0261; Dong-Qiu Dai 0000-0002-1154-3276.

S-Editor: Gao CC
L-Editor: A
P-Editor: Gao CC

REFERENCES

1 **Zhang C**, Ma MH, Liang Y, Wu KZ, Dai DQ. Novel long non-coding RNA LINC02532 promotes gastric cancer cell proliferation, migration, and invasion *in vitro*. *World J Gastrointest Oncol* 2019; **11**: 91-101 [PMID: 30788037 DOI: 10.4251/wjgo.v11.i2.91]

Published by **Baishideng Publishing Group Inc**
7041 Koll Center Parkway, Suite 160, Pleasanton, CA 94566, USA
Telephone: +1-925-3991568
E-mail: bpgoffice@wjgnet.com
Help Desk: https://www.f6publishing.com/helpdesk
https://www.wjgnet.com